THE FRAGMENTATION OF PRESTELLAR CLOUDS

Miguel H. Ibañez S.

Presented for the Degree of Doctor of Philosophy

at the University of Edinburgh,

October, 1979.

This thesis was composed by me and consists

entirely of my own work

October, 1979

ACKNOWLEDGEMENTS

It is a pleasure to express my gratitude to Professor V.C. Reddish for accepting me as one of his last supervised students, for introducing me to the exciting field of stellar formation and for his guidance and advice during my stay at the Department of Astronomy of the University of Edinburgh.

I am also indebted to Dr D.H. Morgan for having devoted so much of his time to advising and discussing many vital aspects on radiative transfer.

I acknowledge Mr L.C. Lawrence for his assistance with the computing and Mrs J. Shand for her patience and skill in typing this thesis.

I am grateful to Facultad de Ciencias and CDCH, Universidad de los Andes, Venezuela, for financial assistance.

M. Ibañez S.

ABSTRACT

The radiative heating problem has been solved analytically, in first approximation, for a semi-infinite cloud model with transverse fluctuations in extinction, in terms of the parameters: albedo for a single scattering $\bar{\omega}$, the greenhouse parameter η, amplitude of the fluctuations a, and the parameter r which is a measure of the reciprocal optical thickness of the fluctuations. For $r << 1$, density fluctuations become radiatively disconnected (in the visual) and the solutions of the radiative heating problem tend to the homogeneous case. For $r >> 1$ temperature fluctuations are extinguished. There is a strong coupling between temperature fluctuations $\Delta T_d/\bar{T}_d$ and mean optical depth Z. Fluctuations with r such that $1 \lesssim r \lesssim 2$, the exact value depending on the Z value at which T_{cri} is reached, can provide temperature fluctuations which result in chemical discontinuity in H_2 formation and the onset of the fragmentation process.

The radiative heating problem has been solved with the help of a numerical (approximated) method for the following models: a) semi-infinite cloud with transverse fluctuations in extinction. b) finite cloud with mean optical thickness τ_o and transverse fluctuations in extinction. The visual radiation field was calculated and the fluctuation $\Delta T_d/\bar{T}_d$ was obtained for the different values of the basic parameters $\bar{\omega}$, η, r, a and τ_o.

Assuming isobaricity as a first approximation, the chemical equation for H_2 formation (in non-equilibrium condition) and the energy equation were solved numerically like a two boundary-value

problem. The values of the chemical parameter x, the gas temperature T and the mass density ρ were obtained explicitly as functions of time and they were compared with the change in the mean density produced by the free-fall. The ability of H_2 formation to act as a direct non-linear amplifier of density inhomogeneities in prestellar clouds depends critically on the initial values of the number density of particles n_o, the temperature T_o and the percentage of chemical heat input to the gas, ε. In particular, if the remainder of the binding energy of H_2 formation is radiated by the grains, H_2 formation can induce fragmentation in a contracting cloud providing that $T_o > 60^oK$ and $n_o \gtrsim 10^2\ cm^{-3}$.

A study (in orders of magnitude) of the turbulence as a mechanism generator of density fluctuations has been done. If the Kolmogorov spectral law is assumed, subsonic turbulence is enough to provide any prestellar cloud with the elemental fluctuations which are effectively amplified by molecule formation in a time shorter than one free-fall.

CONTENTS

CHAPTER I

1. INTRODUCTION

Observations support the idea that interstellar clouds consist mainly of atomic hydrogen, dust and traces of heavy elements, neutral and ionized and also that they evolve towards denser states and occasionally cross the Jeans limit and start to contract under their own self-gravitation. One can say that this last period is rather well understood, at least in the case of a spherical and initially homogeneous cloud, and an abundant literature has appeared since the classical paper of McVittie (1957). See for instance, Hayashi (1966), Bodenheimer (1968), Larson (1969), Disney (1969), Larson (1977). However, two fundamental problems remain to be clarified: a. the onset of the collapse itself* and b. the fragmentation problem, i.e. why, when and how a prestellar cloud, probably during its gravitational contraction, splits into independent units, some of them going on to reach high densities and high opacities (at wavelengths corresponding to the cooling radiation) and in an adiabatic state dramatically increase their temperature while evolving toward the proto-stellar stage.

A qualitative review of the main ideas proposed to explain the onset of fragmentation of clouds as a first stage in the star formation process will be presented in Section 2.

There are reasons to believe that the fragmentation process of prestellar clouds is not a consequence simply of the dynamical (gravitational) properties and that many of the physical processes

* For a recent review on this particular problem, see Woodward, P.R. (1978).

and fields involved, like turbulence, chemistry, radiation, magnetic and gravitational fields, probably play their own role, but because of the mathematical complexity which appears if one tries to incorporate all of these aspects at the same time, they have usually been treated separately.

In this thesis an exploration of a possible way by which turbulence, chemistry, radiation and gravitational fields can instigate fragmentation will be presented starting with the chemistry of the H_2 molecule.

The thermodynamics and in particular the chemistry of interstellar clouds is extremely complex. The diversity of physico-chemical processes, Watson (1976) and the number and diversity of molecules is enormous. Many molecules have been observed in the last few years, Herbst (1978); but the crucial role the H_2 molecule plays in the evolution of any interstellar cloud can be seen from the following general considerations:

a. The H_2 molecule is the most abundant and its formation alters directly the number density of particles of the gas.

b. The H_2 molecule initiates most of the chemical evolution in any interstellar cloud, Oppenheimer and Dalgarno (1975). Most of the molecular chemistry, in particular the CO generation, is inoperative unless sufficient H_2 is present, Gerola and Glassold (1978).

c. The presence of H_2 (and HD) involves a drastic and irreversible change in the thermo-dynamic properties of any cloud because of the change in the cooling agents from atomic to molecular

form. It is likely that this aspect is the most important one as far as the fragmentation process is concerned because of the strong implication on the thermal stability of the cloud. The generation of a new coolant and the change in the number of particles in discrete regions through any non-homogeneous cloud could be the key processes that induce fragmentation: this will be explored in this thesis.

d. The presence of H_2 molecules shields regions against the UV field in the region 912 - 1108 Å, Solomon (1969), Spitzer (1976), Federman et al (1979).

Finally, we quote from Spitzer (1976): "In theories of star formation, condensation of H into H_2 as a cloud contracts seems a very realistic assumption, ..."

In Section 3, the problem to be tackled will be enunciated and the justification for the two main hypotheses introduced i.e. (a) H_2 formation is completely determined by the critical grain temperature T_{cri} if the number density of gas particles $n > 10^2\ cm^{-3}$ and gas temperature $T \approx 100^{\circ}K$. (b) Radiative equilibrium between the dust and the radiation field holds.

In Section 4, an adaptation of the radiative-heating equations valid in the general case of a multidimensional inhomogeneous medium will be presented. These equations are solved, in Section 5, analytically in a first approximation for an inhomogeneous cloud model, i.e. a semi-infinite cloud with sinusoidal transverse fluctuation in density which are taken as a first and schematic representation of random inhomogeneities, possibly generated by turbulence.

The importance of the inhomogeneities at scales with optical thickness $\pi/2$ is shown.

In Section 6 an approximate numerical integration of the visual radiation field in inhomogeneous cloud models is presented introducing approximations justified by the results of Section 5, and a further constraint on the scale of inhomogeneities at large values ($>\pi$) is discussed.

In Section 7, the effects due only to H_2 formation are calculated, schematising the H_2 production as starting in bubbles with radius $\approx \pi/4\overline{\kappa}$, $\overline{\kappa}$ being the mean extinction coefficient. The chemical parameter x, density ρ and temperature T of the gas are evaluated numerically as functions of time and compared with the change in density produced by a hypothetical free-fall collapse, starting with the same initial density at which H_2 formation is switched on.

All the results are shown in graphs which seems the most direct way to present them, avoiding lengthy explanations.

The very complex gas-dynamical aspects have been evaded in this first exploration with an hypothesis of isobaricity which has some degree of justification as discussed in Sections 7 and 8. This is the strongest assumption made, which we hope to remove in a further treatment of the problem.

The summary and further discussion is presented in Section 8. In Section 9 some problems of interest which emerged during the preparation of this thesis have been quoted. It is hoped that they may be tackled in the future.

Appendix A contains a summary of the fundamental equations and basic hypotheses which permit one to introduce drastic simplifications to the formal equations, in particular to the radiative transfer equation. In this appendix some timescales of interest in this study are defined too.

Turbulence as a generator of density fluctuations is studied in orders of magnitude in appendix B.

Appendix C contains a detailed derivation of the Giovanelli equation which is solved analytically in a first approximation in Section 5 and from where a first insight into the radiative heating in inhomogeneous clouds has been obtained.

2. REVIEW OF STELLAR FORMATION THEORIES

The onset of the fragmentation process of prestellar clouds is only a particular aspect of the vast field of stellar formation. Therefore, a review of the theories of star formation with emphasis on the fragmentation problem is helpful.

Kant (1755) speculated that the stars are formed through gravitational collapse of nebular material thereby raising the temperature of the cold gas. Laplace (1796) suggested that cooling would help to initiate the collapse and that rotation might play an important role in the first stages of star formation. However, it was not until 1928 when Jeans published his classical paper that this problem received a quantitative analysis.

Jeans assumed an initially infinite and uniform gas at rest in which an infinitesimal perturbation was allowed for. He solved the motion and continuity equations - equations (A-16) and (A-15) - and found that the marginal state had a characteristic wavelength

$$\lambda_J = \left(\frac{\pi R}{G} \frac{T}{\rho_o} \right)^{\frac{1}{2}} \qquad (2\text{-}1)$$

where T and ρ_o are the unperturbed temperature and density respectively. Therefore, perturbations with wavelength $\lambda > \lambda_J$ would grow exponentially while those with $\lambda < \lambda_J$ would be damped. Although the basic assumption of Jeans was wrong*, nobody now doubts the certainty of his basic conclusion which is a formal

* An infinite static and uniform state is not a solution of the system of equations (A-15) and (A-16).

statement that when a mass is high enough, that is when

$$M > M_J = \left(\frac{\pi R}{G}\right)^{3/2} T^{3/2} \rho^{-\frac{1}{2}} \qquad (2\text{-}2)$$

where M_J = Jeans mass, self gravitation dominates over the thermal pressure. In the context of the consistent solutions of the motion equation the Jeans problem has been reworked by Bonnor (1957) in his classical paper. Chandrasekhar (1951) generalized Jeans' work to an infinite turbulent medium and Sasao (1971) went further in the same way to an isothermal contracting gas sphere. A formal treatment of the Jeans instability has been given by Chandrasekhar (1961) and a less formal one by Mestel (1965). Recently a further generalization of Jeans' criterion introducing the energy balance condition has been made by Kegel and Traving (1976). But although Jeans' criterion may play the main role in determining the initial mass which may start to collapse, Disney et al. (1969) have showed that such a criterion may be irrelevant for fragmentation, at least at scales of galactic prestellar clouds, where this process is only determined by the strong coupling between the dynamics of collapse and atomic properties.

A theory of star formation was put forward by von Weizsäcker (1951) with the aim of explaining in a unified manner the formation of galaxies, stars, planets and satellites where the turbulence would provide the necessary hierarchy of density inhomogeneities on which Jeans' criterion would operate. According to von Weizsäcker, a cloud of dimensions L and characteristic turbulent velocity v evolves towards a flat non-uniform rotating disk in a time scale

$$t = \alpha \frac{L}{v} \qquad (2\text{-}3)$$

where $\alpha \approx 5$. Angular momentum prevents contraction of the body as a whole, resulting in a contraction of part of the body towards the centre. The gravitational energy set free by this contraction prevents the collapse of the rest of the external mass. As a result, a slowly rotating spheroidal mass develops in the centre which von Weizsäcker identified with an early stage of evolution of an elliptical galaxy. The remaining disk acquires enough angular momentum to escape.

In the context of this theory, the part concerning the star formation problem was directed towards the explanation of Baade's (1944) two stellar populations of the Galaxy. The oldest stars (population II) would have condensed before the cloud had contracted appreciably and when the turbulence was great. Therefore, these stars would form spherical systems (globular clusters) and would present in general the largest peculiar motions. The youngest stars (population I) would have formed after the decay of the initial turbulence or in its last phase when the cloud was a flat disk so they would move in nearly circular orbits in the galactic plane. Because the timescale for the formation of a cloud of stellar mass is

$$t_c \approx \ell^{\frac{2}{3}} \approx 5 \times 10^6 \text{ years} \qquad (2\text{-}4)^*$$

ℓ being the corresponding scale of turbulent elements, von Weizsäcker is forced to assume, ad hoc, that no formation of stars is possible today because the presence of stars inhibits the formation of new stars. In addition to this particular point, the main criticism to the

* This order of magnitude is obtained by applying the Kolmogorov spectral law.

von Weizsäcker theory, according to Mestel (1965) is that supersonic turbulence has to be invoked and this is unlikely because of the strong dissipation of energy in shocks. However, although turbulence by itself is unable to induce the star formation process as von Weizsäcker suggested, subsonic turbulence, which is likely to be present in prestellar clouds, Roberts (1969), is probably the most efficient mechanism to generate inhomogeneities which, assisted by another mechanism to amplify these inhomogeneities may induce fragmentation, at least at scales of galactic prestellar clouds. The most natural of such mechanisms is molecule formation, Oppenheimer and Dalgarno (1975), Reddish (1978). Turbulence as an elemental process in the formation of density inhomogeneities is considered in appendix B.

Hoyle (1953) following the same general line as von Weizsäcker proposed that "gravitational" rather than hydrodynamical turbulence is the mechanism by which the following observational data are explained: (a) Galaxies tend to occur in clusters, (b) The masses of galaxies are in the range $3 \times 10^9 M_\odot - 3 \times 10^{11} M_\odot$ with a tendency to fall into two groups at the ends of this range. (c) The typical mass of type II stars is $\sim 1 M_\odot$. (d) The ages of these stars are the same as the age of the galaxy.

Whilst, in the von Weizsäcker theory, fragmentation in general would be a direct consequence of the non-steady regime caused by turbulence which is established where the Reynolds number $\tilde{R} > \tilde{R}_{cri}$, in Hoyle's scheme, fragmentation would be a consequence of the non-steady regime established where $M > M_J$. It seems that from the strong

analogy, Hoyle called his theory "gravitational turbulence".

The core of the physical argument invoked by Hoyle is as follows: when $M > M_J$, i.e. $t_{ff} < t_e$, see appendix A, the cloud has to contract as a whole due to the action of its own gravity. When the contraction proceeds and if $t_c < t_{ff}$, i.e., the cooling efficiency is enough that $M_J \propto T^{3/2} \rho^{-1/2}$ decreases, the cloud can break up and a fragmentation process can continue as long as M_J continues decreasing. The process must stop when the opacity, for the coolant radiation, becomes so high that $t_c \gtrsim t_{ff}$; then further increases in density become adiabatic, i.e. $T \propto \rho$, $M_J \propto \rho^{1/2}$ and the Jeans mass increases.

Hoyle establishes a hierarchical structure starting with a primordial spherical condensation of hydrogen of density $\sim 10^{-27}$ g cm^{-3}, mass $> 1.4 \times 10^{10}$ $M_\odot$ and temperature $\sim 1.5 \times 10^4$ ^oK, which contracts by a factor $k^{2/3}$ and divides into k equal masses. Each fragment undergoes the same process and it is repeated until the opaque stage is reached. The fragments of the first generations would be identified with galaxies and fragments of the n^{th} generation ($n \approx 13$) with type II stars, which would have a corresponding mass $M \approx M_o/k^n \approx 1.5$ $M_\odot$, if $M_o \approx 3.6 \times 10^9$ $M_\odot$ and $k \approx 5$. If further fragmentation occurs masses about 0.3 $M_\odot$ are easy to obtain. However, according to Hoyle "a second and radically different case arises, if dust has been produced in the condensing gas. Dust allows molecules to be formed, and molecules are able to radiate at low temperatures, in contrast to hydrogen, which cannot radiate, once the electron and proton recombines to form atomic hydrogen ...".

In the context of Hoyle's scheme, according to Hunter (1962, 1964), fragmentation could result as a consequence of the amplification of non-uniformities, present at the onset of the contraction, due to the dynamics of the collapse. Such results have been severely criticised by Layzer (1963a,b, 1964).

Assuming hierarchical fragmentation, the problem of the last fragmentation and minimum mass of fragments has been studied by Smith and Wright (1975), Suchkov and Shchekinov(1976), Low and Lynden-Bell (1976), Rees (1976) and Smith (1977). In particular, according to Low and Lynden-Bell, the minimum mass would be $7 \times 10^{-3}\ M_{\odot}$ as determined by opacity or $10^{-3}\ M_{\odot}$ if fragmentation occurs at the hydrogen ionization stage.

Recent numerical calculations, Larson (1977, 1978), Tohline (1978, 1979) have questioned such a hierarchical scheme. In particular, according to Larson (1977), the bulk of fragmentation would have to occur as a one shot process and during the initial collapse of the cloud. This form of fragmentation would offer the additional advantage of minimising the Layzer (1963a) objection to fragments coalescence.

Because the fragmentation process involves an effective separation of the collapsing fragments, one can see that any process capable of instigating amplification of density contrast, at early stages of the cloud contraction, has to be the key in determining the main characteristic of the whole process, in particular, the resulting mass function distribution. Jeans' criterion only provides a necessary but not sufficient condition, to be fulfilled by the cloud as a whole and by the fragments themselves, to induce fragmentation

in any prestellar cloud. Fragmentation, for instance, is impossible in an ideal initially uniform cloud although the condition $M > M_J$ is fulfilled, Disney et al. (1969).

Ambartsumian (1955, 1960) put forward the idea that the origin of stars, gas and dust is closely related to the nuclei activity of galaxies. This theory has still to be developed and it constitutes a completely different point of departure from the conventional one.

Another star formation theory has been proposed and developed by Layzer (1954, 1956, 1963a,b, 1964) in which he starts by distinguishing between fragmentation and clustering. The first process, according to him, is related to local and the second one, to global properties of the system. He assumes that an isotropic and homogeneous cosmic distribution of mass is similar to a uniform imperfect gas. In this, if an adiabatic expansion takes place, formation of liquid droplets arises, and the same would occur on a large scale, in the gravitating gas.

The main difficulty arising in the Layzer model is the explanation of the star formation process at scales of galactic clouds without appealing to hypothesis ad hoc and without invoking other mechanisms capable of acting at these scales. Layzer put forward the idea that the birth of O stars "would initiate a chain reaction triggering the gravitational collapse of all surviving prestars within a certain radius"and therefore, according to him, Baade's view that "star formation is a contagious disease" would receive a natural explanation. This idea has been developed recently by Elmegren and Lada (1977).

McCrea (1960) proposed a random accretion theory principally with the aim of linking the formation of the solar system with the star formation problem. He suggested that once the original cloud has collapsed to the dimensions of the solar system, it can be represented by a set of non-interacting "condensations" or "floccules" composed mainly of molecular hydrogen with temperature about $50^{o}K$ velocities of 1 Km/s and mean paths of the same order as the size of the present solar system. For successive collisions, some floccules can reach sufficient mass and they become gravitationally bound. Although in this theory there is some difficulty with the stability of the "floccules", it predicts remarkably well the value of the angular momentum of the Sun which would be 7×10^{48} g $cm^2 s^{-1}$ differing only from the accepted value (2×10^{48} g $cm^2 s^{-1}$) by a factor 3.5.

Grzedzielski (1966), following the McCrea line, has developed a theory in which instead of floccules, shockwaves would be generated by large velocity differences supposed to be present initially. His two basic assumptions are: a) The typical scale of chaotic motions is large, corresponding to velocity cells with masses of the order of $10^9 M_\odot$. b) The kinetic energy of these motions is comparable to the gravitational potential energy of the pregalaxy. From these hypotheses he concludes that the pregalaxy may fragment into smaller objects of the order of 10^8 $M_\odot$ and if heavy elements are present within these subcondensations, a further stage of fragmentation would be possible, giving rise to masses of the same order as those of globular clusters.

Recently Woolfson (1979), following the line traced by McCrea

and Grzedzielski, but invoking the turbulence explicitly, has attempted to exlain the star formation process in galactic clusters. He represents the turbulent elements as gas spheres each of mass M_J(?) and moving at the same speed but in random direction. With these assumptions, he removes the stability problems of McCrea's floccules and the inherent difficulties of the fragmentation process. Although the model offers some interesting attractions, it seems unable, at least in its present status, to fit the observed mass function distribution.

Some authors have treated the fragmentation problem specifically as a random process. Auluck and Kothari (1954, 1965) assumed a distribution of the form

$$N(V) \sim N_o\left(\frac{V}{V_o}\right) \exp\left[-3\left(\frac{V}{V_o}\right)^{\frac{1}{3}}\right] \qquad (2\text{-}5)$$

where N(V) is the number of fragments with volume equal to or greater than V, N_o is the total number of fragments and V_o the average volume of a fragment. In the same way Kruszewski (1961) fits an expression for the initial mass spectrum obtained by Limber (1960) in a mass range from 0.1 $M_\odot$ to 10^2 $M_\odot$.

Larson (1973) studied the fragmentation problem as a temporal random process. Although he found an approximated gaussian function for the stellar mass spectrum, his results (as he himself pointed out) do not provide a solution to the problem of the stellar mass spectrum.

One can see that the random approach is rather an elegant way of hiding the physical mechanisms which, although they can be quite complex, do determine spatially and temporally the behaviour of any actual cloud.

An attractive but not well explored theory that fulfils Larson's (1977, 1978) requirements, and predicts remarkably well the Salpeter (1955) initial mass function and other observed properties of the star formation process, has been outlined by Reddish (1975, 1978). In it, the formation of the hydrogen molecule plays a crucial role as the initial instigator of the fragmentation process.

Speaking in very general terms, according to Reddish, spatial density fluctuations of the dust component lead to spatial fluctuations of the radiation field (the main source of this field is the mean star light radiation field) which produce spatial fluctuations of the dust temperature T_d. Because the rate of H_2 formation depends critically on T_d, Solomon and Wickramasinghe (1969), hereafter SW (1969), Lee (1972, 1975), regions appear where the rate of molecule formation is faster and others where this process is slower, or does not occur at all. This would produce instabilities with length scales of the order of one unit of optical depth in visual extinction by grains and in a time shorter than one free-fall time.

Because of the connection between some works on H_2 and CO formation and the basic ideas of Reddish a short review of these will be given, to conclude this section.

With the implicit assumption that $T_d < T_{cri}$ through the whole cloud, Hollenback et al. (1971) have calculated the number density of H_2 as function of the mean optical thickness τ_o and the position into the cloud for static clouds in chemical equilibrium.

The thermo-dynamical problem of a reacting hydrogen gas, in particular, the stability of the chemical equilibrium has been worked out by Yoneyama (1973) and Giaretta (1977), following standard methods of marginal stability, Chandrasekhar (1961) and with the assumption that $T_d < T_{cri}$ through the whole cloud and therefore where T_d does not play a role at all in the control of the rate of H_2 formation.

Although Reddish (1978) appealed to an early paper of Schatzman (1958) who proposed a kind of instability related to the change of the number of particles in an isothermal gas as a result of recombination, the two problems are different.

Schatzman considered a slab of ionized hydrogen with radiation flux incident on both sides and found the marginal states for such a slab of gas. He concluded that there appears to be a collapse of the slab (the hydrogen would recombine entirely and it would form a cool HI cloud) for thickness $\ell > \ell_{cri}$. However Giaretta (1977) has proved that there was a mistake in the above paper and no instability really takes place, at least under the particular conditions assumed there.

In an early paper, Yoneyama (1973), carried out a generalisation of the work of Field (1965), introducing the chemical kinetic equation in addition to the three basic equations of Field. He found that a new type of instability "the thermo-chemical" one, could appear in gases where chemical reactions occur. In particular he considered the hydrogen recombination on grains at high gas temperatures $10^3 \leq T \leq 10^4$ ^oK and the case where hydrogen molecules accreted on grains.

Part of Giaretta's work is in essence a further generalisation of Yoneyama's but he introduces a simplified radiative transfer equation to take into account the coupling gas-radiation field via absorption effects only. His analysis is made in a one dimensional infinite medium. Physically, Giaretta looked for the conditions under which infinitesimal perturbations on the, initially assumed, equilibrium state could grow at a rate faster than that of gravitational perturbations. He assumed that the H_2 formation is controlled by the gas parameters which would control the UV field too.

As will be seen in the next section, the situation under consideration in this study is different from that considered by the above authors. In particular, the dust temperature is the critical parameter in determining the rate at which H_2 can form on dust grains.

Several authors have studied other molecules, in particular CO, as possible generators of thermo-chemical instabilities, Glassgold and Langer (1976), Oppenheimer (1977), Sabano and Kannari (1978). However, according to the most accepted scheme for the chemical evolution of interstellar clouds, the CO production is conditioned to the presence of H_2 in appreciable amounts, Oppenheimer and Dalgarno (1975). In particular CO instabilities require an H_2 concentration of 50%, Sabano and Kannari (1978). According to de Jong (1977), such CO instabilities disappear if the quenching of the CO cooling by radiation trapping is allowed for.

3. THE PROBLEM

The starting point of Reddish's scenario is a cloud, initially of pure atomic hydrogen and dust particles, at the verge of gravitational contraction, in a turbulent (subsonic) state which provides the mechanism generator of density fluctuations*. The mean diffuse galactic radiation field is incident on the boundary surface of the cloud and the 2.7 ^{o}K background radiation field is also present. Initially the particle number density is probably $n \gtrsim 10^2$ cm^{-3} and the gas temperature $T \approx 10^2$ K.

Strictly speaking, to follow the exact evolution of the above dusty cloud one would have to solve in a self-consistent manner the equations of gas dynamics (dusty gas dynamics) complicated by the radiative transfer equation taking into account the interaction of the radiation field with dust and gas (Appendix A). In addition to the inherent difficulty caused by a non-steady regimen, because of both the contraction and turbulence, the presence of chemical reactions completes the set of difficulties, because unfortunately with the problem enunciated in the above form there is no way to separate the chemical problem from the gas dynamical one. Fortunately, some assumptions can be introduced without losing the basic ingredients and some insight into the whole problem can be obtained with the help of schematic solutions, as will be indicated as follows.

* This seems to be the state in which HI clouds are left by the compression of the stationary spiral density wave of the galaxy, Roberts (1969), Clayton (1978).

The rate of hydrogen recombination on the grain surface is given by SW (1969), Spitzer (1978)

$$\frac{dn_{H_2}}{dt} = \gamma < \tilde{\sigma}_d > < v_H > n_d \, n_H \qquad (3\text{-}1)$$

where n_{H_2}, n_H and n_d are the number density per cm^3 of H_2 formed, hydrogen atoms and dust particles respectively, $< \tilde{\sigma}_d >$ is the mean geometrical cross section of a single grain, $< v_H >$ is the mean velocity of hydrogen atoms and γ the total recombination efficiency which depends on the sticking probability and the recombination efficiency, Hollenback and Salpeter (1971) and probably on the surface contamination with H_2, Marenco et al. (1972). But in the range of interest $T \approx 10^2$ K and $n \gtrsim 10^2$, SW (1969) propose the following schematical representation

$$\gamma = \begin{cases} 0.5 & \text{if } T_d < T_{cri} \\ 0.0 & \text{if } T_d > T_{cri} \end{cases} \qquad (3\text{-}2)$$

In a less schematic model, however, $\left|\frac{\delta\gamma}{\delta T}\right|_{T_{cri}} \neq \infty$ and the amplitude of the fluctuation around T_{cri}, $\Delta T/T_{cri}$, required to produce sensible changes in the rate of H_2 formation has to leave a non-zero width which can be estimated with the help of the relations given by Reddish (1978) but corrected by the fact that when the length of time which an adsorbed atom spends on a grain, τ, is shorter or of the order of the interval between successive adsorptions of atoms on a grain t, the recombination coefficient γ is proportional to the probability that at least <u>two atoms</u> meet on a grain at the same

time i.e.

$$\gamma \sim \left(\frac{\tau}{t}\right)^2 \sim \exp(2E/kT_d) \qquad (3\text{-}3)$$

E being the adsorption energy of the atoms on the surface.

From equation (3-3) it follows that a fractional change in the recombination coefficient, due to a change in T_d where $T_d \approx T_{cri}$, would be given by

$$\left[\frac{\Delta\gamma}{\gamma(T_{cri})}\right] = -\frac{2E}{kT_{cri}}\left(\frac{\Delta T_d}{T_{cri}}\right) \qquad (3\text{-}4)$$

Graphite, for instance, according to the experimental results of Lee (1975) has $T_{cri} = 25^{o}K$ and $E/k = 785$, therefore a change in temperature of 1.6% around T_{cri} would produce a change in the rate of H_2 formation of 99%. All the substrata studied experimentally by Lee present similar behaviour, in particular the quantity $(2E/k\,T_{cri})^{-1}$ is practically insensitive to the particular kind of substrata as can be seen from the experimental values given by this author:

substrate	$(2E/k\,T_{cri})^{-1}$
H_2O	0.015942
CO_2	0.016406
Graphite	0.015924

Marenco et al. (1972) have found experimentally that the energy given to the cold surface by the hydrogen atoms arriving to it is a function of the surface contamination with H_2. For reasons of

saturation, they excluded the chemisorption process as a possible explanation. Then, either of the following possibilities, to explain the above result, remain: 1) The presence of H_2 on the surface influences the recombination rate. 2) The presence of H_2 is only useful to obtain an increased accommodation at the surface temperature of the formed excited H_2 molecules.

Reddish (1975, 1978) assumed that the above first interpretation is the correct one and modified the recombination rate (3-1) in the form

$$\frac{dn_{H_2}}{dt} = \gamma_o \langle \tilde{\sigma}_d \rangle \langle v_H \rangle \, n_d \, n_H \, n_{H_2} \qquad (3\text{-}5)$$

with $(\gamma_o n_{H_2})_{max} = 1.0$, where γ_o would contain the dependence of the recombination coefficient on the sticking probability (depending on the gas parameters) and on the recombination efficiency (which depends sensibly on T_d). However, to keep (3-5) consistent, a redefinition of γ_o would be required and from the pure dimensional standpoint γ_o would have to be a probability per unit density of particles. However, the value $\gamma_o = 1$ was assumed by Reddish, which indeed invalidated (3-5).

The above error indeed (contrary to the Silk (1978) criticism) is not crucial for Reddish's scenario of fragmentation, because even with the classical equation, Spitzer (1978), equation (3-1), the H_2 formation could instigate density amplification in a contracting cloud, as can be seen throughout the present work.

On the other hand, Silk (1978), took the second possibility to

explain the Marenco et al. results, however one sees that he is in no better position than Reddish. More experimental work would have to be done or a very careful theoretical quanto-mechanic treatment would be required to decide in this respect.

In a first approximation, if the rate of hydrogen molecule formation is enhanced by the contamination of the surface with H_2, assuming that the degree of contamination is simply proportional to the H_2 concentration in the gas, the recombination coefficient would be of the form

$$\gamma = S(E_{gas})\ \gamma'(T_d)\ \gamma''(n_{H_2}) \qquad (3\text{-}6$$

where S is the sticking probability (fraction of atoms incident on the surface which becomes adsorbed), γ' is the recombination coefficient(fraction of atoms that recombine instead of evaporating) and γ'' a coefficient proportional to n_{H_2}. This form for the total recombination coefficient, would give a stronger sharpness to the boundaries separating regions where $T_d < T_{cri}$ and where H_2 formation can proceed easily, from those where $T_d > T_{cri}$ and the gas remains mainly atomic, and corrections to (3-4) to take into account such effect would give a steeper dependence near to T_{cri}.

The H_2 molecules can be dissociated by UV photons of the Lyman and Werner bands, Stecher and Williams (1967), Spitzer (1978). The disassociation rate can be expressed in the form

$$\frac{dn'_{H_2}}{dt} = Bn_{H_2} \qquad (3\text{-}7)$$

where n'_{H_2} is the number density of molecules dissociated and B is a function depending on the local value of the UV field in wavelength range $912 \leq \lambda \leq 1108$ Å and on internal parameters of the H_2 molecule; for a free H_2 molecule exposed to the mean galactic UV field, $B \approx 10^{-10} sec^{-1}$, Hollenbach et al. (1971).

As shown by SW (1969), in clouds with $T \approx 10^2$, and $n > 10^2$ cm^{-3}, with reaction and destruction rates given by equations (3-1) and (3-7) respectively, wherever $T_d < T_{cri}$, chemical equilibrium would be reached for $n_{H_2} \leq 8.10^{-3} cm^{-3}$, assuming a normal dust/gas ratio of $n_d/n = 10^{-12}$, i.e. "the dissociating radiation is completely ineffective and may be neglected except for a thin shell, Solomon (1969). Therefore, in clouds under consideration, the only factor governing the extent of recombination is the critical grain temperature." Recent and more detailed calculations, Federman et al. (1979) confirm this conclusion. Therefore this first simplification emerges.

The dust temperature at any point in a cloud is determined by the local energy balance equation

$$\int_o^\infty n_d(\underline{r}) \left[\left\langle \tilde{\sigma}_d \, Q_{abs} \right\rangle_\nu B_\nu (T_d(\underline{r})) - \left\langle \tilde{\sigma}_d \, Q_{abs} \right\rangle_\nu J_\nu (\underline{r}) \right] d\nu = \frac{1}{4\pi} E(\underline{r}) \qquad (3\text{-}8)$$

where $\left\langle \tilde{\sigma}_d \, Q_{abs} \right\rangle$ is a mean absorption cross section per grain at frequency ν, $B_\nu(T_d(\underline{r}))$ the Planck function, $J_\nu(\underline{r})$ the local mean intensity of the radiation field at frequency ν and $E(\underline{r})$ represents the net amount of energy lost by the non-radiative processes: gas-dust collision and H_2 formation. At $T \lesssim 150$ K and $n < 10^6 cm^{-3}$ the transfer of energy by gas-dust collision is negligible in comparison with the radiation heating, Hayashi and Nakano (1965), and for

$n \lesssim 10^4\ cm^{-3}$ the energy by H_2 formation imput can also be neglected, if the local radiation field can maintain the dust temperature above about 9^oK, SW (1969). Indeed, this limit was obtained by these authors assuming that all the binding energy can be absorbed by the grain. However, according to Hunter and Watson (1978), H_2 probably recombines into high rotational states and new molecules return to the gas in rotational states $J \gtrsim 7$. Therefore, the above temperature would represent an upper limit and equation (3-8) becomes

$$\int_o^\infty \left\langle \bar{\sigma}_d Q_{abs} \right\rangle_\nu \; J_\nu (\underline{r})\, d\nu = \int_o^\infty \left\langle \bar{\sigma}_d Q_{abs} \right\rangle_\nu \; B_\nu (T_d(\underline{r}))\, d\nu \qquad (3\text{-}9)$$

i.e. the common radiative heating equation. This is the second simplification.

From the above discussion one may see that at least in the range $T \lesssim 150\,K$, $T_d \approx 20^oK$, $n \lesssim 10^4\ cm^{-3}$, the H_2 formation is controlled by the dust temperature which is determined at each point in any dusty cloud by the radiative transport controlled mainly by the dust optics, van de Hulst (1946), Werner and Salpeter (1969), hereafter WS (1969), Leung (1975), Aiello et al. (1977). Because a random density distribution is probably a common characteristic in real interstellar clouds, Zuckerman and Palmer (1974), Zuckerman and Evans (1974), "tongues" of radiation penetrate into the clouds producing an irregular T_d distribution. This means that patches in the cloud become cold enough ($T_d < T_{cri}$) and H_2 formation starts there first. One must recognise, just at this stage, that one is dealing with a multi - dimensional radiative heating problem.

Despite the intrinsic complexity of the above problem, one can say with confidence that equation (3-9) remains valid because the radiative equilibrium between the dust and the radiation field is fulfilled as can be seen from the following simple argument.

The timescale to re-establish radiative equilibrium between dust and radiation field is given in a first approximation by the timescale for diffusion of the photons responsible for the heating of the grains, through the cloud, i.e.

$$t_d \approx \tau_o \frac{R}{c} \tag{3-10}$$

where τ_o is the mean optical depth to the centre of the cloud of dimensions R, measured at wavelengths of importance for the heating of the dust, and c the light speed.

An appropriate upper limit to the above diffusion time would be given by the diffusion of the visual photons. In this case, equation (3-10) becomes

$$t_d \approx \frac{\tau_o^2}{n_d \left\langle Q_{abs} \tilde{\sigma}_d \right\rangle_o c} = \left[\left(\frac{n_d}{n} \right) \left\langle Q_{ext} \tilde{\sigma}_d \right\rangle_o c \right]^{-1} \tau_o^2 \, n^{-1} \tag{3-11}$$

If one compares this timescale with the other three timescales of interest in the present study, i.e., the free-fall time t_{ff}, the H_2 formation time t_{H_2}, equations (A-21) and (A-36) respectively, and the timescale for turbulence at the scales corresponding to visual optical thickness of $\pi/2$*, t_t, given by equation (B-23), one

* The importance of this scale will be shown in Section 5.

obtains the following relations

$$\frac{t_d}{t_{ff}} = 2.0 \times 10^{-26} \left[\frac{n_d}{n} \langle Q_{ext} \tilde{\sigma}_d \rangle \right]^{-1} \tau_o^{\,2}\, n^{-\frac{1}{2}} \qquad (3\text{-}12)$$

$$\frac{t_d}{t_{H_2}} = 2.6 \times 10^{-7} \left\langle Q_{ext} \right\rangle^{-1} T^{\frac{1}{2}}\, \tau_o^{\,2} \qquad (3\text{-}13)$$

$$\frac{t_d}{t_{t_1}} = 1.9 \times 10^{-7}\, T^{\frac{1}{2}}\, \tau_o^{\,6/3} \qquad (3\text{-}14)$$

and assuming the mean values $\frac{n_d}{n} \approx 10^{-12}$, $\langle Q_{ext} \rangle \approx 2$, $\tilde{\sigma}_d = 7 \times 10^{-10} \mathrm{cm}^2$ one obtains

$$\frac{t_d}{t_{ff}} \approx 1 \times 10^{-5}\, \tau_o^{\,2}\, n^{-\frac{1}{2}} \qquad (3\text{-}15)$$

$$\frac{t_d}{t_{H_2}} \approx 1 \times 10^{-7}\, T^{\frac{1}{2}} \tau_o^{\,2} \qquad (3\text{-}16)$$

$$\frac{t_d}{t_{t_1}} \approx 2 \times 10^{-7}\, T^{\frac{1}{2}}\, \tau_o^{\,5/3} \qquad (3\text{-}17)$$

For the situation at hand $\tau_o \approx 5$, $n \approx 10^3\ \mathrm{cm}^3$ and $T \approx 10^2\ \mathrm{K}$

$$\frac{t_d}{t_{ff}} \approx 8 \times 10^{-4};\ \frac{t_d}{t_{H_2}} \approx 3 \times 10^{-5} \text{ and } \frac{t_d}{t_{t_1}} \approx 3 \times 10^{-5} \qquad (3\text{-}18)$$

and therefore the timescale to re-establish radiative equilibrium is very short compared with any other time of interest and static models give a good representation of the spatial distribution of the dust temperature. Note that if $\tau_o \lesssim 1$, the diffusion timescale given by equation (3-10) becomes simply $t_d \simeq R/c$.

With the two basic simplifications introduced in this section i.e., the H_2 production is totally controlled by T_{cri} and radiative equilibrium between dust and radiation fields holds, the problems to tackle are: (a) To find the effective scale length at which the dust temperature T_d fluctuates around T_{cri}. (b) To show that regions $T_d < T_{cri}$ (and where H_2 starts) could become effectively denser and cooler with respect to regions where $T_d > T_{cri}$ and in a time shorter than one free-fall.

The above two crucial problems in the Reddish scenario for fragmentation are the aim of this thesis. They will be studied in first (and schematical) approximation in the next sections.

CHAPTER II

4. THE RADIATIVE HEATING PROBLEM IN INHOMOGENEOUS MEDIA

In this section the basic equations of the radiative heating problem, valid for the general case of a non-uniform 3-D medium will be adapted for our particular problem. Although the range of applicability of such equations is general, limited only by the restrictions explicitly enunciated, this discussion will be made with the interstellar dust clouds in mind.

In this study the main interest is focussed on the early stages of evolution of prestellar clouds when the transition of H_1 to H_2 has to occur and therefore no internal sources of radiative energy are expected to be present. Only the diluted stellar mean radiation field, as that compiled by Watson (1976) is considered incident on the free surface of the interstellar dust clouds. In addition, strictly speaking, any interstellar cloud has to be considered embedded in the $2.7^{o}K$ background field. The main role of this field is to prevent the dust temperature falling below $2.7^{o}K$ at any depth, WS (1969), Greenberg (1971).

The radiative transfer equation, (appendix B), can be written in the form

$$\frac{dI_\nu(s,\underline{\Omega})}{ds} = -\kappa_\nu(s)\, I_\nu(s,\underline{\Omega}) + j_\nu(s,\underline{\Omega}) \qquad (4\text{-}1)$$

Formal integration of this equation yields

$$I_\nu(s,\underline{\Omega}) = I_\nu(o,\underline{\Omega})\, \exp\left(-\tau_\nu(o,s)\right) + \int_o^s j_\nu(s,\underline{\Omega})\, \exp\left(-\tau(s,s')\right) d\, s' \qquad (4\text{-}2)$$

where $\tau_\nu(o,s)$ is the optical depth from the boundary to the point s measured along the direction $\underline{\Omega}$, i.e.

$$\tau_\nu(o,s) = \int_o^s K_\nu(s')\, d\, s' \qquad (4\text{-}3)$$

and $\tau_\nu(s,s')$ is the optical thickness between the points s and s' along the direction $\underline{\Omega}$, i.e.

$$\tau_\nu(s,s') = \int_s^{s'} K_\nu(s'')\, d\, s'' \qquad (4\text{-}4)$$

(Chandrasekhar 1960).

From equation (4-2) it follows readily that the radiation field at any point in a cloud can be represented by the sum of two components: (a) The reduced incident radiation field, i.e. the incident field reaching any point s in the cloud without having suffered any absorption or scattering - the first term on the right-hand side of equation (4-2). This field will be called simply the attenuated field. (b) The diffuse radiation field, i.e., the field at any point s in the cloud originated by scattering and emission processes - the second term on the right-hand side of equation (4-2).

a. Attentuated Field

The mean attentuated radiation field at any point $\underline{r}$ in the cloud is

$$J_\nu^a(\underline{r}) = \frac{1}{4\pi} \int_{4\pi} I_\nu^a(\underline{r}, \underline{\Omega})\, d\Omega \qquad (4\text{-}5)$$

where $I_\nu^a(\underline{r}, \underline{\Omega})$ is the intensity of the attentuated field in the

particular direction $\underline{\Omega}$, i.e.

$$I^a_\nu(\underline{r},\underline{\Omega}) = I^o_\nu(\underline{r}_o,\underline{\Omega}) \exp(-\tau_\nu(o,s)) \tag{4-6}$$

$I^o_\nu(\underline{r}_o,\underline{\Omega})$ being the intensity at the boundary and $\tau_\nu(o,s)$ the optical depth from the boundary to the point $\underline{r}$.

It is clear that the explicit value of $J^a_\nu(\underline{r})$ depends on the type of incidence and the geometry involved.

For plane parallel incidence with direction μ_o and ϕ_o, the inwards intensity $I^o_\nu(-\mu,\phi)$ becomes

$$I^o_\nu(-\mu,\phi) = \pi F_{o\nu}\, \delta(\mu-\mu_o)\, \delta(\phi-\phi_o) \tag{4-7}$$

where μ is the cosine of the angle between the outwards normal to the surface and the $\underline{\Omega}$ direction, ϕ is the azimuth angle and $\pi F_{o\nu}$ the flux crossing a unit surface normal to the direction of incidence μ_o, ϕ_o, and the δ's are Dirac delta functions, Chandrasekhar (1960).

For plane geometry, from equations (4-5) and (4-7) one obtains

$$J^a_\nu(\underline{r}) = \frac{F_{o\nu}}{4} \exp(-\tau_{o\nu}(o,s;\mu_o,\phi_o)) \tag{4-8}$$

b. Diffuse Field

According to equation (4-2) the total intensity $I_\nu(\underline{r},\underline{\Omega})$ can be written in the form

$$I_\nu(\underline{r},\underline{\Omega}) = I_\nu{}^d(\underline{r},\underline{\Omega}) + I_\nu{}^a(\underline{r},\underline{\Omega}) \tag{4-9}$$

where the upper index d denotes "diffuse".

Substituting equation (4-9) in the radiative transfer equation (4-1) one obtains

$$\frac{d}{ds}\,(I_\nu^{\,d} + I_\nu^{\,a}) \;=\; -\kappa_\nu(I_\nu^{\,d} + I_\nu^{\,a}) + j_\nu \tag{4-10}$$

If isotropic scattering is assumed, according to equation (A-54) the emission coefficient is

$$j_\nu \;=\; \kappa_\nu S_\nu \;=\; \alpha_\nu B_\nu + \sigma_\nu(J_\nu^{\,d} + J_\nu^{\,a}) \tag{4-11}$$

With the help of equations (4-3) and (4-4), from equation (4-10) one obtains the radiative transfer equation for the diffuse field i.e.

$$\frac{dI_\nu^{\,d}}{ds} \;=\; -\kappa_\nu I_\nu^{\,d} + \sigma_\nu J_\nu^{\,d} + \kappa_\nu \tilde{S}_\nu \tag{4-12}$$

where the function $\tilde{S}$ is defined by

$$\kappa_\nu \tilde{S}_\nu \;=\; \alpha_\nu B_\nu + \sigma_\nu J_\nu^{\,a} \tag{4-13}$$

Hereafter the upper index d will be dropped, i.e. the radiative transfer equation for the diffuse field will be simply

$$\frac{dI_\nu}{ds} \;=\; -\kappa_\nu I_\nu + \sigma_\nu J_\nu + \kappa_\nu \tilde{S}_\nu \tag{4-14}$$

Using this equation, Giovanelli (1959, 1963) constructed a generalization to the Eddington approximation for inhomogeneous atmospheres.

By writing the general solution of equation (4-14) in the form

$$I \;=\; \sum_{n=o}^{\infty} \{I_n P_m(\mu) + \sum_{m=1}^{n} [a_n^{\,m} \cos(m\phi) + b_n^{\,m} \sin(m\phi)]\; P_n^{\,m}(\mu) \tag{4-15}$$

where $P_m(\mu)$ and $P_n^m(\mu)$ are the Legendre polynomials and Legendre associated functions, I_n, a_n^m and b_n^m coefficients depending on frequency and position but not of directions (μ,ϕ), Giovanelli showed that if only first order effects of μ and ϕ are taken into account, i.e. $I_2 = 0$ and $\frac{\partial a_2^1}{\partial x} = \frac{\partial b_2^1}{\partial y} = 0$, from equations (4-14) and (4-15) the following equation is obtained

$$\underline{\nabla}\left[\frac{1}{\kappa_\nu(\underline{r})}\,\underline{\nabla} J_\nu(\underline{r})\right] = 3\left[\alpha_\nu(\underline{r})\, J_\nu(\underline{r}) - \kappa_\nu(\underline{r})\,\tilde{S}_\nu(\underline{r})\right] \qquad (4\text{-}16)$$

see appendix C.

According to Giovanelli, equation (4-16) leads to results for 3-D non-uniform media of the same degree of validity as those obtained from the Eddington approximation in the 1-D case. Unno and Spiegel (1966) have arrived independently at the same equation (4-16) and they proved formally that their solutions are reasonably accurate over the whole range of optical thickness.

c. Radiative Heating Problem

As shown in Section 3, the dust temperature in interstellar dust clouds is controlled in assence by the radiation field through the heat balance equation (3-9) i.e.

$$\int_o^\infty \langle \tilde{\sigma}_d Q_{abs} \rangle_\nu\, J_\nu(\underline{r})\, d\nu = \int_o^\infty \langle \tilde{\sigma}_d Q_{abs} \rangle_\nu\, B_\nu(T_d(\underline{r}))\, d\nu \qquad (4\text{-}17)$$

The mean radiation field $J(\underline{r})$ at a particular point $\underline{r}$ in any cloud is determined by the radiative transport into the cloud of the incident radiation field on the free surface of the cloud. According to Zimmerman (1964), Krishna Swamy and Wickramasinghe (1968), this

ield is well represented by a black-body radiation field corresponding to a temperature of about $10^4\,^oK$ but diluted by a factor $W = 10^{-14}$*. The exact value depends in general on the exact location in the galaxy and generally speaking, on the type of galaxy and stage of evolution. In this thesis, however, attention is focussed on clouds in our own galaxy.

If the grains were black-bodies and they were located in the free space, equation (4-17) would be simply

$$J = \sigma_o W T_r^4 = \sigma_o T_d^4 \qquad (4\text{-}18)$$

T_r being the dilute radiation field temperature and σ_o the Stefan-Boltzmann constant. If one takes into account the 2.7^oK background radiation, the extra term $\sigma_o (2.7)^4$ has to be added to the mean radiation field J, i.e.

$$W T_r^4 + (2.7)^4 = T_d^4 \qquad (4\text{-}19)$$

The Planckian distribution of the radiation field has its maximum at wavelengths $\lambda_{mr} = \text{const}/T$ and that corresponding to the grain emission at wavelengths λ_{md}. But

$$\lambda_{mr} T_r = \lambda_{md} T_d$$

or (4-20)

$$\frac{\lambda_{mr}}{\lambda_{md}} = \left[1 + \left(\frac{2.7}{W T_r} \right)^4 \right]^{\frac{1}{4}} W^{\frac{1}{4}}$$

* Strictly speaking, this field is a good representation of the field in the vicinity of the Sun. A more sophisticated representation of this field has been discussed by Werner and Salpeter (1969) and Greenberg (1971).

which for the problem of interest would give

$$\frac{\lambda_{mr}}{\lambda_{md}} = 3.5 \times 10^{-4} \qquad (4\text{-}21)$$

This means that the integrals of equation (4-17) involve two different spectral regions, towards the visual in the left-hand side and towards the infrared in the right-hand side. Therefore, it can be split in the form

$$\int_{\nu_1}^{\infty} (\tilde{\sigma}_d Q_{abs})_\nu \, J_\nu(\underline{r}) \, d\nu = \int_{o}^{\nu_2} (\tilde{\sigma}_d Q_{abs}) \, B_\nu(T(\underline{r})) \, d\nu \qquad (4\text{-}22)$$

in a first approximation.

Although it is true that grains are not black-body radiators, this fact does not invalidate equation (4-22) and one can split the ν-range in two parts: the visual s and infrared p. Defining the mean absorption coefficients α_s and α_p for each one of the two regions*, equation (4-22) takes the very simple form

$$\alpha_s J_s = \alpha_p B(T)$$

or (4-23)

$$T^4 = \left(\frac{1}{\sigma_o}\right) \frac{\alpha_s}{\alpha_p} J_s$$

σ_o being the Stefan-Boltzmann constant. Therefore, $T > T_{b-b}$ (black-body temperature) if $\frac{\alpha_s}{\alpha_p} > 1$ and $T < T_{b-b}$ if $\frac{\alpha_s}{\alpha_p} < 1$, i.e. an absorber

* Hereafter the notation used in radiative transfer literature on planetary atmospheres will be employed: sub or upper indices s and p will denote visual and infrared regions respectively.

exposed at the same radiation field J_s, can obtain a higher or lower temperature than that corresponding to a black-body (for which $\frac{\alpha_s}{\alpha_p} = 1$) according to the ratio $\frac{\alpha_s}{\alpha_p}$ is greater or less than 1. Typical grains of the interstellar medium are likely to have large values ($\gtrsim 10^2$) of the ratio $\frac{\alpha_s}{\alpha_p}$, Werner and Salpeter (1969), Greenberg (1971) and Leung (1975).

The temperature of grains in dust clouds can be evaluated in the same manner by considering the cloud to be grey in the visual and infrared regions of the spectrum; but in this case the left-hand side of equation (4-22) also includes the diffuse visual and infrared radiation fields.

Following Wildt (1966) and Stibbs (1971) works, one defines the Greenhouse parameter η by the relation

$$\eta = \frac{\kappa_s}{\kappa_p} \tag{4-24}$$

Because the mean free paths of photons in the visual and infrared are $\sim 1/\kappa_s$ and $\sim 1/\kappa_p$ respectively, the η parameter is a measure of the relative thickness of the medium at either of the two fields: visual and infrared. Therefore, this parameter contains schematically the (other way) very complex dependence on frequency characteristic of the dust (or gas) optics, Andriesse (1977). It will be of particular importance in the forthcoming sections.

It is convenient to define a dimensionless function $\psi(\underline{r})$

containing the spatial dependence of the extinction such that

$$\kappa_i = \left(Q_{ext} \tilde{\sigma}_d \right)_i \bar{n}_d \psi(\underline{r}) ,$$

or (4-25)

$$\kappa_i = \bar{\kappa}_i \psi(\underline{r}) , \quad i = s,p$$

$\bar{\kappa}_i$ being a mean value for the extinction. Similar relations can be given for the absorption and scattering coefficients α_i and σ_i respectively.

d. Visual Field

In the visual region the emission coefficient j_s is the radiation scattered from the attenuated and diffuse radiation fields and the thermal emission, assumed to be zero in this region. Therefore the function $\tilde{S}$ is given by

$$\kappa_s \tilde{S}_s = \frac{\sigma_s}{4\pi} \int_{4\pi} I_s^o (\underline{\Omega}) \exp(-\tau_s(o,s)) \, d\Omega \qquad (4-26)$$

or

$$\tilde{S}_s = \frac{\bar{\omega}}{4\pi} \int_{4\pi} I_s^o(\underline{\Omega}) \exp(-\tau_s(o,s)) \, d\Omega \qquad (4-27)$$

$\bar{\omega}$ being the albedo for single scattering σ_s/κ_s. Therefore, the equation (4-16) becomes

$$\underline{\nabla} \cdot \left[\frac{1}{\kappa_s(r)} \underline{\nabla} J_s(\underline{r}) \right] = 3 \kappa_s(\underline{r}) \left[\lambda J_s(\underline{r}) - \bar{\omega} J_s^a(\underline{r}) \right] \qquad (4-28)$$

where $\lambda = 1 - \bar{\omega}$ is the scattering parameter. This equation in terms of the function $\psi(\underline{r})$ and mean extinction $\bar{\kappa}_s$ becomes

$$\underline{\nabla} \cdot \left[\frac{1}{\psi(\underline{r})} \underline{\nabla} J_s(\underline{r}) \right] = 3\bar{\kappa}_s^2 \psi(\underline{r}) \left[\lambda J_s(\underline{r}) - \bar{\omega} J_s^a(\underline{r}) \right] \qquad (4\text{-}29)$$

For plane geometry and plane parallel incidence with directions $\cos^{-1} \mu_o$, ϕ_o and radiance πF in the visual, from equation (4-8) and (4-29) one obtains

$$\underline{\nabla} \cdot \left[\frac{1}{\psi(\underline{r})} \underline{\nabla} J_s(\underline{r}) \right] = 3\bar{\kappa}_s^2 \psi(\underline{r}) \left[\lambda J_s(\underline{r}) - \bar{\omega} \frac{F}{4} \exp(-\tau_o(s; \mu_o, \phi_o)) \right] \qquad (4\text{-}30)$$

$\tau_o(s; \mu_o, \phi_o)$ being the optical depth of the point $\underline{r}$ along the incident beam.

e. Infrared Field

The emission coefficient in the infrared j_p is the sum of the terms: the thermal radiation absorbed and re-emitted, the visual radiation converted into infrared and the scattered infrared radiation, assumed to be zero, i.e.

$$j_p = \kappa_p \tilde{S}_p = \alpha_p(\underline{r}) J_p(\underline{r}) + \alpha_s(\underline{r}) \left[J_s(\underline{r}) + J_s^a(\underline{r}) \right] \qquad (4\text{-}31)$$

or in terms of the Greenhouse parameter η defined by (4-24), one obtains

$$\tilde{S}_p = J_p(\underline{r}) + \lambda\eta \left[J_s(\underline{r}) + J_s^a(\underline{r}) \right] \qquad (4\text{-}32)$$

Substituting equation (4-32) in (4-16) and with the help of the definitions (4-25) one obtains the radiative transfer equation in the infrared

$$\underline{\nabla} \cdot \left[\frac{1}{\psi(\underline{r})} \underline{\nabla} J_p(\underline{r}) \right] = -3 \lambda \eta^{-1} \bar{\kappa}_s^{\,2} \psi(\underline{r}) \left[J_s(\underline{r}) + J_s^{\,a}(\underline{r}) \right] \tag{4-33}$$

which for plane parallel incidence with angles $\cos^{-1} \mu_o$ and ϕ_o and plane geometry becomes

$$\underline{\nabla} \cdot \left[\frac{1}{\psi(\underline{r})} \underline{\nabla} J_p(\underline{r}) \right] = -3 \lambda \eta^{-1} \bar{\kappa}_s^{\,2} \psi(\underline{r}) \left[J_s(\underline{r}) + \frac{F}{4} \exp(-\tau_o(s;\mu_o,\phi_o)) \right] \tag{4-34}$$

f. Boundary Conditions

The Giovanelli approximation, see appendix C, is a representation of $I_\nu(\underline{r},\underline{\Omega})$ in the form

$$I_\nu(\underline{r},\underline{\Omega}) = J_\nu(\underline{r}) + \underline{I}_1 \cdot \underline{\Omega} + \sum_{n=3}^{\infty} \left[I_n P_n(\mu) + \sum_{m=1}^{n} (a_n^m \cos m\phi + b_n^m \sin m\phi) P_n^m(\mu) \right] \tag{4-35}$$

where

$$\underline{I}_1(r) = \frac{3}{4\pi} \int_{4\pi} I_\nu(\underline{r},\underline{\Omega}) \, \underline{\Omega} \, d\Omega \tag{4-36}$$

which results from direct integration of equation (4-36) with $I_\nu(\underline{r},\underline{\Omega})$ given by (4-35).

For the diffuse field, the boundary condition consistent with

approximation (4-35), according to Wilson (1968) is

$$J_\nu(\underline{r}_o) = \frac{1}{\sqrt{3}} \underline{n}.\underline{I}_1(\underline{r}_o) \tag{4-37}$$

$\underline{r}_o$ denotes any point on the boundary surface and $\underline{n}$ is a unit outward vector.

From equation (4-37) and (C-19) one obtains

$$\underline{n}.\underline{\nabla} J_\nu(\underline{r}_o) = -\sqrt{3}\, \kappa_\nu J_\nu(\underline{r}_o) \tag{4-38}$$

This boundary condition (4-38) with the help of equations (4-25) becomes

$$\underline{n}.\underline{\nabla} J(\underline{r}_o) = -\sqrt{3}\, \bar{\kappa}_s \psi(\underline{r}_o) J_s(\underline{r}_o) \tag{4-39}$$

in the visual, and

$$\underline{n}.\underline{\nabla} J_p(\underline{r}_o) = -\sqrt{3}\, \eta^{-1} \bar{\kappa}_s \psi(\underline{r}_o) J_p(\underline{r}_o) \tag{4-40}$$

in the infrared.

g. Temperature

From equations (4-13), (4-17) and (4-31) it follows that the integrated Planck function is given by

$$B_p(\underline{r}) = J_p(\underline{r}) + \lambda\eta\left[J_s(\underline{r}) + J_s^a(\underline{r})\right] \tag{4-41}$$

and the temperature at any point $\underline{r}$ will be given by

$$T^4(\underline{r}) = \frac{\pi}{\sigma_o} B_p(\underline{r}) \tag{4-42}$$

If one defines the effective temperature of the incident

radiation field by the relation

$$\sigma_o T_o^4 = \pi F \tag{4-43}$$

the temperature at any point of a particular cloud normalized to T_o will be given by

$$\frac{T(\underline{r})}{T_o} = \left(\frac{B_p(\underline{r})}{F} \right)^{\frac{1}{4}}$$

or from equation (4-41)

$$T(\underline{r}) = \{ J_p(\underline{r}) + \lambda\eta \left[J_s(\underline{r}) + J_s^a(\underline{r}) \right] \}^{\frac{1}{4}} \tag{4-44}$$

where the substitutions $T(\underline{r})/T_o \rightarrow T(\underline{r})$ and $J_i/F \rightarrow J_i$ have been made. This notation will be adopted hereafter.

In the particular case of plane geometry and plane parallel incident radiance πF, equation (4-44) becomes

$$T(\underline{r}) = \{ J_p(\underline{r}) + \lambda\eta \left[J_s(\underline{r}) + \tfrac{1}{4} \exp\left(-\tau_o(s; \mu_o, \phi_o)\right) \right] \}^{1/4} \tag{4-45}$$

5. A CLOUD MODEL. ANALYTICAL SOLUTION

The simplest model that one may propose to schematise a non-uniform cloud and gain some insight, by analytical means, into the general behaviour of the radiative field and in particular the dependence between the optical thickness of the inhomogeneities and the temperature fluctuations, is a semi-infinite cloud with a density distribution of the form

$$\psi(x,z) = 1 + a \cos \ell x \qquad (5\text{-}1)$$

where $a < 1$ and $\ell = 2\pi/\lambda_d$ indicates the wavelength number of the density fluctuation. The free surface is the plane $z = 0$, on which a parallel beam of net flux πF normal to itself is incident in some specific direction $\cos^{-1}\mu_o, \phi_o$. Later $\mu_o = 1/\sqrt{3}$ and $\phi_o = \pi/4$ will be taken as two quadrature points to represent the nearly isotropic mean incident galactic field, see Figure 5-1.

One defines two dimensionless variables X and Z and the parameter r as follows

$$X = \ell x, \quad Z = \overline{\kappa}_s z, \quad r = \ell/\overline{\kappa}_s = 2\pi/\lambda_d \, \overline{\kappa}_s \qquad (5\text{-}2)$$

Therefore, X will be measured in units of wavelength λ_d, Z is the mean optical depth which corresponds to the optical depth in the homogeneous case ($a = 0$) or the actual optical depth measured at $X = \pi/2$. The parameter r is a measure of the optical thickness of the fluctuation.

From equation (5-2), it is clear that the following simple

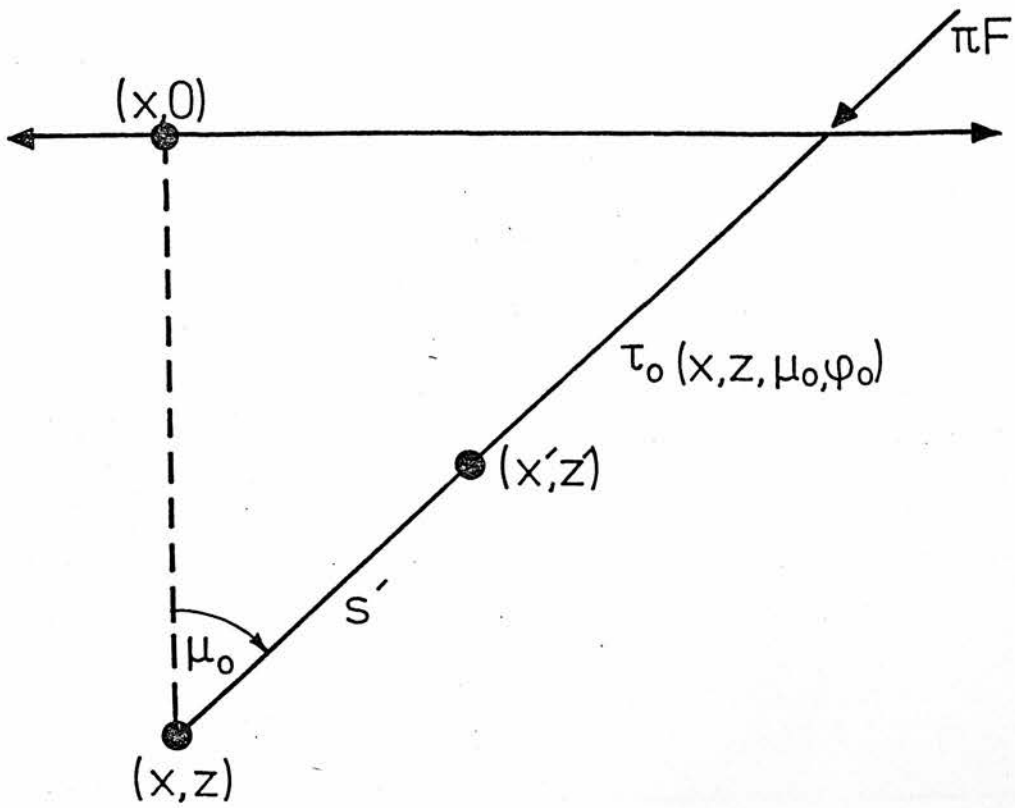

Fig. 5-1 The cross section of an inhomogeneous semi-infinite cloud in the plane of the incident radiation.

relations hold

$$\frac{\partial}{\partial x} = \ell \frac{\partial}{\partial X} , \quad \frac{\partial}{\partial z} = \bar{\kappa}_s \frac{\partial}{\partial Z} \tag{5-3}$$

and therefore

$$\begin{aligned} \underline{\nabla}_{xz} &= \bar{\kappa}_s \ \underline{\nabla}_{XZ} \\ \underline{\nabla}^2_{xz} &= \bar{\kappa}_s^{\,2} \ \underline{\nabla}^2_{XZ} \end{aligned} \tag{5-4}$$

where

$$\underline{\nabla}_{xz} = \left(\frac{\partial}{\partial x} , \frac{\partial}{\partial z} \right)$$

and (5-5)

$$\underline{\nabla}_{XZ} = \left(r \frac{\partial}{\partial X} , \frac{\partial}{\partial Z} \right)$$

With the help of equations (5-1) to (5-5) the basic equations (4-30), (4-34), (4-39) and (4-40) are simplified as follows.

a. Visual Field

With the density distribution (5-1) and in terms of the variables defined above, equation (4-30) becomes

$$(1 + a\cos X) \left(r^2 \frac{\partial^2 J_s}{\partial X^2} + \frac{\partial^2 J_s}{\partial Z^2} \right) + r^2 a \sin X \frac{\partial J_s}{\partial X} =$$

$$3(1 + a\cos X)^3 \left[\lambda J_s - \frac{\bar{\omega}}{4} \exp\left(-\tau_o(X,Z,\mu_o,\phi_o)\right) \right] \tag{5-6}$$

where $\tau_o(X,Z,\mu_o,\phi_o)$ is the optical depth of the point (X,Z) along the direction defined by the angles $\cos^{-1}\mu_o$ and ϕ_o, Figure 5-1, which can be evaluated easily as follows; from the definition

$$\tau_o(s,z,\mu_o,\phi_o) = \int_o^{s(x,z,\mu_o,\phi_o)} \kappa(s')\, d\, s' \tag{5-7}$$

and from the geometry of Figure 5-1, results

$$\begin{aligned} x' &= x + s'\,(1-\mu_o^2)^{\frac{1}{2}} \cos\phi_o \\ z' &= s'\,\mu_o \end{aligned} \tag{5-8}$$

Substituting equations (5-1) and (5-8) in (5-7), integrating this last equation and changing to the dimensionless variables defined by (5-2) one obtains

$$\tau_o(X,Z,\mu_o,\phi_o) = \frac{Z}{\mu_o} + a\left[f_1(Z,\mu_o,\phi_o)\cos X + f_2(Z,\mu_o,\phi_o)\sin X \right] \tag{5-9}$$

where

$$\begin{aligned} f_1(Z,\mu_o,\phi_o) &= \sin\delta Z/\mu_o\delta && \text{(a)} \\ f_2(Z,\mu_o,\phi_o) &= (\cos\delta Z - 1)/\mu_o\delta && \text{(b)} \\ \delta &= r(1/\mu_o^2 - 1)^{\frac{1}{2}} \cos\phi_o && \text{(c)} \end{aligned} \tag{5-10}$$

When $\delta \to 0$, $f_1 \to Z/\mu_o$ and $f_2 \to 0$, this occurs when $\mu_o \to 1$ (normal incidence) and/or $\phi_o \to \pi/2$, and/or $r \to 0$ (homogeneous case with constant extinction $\bar{\kappa}_s(1+a)$). This case will be called the asymptotic case and will be treated in parallel with the case $\delta \neq 0$.

The exponential exp $(-\tau_o)$ can be expanded as a power series which for a < 1 converges very fast and the error remains small if enough terms are taken in the expansion. In addition, if any power of the functions sinX and cos X are expressed by harmonic sums the exponential becomes

$$\exp(-\tau_o(X,Z,\mu_o,\phi_o)) = \exp\left(-\frac{Z}{\mu_o}\right)\Big\{g_o(Z) + g_1(Z)\cos X + g_2(Z)\cos 2X + \ldots$$

$$+ h_1(Z)\sin X + h_2(Z)\sin 2X + \ldots\ldots\Big\} \qquad (5\text{-}11)$$

where

$$g_o(Z) = 1 + \frac{a^2}{4}(f_1^{\,2} + f_2^{\,2}) + \ldots \qquad \text{(a)}$$

$$g_1(Z) = -a f_1\left[1 + \frac{a^2}{8}(f_1^{\,2} + f_2^{\,2}) + \ldots.\right] \qquad \text{(b)}$$

$$g_2(Z) = \frac{a^2}{4}\left[f_1^{\,2} - f_2^{\,2} + \ldots.\right] \qquad \text{(c)}$$

$$h_1(Z) = -a f_2\left[1 + \frac{a^2}{8}(f_1^{\,2} + f_2^{\,2}) + \ldots.\right] \qquad \text{(d)} \qquad (5\text{-}12)$$

$$h_2(Z) = \frac{a^2}{2} f_1 f_2 + \ldots.. \qquad \text{(e)}$$

From equation (5-11) it is seen that it is reasonable to look for solutions of equation (5-6) of the form

$$J_s(X,Z) = \sum_{k=0}^{\infty} J_k^{\,s}(Z)\cos k X + \sum_{m=1}^{\infty} H_m^{\,s}(Z)\sin m X \qquad (5\text{-}13)$$

Substituting equations (5-12) and (5-13) in (5-6) and equating the coefficients for the different harmonics of X, a set of simultaneous

differential equations of the form

$$b_{ij}\, J_j''(Z) + c_{ij}\, J_i(Z) = W_i^{s}(Z) \qquad \text{(a)}$$

$$d_{ik}\, H_k''(Z) + e_{ik}\, H_k(Z) = U_i^{s}(Z) \qquad \text{(b)} \qquad (5\text{-}14)^{*}$$

$$i = 0, 1, \ldots N$$

$$j = 0, 1, \ldots N$$

$$k = 0, 1, \ldots N$$

is obtained, where b_{ij}, c_{ij}, d_{ik} and e_{ik} are known coefficients depending on the parameters r, λ and a and $W_i(Z)$, $U_i(Z)$ known functions of the form

$$W_i^{s}(Z) = W(g_o, g_1 \ldots) \exp(-Z/\mu_o) \qquad \text{(a)}$$

$$U_i^{s}(Z) = U(h_1, h_2, \ldots) \exp(-Z/\mu_o) \qquad \text{(b)} \qquad (5\text{-}15)$$

This system of equation together with the corresponding set obtained from the boundary condition (4-36) can be solved with the help of an appropriate numerical technique. Analytically, however, only a small number of harmonics can be retained.$^{\neq}$ Fortunately the terms involving harmonics greater than, or equal to 2, are small and may be neglected when $a < 1$ in a first approximation.

* Einstein's sum convention is used.

$\neq$ The numerical solutions of the set of equation (5-14) and the possible generalisation to more realistic (and complex) ψ distributions will be carried out in a further

Reducing the solutions (5-13) to the form

$$J_s(X,Z) = J_o^s(Z) + J_1^s(Z)\cos X + H_1^s(Z)\sin X \qquad (5\text{-}16)$$

the system of equations (5-14) is reduced to

$$J_o^{s\,''}(Z) + \frac{a}{2}J_1^{s\,''}(Z) - 3(1+\frac{3}{2}a^2)\lambda J_o^s(Z) - \left[ar^2 + \frac{9}{2}a\,(1+\frac{a^2}{4})\lambda\right]J_1^s(Z)$$

$$= -\frac{3\bar{\omega}}{4}(1+\frac{3}{2}a^2)\,g_o(Z) - \frac{9\bar{\omega}}{8}a\,(1+\frac{a^2}{4})\,g_1(Z) = W_o^s(Z) \qquad (a)$$

$$aJ_o^{s\,''}(Z) + J_1^{s\,''}(Z) - 9a(1+\frac{a^2}{4})\lambda\, J_o^s(Z) - \left[r^2 + 3(1+\frac{9}{4}a^2)\lambda\right]J_1^s(Z) \qquad (5\text{-}17)$$

$$= -\frac{9\bar{\omega}}{4}(1+\frac{a^2}{4})\,g_o(Z) - \frac{3\bar{\omega}}{4}(1+\frac{9}{4}a^2)\,g_1(Z) = W_1^s(Z) \qquad (b)$$

$$H_1^{s\,''}(Z) - \left[r^2 + 3(1+\frac{3}{4}a^2)\lambda\right]H_1^s(Z) = -\frac{3\bar{\omega}}{4}(1+\frac{3}{4}a^2)\,h_1(Z) = U_1^s(Z) \qquad (c)$$

where dashes denote derivatives with respect to Z.

The boundary condition (4-36) gives three equations

$$J_o^{s\,'}(Z)\Big|_{Z=0} = \sqrt{3}\left[J_o^s(o) + \frac{a}{2}J_1^s(o)\right] \qquad (a)$$

$$J_1^{s\,'}(Z)\Big|_{Z=0} = \sqrt{3}\left[J_1^s(o) + a\,J_o^s(o)\right] \qquad (b) \qquad (5\text{-}18)$$

$$H_1^{s\,'}(Z)\Big|_{Z=0} = \sqrt{3}\,H_1^s(o) \qquad (c)$$

In this particular case of a semi-infinite cloud, the condition

$$J(X,Z)\exp\left(-\frac{Z}{\mu_o}\right) \to 0 \qquad \text{when } Z \to \infty \qquad (5\text{-}19)$$

Chandrasekhar (1960), provides three additional equations. Therefore, the system of simultaneous equations (4-17) is completely determined.

The analytical solution of equations (5-17) is rather cumbersome and the procedure is as follows:

If terms with powers of a greater than three are neglected, from equations (5-17 a,b) one obtains

$$J_1^{s''}(Z) = a_o J_o^{s}(Z) + a_1 J_1^{s}(Z) + \frac{W_1 - aW_o}{1 - a^2/2} \qquad (5\text{-}20)$$

where

$$a_o = 3a(2 - \tfrac{3}{4}a^2)\lambda\,(1 - a^2/2)^{-1}$$

$$a_1 = \{(1-a^2)r^2 + 3\left[1 + \frac{3a^2}{4}(1 - a^2/2)\right]\}\,(1 - a^2/2)^{-1}$$

From equations (5-17a) and (5-20) results

$$J_1^{s}(Z) = a_2 J_o^{s''}(Z) - a_3 J_o^{s}(Z) - a_4 W_o - a_5 W_6 \qquad (5\text{-}21)$$

where

$$a_2 = a^{-1}\left[r^2 + \tfrac{9}{2}(1 - a^2/4) - \tfrac{1}{2}.a_1\right]^{-1}$$

$$a_3 = a_2\left[3\lambda\,(1 + \frac{3}{2}a^2) - \frac{a}{2}a_o\right]$$

$$a_4 = a_2\,(1 - a^2/2)^{-1}$$

$$a_5 = \frac{aa_2}{2}\,(1 - a^2/2)^{-1}$$

Substituting equation (5-21) in (5-20), after lengthy calculation one finds a fourth order differential equation for $J_o^s(Z)$, i.e.

$$J_o^{s(4)}(Z) + b_2 J_o^{s''}(Z) + b_o J_o^{s}(Z) =$$

$$\rho_o \exp\left(-\frac{Z}{\mu_o}\right) + \left[\rho_1 \cos\delta Z + \rho_2 \sin\delta Z\right] \exp\left(-\frac{Z}{\mu_o}\right) \qquad (5\text{-}22)$$

where

$$b_o = -a_o a\left[r^2 + \frac{9}{2}\left(1+\frac{a^2}{4}\right)\lambda\right] + \frac{a_o a_1}{2}(9-a) + 3\lambda a_1\left(1+\frac{3}{2}a^2\right)$$

$$b_2 = \tfrac{1}{2} a a_o - a_1 - 3\lambda\left(1+\frac{3}{2}a^2\right)$$

$$\rho_o = \frac{3\bar{\omega}}{4}\frac{1+a^2/2\mu_o^2\delta^2}{(1-a^2/2)}\left\{a_1\left[1+3a^2(1-a^2/2)\right] - 3a^2\left(2-\frac{3}{4}a^2\right)\left[r^2+\frac{9\lambda}{2}(1+a^2/4)\right]\right.$$

$$\left. - \frac{3}{\mu_o^2}\left[1+3a^2(1+a^4/8)\right]\right\}$$

$$\rho_1 = \frac{3\bar{\omega}}{4}\frac{a^2}{(1-a^2/2)}\left\{\frac{-2+\frac{3}{2}a^2}{\mu_o^2} + \frac{1}{2\mu_o^2\delta^2}\left[\left(\frac{1}{\mu_o^2}-\delta^2\right) - a_1\left(1+\frac{a^2}{2}\left(5-\frac{3}{4}a^2\right)\right)\right]\right.$$

$$\left. + a^2\left[\frac{3}{2}\left(1+\frac{a^2}{4}\right) + \left(2-\frac{3}{4}a^2\right)\left(r^2+\frac{9}{2}\lambda\left(1+\frac{a^2}{2}\right)\right)\right]\right\}$$

$$\rho_2 = \frac{3\bar{\omega}}{4}\frac{a^2}{\delta\mu_o(1-a^2/2)}\left\{\frac{1}{\mu_o^2}\left(1-\frac{3}{8}a^4\right) - \left(\delta^2-\frac{1}{\mu_o^2}\right)\left(1-\tfrac{3}{4}a^2\right) - 2a_1\left(1-\tfrac{3}{4}a^2\right)\right.$$

$$\left. -\left(\frac{3}{2}a-1\right)\left(1+\frac{9}{4}a^2\right)\left[r^2+\frac{9}{2}\left(1+\frac{a^2}{4}\right)\lambda - \tfrac{1}{2}a_1\right]\right\}$$

The solution of the differential equation (5-22) is

$$J_o^s(Z) = J_{o\,hom.}^s(Z) + J_{o\,part.}^s(Z) \qquad (5\text{-}23)$$

$J_{o\,hom.}^s(Z)$ being the solution of the homogeneous equation corresponding to equation (5-22) and $J_{o\,part.}^s(Z)$ a particular solution of equation (5-22).

The homogeneous solution $J_{o\,hom.}^s(Z)$ becomes

$$J_{o\,hom.}^s(Z) = c_1\exp(\alpha_1 Z) + c_2\exp(\alpha_2 Z) + c_3\exp(\alpha_3 Z) + c_4\exp(\alpha_4 Z) \qquad (5\text{-}24)$$

where c_1, c_2, c_3, c_4 are arbitrary constants and α_1, α_2, α_3, α_4 the roots of the characteristic equations corresponding to (5-22), i.e.

$$\alpha_1 = \left\{\tfrac{1}{2}\left[-b_2 + (b_2^2 - 4b_o)^{\frac{1}{2}}\right]\right\}^{\frac{1}{2}}$$

$$\alpha_2 = -\left\{\tfrac{1}{2}\left[-b_2 + (b_2 - 4b_o)^{\frac{1}{2}}\right]\right\}^{\frac{1}{2}}$$

$$\alpha_3 = \left\{\tfrac{1}{2}\left[-b_2 - (b_2^2 - 4b_o)^{\frac{1}{2}}\right]\right\}^{\frac{1}{2}}$$

$$\alpha_4 = -\left\{\tfrac{1}{2}\left[-b_2 - (b_2^2 - 4b_o)^{\frac{1}{2}}\right]\right\}^{\frac{1}{2}}$$

In order to preserve the condition (5-19), the constants c_1 and c_3 must be identically zero. So, equation (5-24) is reduced to

$$J_{o\,hom.}(Z) = c_2\exp(\alpha_2 Z) + c_4\exp(\alpha_4 Z) \qquad (5\text{-}25)$$

On the other hand, using the method of undetermined coefficients a particular solution of (5-22) is found in the form

$$J_{o\,part.}(Z) = \left[d_o + d_1 \cos \delta Z + d_2 \sin \delta Z\right] \exp\left(-\frac{Z}{\mu_o}\right) \tag{5-26}$$

where

$$d_o = \rho_o \left[\frac{1}{\mu_o^4} + \frac{b_2}{\mu_o^2} + b_o\right]^{-1}$$

$$d_1 = \{\rho_1 \left[\left(\frac{1}{\mu_o^2} - \delta^2\right)^2 - \frac{4\delta^2}{\mu_o^2} + b_2\left(\frac{1}{\mu_o^2} - \delta^2\right) + b_o\right] - \rho_2\left[\frac{4\delta}{\mu_o}\left(\frac{1}{\mu_o^2} - \delta^2\right) + b_2\frac{2\delta}{\mu_o}\right]\} \Delta^{-1}$$

$$d_2 = \{\rho_2 \left[\left(\frac{1}{\mu_o^2} - \delta^2\right)^2 - \frac{4\delta^2}{\mu_o^2} + b_2\left(\frac{1}{\mu_o^2} - \delta^2\right) + b_o\right] - \rho_1\left[\frac{4\delta}{\mu_o}\left(\frac{1}{\mu_o^2} - \delta^2\right) + b_2\frac{2\delta}{\mu_o}\right]\} \Delta^{-1}$$

and

$$\Delta = \left[\left(\frac{1}{\mu_o^2} - \delta^2\right)^2 - \frac{4\delta^2}{\mu_o^2} + b_2\left(\frac{1}{\mu_o^2} - \delta^2\right) + b_o\right]^2 + \left[\frac{4\delta}{\mu_o}\left(\frac{1}{\mu_o^2} - \delta^2\right) + b_2\frac{2\delta}{\mu_o}\right]^2 .$$

The solution (5-25) therefore takes the form

$$J_o(Z) = c_2 \exp(\alpha_2 Z) + c_4 \exp(\alpha_4 Z) + \left[d_o + d_1 \cos\delta Z + d_2 \sin\delta Z\right] \exp\left(-\frac{Z}{\mu_o}\right) \tag{5-27}$$

where c_2 and c_4 are constants to be determined from the boundary conditions (5-18).

Once $J_o(Z)$ is known, $J_1(Z)$ is obtained directly from equation (5-21), i.e.

$$J_1(Z) = \beta_2 c_2 \exp(\alpha_2 Z) + \beta_4 c_4 \exp(\alpha_4 Z) + \left[q_o + q_1 \cos\delta Z + q_2 \sin\delta Z \right] \exp(-\frac{Z}{\mu_o}) \tag{5-28}$$

where

$$\beta_2 = \left[\alpha_2^2 - 3(1 + \frac{3}{2}a^2)\lambda + \tfrac{1}{2} a a_o \right] / a\left[r^2 + \frac{9}{2}(1 + \frac{a^2}{4})\lambda - \tfrac{1}{2} a_1 \right]$$

$$\beta_4 = \left[\alpha_4^2 - 3(1 + \frac{3}{2}a^2)\lambda + \tfrac{1}{2} a a_o \right] / a\left[r^2 + \frac{9}{2}(1 + \frac{a^2}{4})\lambda - \tfrac{1}{2} a_1 \right]$$

$$q_o = \{ \left[d_o(\frac{1}{\mu_o^2} - 3(1 + \frac{3}{2}a^2)\lambda + \tfrac{1}{2} a a_o \right] + \frac{3}{4}\bar{\omega} \frac{(1 + a^2/2\,\mu_o^2\delta^2)}{(1 - a^2/2)} (1 + \frac{9}{8}a^2 - \frac{3}{32}a^4) \} a_2$$

$$q_1 = \{ d_1 \left[(\frac{1}{\mu_o^2} - \delta^2) - 3(1 + \frac{3}{2}a^2)\lambda + \tfrac{1}{2} a a_o \right] - d_2 \frac{2\delta}{\mu_o} - \frac{3\bar{\omega}}{4} \frac{\tfrac{1}{2}(1 - \frac{3}{8}a^4)}{(1 - a^2/2)} \} a_2$$

$$q_2 = \left\{ d_1 \frac{2\delta}{\mu_o} + d_2 \left[(\frac{1}{\mu_o^2} - \delta^2) - 3(1 + \frac{3}{2}a^2)\lambda + \tfrac{1}{2} a a_o \right] - \frac{3\bar{\omega}}{4} \frac{a^2(1 - \frac{3}{4}a^2)}{\mu_o \delta (1 - a^2)} \right\} a_2$$

Finally, equation (5-17c) may be integrated straightforwardly and one obtains

$$H_1(Z) = k_2 \exp(-vz) + \left[\ell_o + \ell_1 \cos\delta Z + \ell_2 \sin\delta Z \right] \exp(-\frac{Z}{\mu_o}) \tag{5-29}$$

where k_2 is a constant to be evaluated from the boundary conditions

and v, ℓ_o, ℓ_1, ℓ_2 are given by

$$v = \sqrt{r^2 + 3(1 + \tfrac{3}{4}a^2)\lambda}$$

$$\ell_o = \frac{3\bar{\omega}}{4} \frac{a(1 + \frac{3}{4}a^2)\lambda}{\mu_o \delta (v^2 - \frac{1}{\mu_o^2})}$$

$$\ell_1 = -\frac{3\bar{\omega}}{4} \frac{a(1 + \frac{3}{4}a^2)}{2\mu_o \delta v} \{(v - \frac{1}{\mu_o})/[(v - \frac{1}{\mu_o})^2 + \delta^2] + (v + \frac{1}{\mu_o})/[(v + \frac{1}{\mu_o})^2 + \delta^2]\}$$

$$\ell_2 = \frac{3\bar{\omega}}{4} \frac{(1 + \frac{3}{4}a^2)}{2\mu_o v} (v^2 - \frac{1}{\mu_o^2})^2 / \left[(v + \frac{1}{\mu_o})^2 + \delta^2\right]\left[(v - \frac{1}{\mu_o}) + \delta^2\right]$$

In obtaining equation (5-29) condition (5-19) has been used.

The boundary conditions (5-18) give the necessary equations to evaluate the constants of integration c_2, c_4 and k_2. After some algebraic calculation one obtains

$$c_2 = \{\left[\frac{1}{\mu_o}(d_o + d_1) - \delta d_2 + \sqrt{3}(d_o + d_1 + \tfrac{1}{2}aq_o + \tfrac{1}{2}aq_1)\right]\left[\alpha_4\beta_4 - \sqrt{3}(\beta_4 + a)\right] -$$

$$\left[\frac{1}{\mu_o}(q_o + q_1) - \delta q_2 + \sqrt{3}(q_o + q_1 + ad_o + ad_1)\right]\left[\alpha_4 - \sqrt{3}(1 + \tfrac{1}{2}a\beta_4)\right]\} / \Delta_1$$

$$c_4 = \{\left[\frac{1}{\mu_o}(q_o + q_1) - \delta q_2 + \sqrt{3}(q_o + q_1 + ad_o + ad_1)\right]\left[\alpha_2 - \sqrt{3}(1 + \tfrac{1}{2}a\beta_2)\right] -$$

$$\left[\frac{1}{\mu_o}(d_o + d_1) - \delta d_2 + \sqrt{3}(d_o + d_1 + \tfrac{1}{2}aq_o + \tfrac{1}{2}aq_1)\right]\left[\alpha_2\beta_2 - \sqrt{3}(\beta_2 + a)\right]\} / \Delta_1$$

$$\Delta_1 = \left[\alpha_2 - \sqrt{3}(1 + \tfrac{1}{2}a\beta_2)\right]\left[\alpha_4\beta_4 - \sqrt{3}(\beta_4 + a)\right] - \left[\alpha_4 - \sqrt{3}(1 + \tfrac{1}{2}a\beta_4)\right]\left[\alpha_2\beta_2 - \sqrt{3}(\beta_2 + a)\right]$$

$$k_2 = \left[\delta\ell_2 - (\sqrt{3} + \frac{1}{\mu_o})(\ell_o + \ell_1)\right] / (v + \sqrt{3}).$$

In the particular case when $\delta = o$, instead of equation (5-22), one finds

$$J_o^{(4)}(Z) + b_2 J_o''(Z) + b_o J_o(Z) = (p_o + p_1\frac{Z}{\mu_o} + p_2\frac{Z^2}{\mu_o^2})\exp(-\frac{Z}{\mu_o})$$

where (5-30)

$$p_o = \frac{3\bar{\omega}}{4}\frac{1}{(1-a^2/2)}\{\frac{1}{\mu_o^2}(1 + a^2 - \frac{15}{8}a^4) + (1 - \frac{3}{8}a^4)a_1 - a^2(2 - \tfrac{3}{4}a^2)\, x$$

$$\left[r^2 + \frac{9\lambda}{2}(1 + \frac{a^2}{4}) - \tfrac{1}{2}a_1\right]\}$$

$$p_1 = \frac{3\bar{\omega}}{4}\frac{a^2}{(1-a^2/2)}\{\frac{1}{2\mu_o^2}(3 + \frac{7}{4}a^2 - \tfrac{3}{4}a^4) - a_1(1 - \tfrac{3}{4}a^2) - (\frac{3}{2}a - 1)(1 + \frac{9}{4}a^2)\left[r^2 +\right.$$

$$\left.\frac{9\lambda}{2}(1 + \frac{a^2}{4}) - \tfrac{1}{2}a_1\right]\}$$

$$p_2 = \frac{3\bar{\omega}}{4} \frac{a^2}{4(1-a^2/2)} \{-\frac{1}{\mu_o^2}(1-\frac{3}{8}a^4) + a_1\left[1+\frac{a^2}{2}(5-\tfrac{3}{4}a^2)\right] - a^2\left[\frac{3}{2}(1+\frac{a^2}{4})\right.$$

$$\left. + (2-\tfrac{3}{4}a^2)\left[r^2+\frac{9\lambda}{2}(1+a^2/2)\right]\right] \}$$

Following the same procedure as in the case $\delta \neq o$ the solution of (5-30) becomes

$$J_o^s(Z) = c_2^{(o)} \exp(\alpha_2 Z) + c_4^{(o)} \exp(\alpha_4 Z) + \left[d_o^{(o)} + d_1^{(o)} \frac{Z}{\mu_o} + d_2^{(o)} \frac{Z^2}{\mu_o^2}\right] \exp(-Z/\mu_o)$$

(5-31)

where $c_2^{(o)}$ and $c_4^{(o)}$ are constants of integration which will be determined from the boundary conditions in the same way that c_2 and c_4 were calculated; the coefficients $d_o^{(o)}$, $d_1^{(o)}$ and $d_2^{(o)}$ are given by

$$d_2^{(o)} = p_2 \left[\frac{1}{\mu_o^4} + \frac{b_2}{\mu_o^2} + b_o\right]^{-1}$$

$$d_1^{(o)} = \left[p_1 + 4 d_2 (\frac{2}{\mu_o^4} + \frac{b_2}{\mu_o^2})\right]\left[\frac{1}{\mu_o^4} + \frac{b_2}{\mu_o^2} + b_o\right]^{-1}$$

$$d_o^{(o)} = \left[p_o + 2d_1(\frac{2}{\mu_o^4} + \frac{b_2}{\mu_o^2}) - 2d_2(\frac{6}{\mu_o^4} + \frac{b_2}{\mu_o^2})\right]\left[\frac{1}{\mu_o^4} + \frac{b_2}{\mu_o^2} + b_o\right]^{-1}$$

With the help of equation (5-31) one obtains the corresponding

solution $J_1(Z)$ which becomes

$$J_1^s(Z) = \beta_2 c_2^{(o)} \exp(\alpha_2 Z) + \beta_4 c_4^{(o)} \exp(\alpha_4 Z) + \left[q_o^{(o)} + q_1^{(o)} \frac{Z}{\mu_o} + q_2^{(o)} \frac{Z^2}{\mu_o^2} \right] \exp(-\frac{Z}{\mu_o}) \qquad (5\text{-}32)$$

where

$$q_o^{(o)} = \{ (d_o^{(o)} - 2d_1^{(o)} + 2d_2^{(o)})/\mu_o^2 - d_o \left[3\lambda(1 + \tfrac{3}{2}a^2) - \tfrac{1}{2} a a_o \right] - \frac{3\bar{\omega}}{4(1-a^2/2)} \left[(1 - \tfrac{3}{2}a^2 - \tfrac{3}{4}a^4) \right] \} a_2$$

$$q_1^{(o)} = \{ (d_1^{(o)} - 4d_2^{(o)})/\mu_o^2 - \left[3\lambda(1 + \tfrac{3}{2}a^2) - \tfrac{1}{2} a a_o \right] - \frac{3\bar{\omega}}{4} \frac{a^2}{(1-a^2/2)} (1 - \tfrac{3}{2}a^2) \} a_2$$

$$q_2^{(o)} = \{ d_2^{(o)}/\mu_o^2 - d_2 \left[3(1 + \tfrac{3}{2}a^2)\lambda - \tfrac{1}{2} a a_o \right] + \frac{3\bar{\omega}}{4} \frac{a^2}{4(1-a^2/2)} (1 - \tfrac{3}{8}a^4) \} a_2 .$$

The constants $c_2^{(o)}$ and $c_4^{(o)}$ are calculated from the boundary equation (5-18); the result is

$$c_2^{(o)} = \{ \left[(d_o^{(o)} - d_1^{(o)})/\mu_o + \sqrt{3}(d_o^{(o)} + \tfrac{1}{2} a q_o^{(o)}) \right] \left[\alpha_4 \beta_4 - \sqrt{3}(\beta_4 + a) \right] -$$

$$\left[(q_o^{(o)} - q_1^{(o)})/\mu_o + \sqrt{3}(q_o^{(o)} + a d_o^{(o)}) \right] \left[\alpha_4 - \sqrt{3}(1 + \tfrac{1}{2} a \beta_4) \right] \} / \Delta_2$$

$$c_4^{(o)} = \{\left[(q_o^{(o)} - q_1^{(o)}) / \mu_o + \sqrt{3}(q_o^{(o)} + a d_o^{(o)})\right]\left[\alpha_2 - \sqrt{3}(1 + \tfrac{1}{2}a\beta_2)\right] -$$

$$\left[(d_o^{(o)} - d_1^{(o)})/\mu_o + \sqrt{3}(d_o^{(o)} + \tfrac{1}{2}a q_o^{(o)})\right]\left[\alpha_2\beta_2 - \sqrt{3}(\beta_2 + a)\right]\} / \Delta_2$$

$$\Delta_2 = \left[\alpha_2 - \sqrt{3}(1 + \tfrac{1}{2}a\beta_2)\right]\left[\alpha_4\beta_4 - \sqrt{3}(\beta_4 + a)\right] -$$

$$\left[\alpha_4 - \sqrt{3}(1 + \frac{a}{2}\beta_4)\right]\left[\alpha_2\beta_2 - \sqrt{3}(\beta_2 + a)\right]$$

Equation (5-16), with $J_o^s(Z)$, $J_1^s(Z)$ and $H_1(Z)$ given by equations (5-27), (5-28) and (5-29) respectively, is the solution of Giovanelli's equation for the diffuse field in a semi-infinite cloud with sinusoidal transverse density fluctuations.

b. Infrared Field

Once the visual field has been evaluated for the model studied in this section the infrared field will be calculated solving equation (4-34) with the density distributions given by (5-1).

Proceeding in the same manner as in the previous sub-section, equation (4-34) can be written as follows

$$(1 + a\cos X)\left(r^2 \frac{\partial^2 J^p}{\partial X^2} + \frac{\partial^2 J^p}{\partial Z^2}\right) + r^2 a \sin X \frac{\partial J^p}{\partial X} =$$

$$-3\eta^{-1}\lambda(1 + a\cos X)^3\left[J^s(X,Z) + \tfrac{1}{4}\exp\left(-\tau_o(X,Z,\mu_o,\phi_o)\right)\right] \qquad (5\text{-}33)$$

If one assumes a solution of equation (5-33) in the same form as equation (5-13) taking into account only the first harmonics, i.e.

$$J^p(X,Z) = J_o^p(Z)\cos X + H_1^p(Z)\sin X \qquad (5\text{-}34)$$

the equation (5-33) is reduced to the following system of differential equations

$$J_o^{p''} + \tfrac{1}{2}a J_1^{p''} - a r^2 J_1 = W_o^p(Z) \qquad (a)$$

$$a J_o^{p''} + J_1^{p''} - r^2 J_1 = W_1^p(Z) \qquad (b) \qquad (5\text{-}35)$$

$$H_1^{p''} - r^2 H_1 = U_1^p(Z) \qquad (c)$$

where

$$W_o^p(Z) = -3\eta^{-1}\lambda\left[(1+\frac{3}{2}a^2)(J_o^s(Z) + \tfrac{1}{4}g_o(Z)) + \frac{3}{2}a\,(1+\frac{a^2}{4})(J_1^s(Z) + \tfrac{1}{4}g_1(Z))\right]$$

$$W_1^p(Z) = -3\eta^{-1}\lambda\left[(1+\frac{a}{4}a^2)(J_1^s(Z) + \tfrac{1}{4}g_1(Z)) + 3a(1+\frac{a^2}{4})(J_o^s(Z) + \tfrac{1}{4}g_o(Z)\right]$$

$$U_1^p(Z) = -3\eta^{-1}\lambda\,(1+\tfrac{3}{4}a^2)\left[H_1^s(Z) + \tfrac{1}{4}h_1(Z)\right]$$

where $g_o(Z)$, $g_1(Z)$, $h_1(Z)$ are given by equations (5-12).

From the boundary condition (4-40) the following equations are obtained

$$J_o^{p'}(Z)\Big|_{Z=o} = \frac{\sqrt{3}}{\eta}\left[J_o^p(o) + \tfrac{1}{2}a J_1^p(o)\right] \qquad (a)$$

$$J_1^{p'}(Z)\Big|_{Z=o} = \frac{\sqrt{3}}{\eta}\left[J_1^p(o) + a\,J_o^p(o)\right] \qquad (b) \qquad (5\text{-}36)$$

$$H_1^{p'}(Z)\Big|_{Z=o} = \frac{\sqrt{3}}{\eta}\,H_1^p(o) \qquad (c)$$

Equation (5-36) together with condition (5-19) applied to the infrared

field, provide the necessary conditions to determine the solutions of equations (5-35).

The solution to the system of equations (5-35) is obtained as follows: from equation (5-35a) one gets the expression

$$J_o^{p''}(Z) = -\tfrac{1}{2}a\,J_1''(Z) + a\,r^2 J_1(Z) + W_o^{p}(Z) \qquad (5\text{-}37)$$

and substituting (5-37) in (5-35b) one obtains a differential equation for $J_1^{p}(Z)$, i.e.

$$J_1^{p''} - R^2 J_1 = (W_1^{p}(Z) - aW_o^{p}(Z)) \Big/ (1 - a^2/2) \qquad (5\text{-}38)$$

with $$R = \sqrt{\frac{1 - a^2}{1 - \frac{1}{2}a^2}}\; r$$

Integrating (5-38) one obtains

$$J_1^{p}(Z) = C_2\exp(-RZ) + S_2\exp(\alpha_2 Z) + S_4\exp(\alpha_4 Z) + \left[Q_o + Q_2\cos\delta Z + Q_1\sin\delta Z \right] \exp\left(-\frac{Z}{\mu_o}\right) \qquad (5\text{-}39)$$

where C_2 will be determined later and the coefficients in equation (5-39) are given by

$$S_2 = \frac{3\eta^{-1}\lambda}{(\alpha_2^2 - R^2)(1 - a^2/2)} \left\{ -\left[a\left(1+\frac{a^2}{4}\right) + \beta_2\left(1+\frac{9}{4}a^2\right) \right] c_2 + a\left[\left(1+\frac{3}{2}a^2\right) + \beta_2 \frac{3}{2}a\left(1+\frac{a^2}{4}\right) \right] \right\}$$

$$S_4 = \frac{3\eta^{-1}\lambda}{(\alpha_4^2 - R^2)(1 - a^2/2)} \{ -\left[3a(1+a^2/4) + \beta_4(1 + \frac{9}{4}a^2) \right] c_4 + a\left[(1 + \frac{3}{2}a^2) \right.$$

$$\left. + \beta_4 \frac{3}{2}a(1 + \frac{a^2}{4}) \right] \}$$

$$Q_o = \frac{3\eta^{-1}\lambda}{(R^2 - 1/\mu_o^2)(1 - a^2/2)} \{ \frac{5}{4} a^2 \left[d_o + \tfrac{1}{4}(1 + \frac{a^2}{2\mu_o^2\delta^2}) \right] - q_o \left[1 + \frac{a^2}{4}(5 - a^2) \right] \}$$

$$Q_1 = \frac{3\eta^{-1}\lambda}{R(1 - a^2/2)} \{ \frac{B_1}{(R - 1/\mu_o)^2 + \delta^2} + \frac{B_2}{(R + 1/\mu_o)^2 + \delta^2} \}$$

$$B_{\frac{1}{2}} = \pm 2\delta \left[a(1 + \frac{a^2}{4})(d_1 - \frac{a^2}{8\mu_o^2\delta^2}) + (1 + \frac{9}{4}a^2)q_1 - a(1 + \frac{3}{2}a^2)(d_1 - \frac{a^2}{8\mu_o^2\delta^2}) \right.$$

$$\left. - \frac{3}{2}a^2(1 + \frac{a^2}{4})q_1 \right] + 2\left[3a(1 + \frac{a^2}{4})d_2 + (1 + \frac{9}{4}a^2)(q_2 - \frac{a}{4\mu\delta}) \right.$$

$$\left. - a(1 + \frac{3}{2}a^2)d_2 - \frac{3}{2}a^2(1 + \frac{a^2}{4})(q_2 - \frac{a}{4\mu_o\delta}) \right] (R \mp \frac{1}{\mu_o})$$

$$Q_2 = \frac{3\eta^{-1}\lambda}{R(1 - a^2/2)} \{ \frac{B_3}{(\frac{3}{4}R - 1/\mu_o)^2 + \delta^2} + \frac{B_2}{(R + 1/\mu_o)^2 + \delta^2} \}$$

$$B_3 = 2(R-\frac{1}{\mu_o})\left[a(1+\frac{a^2}{4})(d_1 - \frac{a^2}{8\mu_o^2\delta^2}) + (1+\frac{9}{4}a^2)\,q_1 - a(1+\frac{3}{2}a^2)(d_1 - \frac{a^2}{8\mu_o^2\delta^2})\right.$$

$$\left. -\frac{3}{2}a^2(1+\frac{a^2}{4})q_1\right] + 2\delta\left[3a(1+\frac{a^2}{4})d_2 + (1+\frac{9}{4}a^2)(q_2 - \frac{a}{4\mu\delta})\right.$$

$$\left. - a(1+\frac{3}{2}a^2)d_2 - \frac{3}{2}a^2(1+\frac{a^2}{4})(q_2 - \frac{a}{4\mu_o\delta})\right]$$

Now, substituting the solution (5-39) in equation (5-37) and integrating, the following expression for $J_o^p(Z)$ is obtained

$$J_o^p(Z) = \frac{P_2}{\alpha_2^2}\exp(\alpha_2 Z) + \frac{P_4}{\alpha_4^2}\exp(\alpha_4 Z) + \frac{a}{2(1-a^2)}C_2\exp(-RZ)$$

$$+\left[V_o + V_2\cos\delta Z + V_1\sin\delta Z\right]\exp(-\frac{Z}{\mu_o}) + C_4 \qquad (5\text{-}40)$$

where C_4 is a constant to be evaluated from the boundary conditions and the coefficients are given by

$$P_2 = (r^2 - \tfrac{1}{2}\alpha_2^2)aS_2 - 3\eta^{-1}\lambda\left[(1+\frac{3}{2}a^2) + \frac{3}{2}a\beta_2\ (1+\frac{a^2}{4})\right]$$

$$P_4 = (r^2 - \tfrac{1}{2}\alpha_4^2)aS_4 - 3\eta^{-1}\lambda\left[(1+\frac{3}{2}a^2) + \frac{3}{2}a\beta_2(1+\frac{a^2}{4})\right]$$

$$V_o = \mu_o^2\{(r^2 - \frac{1}{2\mu_o^2})aQ_o - 3\eta^{-1}\lambda\left[(1+\frac{3}{2}a^2)(d_o + \tfrac{1}{4}(1+\frac{a^2}{2\mu_o^2\delta^2})) + \frac{3}{2}aq_o(1+\frac{a^2}{4})\right]\}$$

$$V_1 = \frac{1}{(\frac{1}{\mu_o^2} + \delta^2)^2} \Big(- \frac{2\delta}{\mu_o} \{ a r^2 Q_2 - \frac{a}{2} \Big[(\frac{1}{\mu_o^2} - \delta^2) Q_2 - \frac{2\delta}{\mu_o} Q_1 \Big]$$

$$- 3\eta^{-1}\lambda \Big[(1 + \frac{3}{2}a^2)(d_1 - \frac{a^2}{8\mu_o^2\delta^2}) + \frac{3}{2} a (1 + \frac{a^2}{4}) q_1 \Big] \} +$$

$$(\frac{1}{\mu_o^2} - \delta^2) \{ a r^2 Q_1 - \frac{a}{2} \Big[\frac{2\delta}{\mu_o} Q_2 + (\frac{1}{\mu_o^2} - \delta^2) Q_1 \Big]$$

$$- 3\eta^{-1}\lambda \Big[(1 + \frac{3}{2}a^2) d_2 + \frac{3}{2} a (1 + \frac{a^2}{4}) (q_2 - \frac{a}{4\mu\delta}) \Big] \} \Big)$$

$$V_2 = \frac{1}{(\frac{1}{\mu_o^2} + \delta^2)^2} \Bigg((\frac{1}{\mu_o^2} - \delta^2) \{ a r^2 Q_2 - \frac{a}{2} \Big[(\frac{1}{\mu_o^2} - \delta^2) Q_2 - \frac{2\delta}{\mu_o} Q_1 \Big]$$

$$-3\eta^{-1}\lambda \Big[(1+\frac{3}{2}a^2) (d_1 - \frac{a^2}{8\mu_o^2\delta^2}) + \frac{3}{2} a (1 + \frac{a^2}{4}) q_1 \Big] \}$$

$$+ \frac{2\delta}{\mu_o} \{ a r^2 Q_1 - \frac{a}{2} \Big[(\frac{1}{\mu_o^2} - \delta^2) Q_2 - \frac{2\delta}{\mu_o} Q_1 \Big]$$

$$- 3\eta^{-1}\lambda \Big[(1 + \frac{3}{2}a^2) d_2 + \frac{3}{2} a (1 + \frac{a^2}{2}) (q_2 - \frac{a}{4\mu\delta}) \Big] \} \Bigg)$$

Furthermore, integration of equation (5-35c) results in

$$H_1^p(Z) = K_2 \exp(-rZ) + L_3 \exp(-vZ) + \Big[L_o + L_2 \cos\delta Z + L_1 \sin\delta Z \Big] \exp(-\frac{Z}{\mu_o})$$

(5-41)

where K_2 is a constant of integration, to be determined, and the coefficients L become

$$L_o = \frac{3\eta^{-1}\lambda}{(r^2 - \frac{1}{\mu_o^2})} \left(1 + \tfrac{3}{4}a^2\right)\left(\ell_o + \frac{a}{4\mu_o\delta}\right)$$

$$L_1 = \frac{3\eta^{-1}\lambda(1 + \frac{3}{4}a^2)}{r} \left\{\frac{\frac{1}{2}(\ell_1 - \frac{a}{4\mu_o\delta})\delta + \frac{1}{2}\ell_2(r - \frac{1}{\mu_o})}{(r - \frac{1}{\mu_o})^2 + \delta^2}\right.$$

$$\left. + \frac{-\frac{1}{2}(\ell_1 - \frac{a}{4\mu_o\delta})\delta + \frac{1}{2}\ell_2(r + \frac{1}{\mu_o})}{(r + \frac{1}{\mu_o})^2 + \delta^2}\right\}$$

$$L_2 = \frac{3\eta^{-1}\lambda(1 + \frac{3}{4}a^2)}{r} \left\{\frac{(\ell_1 - \frac{a}{4\mu_o\delta})(r - \frac{1}{\mu_o}) - \frac{1}{2}\ell_2\delta}{(r - \frac{1}{\mu_o})^2 + \delta^2}\right.$$

$$\left. \frac{(\ell_1 - \frac{a}{4\mu_o\delta})(r + \frac{1}{\mu_o}) + \frac{1}{2}\ell_2\delta}{(r + \frac{1}{\mu_o})^2 + \delta^2}\right\}$$

$$L_3 = \frac{3\eta^{-1}\lambda(1 + \frac{3}{4}a^2)}{(r^2 - v^2)} k^2.$$

Now, substituting (5-40) and (5-41) in equations (5-36), the constants C_2, C_4 and K_2 are calculated. The results are as follows

$$C_2 = (M_2 - aM_1) / (m_2 - am_1)$$

$$C_4 = \frac{\eta}{\sqrt{3}} (m_1 C_2 - M_1)$$

$$K_2 = \frac{-1}{(r + \sqrt{3}/\eta)} \left[vL_3 + \frac{1}{\mu_o} (L_o + L_2) - \delta L_1 + \frac{\sqrt{3}}{\eta} (L_o + L_2 + L_3) \right]$$

where

$$M_1 = \frac{1}{\mu_o} (V_o + V_2) - \frac{P_2}{\alpha_2} - \frac{P_4}{\alpha_4} - \delta V_1 + \frac{\sqrt{3}}{\eta} \left[\frac{P_2}{\alpha_2^2} + \frac{P_4}{\alpha_4^2} + V_o + V_2 + \frac{a}{2}(S_2 + S_4 + Q_o + Q_2) \right]$$

$$M_2 = \frac{1}{\mu_o} (Q_o + Q_2) - (\alpha_2 S_2 + \alpha_4 S_4 + \delta Q_1) + \frac{\sqrt{3}}{\eta} \left[S_2 + S_4 + Q_o + Q_2 + a\left(\frac{P_2}{\alpha_2^2} + \frac{P_4}{\alpha_4^2} + V_o + V_2\right) \right]$$

$$m_1 = - \frac{a}{2(1 - a^2)} \left[R + \frac{\sqrt{3}}{2\eta} (3 - a^2) \right]$$

$$m_2 = -R - \frac{\sqrt{3}}{2\eta} \frac{2 - a^2}{1 - a^2}$$

In the particular case when $\delta = o$, the integration of equations (5-35a,b) gives

$$J_1^{p}(Z) = C_2^{(o)} \exp(-RZ) + S_2 \exp(\alpha_2 Z) + S_4 \exp(\alpha_4 Z) + \left[Q_o^{(o)} + Q_1^{(o)} \frac{Z}{\mu_o} + Q_2^{(o)} \frac{Z^2}{\mu_o^2} \right] \exp\left(-\frac{Z}{\mu_o}\right) \tag{5-42}$$

and

$$J_o^{p}(Z) = \frac{P_2^{(o)}}{\alpha_2^2} \exp(\alpha_2 Z) + \frac{P_4^{(o)}}{\alpha_4^2} \exp(\alpha_4 Z) + \frac{a}{2(1-a^2)} C_2^{(o)} \exp(-RZ) + \left[V_o^{(o)} + V_1^{(o)} \frac{Z}{\mu_o} + V_2^{(o)} \frac{Z^2}{\mu_o^2} \right] \exp\left(-\frac{Z}{\mu_o}\right) + C_4^{(o)} \tag{5-43}$$

where

$$Q_o^{(o)} = \frac{6\eta^{-1}\lambda}{(R^2 - \frac{1}{\mu_o^2})(1 - a^2/2)} \left\{ -a\left(1 + \frac{7}{8}a^2\right)\left(d_o^{(o)} + \tfrac{1}{4}\right) + \tfrac{1}{4}\left[1 + \frac{3a^2}{4}(1 - 6a^2) \right] + \frac{1}{\mu_o^2 (R^2 - \frac{1}{\mu_o^2})} \left[-2a\left(1 + \frac{7}{8}a^2\right) d_1^{(o)} + 1 + \frac{3a^2}{4}(1 - 6a^2) \right] \right\}$$

$$Q_1^{(o)} = \frac{6\eta^{-1}\lambda}{(R^2 - \frac{1}{\mu_o^2})(1 - a^2/2)} \{-a(1 + \frac{7}{8}a^2)d_1^{(o)} + \tfrac{1}{2}\left[1 + \frac{3a^2}{4}(1 - 6a^2)\right](q_1^{(o)} - \frac{a}{4})$$

$$+ \frac{4}{\mu_o^2(R^2 - \frac{1}{\mu_o^2})}\left[-a(1 + \frac{7}{8}a^2)(d_2^{(o)} + \frac{a^2}{16}) + \tfrac{1}{2}(1 + \frac{3a^2}{4}(1 - 6a^2))\right] \}$$

$$Q_2^{(o)} = \frac{6\eta^{-1}\lambda}{(R^2 - \frac{1}{\mu_o^2})(1 - a^2/2)} \{-a(1 + \frac{7}{8}a^2)(d_2^{(o)} + \frac{a^2}{16}) + \tfrac{1}{2}\left[1 + \frac{3a^2}{4}(1 - 6a^2)\right]q_2^{(o)}$$

$$P_2^{(o)} = a(r^2 - \tfrac{1}{2}\alpha_2^2)S_2 - \frac{3\eta^{-1}\lambda}{(1 - a^2/2)} \{a(1 + \frac{7}{8}a^2) - \frac{\beta_2}{2}\left[1 + \frac{3a^2}{4}(1 - 6a^2)\right] \}c_2^{(o)}$$

$$P_4^{(o)} = a(r^2 - \tfrac{1}{2}\alpha_4^2)S_4 - \frac{3\eta^{-1}\lambda}{(1 - a^2/2)} \{a(1 + \frac{7}{8}a^2) - \frac{\beta_4}{2}\left[1 + \frac{3a^2}{4}(1 - 6a^2)\right] \} c_4^{(o)}$$

$$V_o^{(o)} = \mu_o^2\{ar^2(Q_o^{(o)} + 2Q_1^{(o)} + 6Q_2^{(o)}) - 3\eta^{-1}\lambda\left[(1 + \frac{3}{2}a^2)(d_o^{(o)} + 2d_1^{(o)} + 6d_2^{(o)}\right.$$

$$\left. + \tfrac{1}{4}(1 + \frac{a^2}{4})) + \frac{3}{2}a(1 + \frac{a^2}{4})(q_o^{(o)} + 2q_o^{(o)} + 6q_2^{(o)} - \frac{a}{4})\right] \} - \frac{a}{2}(Q_o^{(o)} - 8Q_2^{(o)})$$

$$V_1^{(o)} = \mu_o^2\{ar^2(Q_1^{(o)} + 4Q_2^{(o)}) - 3\eta^{-1}\lambda\Big[(1+\frac{3}{2}a^2)(d_1+d_2+\frac{a^2}{16})$$

$$+\frac{3}{2}a(1+\frac{a^2}{4})(q_1^{(o)}+q_2^{(o)}-\frac{a}{4})\Big]\} - \frac{a}{2}(Q_o^{(o)} - 2Q_1^{(o)} + 3Q_2^{(o)})$$

$$V_2^{(o)} = \mu_o^2\{ar^2Q_2^{(o)} - 3\eta^{-1}\lambda\Big[(1+\frac{3}{2}a^2)(d_2^{(o)}+\frac{a^2}{16}) + \frac{3}{2}a(1+\frac{a^2}{4})q_2^{(o)}\Big]\}$$

$$- \frac{a}{2}Q_2^{(o)}$$

The constants of integration are given by

$$C_2^{(o)} = \frac{M_2^{(o)} - aM_1^{(o)}}{m_2 - a m_1} \quad \text{and} \quad C_4^{(o)} = \frac{\eta}{\sqrt{3}}(m_1 C_2^{(o)} - M_1)$$

where

$$M_1^{(o)} = -(\frac{P_2^{(o)}}{\alpha_2} + \frac{P_4^{(o)}}{\alpha_4}) + \mu_o(V_o^{(o)} - V_1^{(o)}) + \frac{\sqrt{3}}{\eta}\Big[\frac{P_2^{(o)}}{\alpha_2^2} + \frac{P_4^{(o)}}{\alpha_4^2} + \mu_o^2 V_o^{(o)}$$

$$+ \frac{a}{2}(S_2 + S_4 + Q_o^{(o)})\Big]$$

$$M_2^{(o)} = -(\alpha_2 S_2 + \alpha_4 S_4) + \frac{1}{\mu_o}(Q_o^{(o)} - Q_1^{(o)}) + \frac{\sqrt{3}}{\eta}\Big[S_2 + S_4 + Q_o +$$

$$a(\frac{P_2^{(o)}}{\alpha_2^2} + \frac{P_4^{(o)}}{\alpha_4^2} + \mu_o^2 V_o^{(o)})\Big]$$

Equation (5-34), with $J_o^s(Z)$, $J_1^P(Z)$ and $H_1^P(Z)$ given by equations (5-40), (5-39) and (5-41) respectively, is the solution of Giovannelli's equation for the infrared field in a semi-infinite cloud with sinuisoidal transverse density fluctuation.

c. Temperature

From equation (4-43) the temperature distribution can be obtained straightforwardly, i.e.

$$T(X,Z) = \{J_p(X,Z) + \lambda\eta\left[J_s(X,Z) + \tfrac{1}{4}\exp\left(-\tau_o(X,Z;\mu_o,\phi_o)\right)\right]\}^{\frac{1}{4}} \qquad (5\text{-}44)$$

where $J_p(X,Z)$ is given by equation (5-16) and $J_s(X,Z)$ by equation (5-34). The attenuated field is calculated simply with the help of equation (5-9).

d. Results and Discussion

With the help of the approximate analytical solutions obtained in the foregoing sections, an attempt to gain insight into the physics of the radiative heating problem in non-homogeneous clouds will be made in this section.

The basic parameters defining the semi-infinite cloud model are: the amplitude of the density fluctuation a, the albedo for single scattering $\bar{\omega}$, the Greenhouse parameter η and the parameter r which measures the optical thickness of the density fluctuations. Each set of values (a, $\bar{\omega}$, η, r) determines a particular cloud model. Let us fix a = 0.1 this value is a reasonable one to ensure the rapid convergence of the power series of exponentials and the introduction of small errors only. We shall also fix $\bar{\omega}$ = 0.5 which is a reasonable mean value for interstellar dust clouds of interest in this study. With these values we shall consider the behaviour of the radiation field and the temperature in the inhomogeneous semi-infinite model.

In the model under consideration, plane parallel incidence was assumed with polar and azimuthal angles $\cos^{-1}\mu_o$ and ϕ_o. A better representation for the interstellar radiation field falling upon interstellar clouds would be isotropic incidence. An appropriate representation of such an incident field would be a plane parallel field incident with angles $\mu_o = 1/\sqrt{3}$ and $\phi_o = \pi/4$ which is approximately equivalent to integrating the incident isotropic field with one quadrature point in μ_o ($= 1/\sqrt{3}$) and one in ϕ_o ($= \pi/4$).

We consider first the visual field J_s. Within the accuracy of solutions (5-16), calculations between $10^{-4} \leq r \leq 10^{+4}$ show that $J_o^s(Z)$ exhibits only a very weak dependence on r. $J_o^s(Z)$ is shown in Figure 5-2. As expected, $J_o^s(Z)$ is very similar to the solution for the homogeneous cloud showing a rapid increase from the boundary to maximum value at $Z \approx 0.4$ followed by an exponential decay. Curves for different values of r are indistinguishable on the scale of Figure 5-2.

The difference between the radiation field at maximum and minimum density is a measure of the fluctuation of the radiation field. This difference has been plotted in Figure 5-3 as a function of r for several values of Z. It is seen that except for values of Z close to the boundary, $\Delta J_s(Z) = J_s(\pi,Z) - J_s(0,Z)$ tends very quickly to 0 when r is greater than 1.0. When $r >> 1$, the wavelength of the density fluctuation is small with respect to the mean free path of the visual photons, and fluctuations of the diffuse field become negligible. This occurs because visual photons can cross many inhomogeneities before being extinguished. In this case the photons

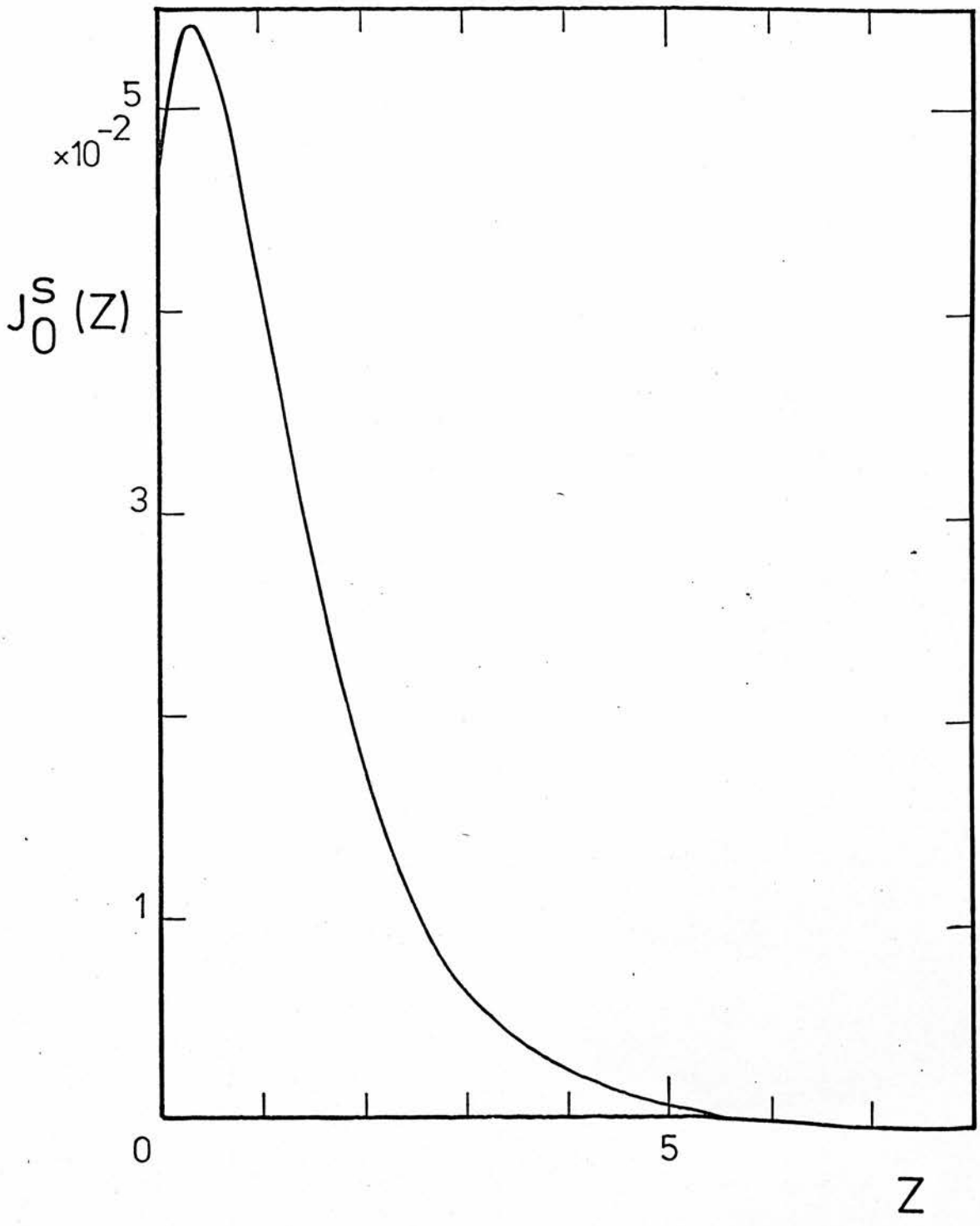

Fig. 5-2 The function $J_o^s(Z)$ for any value of r.
$\bar{\omega} = 0.5$, $a = 0.1$, $\mu_o = 1/\sqrt{3}$, $\phi_o = \pi/4$

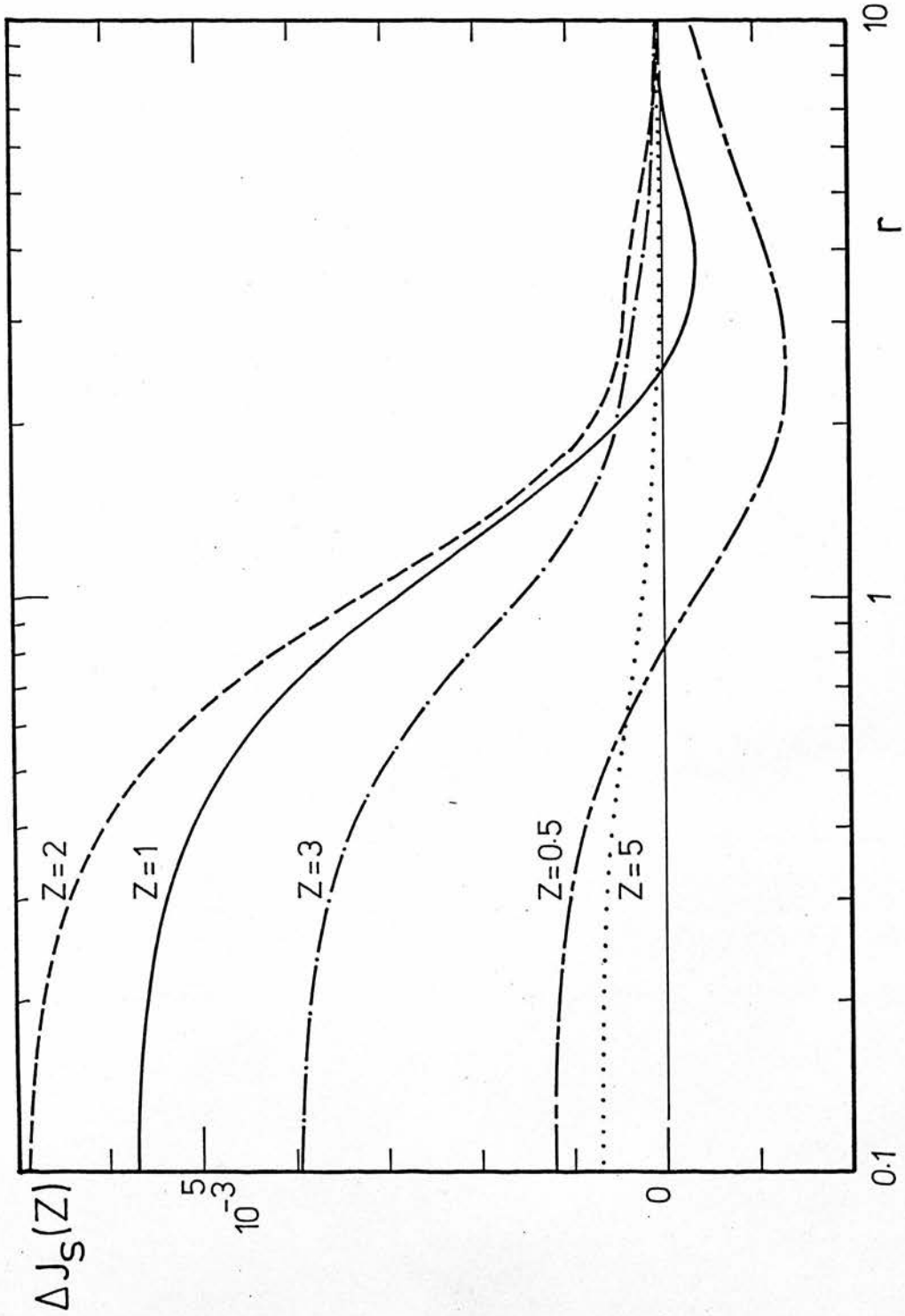

Fig. 5-3 The fluctuation of the visual radiation field $\Delta J_s(Z) = J_s(\pi,Z) - J_s(o,Z)$ as a function of r, for several values of Z. $\bar{\omega} = 0.5$, $a = 0.1$, $\mu_o = 1/\sqrt{3}$, $\phi_o = \pi/4$

"cannot detect" such inhomogeneities and the solution $J_s(X,Z)$ tends to the solution of the homogeneous case.

When $r << 1$, the wavelength of the density fluctuations is greater than the mean free path of the visual photons, $\Delta J_s(Z)$ becomes independent of r and the solution $J_s(X,Z)$ tends to the solution corresponding to the homogeneous case with density determined by the X value.

The function $\Delta J_s(Z)$ has been plotted in figure 5-4 for $r \leq 0.1$, $r = 1.0$ and $r = 10.0$. The strong coupling of $\Delta J_s(Z)$ with Z is evident. Except towards the boundary, $\Delta J_s(Z)$ is positive which means that a maximum density corresponds to a minimum mean intensity, and a minimum density corresponds to a maximum mean intensity. Towards the surface, $Z \lesssim 0.5$ (the exact value depends on r) the above correspondence is reversed. This is due to the face that near the boundary, the diffuse field builds up more slowly in regions of low density than in regions of high density.

Figure 5-4 also shows that each curve presents a maximum near to $Z \simeq 1.5$. The exact value at which the maximum is reached depends on the r value, which means that the fluctuation of the diffuse field is maximised at this depth. This fact is of particular importance because, as will be shown below, it is just at depths $1 \lesssim Z \lesssim 3$* that the visual diffuse field dominates the attenuated and infrared fields.

In Figure 5-5a, the mean infrared field $J_o^p(Z)$ has been plotted for $\eta = 50$, 10^2, 10^3 and 10^4. Within the range of accuracy of

* Strictly speaking, the exact value of this depth depends on the particular $\bar{\omega}$ value and increases for higher values of the albedo up to the asymptotic value corresponding to conservative scattering. This is the main effect of the albedo on the visual field.

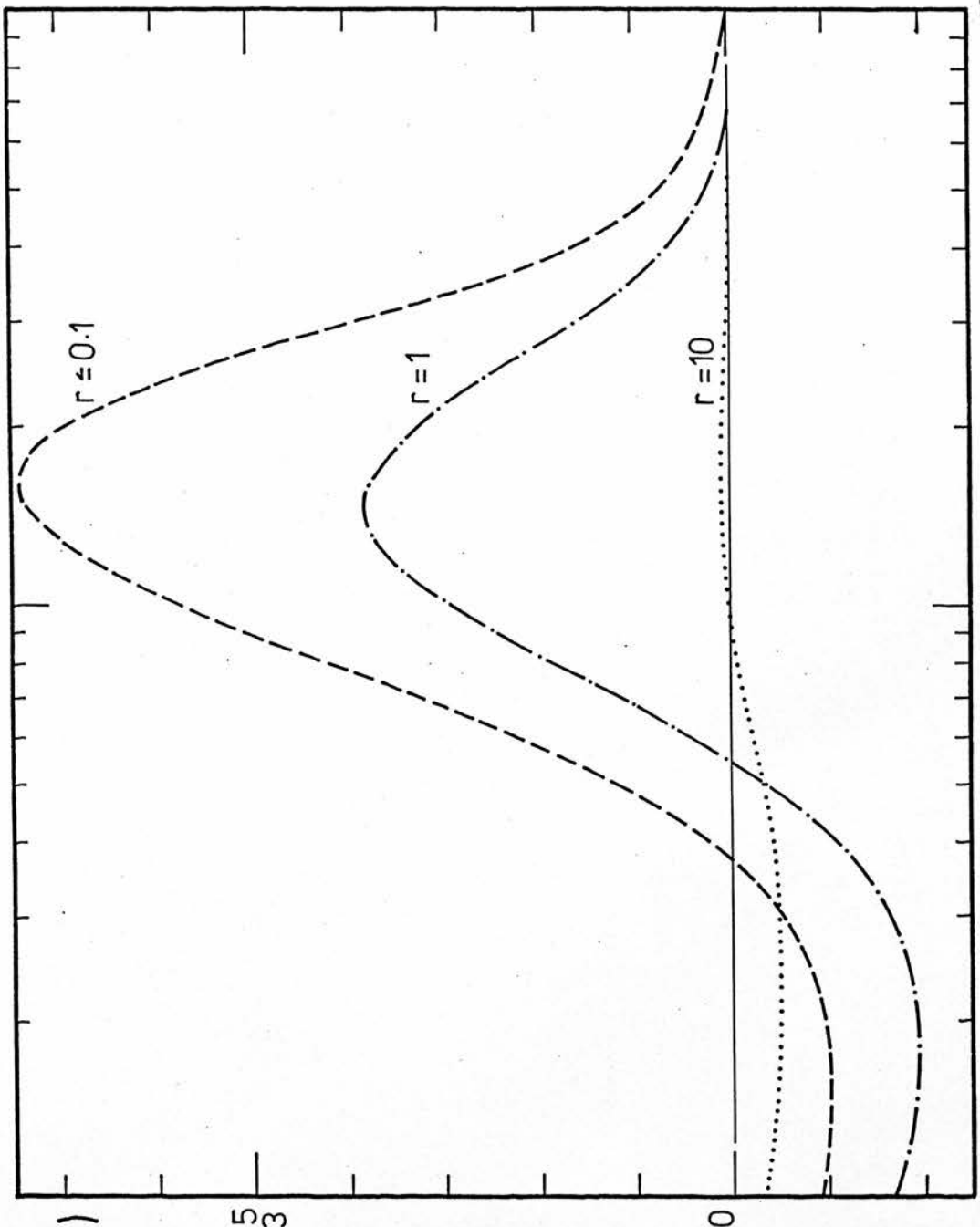

Fig. 5-4 The fluctuation of the visual radiation field $\Delta J_S(Z) = J_S(\pi,Z) - J_S(o,Z)$ as a function of Z for several values of r. $\bar{\omega} = 0.5$, $a = 0.1$, $\mu_o = 1/\sqrt{3}$, $\phi_o = \pi/4$

solution (5-34), as in the visual case, $J_o^p(Z)$ presents only a very weak dependence on r. One notes that for large values of the Greenhouse parameter $\eta(\gtrsim 50)$ $J_o^p(Z)$ is quasi-constant through the cloud. The change between the surface and optical depths of $Z \gtrsim 10$ is 2.82% for $\eta = 50$, 1.41% for $\eta = 10^2$, 0.14% for $\eta = 10^3$ and 0.01% for $\eta = 10^4$. The insensitivity of $J_o^p(Z)$ to the particular value of η, for $\eta \gtrsim 50$, is clear. These results are expected on physical grounds, because for such large values of η the region of the cloud where the thermal radiation is generated tends to be optically thin in the infrared due to the very large mean free path of the infrared photons with respect to the visual ones. The opposite occurs when η is small ($\eta \lesssim 1$). In this case the mean free path of the infrared photons is small and they tend to be trapped into the cloud (Greenhouse effect)*. This explains the steep increases of $J_o^p(Z)$ when one changes η from 10^2 to 1 as shown in Figure 5-5b. Such an effect is still more pronounced if one compares Figures 5-5a and 5-5b with Figure 5-5c where $J_o^p(Z)$ has been plotted for $\eta = 10^{-2}$.

As expected, $J_o^p(Z)$ presents a similar behaviour to the solution for the diffuse visual field in conservative clouds.

The fluctuation in the infrared $\Delta J_p(Z) = J_p(\pi,Z) - J_p(0,Z)$ has been plotted in Figure 5-6a for $\eta = 10^2$. This fluctuation is less, by more than one order of magnitude, than the fluctuation in the visual field, see Figure 5-3, and it will have negligible effect on temperature as will be seen later, for $\eta >> 1$. Nevertheless, it deserves some comments of heuristic value.

* Strictly speaking, this effect occurs for large values of η too. But for $\eta < 1.0$ it is magnified by several orders of magnitude.

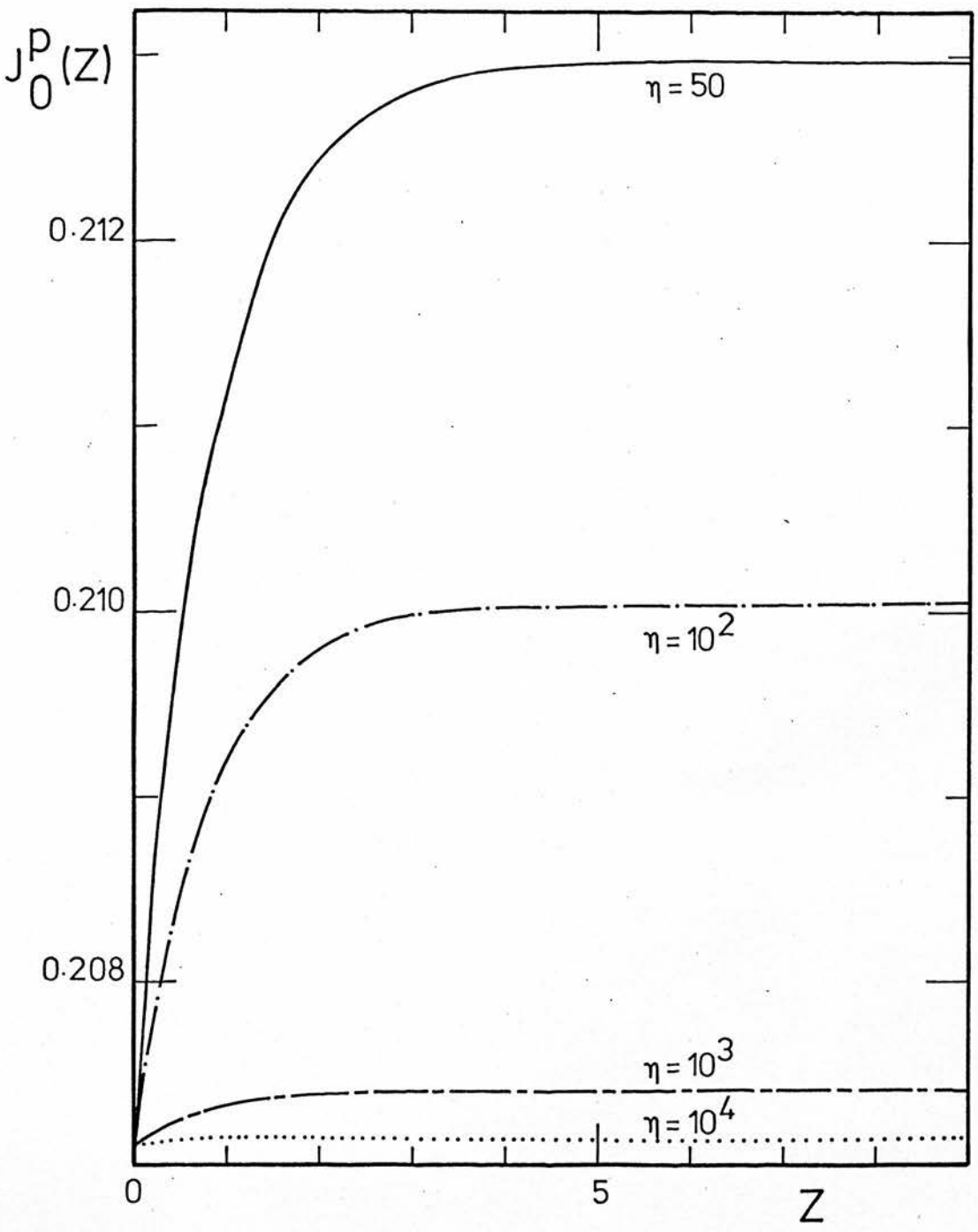

Fig. 5-5a The function $J_o^P(Z)$ for several values of η but any value of r.

$\overline{\omega} = 0.5$, $a = 0.1$, $\mu_o = 1/\sqrt{3}$, $\phi_o = \pi/4$

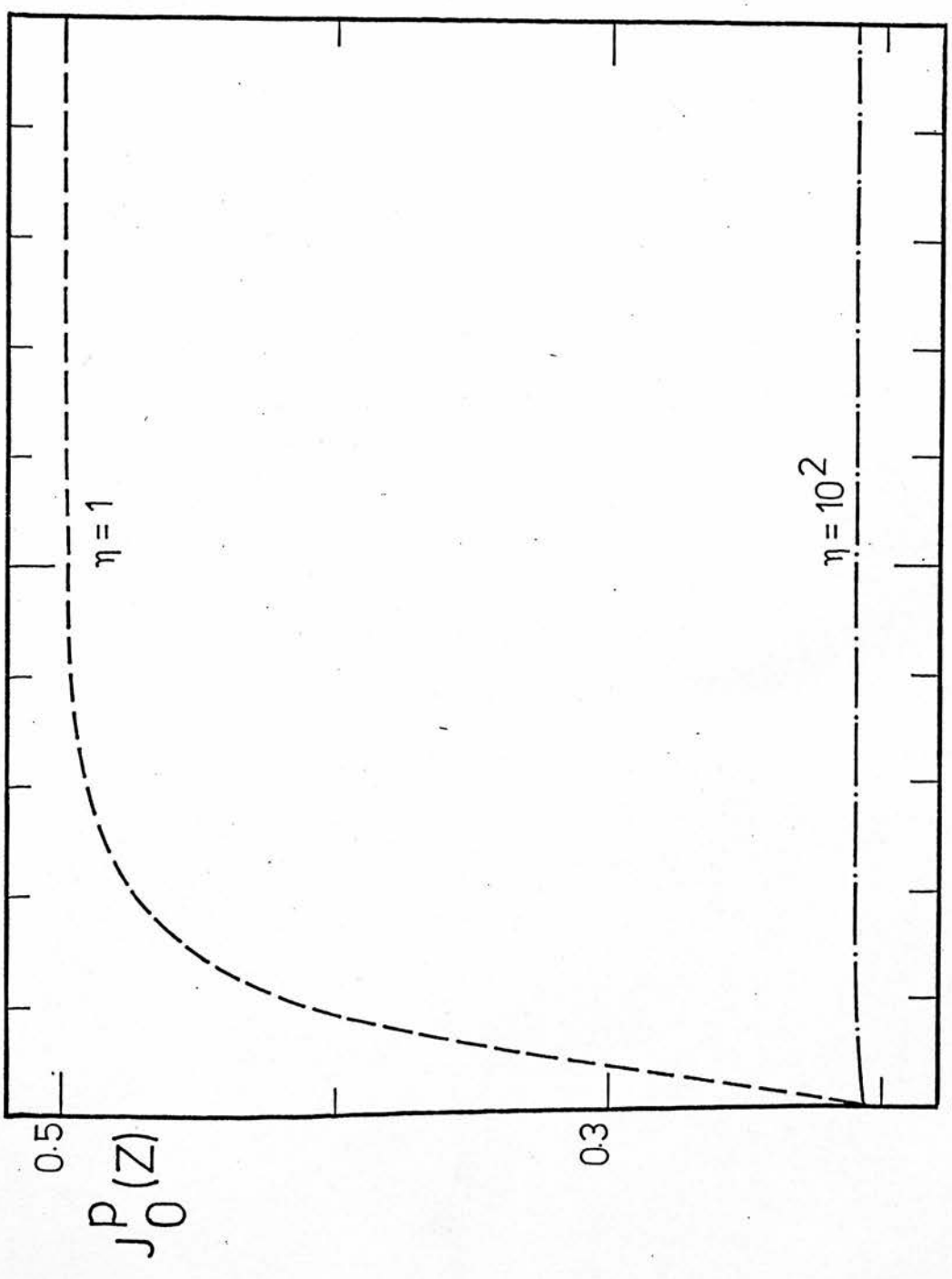

Fig. 5-5b The function $J_o^P(Z)$ for several values of η but any value of r. $\bar{\omega} = 0.5$, $a = 0.1$, $\mu_o = 1/\sqrt{3}$, $\phi_o = \pi/4$

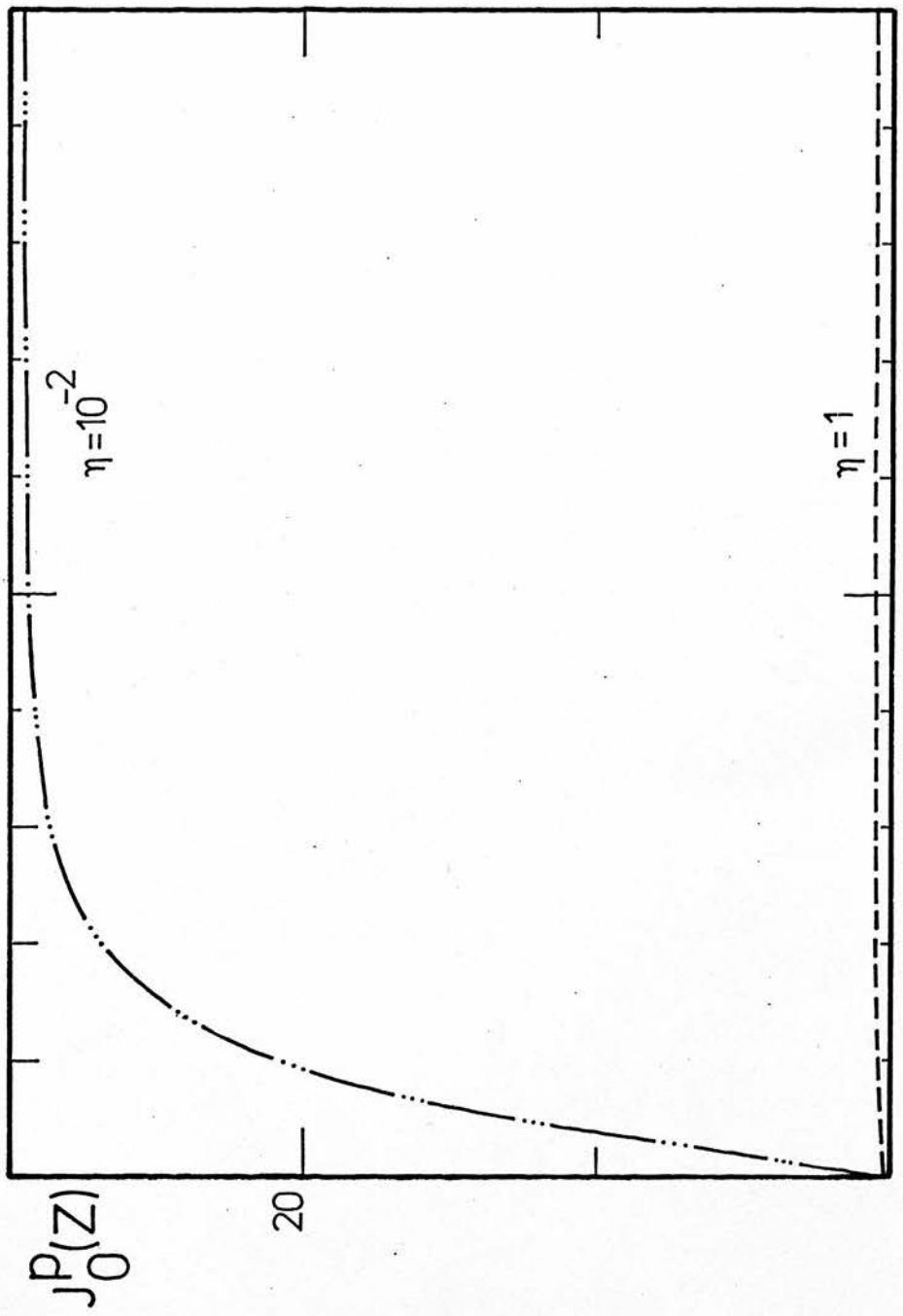

Fig. 5-5c The function $J_o^P(Z)$ for several values of η but any value of r. $\bar{\omega} = 0.5$, $a = 0.1$, $\mu_o = 1/\sqrt{3}$, $\phi_o = \pi/4$

An interesting property of $\Delta J_p(Z)$ is that for $Z \gtrsim 0.5$, always $\Delta J_p(Z) < 0$, i.e., $J_p(\pi,Z) < J_p(0,Z)$ and maxima of density and mean intensity correspond to each other. This effect, although it is very small for $\eta >> 1$, is a manifestation of the fact that infrared photons tend to be trapped in regions where the density of absorbers (and emitters) is larger.

The above behaviour of $\Delta J_p(Z)$ is better illustrated in Figure 5-6b, where $\Delta J_p(Z)$ has been plotted for $Z = 3.0$ and $\eta = 50$, 10^2 and 10^3. The piling up of infrared photons in denser regions increases with decreasing η because for small values of η the mean free path of infrared photons becomes small and hence more infrared photons are trapped in denser regions. This fact is even more clear in Figure 5-6c where $\Delta J_p(Z)$ is shown as a function of η for three different values of Z (1, 3, 5) and $r = 1.0$. There the values of $\Delta J_s(Z)$ are shown too, for comparison. $\Delta J_s(Z) > \Delta J_p(Z)$ for rather modest values of η ($\approx$5). The situation $\eta \lesssim 1$ is of interest in non-homogeneous media where gases and not grains are responsible for the radiative transport, e.g. planetary atmospheres and clouds.

For very large values of η the effect of piling up infrared photons in denser regions decreases as expected, due to the fact that for large mean free-paths the trapping becomes more and more difficult.

The distribution of temperature will now be considered. This aspect of the radiative heating problem is the main aim of this section.

From equation (5-44) it is seen that the temperature at any

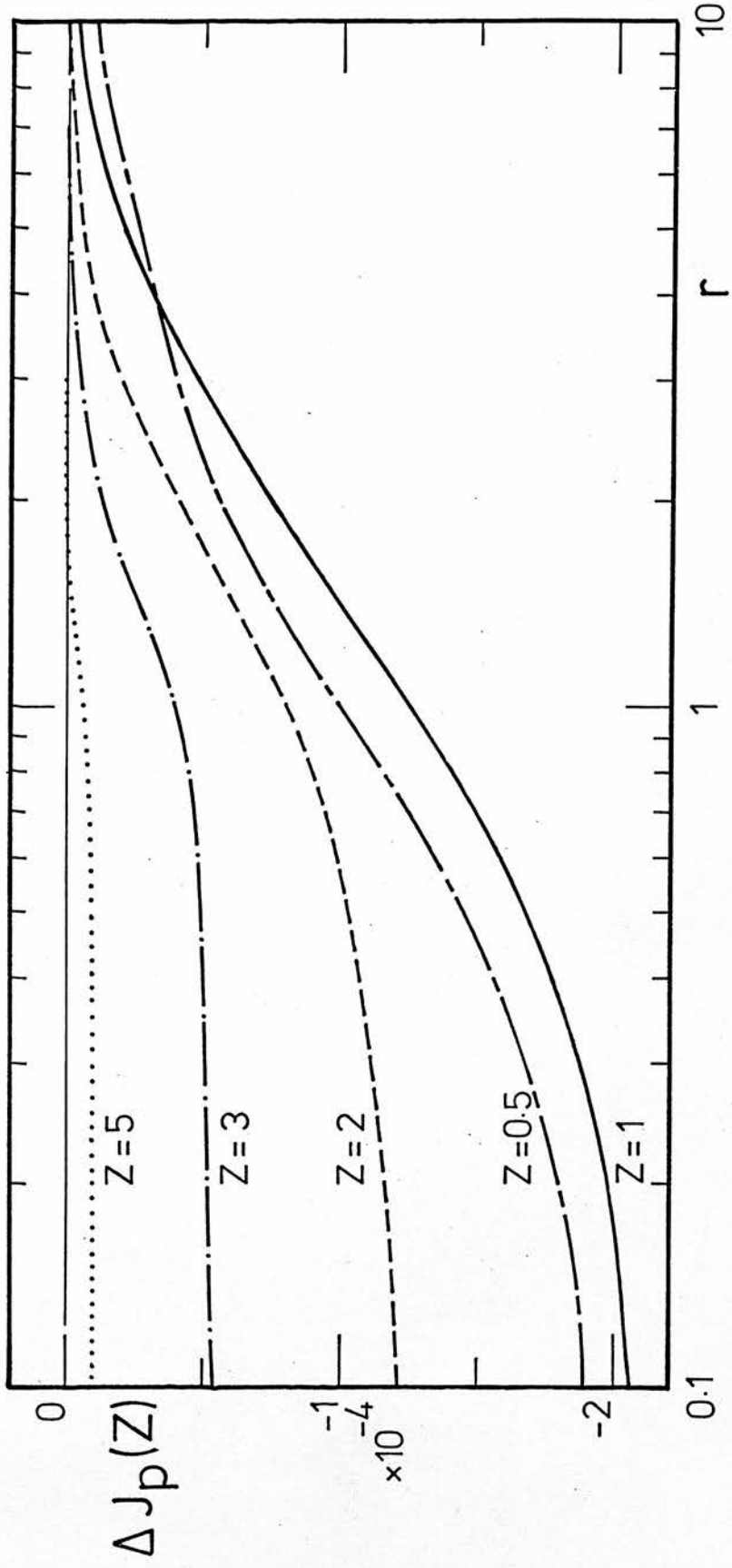

Fig. 5-6a The fluctuation of the infrared field $\Delta J_p(Z) = J_p(\pi,Z) - J_p(0,Z)$ as a function of r for several values of Z. $\eta = 10^2$, $\bar{\omega} = 0.5$, $a = 0.1$, $\mu_o = 1/\sqrt{3}$, $\phi_o = \pi/4$

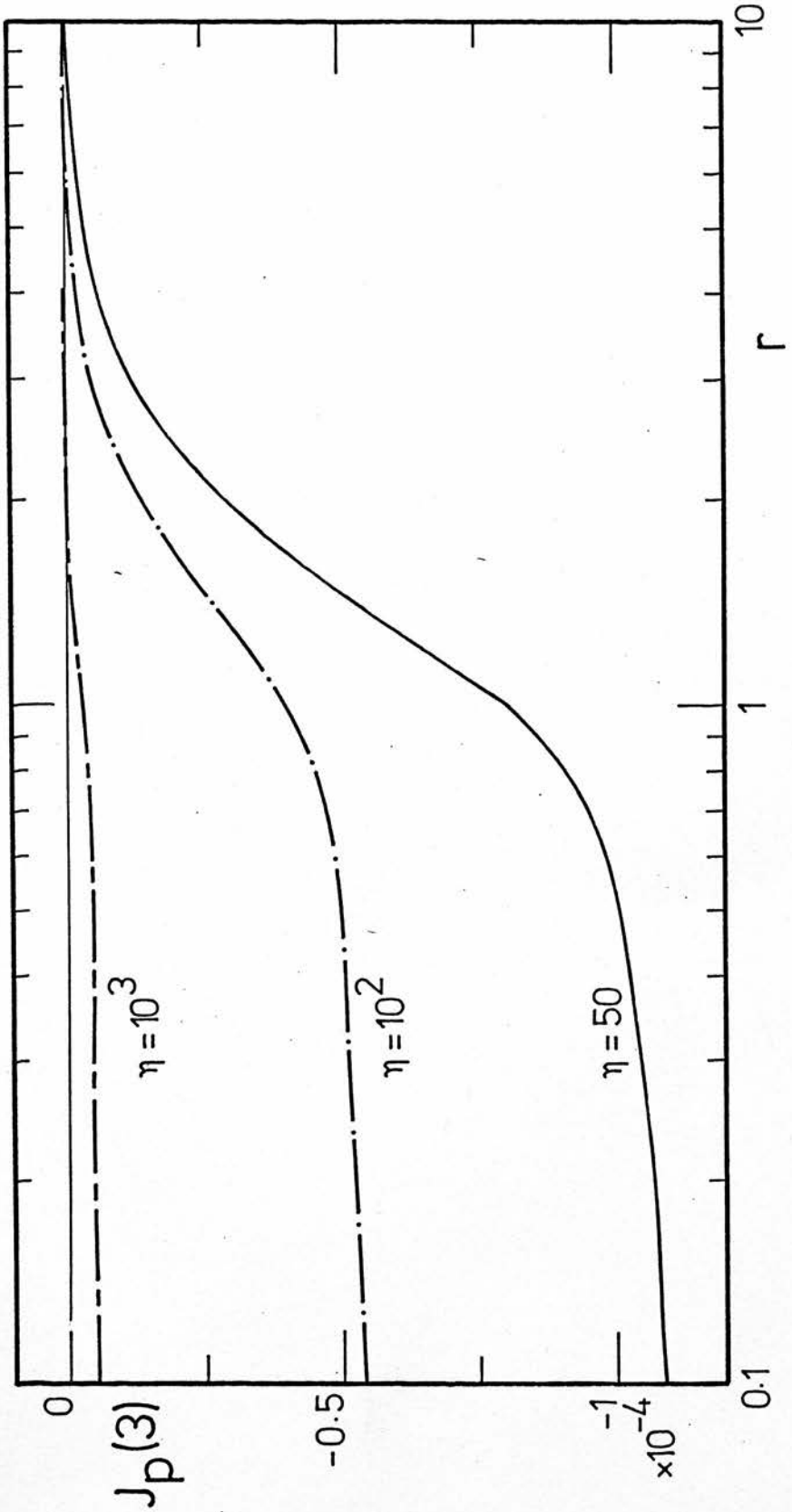

Fig. 5-6b The fluctuation of the infrared field $\Delta J_p(3) = J_p(\pi,3) - J_p(0,3)$ as a function of r for several values of η. $\bar{\omega} = 0.5$, $a = 0.1$, $\mu_o = 1/\sqrt{3}$, $\phi_o = \pi/4$

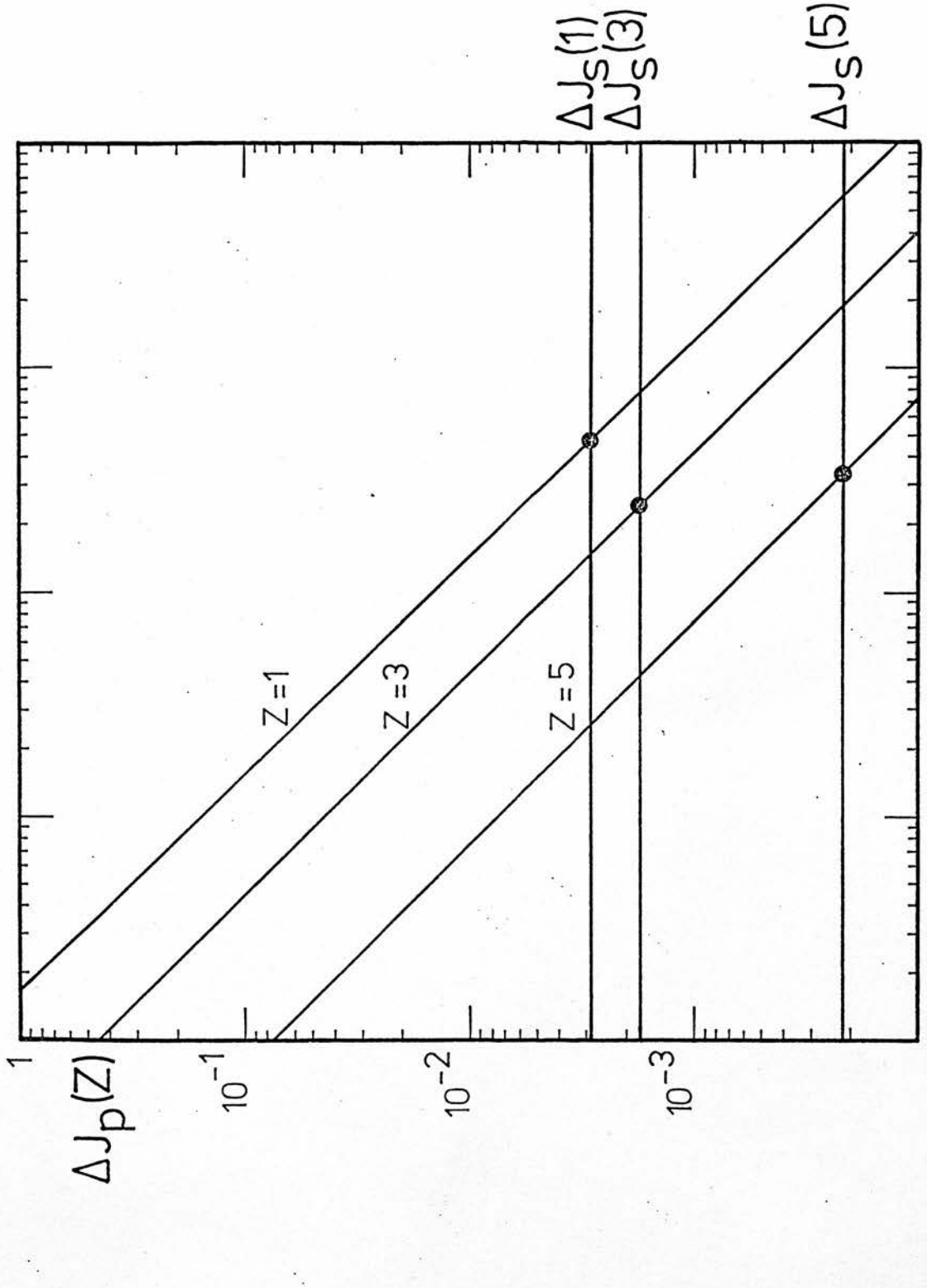

Fig. 5-6c The fluctuation of the infrared field $\Delta J_p(Z)$ as a function of η for several values of Z.
$r = 1.0$, $\bar{\omega} = 0.5$, $a = 0.1$, $\mu_- = 1/\sqrt{3}$, $\phi_- = \pi/4$

point (X,Z) depends on three terms: the infrared field $J_p(X,Z)$, the visual diffuse field $J_s(X,Z)$ and the attenuated field $\frac{1}{4}\exp(-\tau_o(X,Z,\mu_o,\phi_o))$ but these last two terms enter in equation (5-44) multiplied by a factor $(1-\bar{\omega})\eta$. These three terms of equation (5-44) have been plotted in figures 5-7, for different values of η, which give an idea of the range of mean depth Z (measured along $X = \pi/2$) where each field becomes the most important one.

One can say that the grain temperature is practically determined by the attenuated field towards the boundary, i.e. $0 \leq Z \lesssim 1.1$. at greater depths $1.1 < Z \lesssim Z_D$, where $3.0 \lesssim Z_D \lesssim 5$ (the exact value depends on the η value), the diffuse field dominates the infrared. Deep into the cloud, $Z > Z_D$ the temperature is determined by the infrared field as is expected from simple physical considerations.

Figure 5-8 shows the attenuated and visual diffuse fields times $\lambda\eta$ and the infrared J_p for $X = \pi/2$, $Z = 3$ and $r = 1{,}0$, as a function of η. At these depths the mean visual field becomes dominant for rather high values of η (≈ 60).

The temperature $T(X,Z)$ at $X = \pi/2$, which is a measure of the mean temperature, has been plotted in Figure 5-9a for η values, 50.0, 10^2, 10^3 and 10^4. This mean temperature decreases with depth up to values of Z at which the temperature becomes controlled completely by the infrared field. For the rather extreme value of $\eta = 10^4$, this happens at depths of the order of 10. For values of $\eta \approx 10^2$ the value of $T(\pi/2,Z)$ changes by a factor 2.9 between the surface $Z = 0$ and the depths $Z \gtrsim 10$. This value fits well with that obtained

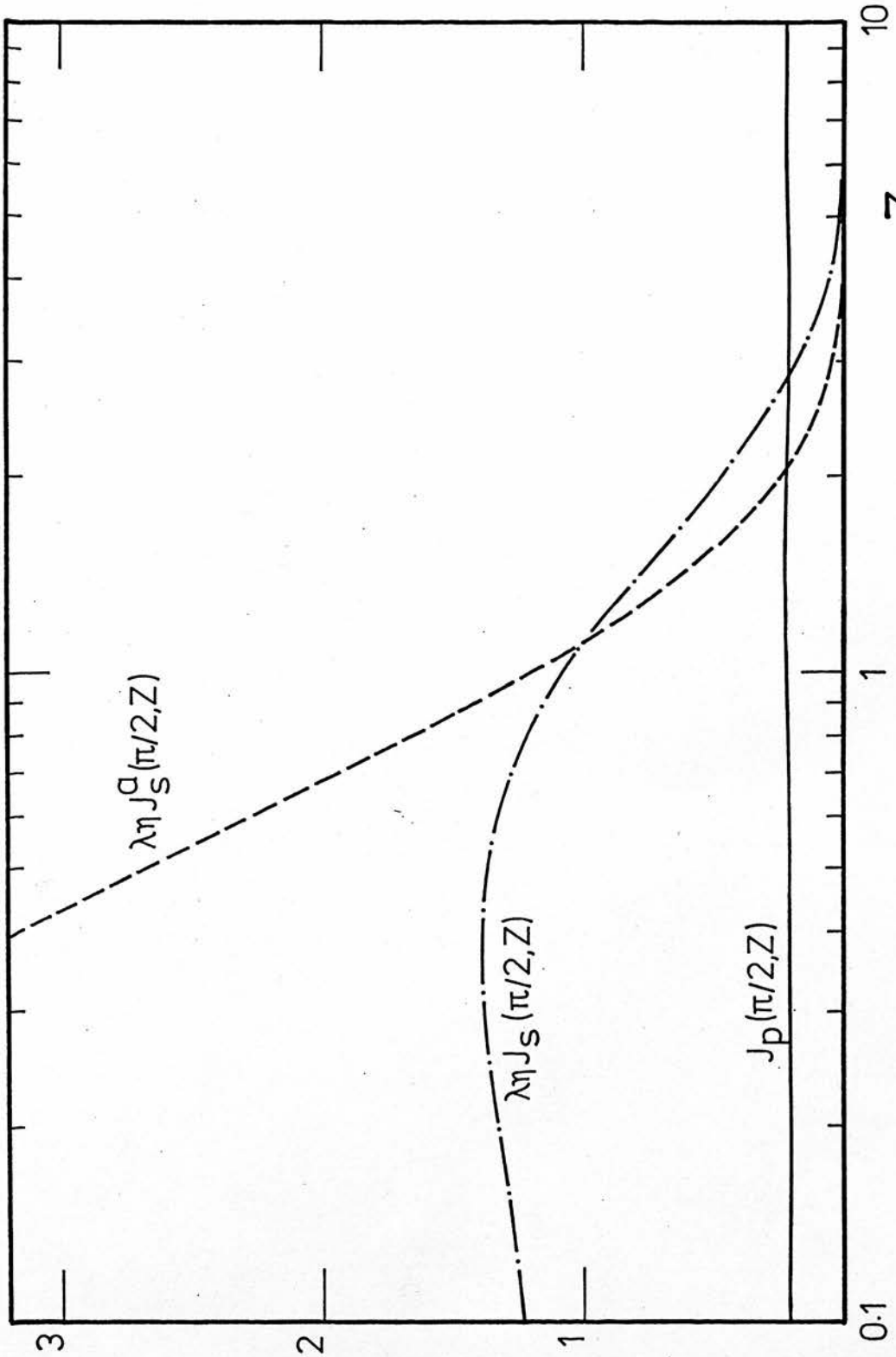

Fig. 5-7a The functions $\lambda\eta J_s(\pi/2,Z)$, $\lambda\eta J_s^a(\pi/2,Z)$ and $J_p(\pi/2,Z)$ as functions of Z.
$\eta = 50$, $r = 1.0$, $\bar{\omega} = 0.5$, $a = 0.1$, $\mu_o = 1/\sqrt{3}$, $\phi_o = \pi/4$

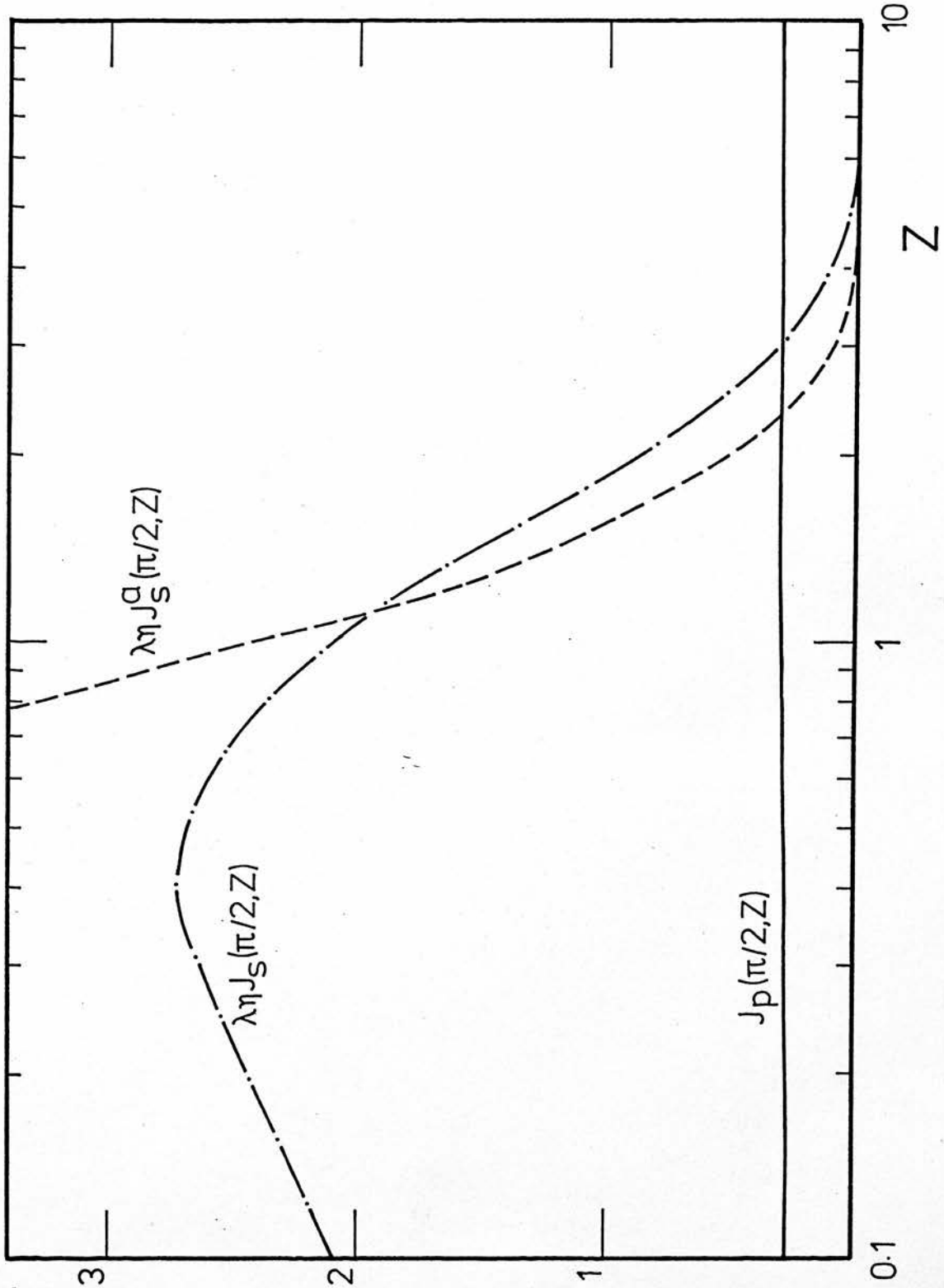

Fig. 5-7b As Fig. 5-7a for $\eta = 10^2$.

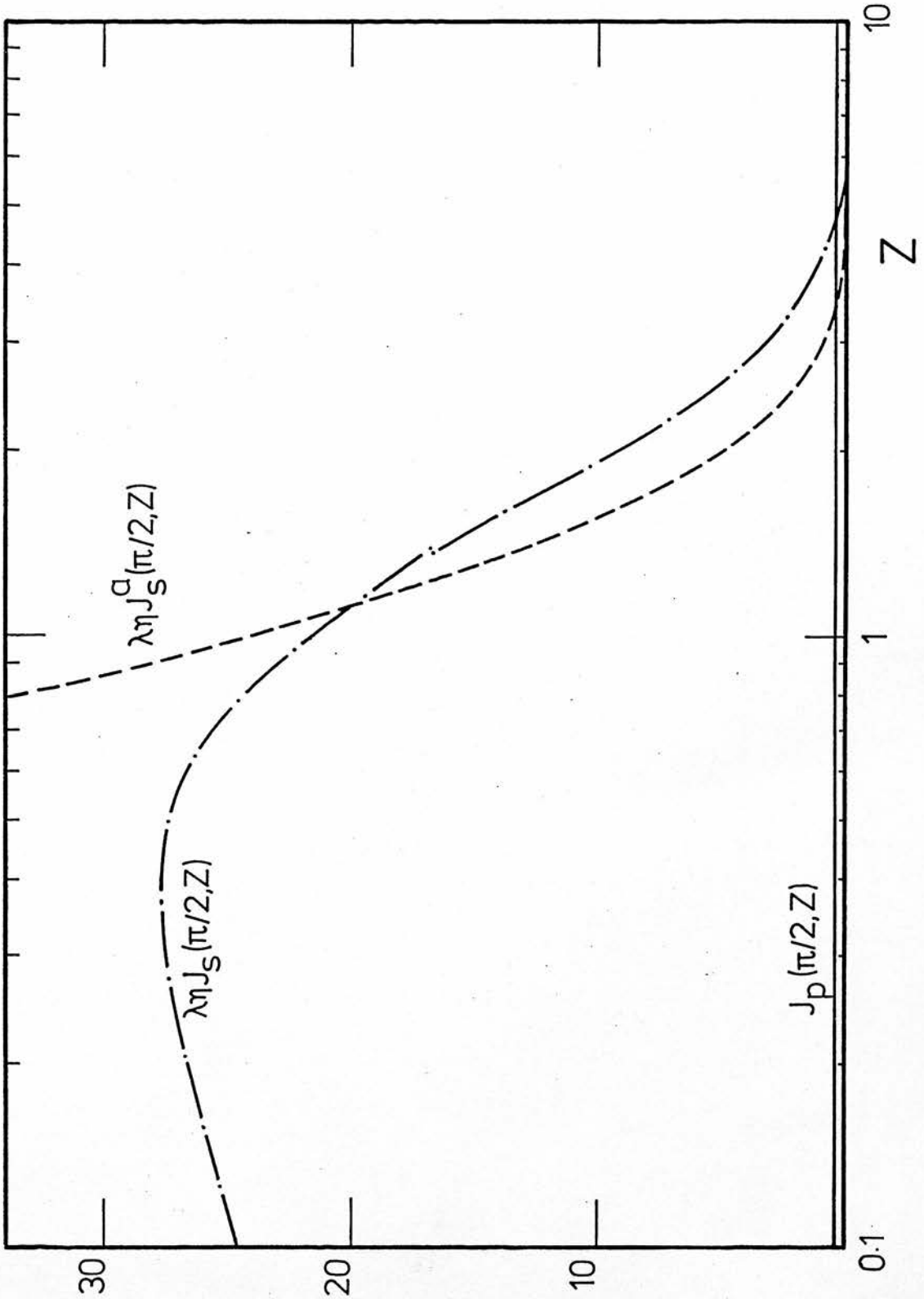

Fig. 5-7c As Fig. 5-7a for $\eta = 10^3$.

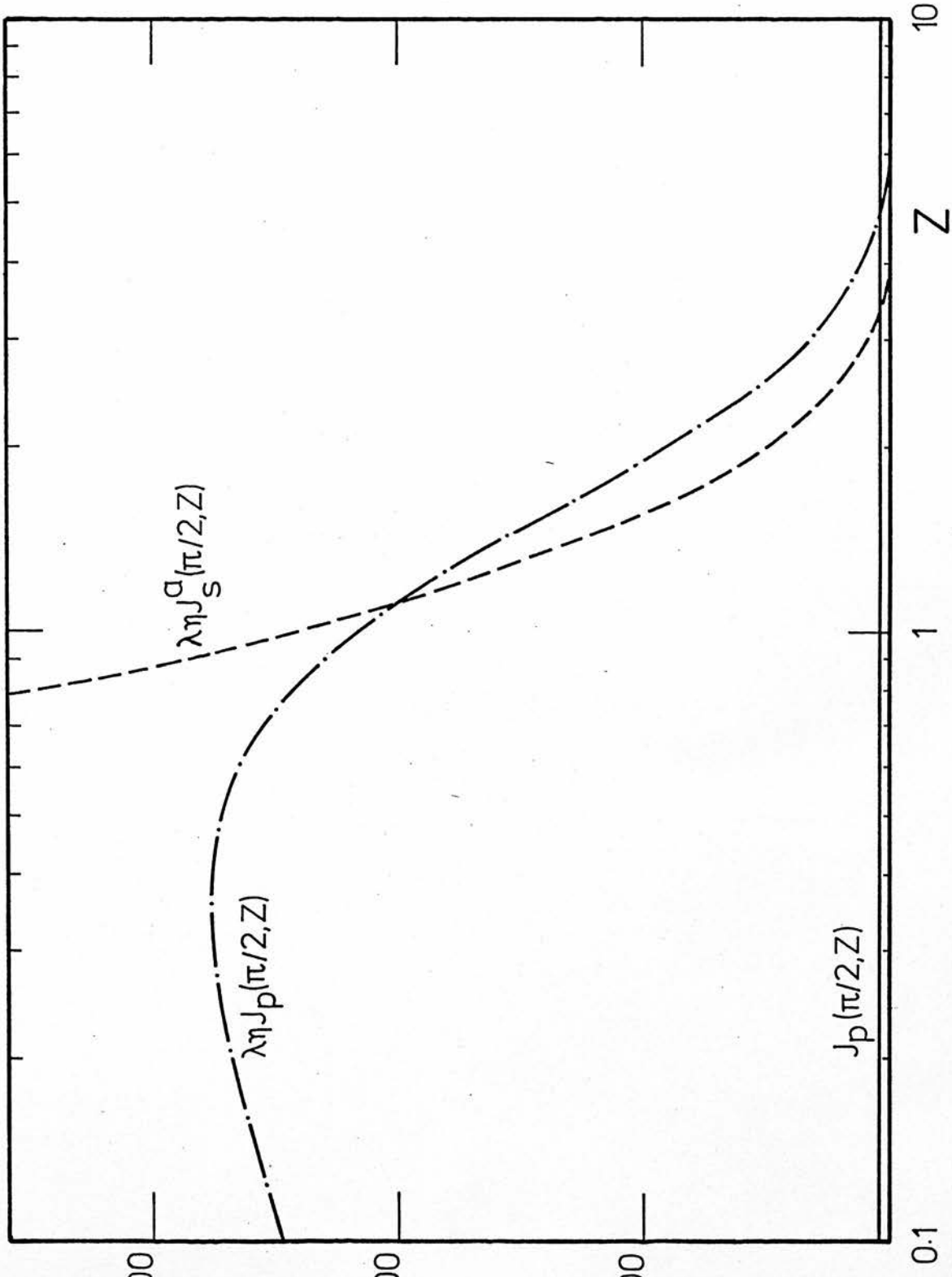

Fig. 5-7d As Fig. 5-7a for $\eta = 10^4$.

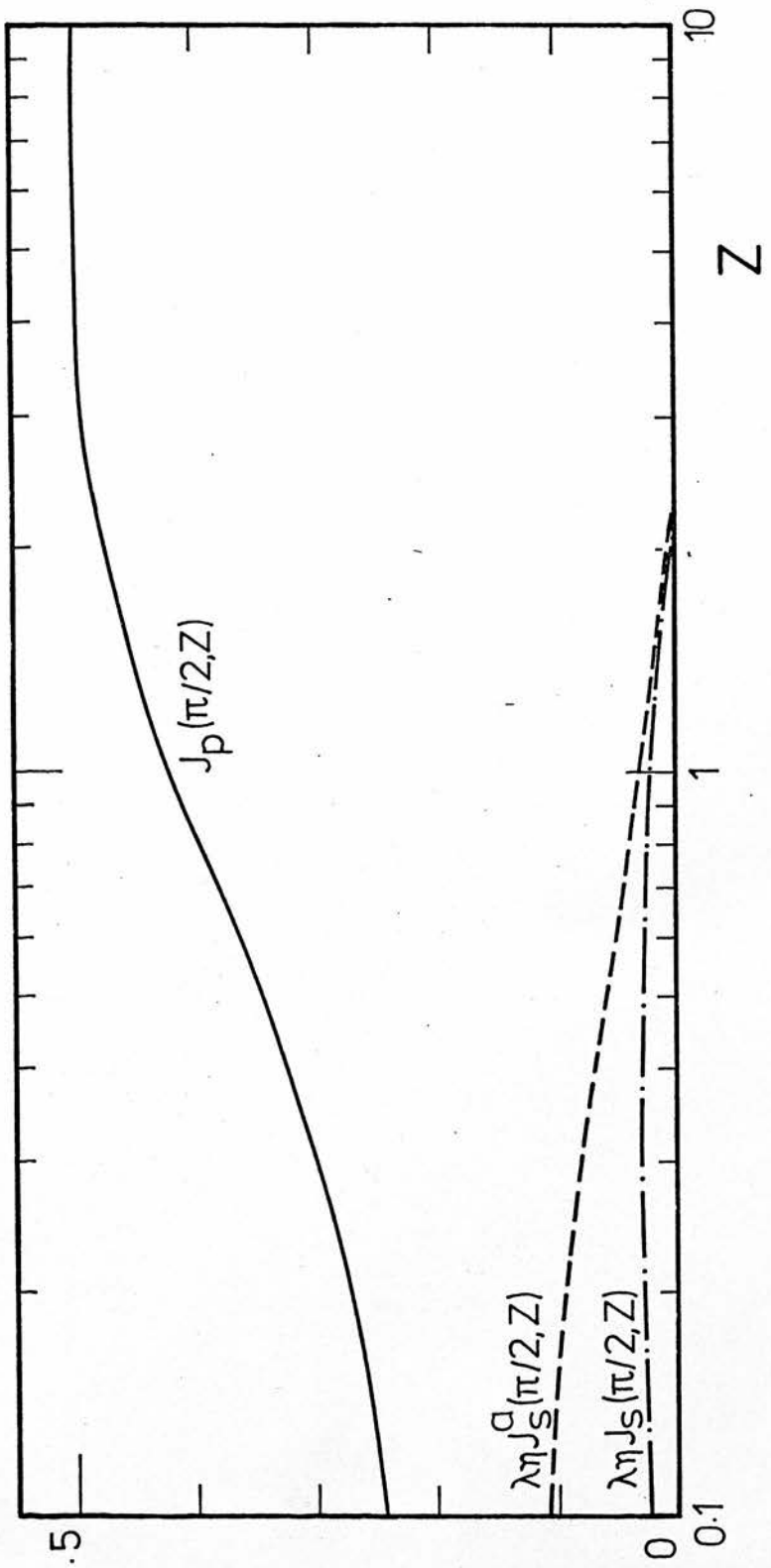

Fig. 5-7e As Fig. 5-7a for $\eta = 1.0$.

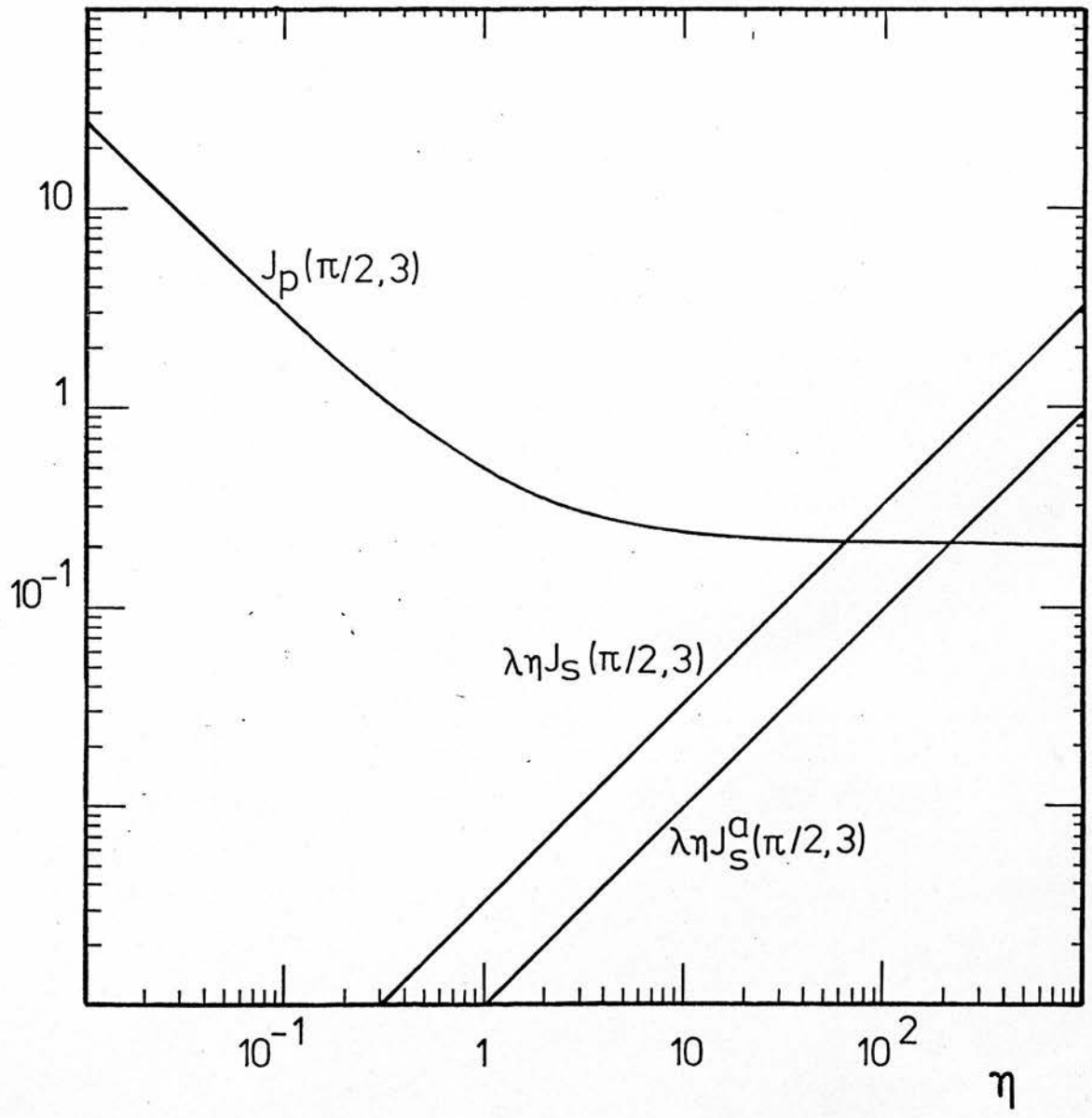

Fig. 5-8 The functions $\lambda\eta\, J_s(\pi/2,3)$, $\lambda\eta\, J_s^a(\pi/2,3)$ and $J_p(\pi/2,3)$ as functions of η. $r = 1.0$, $\bar{\omega} = 0.5$, $a = 0.1$, $\mu_o = 1/\sqrt{3}$, $\phi_o = \pi/4$

from formal homogeneous models.

Figure 5-9b shows the temperature T(X,Z) at $X = \pi/2$ for $\eta = 1.0, 10^{-2}$. For this last value, as expected, the Greenhouse effect becomes evident.

Figures 5-10 show the percentage temperature fluctuation as a function of r at mean optical depths Z = 1.0, 2.0, 3.0, 5.0, where the diffuse field is dominant over or comparable to the attenuated or infrared fields, for $\eta = 50.0, 10^2, 10^3$ and 10^4.

As an illustration, in these figures the horizontal line indicates the percentage of temperature required by equation (3-4) to separate regions where the rate of H_2 formation is given by equation (3-1) with $\gamma = 0.5$ from regions where $\gamma \approx 0.005$.

It is expected that small errors are present mainly due to the somewhat schematic representation to the incident field and to the fact that the source term for the diffuse field $\exp(-\tau_o(X,Z;\mu_o,\phi_o))$ in equation (5-6) has been expanded to a power series in order to solve the system of coupled differential equations. This first aspect is responsible for the small fluctuations appearing for $r > 1.0$ as can be seen if one compares Figure 5-10 with Figure 5-3. As expected, these fluctuations are more exaggerated towards the surface where the attenuated field gains importance.

One important conclusion to be drawn from Figures 5-10 is that although there is a strong coupling between temperature fluctuation and mean optical depth Z, fluctuations with $r > 2.0$ (the exact value depends on η) are unable to produce appreciable temperature fluctuations

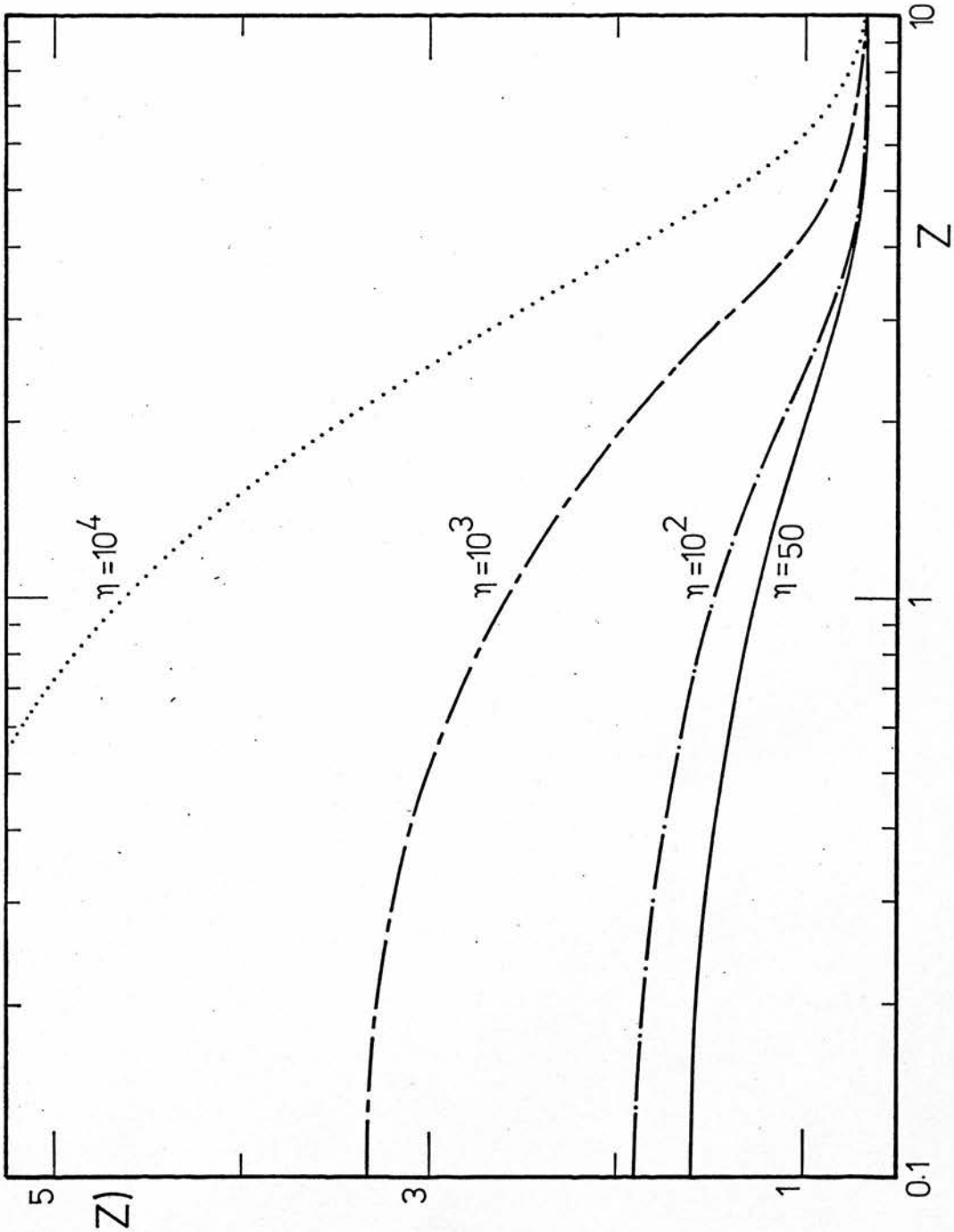

Fig. 5-9a The temperature $T(\pi/2,Z)$ as a function of Z for several values of η.
$r = 1.0$, $\overline{\omega} = 0.5$, $a = 0.1$, $\mu_o = 1/\sqrt{3}$, $\phi_o = \pi/4$

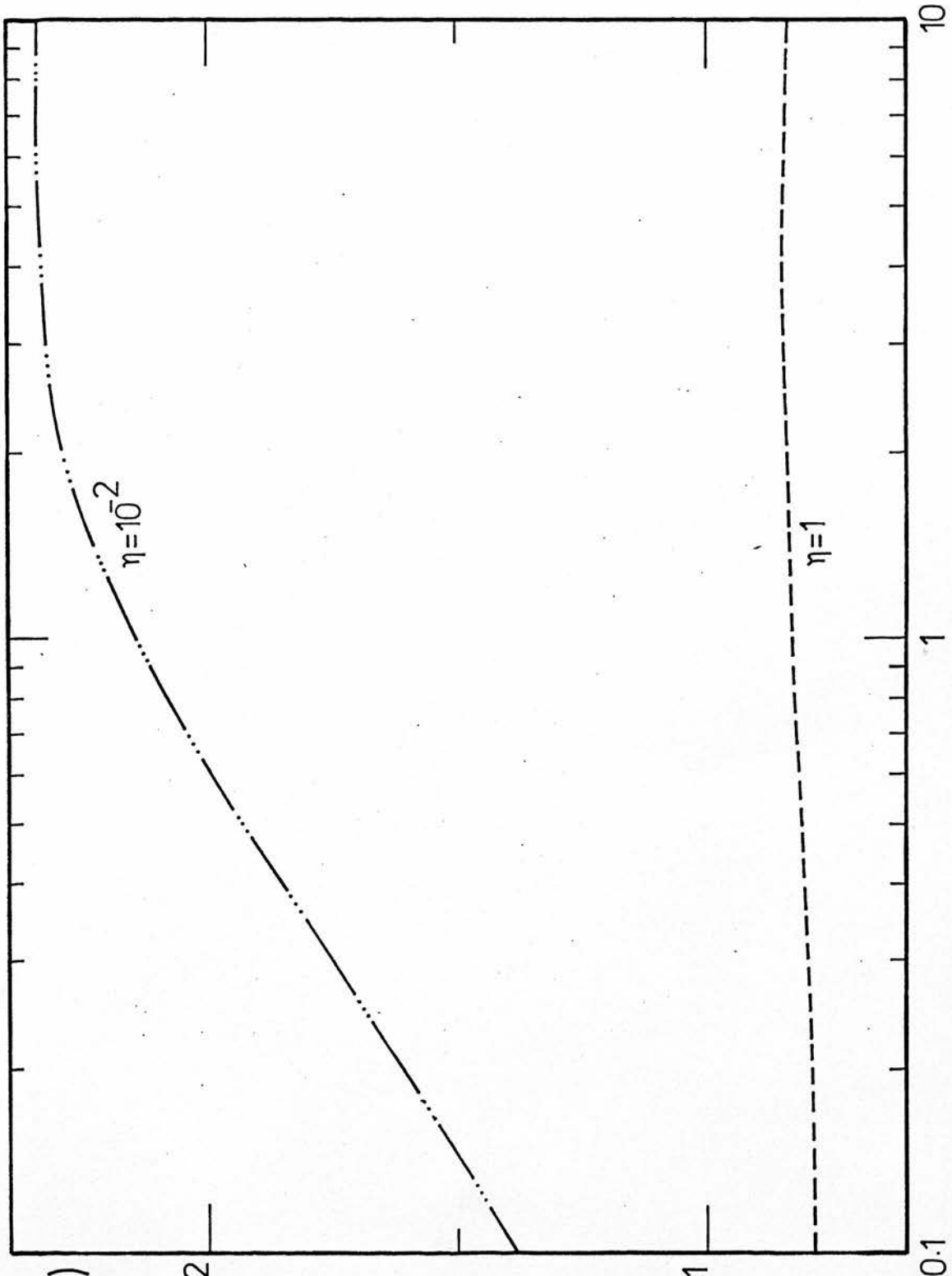

Fig. 5-9b As Fig. 5-9a for η = 1.0 and 10^{-2}.

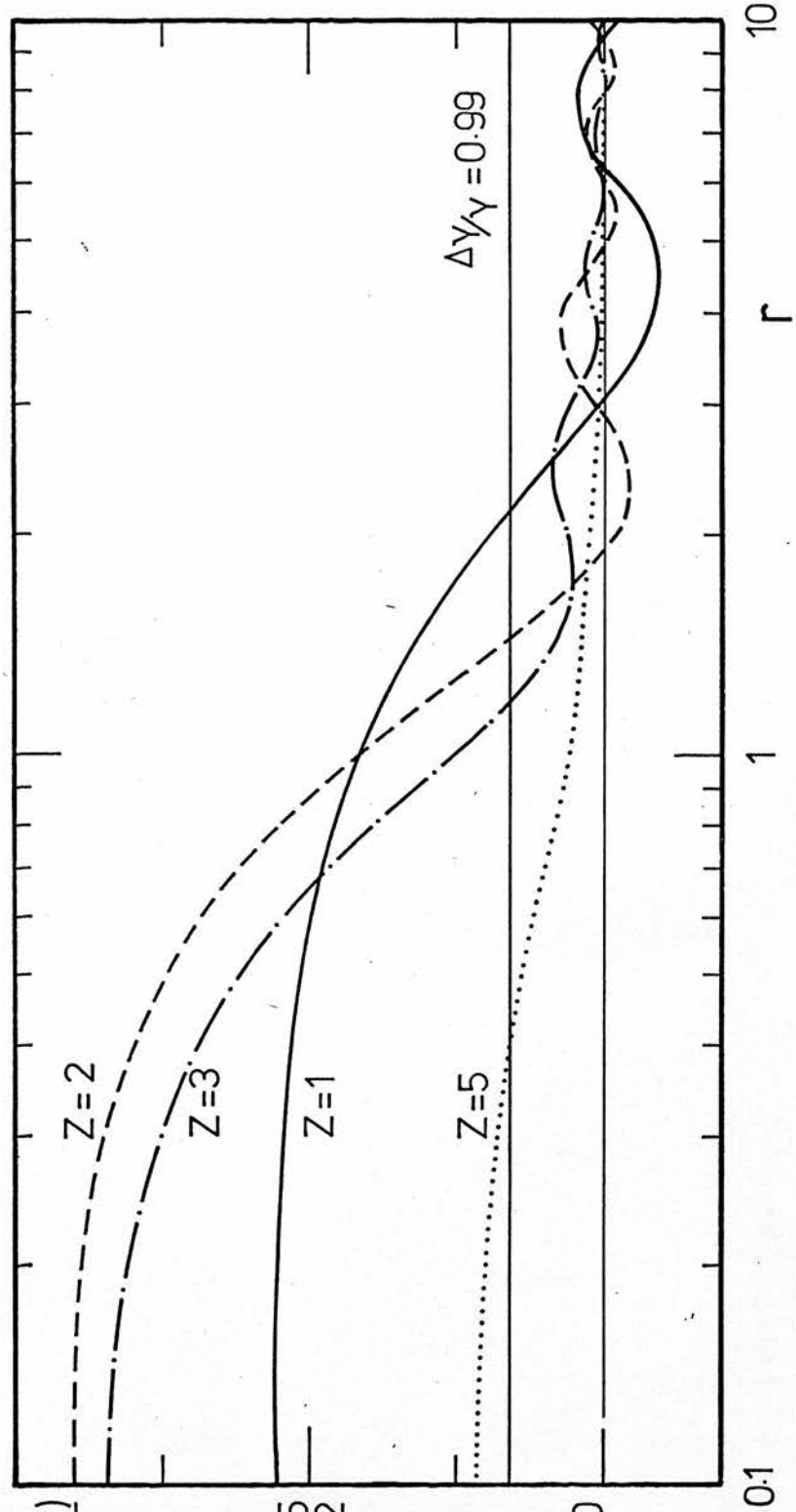

Fig. 5-10a The temperature, fluctuation $\left[T(\pi,Z) - T(0,Z)\right] / T(\pi/2,Z)$ as a function of r for several values of Z. $\eta = 50.0$, $\bar{\omega} = 0.5$, $a = 0.1$, $\mu_o = 1/\sqrt{3}$, $\phi_o = \pi/4$. The horizontal line is the temperature fluctuation required to produce a change in the rate of H_2 formation of 99% if $T(\pi/2,Z) = T_{cri}$.

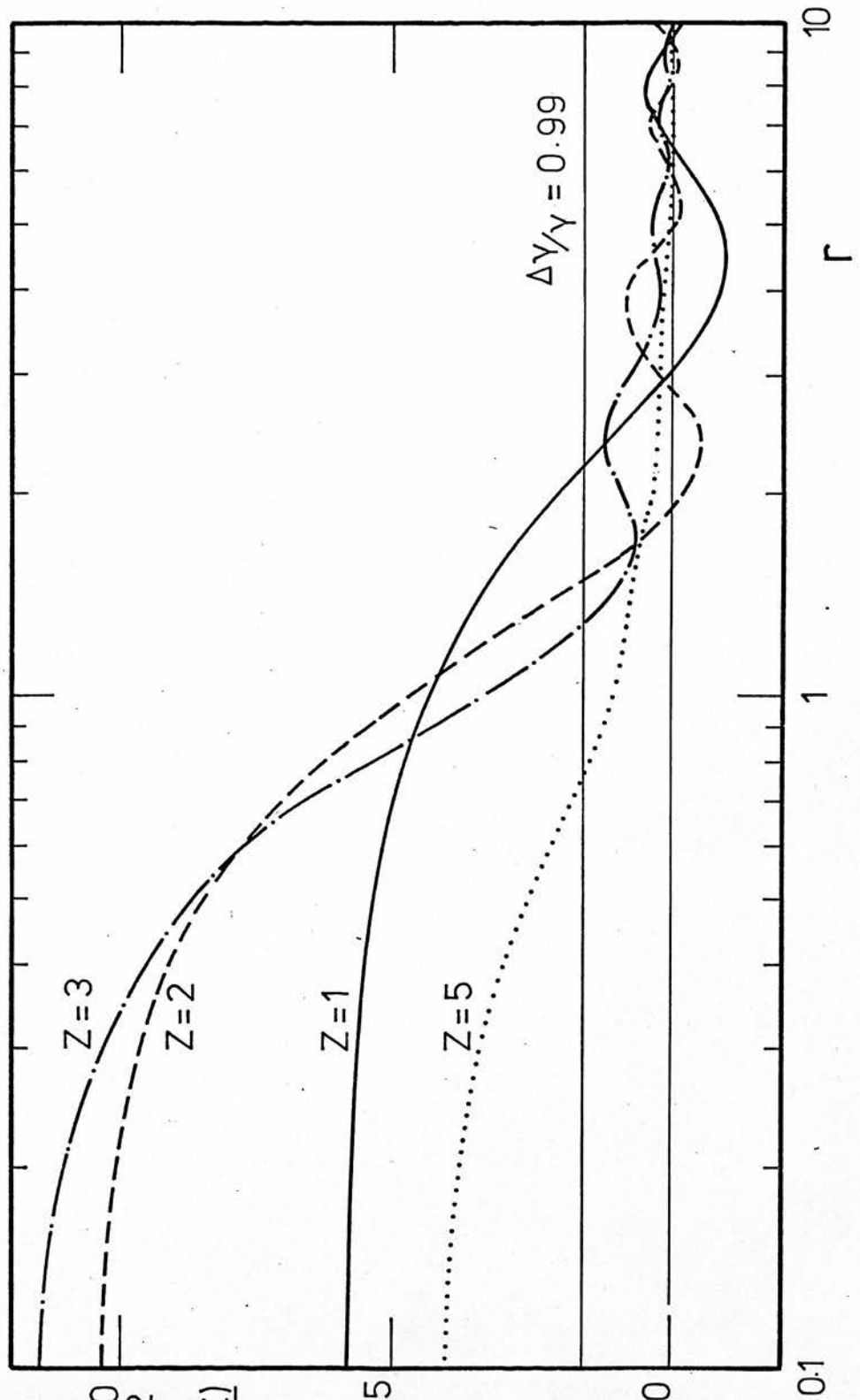

Fig. 5-10b As Fig. 5-10a for $\eta = 10^2$.

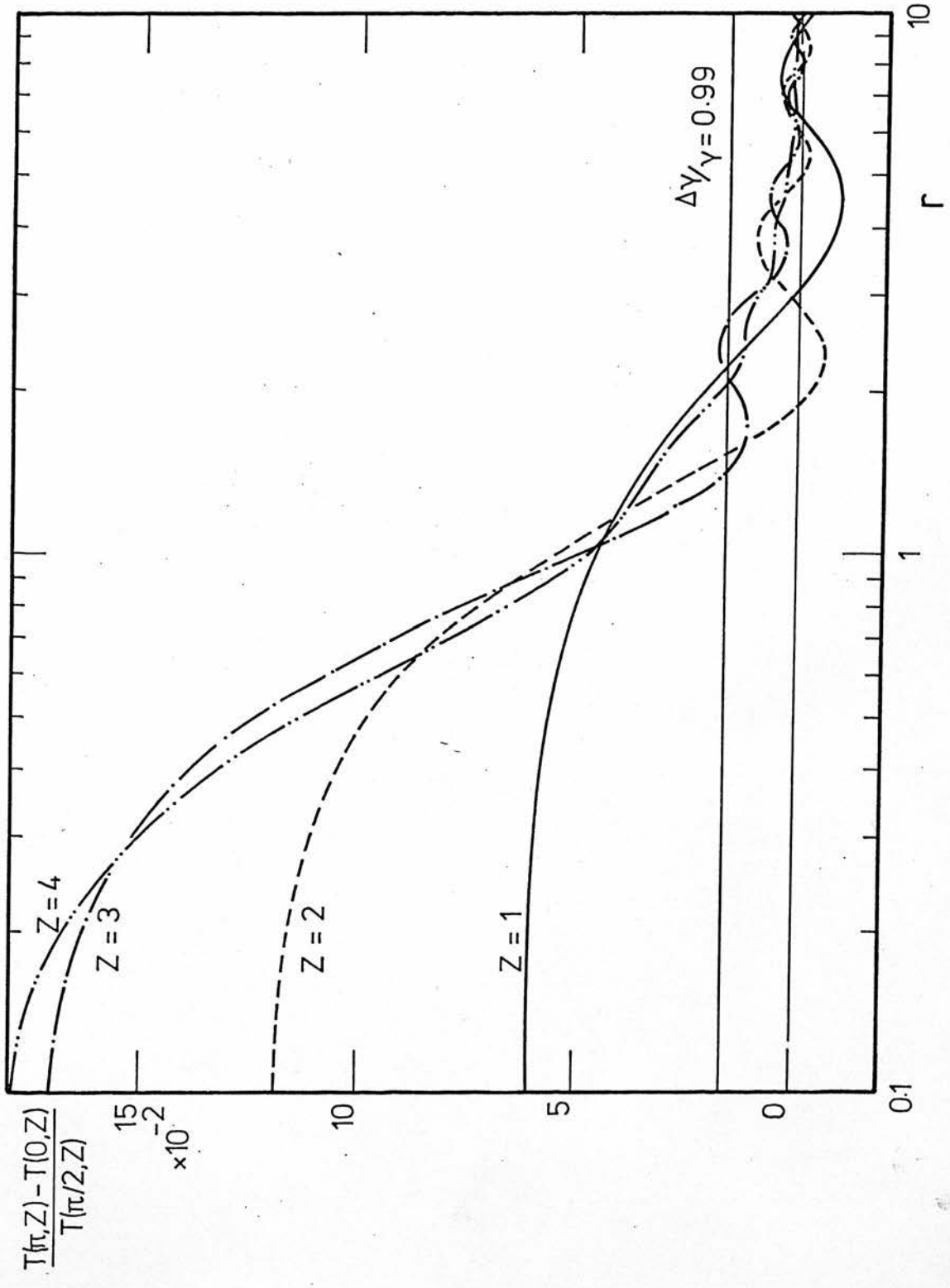

Fig. 5-10c As Fig. 5-10a for $\eta = 10^3$.

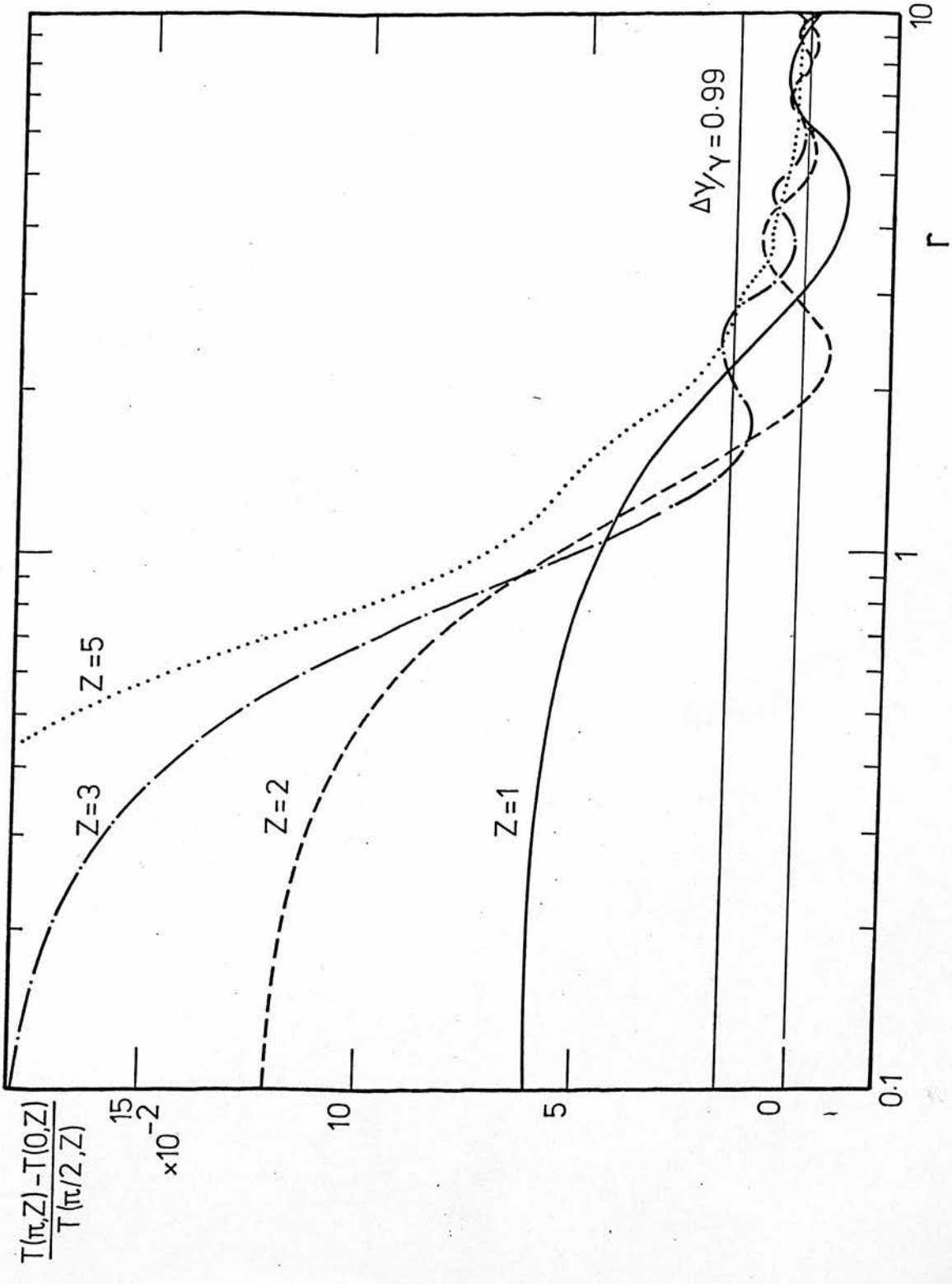

Fig. 5-10d As Fig. 5-10a for $\eta = 10^4$.

at any depth > 1.0. In particular, if one borrows from formal homogeneous models, Leung (1975), the mean optical depth 3 for the depth at which the critical temperature for H_2 formation on graphite grains is reached, fluctuations with $r < r_c$ would be able to produce a change in the rate of H_2 formation of 99%. The value of r_c is very insensitive to the particular η value for the range of interest i.e., $\eta \gtrsim 50$, as can be seen from the following table extracted from Figures (5-10a to 5-10d).

r_c	η
1.1	50.0
1.3	10^2
1.4	10^3
1.4	10^4

A reasonable average to adopt would be $r_c \approx 1.3$, which would give a thickness for the "radius" of the cell, where H_2 proceeds without difficulty, of

$$\bar{\tau} = \frac{\lambda_d \bar{\kappa}_s}{4} = \frac{\pi}{2.6} .$$

In this study the interest in models for which $\eta \lesssim 1.0$ is secondary; however, in Figure 5-11 a plot of the temperature fluctuations has been done for $\eta = 10^{-2}$. It follows from equation (5-44), in this case, contrary to the case when $\eta >> 1$, that the fluctuations in the visual fields, diffuse and attenuated, play a negligible role in determining, directly through equation (5-44), the temperature fluctuations which are determined in essence by the fluctuations

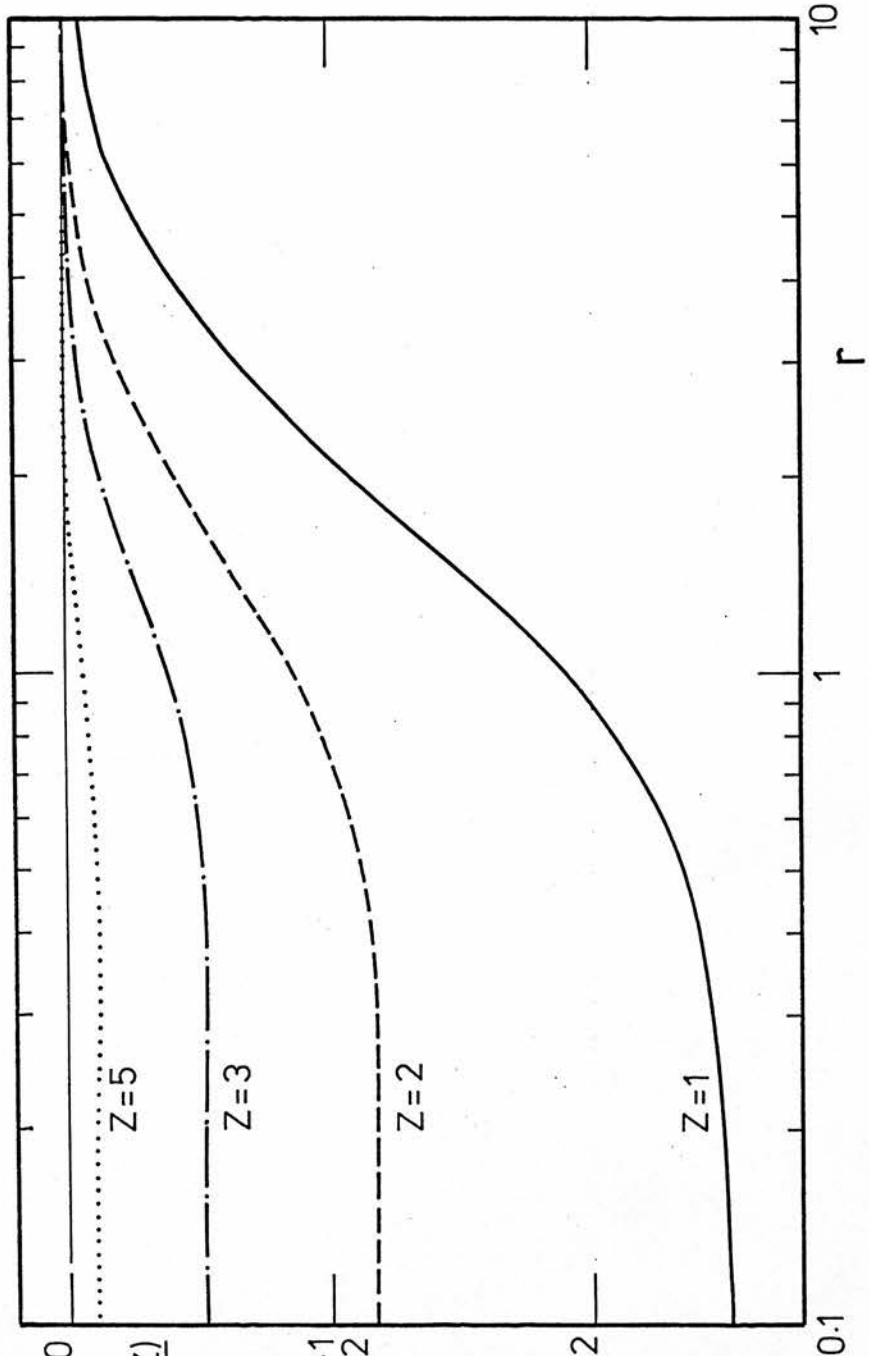

Fig. 5-11 The temperature fluctuation $\left[T(\pi,Z) - T(0,Z)\right]/T(\pi/2,Z)$ as a function of r for several values of Z.
$\eta = 10^{-2}$, $\bar{\omega} = 0.5$, $a = 0.1$, $\mu_o = 1/\sqrt{3}$, $\phi_o = \pi/4$

originated by the infrared field $J_p(X,Z)$.

For $Z \gtrsim 1$ maxima of density always correspond with maxima of temperature and the same is true for minima of density and temperature*. The fast decay of the fluctuation for $r > 1$ is very clear and smooth because there the fluctuations due to the schematic representation of the attenuated field have little effect on the temperature as given by equation (5-44).

* The Greenhouse effect in a non-uniform atmosphere.

6. INHOMOGENEOUS CLOUD MODELS. APPROXIMATED NUMERICAL SOLUTIONS

This section is dedicated to obtain more insight into the radiative heating problem in inhomogeneous media with the help of an approximated numerical method proposed here and which we hope to improve in the future.

From equation (4-2) it follows that the intensity of the visual diffuse field at any point s and in the direction $\cos^{-1}\mu$ and ϕ, see Figure 6-1, is given by

$$I_s(s,\mu,\phi) = \int_s^{sm} j_s(s'') \exp\left(-\tau(s,s'',\mu,\phi)\right) d\,s'' \qquad (6\text{-}1)$$

where the emission coefficient $j_s(s'')$ is given by

$$j_s(s'') = \sigma(s'') \left[J_s(s'') + \frac{F}{4} \exp\left(-\tau_o(s'', \mu_o, \phi_o)\right) \right] \qquad (6\text{-}2)$$

$\sigma(s'')$ being the scattering coefficient and the terms in the brackets, the mean visual diffuse field

$$J_s(s'') = \frac{1}{4\pi} \int_o^{2\pi} \int_{-1}^{1} I_s(s'',\mu,\phi)\, d\mu d\phi \qquad (6\text{-}3)$$

and the mean attenuated field at s''. $\tau_o(s'', \mu_o, \phi_o)$ is the optical distance from surface along path μ_o, ϕ_o.

Given an initial approximated form for $J_s(s'')$ equations (6-1) and (6-3) can be used to provide an iterative sequence for $I_s(s,\mu,\phi)$ and $j_s(s'')$. Since the density fluctuations are considered small ($a \approx 0.1$) a reasonable starting solution for $j_s(s'')$ is that derived

for the homogeneous clouds. The validity of approach can be tested by comparing the results with those obtained in the previous sections by analytical means. Equations (6-1) and (6-3) can be integrated numerically and can therefore be used to deal with density fluctuations beyond the scope of analytical methods.

Analogous equations to (6-1) and (6-3) can be written for the infrared field and a similar iterative procedure adopted. However, because it is necessary to know $J_s(s'')$ at every point in the cloud in order to perform the integrations and the integration of (6-1) and (6-3) to obtain $J_s(s'')$ is itself a lengthy procedure, the calculation of $J_p(s'')$ requires a realtively large amount of computing time.

It was seen in the last section that, for the problem in hand, $\eta >> 1$, the fluctuation of the visual field ΔJ_s is much greater than that of the infrared field ΔJ_p, see Figure 5-6c. Furthermore, ΔJ_s is amplified by a very large factor, $(1 - \bar{\omega})\eta$, in the expression defining the temperature, therefore, the fluctuations in the infrared radiation field have very small influence on those of temperature. That is, the infrared field could be well represented by the solution for the homogeneous cloud. Therefore, in this numerical solution the infrared radiation, $J_p(s'')$, will be represented by the solution for the homogeneous cloud.

The solutions for homogeneous clouds can be obtained in a straightforward manner using the well known Eddington approximation to integrate the radiative transfer equation (4-1). For homogeneous models, the R.T.E. (4-1) with the help of the two emission coefficients given by

equations (4-23) and (4-28), can be written in the form

$$\frac{dI_s}{\kappa_s ds} = -I_s + \bar{\omega} \left[J_s + J_s^a \right] \tag{6-4}$$

in the visual, and

$$\frac{dI_p}{\kappa_s ds} = -\eta^{-1} \left[I_p - J_p \right] + (1 - \bar{\omega}) \left[J_s + J_s^a \right] \tag{6-5}$$

in the infrared.

In plane geometry equations (6-4) and (6-5) become simply

$$\mu \frac{dI_s}{d\tau} = -I_s + \bar{\omega} \left[J_s + J_s^a \right] \tag{6-6}$$

and

$$\mu \frac{dI_p}{d\tau} = \eta^{-1} \left[-I_p + J_p \right] + (1 - \bar{\omega}) \left[J_s + J_s^a \right] \tag{6-7}$$

where $d\tau = \kappa_s dz = \kappa_s \mu ds$, i.e. for homogeneous solutions, the optical depth commonly used in the radiative transfer literature is adopted.

In the Eddington approximation

$$I_i = J_i + I_i^i \mu \qquad i = p,s \tag{6-8}$$

Substituting equation (6-8) in (6-6) and (6-7) and integrating with μ and times μ between -1 and +1 the following relations are obtained

$$\frac{dI_1^s}{d\tau} = -3\,(1-\bar{\omega})\,J_s + 3\bar{\omega}\,J_s^a \tag{6-9}$$

$$\frac{dJ_s}{d\tau} = -I_1^s \tag{6-10}$$

$$\frac{dI_1^p}{d\tau} = 3(1-\bar{\omega})\left[J_s + J_s^a\right] \tag{6-11}$$

$$\frac{dJ_p}{d\tau} = -\eta^{-1}\,I_1^p \tag{6-12}$$

or

$$\frac{d^2J_s}{d\tau^2} = 3(1-\bar{\omega})\,J_s - 3\bar{\omega}J_s^a \tag{6-13}$$

and

$$\frac{d^2J_p}{d\tau^2} = -3(1-\bar{\omega})\,\eta^{-1}\left[J_s + J_s^a\right] \tag{6-14}$$

Equation (6-8) gives the approximated boundary condition at the surface $\tau = 0$ for semi-infinite clouds and at $\tau = 0$ and $\tau = \tau_o$ for finite clouds with optical thickness τ_o, i.e.

$$J_s(0) = \frac{1}{\sqrt{3}}\left.\frac{dJ_s}{d\tau}\right|_{\tau=0} \qquad \text{(a)}$$

$$J_s(\tau_o) = -\frac{1}{\sqrt{3}}\left.\frac{dJ_s}{d\tau}\right|_{\tau=\tau_o} \qquad \text{(b)} \tag{6-15}$$

and

$$J_p(0) = \frac{\eta}{\sqrt{3}} \left.\frac{dJ_p}{d\tau}\right|_{\tau=0} \quad \text{(a)}$$

$$J_p(\tau_o) = -\frac{\eta}{\sqrt{3}} \left.\frac{dJ_p}{d\tau}\right|_{\tau=\tau_o} \quad \text{(b)} \qquad (6\text{-}16)$$

where $\frac{2}{3}$ has been substituted by $\frac{1}{\sqrt{3}}$ as a better quadrature point associated with the Eddington approximation.

For a semi-infinite homogeneous cloud with attenuated field at depth τ given by

$$J_s^a = \tfrac{1}{4} \exp\left(-\frac{\tau}{\mu_o}\right) \qquad (6\text{-}17)$$

integration of (6-13) - (6-14) with boundary condition (6-15a) and (6-15b) leaves

$$J_s = d_1 \exp(-k\tau) + d_2 \exp\left(-\frac{\tau}{\mu_o}\right) \qquad (6\text{-}18)$$

and

$$J_p = -3(1-\bar{\omega})\eta^{-1}\left\{\frac{d_1}{k^2}\exp(-k\tau) + \mu_o^2(\tfrac{1}{4}+d_2)\exp\left(-\frac{\tau}{\mu_o}\right)\right\} + C_1 \qquad (6\text{-}19)$$

where

$$k = \sqrt{3(1-\bar{\omega})} \quad \text{(a)}$$

$$d_1 = -3\bar{\omega}\mu_o^2\left(1+\frac{1}{\sqrt{3}}\mu_o\right) / 4(k^2\mu_o^2-1)(1+k/\sqrt{3}) \quad \text{(b)}$$

$$d_2 = 3\bar{\omega}\mu_o^2 / 4(k^2\mu_o^2-1) \quad \text{(c)} \qquad (6\text{-}20)$$

$$C_1 = \frac{\sqrt{3}}{k^2}(1-\bar{\omega})(k+\sqrt{3}\eta^{-1})d_1 + \sqrt{3}\mu_o^2(1-\bar{\omega})\left(\frac{1}{\mu_o}+\sqrt{3}\eta^{-1}\right)(\tfrac{1}{4}+d_2)$$

(d)

For a finite cloud with optical thickness τ_o and attentuated field at depth τ given by

$$J_s^a = \tfrac{1}{4}\{\exp(\frac{\tau}{\mu_o}) + \exp(-\frac{(\tau_o - \tau)}{\mu_o})\} \tag{6-21}$$

the result of integrating (6-13) and (6-14) with boundary condition (6-15b) and (6-16b) becomes

$$J_s = b_o\{\exp(-\frac{\tau}{\mu_o}) + \exp(-\frac{(\tau_o - \tau)}{\mu_o})\} + b_1 \exp(-\frac{k}{\tau}) + b_2 \exp(\frac{k}{\tilde{\tau}}) \tag{6-22}$$

and

$$J_p = -3(1-\bar{\omega})\eta^{-1}\{\mu_o^2(b_o+\tfrac{1}{4})\exp(-\frac{\tau}{\mu_o}) + \mu_o^2(b_o+\tfrac{1}{4})\exp(-\frac{(\tau_o-\tau)}{\mu_o}) + \frac{b_1}{k^2}\exp(-k\tau) + \frac{b_2}{k^2}\exp(k\tau)\} + C_2\tau + C_3 \tag{6-23}$$

where

$$b_o = \tfrac{3}{4}\,\bar{\omega} \,/\, (k^2 - 1/\mu_o^2) \tag{a}$$

$$b_2 = b_o \frac{k}{\sqrt{3}} \frac{(1+\exp(-k\tau_o))}{1+k/\sqrt{3}} \frac{(1/\sqrt{3}\,\mu_o - 1)\exp(-\tau_o/\mu_o)) - (1/\sqrt{3}\mu_o + 1)}{[1+k/\sqrt{3}\exp(k\tau_o)] - \frac{1-k/\sqrt{3}}{1+k/\sqrt{3}}(1-\frac{k}{\sqrt{3}}\exp(-k\tau_o)} \tag{b}$$

$$b_1 = \frac{b_o}{1+k/\sqrt{3}}\left[(1/\sqrt{3}\mu_o - 1)\exp(-\frac{\tau_o}{\mu_o}) - (1 + 1/\sqrt{3}\mu_o)\right] - \frac{1-k/\sqrt{3}}{1+k/\sqrt{3}}\, b_2 \tag{c}$$

$$C_2 = \frac{\sqrt{3}(1-\bar{\omega})}{k^2\,\tau_o}\{(\sqrt{3}\eta^{-1} - k)(b_1\exp(-k\tau_o) - b_2) + (\sqrt{3}\,\eta^{-1} + k)(b_2\exp(k\tau_o) - b_1)\} \tag{d}$$

$$C_3 = \sqrt{3}(1-\bar{\omega})\mu_o^2(b_o + \tfrac{1}{4})\left[(\sqrt{3}\eta^{-1} + \frac{1}{\mu_o}) + (\sqrt{3}\eta^{-1} - \frac{1}{\mu_o})\exp(-\frac{\tau_o}{\mu_o})\right]$$

$$+ \frac{\sqrt{3}}{k^2}(1-\bar{\omega})\left[(\sqrt{3}\eta^{-1} + k)\, b_1 + (\sqrt{3}\eta^{-1} - k)\, b_2 + C_2\right] \qquad \text{(e)}$$

(6-24)

It is easy to see that solutions (6-22) and (6-23) tend to solutions (6-18) and (6-19) when $\tau_o \to \infty$, as expected.

a. Semi-infinite Cloud

The visual field in a semi-infinite cloud, with the same density distribution as studied in Section 5, will be calculated. The notation is summarised in Figure 6-1. In addition to the dimensionless variables X and Z and the parameter r defined by equation (5-2), the mean optical distance S along the ray s defined by

$$S = \bar{\kappa}_s s \qquad (6\text{-}25)$$

is introduced

Equation (6-1) in terms of the optical distances and the notation of Figure (6-1) is

$$I_s(X,Z;\mu,\phi) = \bar{\omega}\int_o^{S_m} \psi(S'')\{J_s(S'') + \frac{F}{4}\exp -\tau_o(S'',\mu_o,\phi_o)[\}\exp -\tau(X,Z,\mu,\phi,\ S'')]dS''$$

(6-26)

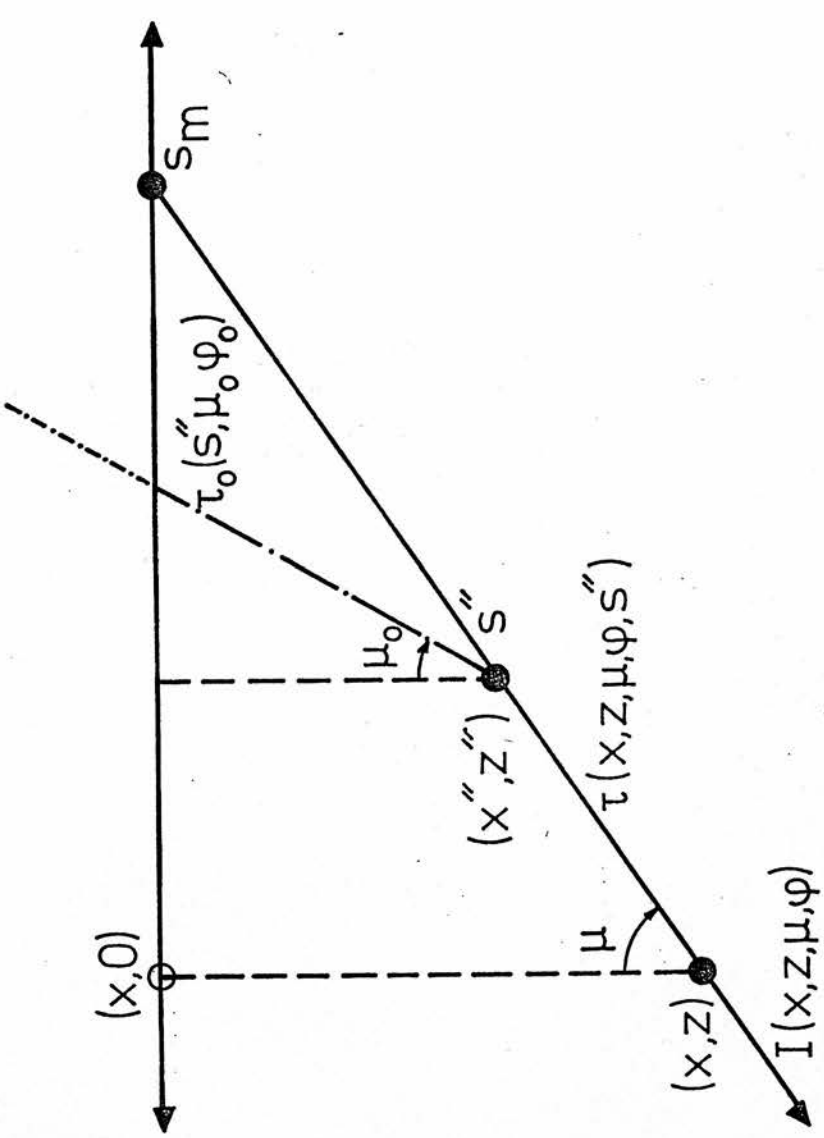

Fig. 6-1 The cross section of an inhomogeneous semi-infinite cloud in the plane of the incident radiation for $\phi = \phi_o$.

where the optical distances τ_o and τ are given by

$$\tau_o(S'', \mu_o, \phi_o) = (S_m - S)\frac{\mu}{\mu_o} + \frac{a}{r(1-\mu_o^2)^{\frac{1}{2}}\cos\phi_o}\{\sin\left[X + r(S''-S)(1-\mu^2)^{\frac{1}{2}}\cos\phi + (S_m - S'')\frac{\mu}{\mu_o} r(1-\mu_o^2)^{\frac{1}{2}}\cos\phi_o\right]$$

$$- \sin\left[X + (S''-S)\, r\,(1-\mu^2)^{\frac{1}{2}}\cos\phi\right]\} \qquad (6\text{-}27)$$

and

$$\tau(X,Z,\mu,\phi,S'') = (S''-S) + \frac{a}{r(1-\mu^2)^{\frac{1}{2}}\cos\phi}\{\sin\left[rS''\,(1-\mu^2)^{\frac{1}{2}}\cos\phi\right]$$

$$- \sin\left[rS(1-\mu^2)^{\frac{1}{2}}\cos\phi\right]\} \qquad (6\text{-}28)$$

The initial value of J(S'') is the solution corresponding to the homogeneous semi-infinite cloud (6-22).

Equation (6-26) can be integrated numerically along S'' for any couple of points X, Z and any values of the angles μ and ϕ. This is done approximating the integral (6-26) to the Gauss-Legendre quadrature formula, i.e.

$$I_s = \sum_{k=1}^{n} A_k F(\xi_k) \qquad (6\text{-}29)$$

where A_k are the weights, $F(\xi_k)$ is the integrand corresponding to equation (6-26) and ξ_k the pivots which are the zeros of the Legendre polynomials.

The same procedure can be used to integrate (6-3) with respect to μ and ϕ, with $I_s(S,\mu,\phi)$ given by (6-26) at appropriate values μ and ϕ. Because there is a sharp peak in I_s around $\mu \approx 0.0$ for $Z \lesssim 1.0$ an appropriate distribution of quadrature points in the μ range $-1.0 \leq \mu \leq +1.0$ is necessary to retain a good accuracy in the integration with μ.

If one attempts to iterate formally the equations (6-1) and (6-3), the computational demands seem severe, but if in the first entry for J(S"), J(S") is given by the solution for a homogeneous cloud of the local density at S" rather than that for a homogeneous cloud of the mean density of the inhomogeneous cloud, the integration seems to converge very quickly.

After one integration a good agreement with the analytical solution is found. The worst discrepancy is 20% which occurs near the surface ($Z < 0.4$). This discrepancy towards the boundary comes partially from the boundary condition involved in the Eddington approximation.

Figures 6-2a and 6-2b are plots of the analytical and numerical solutions for the temperature fluctuation

$[T(\pi,Z) - T(o,Z)]/\, T(\pi/2,Z)$ for $\eta = 10^2$, $Z = 1.0$, $Z = 2.0$ and $Z = 3.0$, $Z = 5.0$ respectively. From there, one can see that although there are differences, they are tolerable and either of these approaches can be used to gain semi-quantitative insight into the radiative heating problem in non-uniform media. The numerical one is more useful if one attempts to tackle more realistic (and

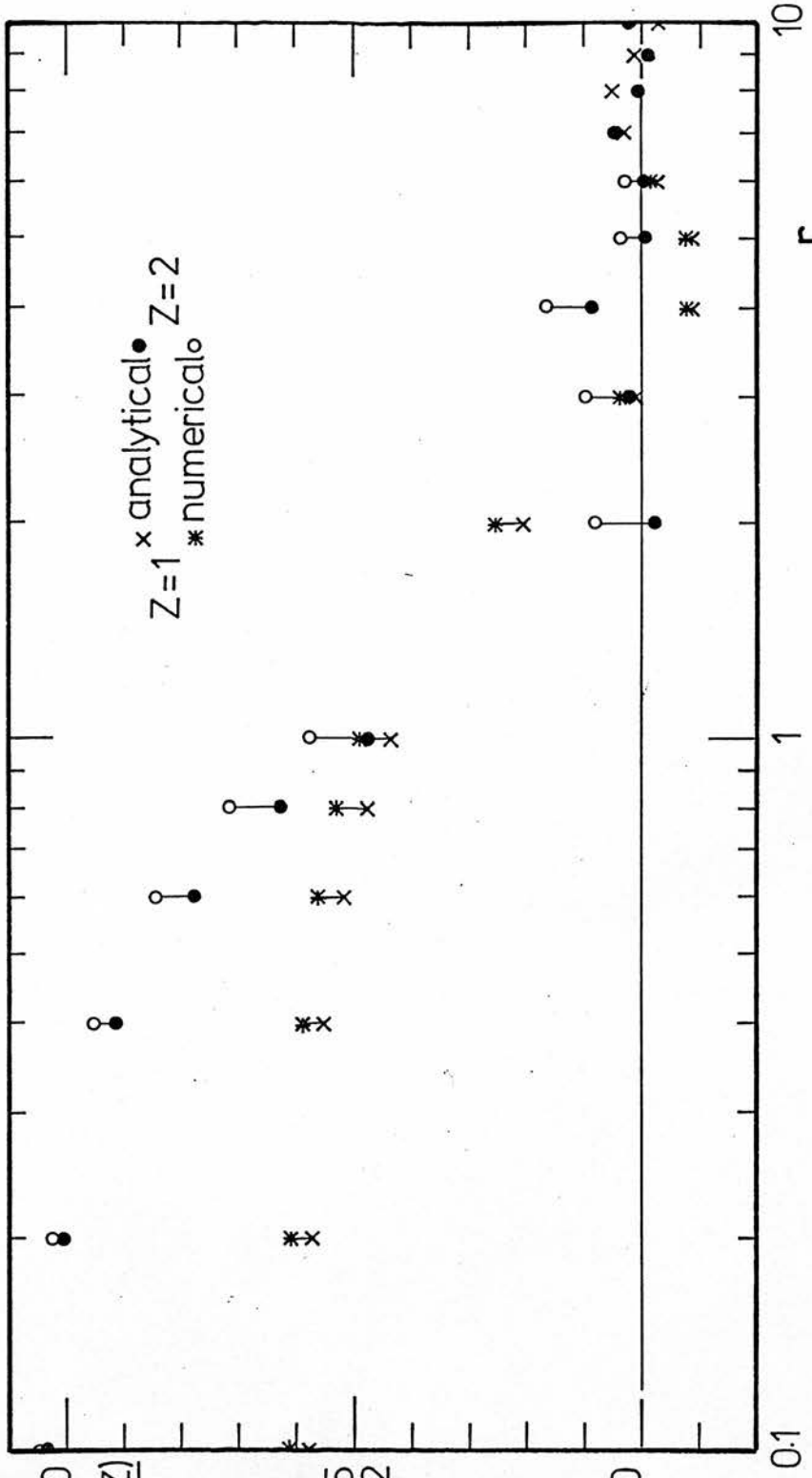

Fig. 6-2a The analytical and numerical solutions for the temperature fluctuation $\left[T(\pi,Z) - T(0,Z)\right]/T(\pi/2,Z)$ as functions of r for Z = 1.0 and Z = 2.0. $\eta = 10^2$, $\bar{\omega} = 0.5$, a = 0.1, $\mu_o = 1/\sqrt{3}$, $\phi_o = \pi/4$

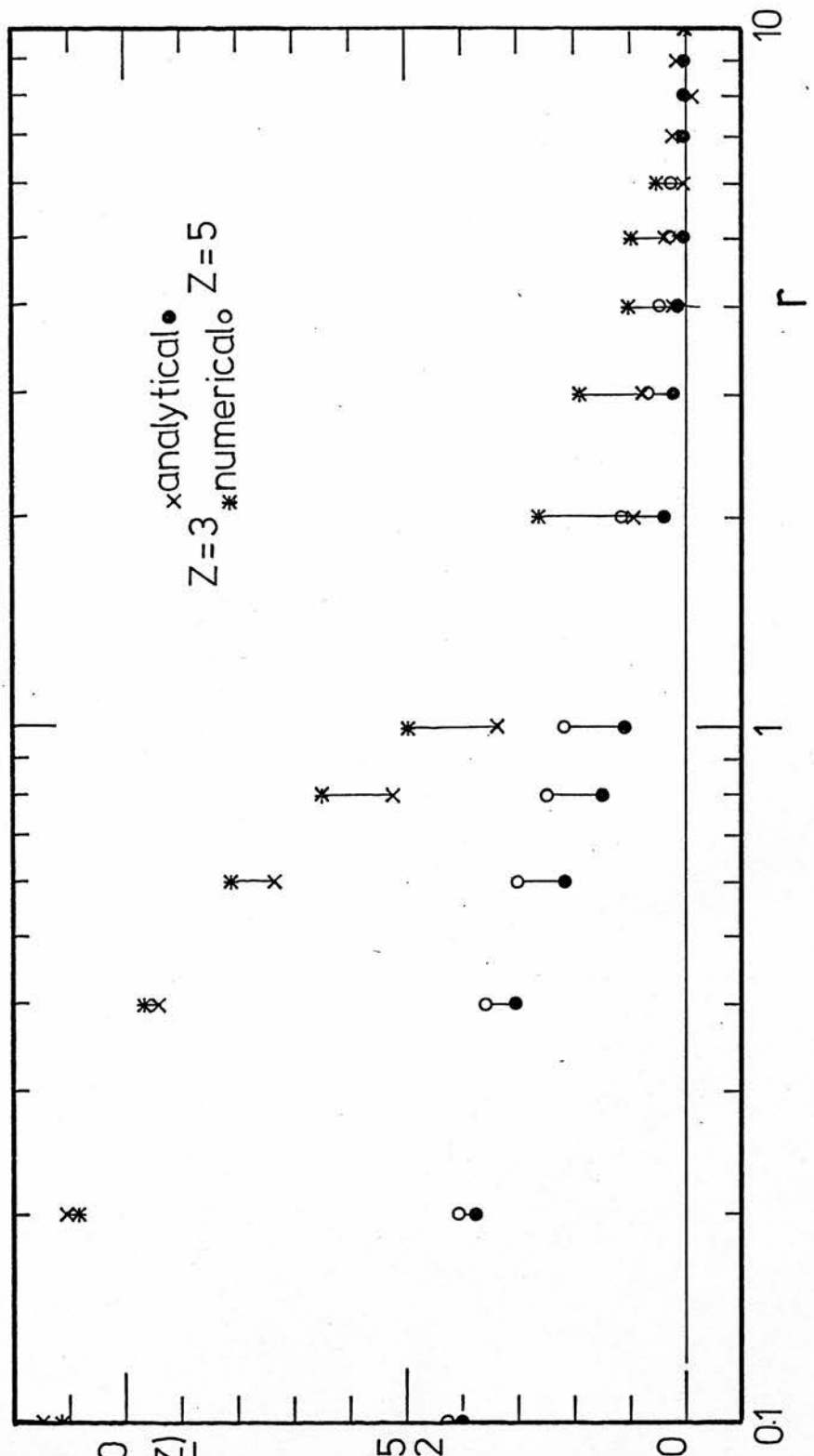

Fig. 6-2b As Fig. 6-2a for Z = 3.0 and Z = 5.0.

therefore more complex) models, where the analytical solution becomes impossible. These results give a check on the numerical method and show that it can be extended to more complex models.

Only the "simplest" model of a non-homogeneous cloud has been worked out in the previous sections, i.e. a semi-infinite cloud with one transverse fluctuation in density of arbitrary value of r. However, real clouds are finite and real fluctuations, in our particular problem, are generated by turbulence which means that many values of r occur simultaneously. But small scale fluctuations are contained in large scale fluctuations which means that the smaller fluctuations peak towards the maxima of the largest ones. One can see from the ideal model studied, that large scale fluctuations ($r << 1.0$) only determine the mean value of T_d. In particular they define the regions where the critical temperature for the H_2 formation is reached first. On the other hand, fluctuations at scales shorter than r_c (≈ 2.0) are unable to produce the minimum value of $\Delta T_d/\overline{T}_d$ required to switch on the chemical discontinuity in the H_2 production. This means that the fluctuations around T_{cri} capable of disconnecting regions where H_2 proceeds with high efficiency from those where it proceeds with very low ones are in the range

$$1.0 \approx r < r_c \approx 2.0 \qquad (6\text{-}30)$$

The above aspect is readily seen with the help of the following idealised model:

Let us again consider the semi-infinite cloud already studied but instead of an extinction of the form

$$\kappa_s = \overline{\kappa}\,(1 + a\cos \ell x) \qquad (6\text{-}31a)$$

two fluctuations overlapped are assumed, i.e.

$$\kappa_2 = \bar{\kappa}\,(1 + a\cos \ell x + a_1 \cos \ell_1 x) \tag{6-31b}$$

The radiative heating problem can be solved in a first approximation by using the approximated numerical method with the help of the following two optical distances: the optical distance between any two points (x,z) and (x",z") separated by a length s" -

$$\tau(x,z;x'',z'') = \bar{\kappa}s'' + \frac{\bar{\kappa}a}{\ell \sin\theta\cos\phi}\{\sin[\ell x + \ell s'' \sin\theta\cos\phi] - \sin \ell x\}$$

$$+ \frac{\bar{\kappa}a_1}{\ell_1 \sin\theta\sin\phi}\{\sin[\ell_1 x + \ell_1 s''\sin\theta\cos\phi] - \sin \ell_1 x\} \tag{6-32}$$

and the optical depth from the boundary to any point (x", z") -

$$\tau_o(x'',z'') = \frac{\bar{\kappa}(z - s''\mu)}{\mu_o} + \frac{\bar{\kappa}a}{\ell \sin\theta_o\cos_o\phi_o}\{\sin[\ell x + s''\ell\sin\theta\cos\phi$$

$$+ \frac{(z-s''\mu)}{\mu_o}\ell \sin\theta_o\cos\phi_o] - \sin[\ell x + s''\ell\sin\theta\cos\phi]$$

$$+ \frac{\bar{\kappa}a_1}{\ell_1\sin\theta_o\cos\phi_o}\{\sin[\ell_1 x + s''\ell_1\sin\theta\cos\phi$$

$$+ \frac{z-s''\mu}{\mu_o}\ell_1\sin\theta_o\cos\phi_o] - \sin[\ell_1 x + s''\ell_1\sin\theta\cos\phi]\} \tag{6-33}$$

The above two optical distances in terms of the dimensionless variables X and Z and parameters $r = \ell/\bar{\kappa}$ and $r_1 = \ell_1/\bar{\kappa}$, become

$$\tau(X,Z;X''Z'') = S'' + \frac{a}{r\sin\theta\cos\phi}\left\{\sin\left[X + S''r\sin\theta\cos\phi\right] - \sin X\right.$$

$$\left. + \frac{a_1}{r_1\sin\theta\cos\phi}\left\{\sin\left[\frac{r_1}{r}X + S''r_1\sin\theta\cos\phi\right] - \sin\frac{r_1}{r}X\right\}\right. \qquad (6\text{-}34)$$

and

$$\tau_o(S'') = \frac{(Z - S''\mu)}{\mu_o} + \frac{a}{r\sin\theta_o\cos\phi_o}\left\{\sin\left[X + rS''\sin\theta\cos\phi\right.\right.$$

$$\left. + \frac{Z - S''\mu}{\mu_o} r\sin\theta_o\cos\phi_o\right] - \sin\left[X + rS''\sin\theta\cos\Phi\right]\left.\right\}$$

$$+ \frac{a_1}{r_1\sin\theta_o\cos\phi_o}\left\{\sin\left[\frac{r_1}{r}X + S''r_1\sin\theta\cos\phi + \frac{Z - S''\mu}{\mu_o} r_1\sin\theta_o\cos\phi_o\right]\right.$$

$$\left. - \sin\left[\frac{r_1}{r}X + S''r_1\sin\theta\cos\phi\right]\right\} \qquad (6\text{-}35)$$

Figure 6-3 shows the fluctuation $\dfrac{T(\pi,Z) - T(o,Z)}{T(\pi/2,Z)}$ for $r = 1.0$ and values of r_1 such that $0.1 \leq r_1 < 10.0$. Figure 6-4 is the same as figure 6-3 but for $r = 2.0$. From there, it is apparent that fluctuations $r_1 << 1$ have little effect on the fluctuation $\Delta T/\bar{T}$ produced by the smallest scale ($r = 1.0$ and 2.0) and they affect mainly the mean value of T as can be seen in figure 6-5 where $T(\pi/2,Z)$ has been plotted for $r_1 = 0.1$ and $r_1 = 10.0$, for $r = 1.0$ in figure 6-5a

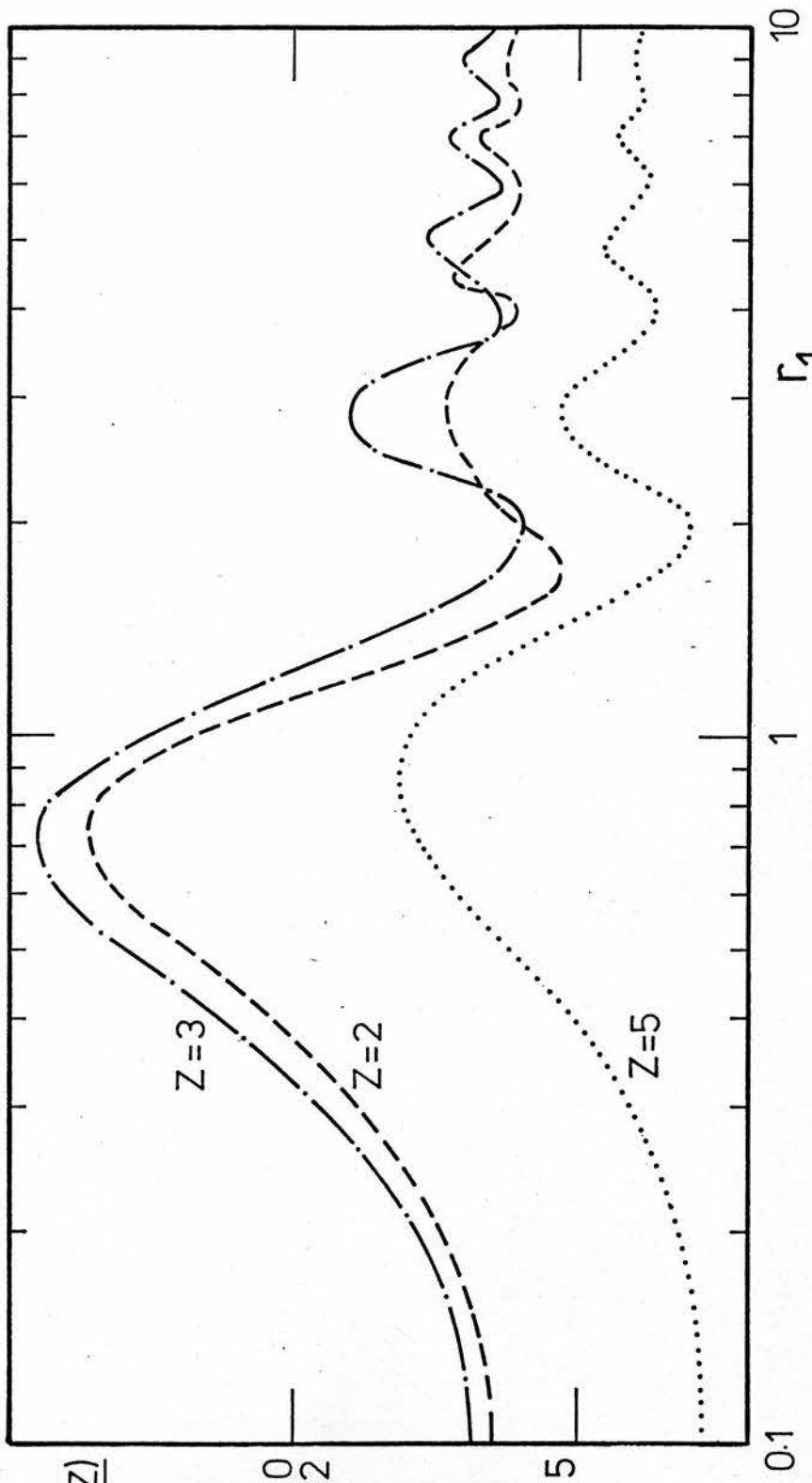

Fig. 6-3 The temperature fluctuation $\left[T(\pi,Z) - T(0,Z)\right] / T(\pi/2,Z)$ for r = 1.0 as a function of r_1.
$\eta = 10^2$, $\bar{\omega} = 0.5$, $a = a_1 = 0.5$, $\mu_o = 1/3$, $\phi_o = \pi/4$

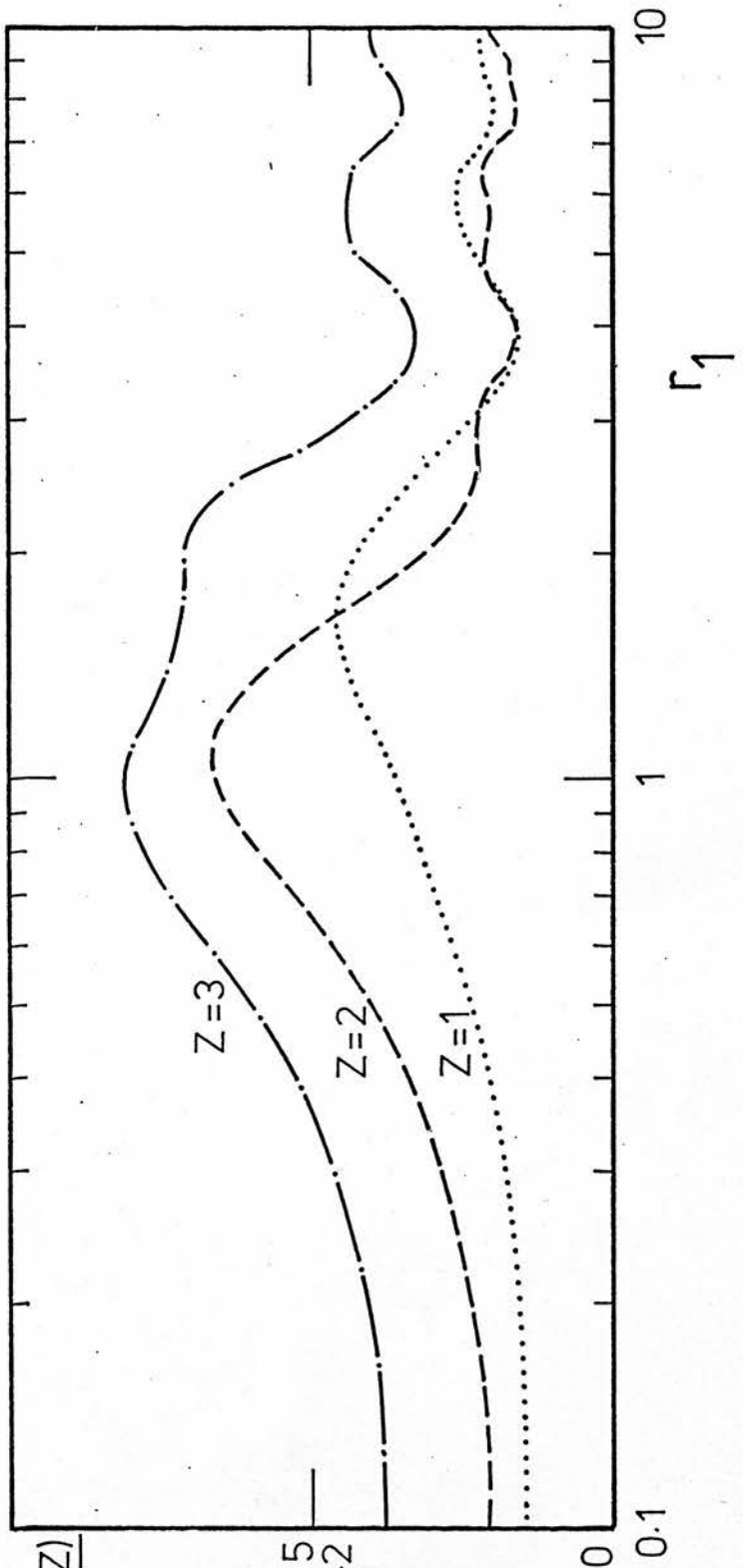

Fig. 6-4 As Fig. 6-3 for r = 2.0.

and r = 2.0 in figure 6-5b.

From figures 6-5 one can see that the value of $T(\pi/2,Z)$ for $r_1 = 0.1$ is lower than the value of $T(\pi/2,Z)$ for $r_1 = 10.0$ as expected, because in the former case κ fluctuates rather around the mean value $\overline{\kappa}(1 + a)$ and when $r_1 = 10.0$, κ fluctuates around the mean value $\overline{\kappa}$, i.e. in a first approximation one can assume that when $r_1 << 1$ the smallest fluctuations occur embedded in a cloud with different mean density.

On the other hand, density fluctuations with $r_1 >> 1.0$ are unable to affect appreciably the temperature fluctuations corresponding at larger scales and therefore the strongest temperature fluctuations around a determined mean value, in the case of interest, $\overline{T} = T_{cri}$, are expected to occur at scales given by the relation (6-30).

b. Finite Cloud with Mean Optical Thickness Z_o

The approximated numerical procedure can be extended to the case of plane-parallel models with finite mean optical thickness Z_o to get a solution to the radiative heating problem for non-homogeneous clouds.

As a first value for the mean intensity of the visual radiation field the solution of the radiative transfer equation in the Eddington approximation in a homogeneous cloud, equation (6-22) is taken. The remaining calculation follows the same course as the semi-infinite case, but in addition to the optical depth τ_o given by equation (6-27) and which will be denoted by τ_o^+, see Figure 6-6, the optical depth from

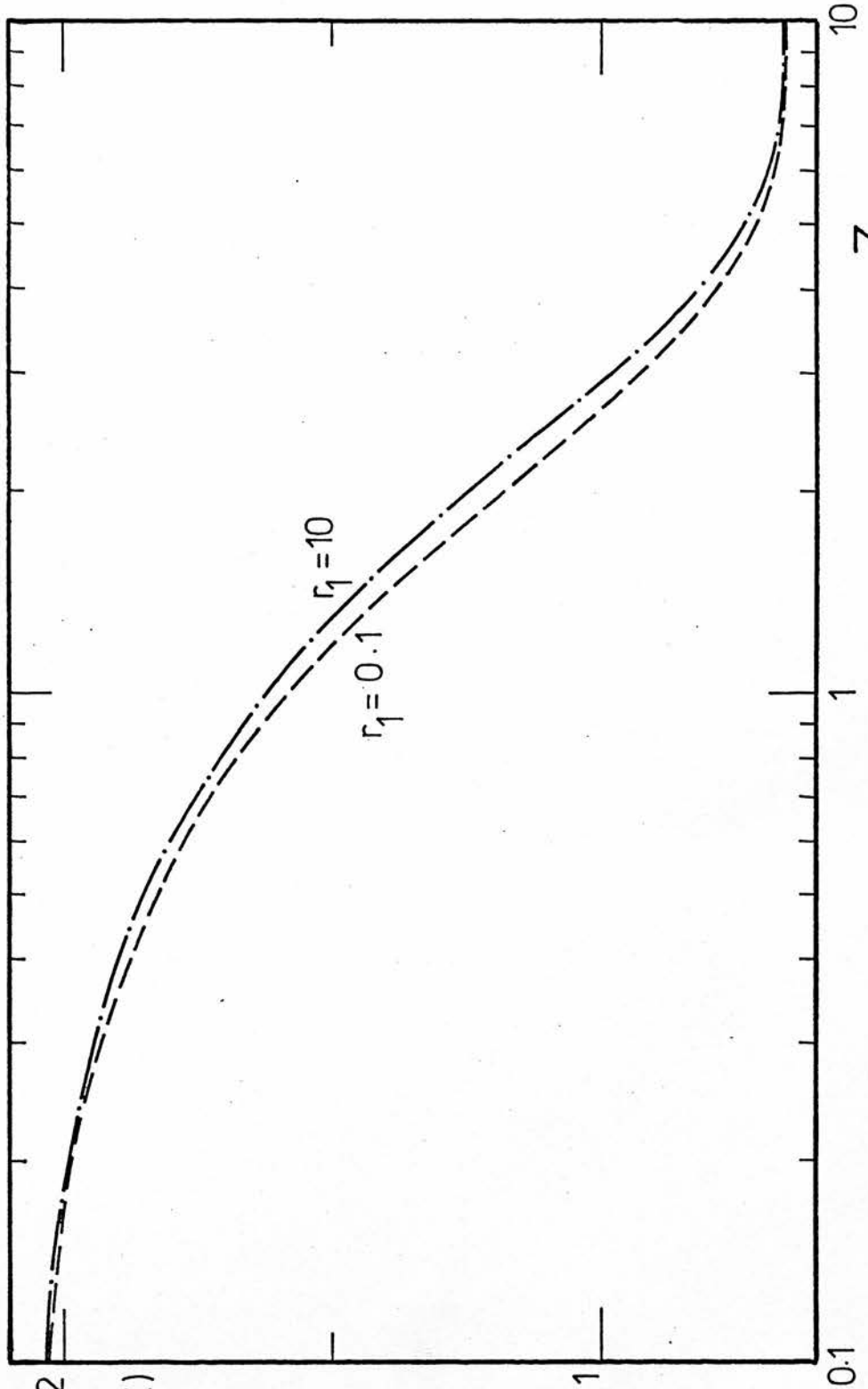

Fig. 6-5a The mean temperature $T(\pi/2, Z)$ as a function of Z for $r_1 = 0.1$ and $r_1 = 10.0$. $r = 1.0$, $\eta = 10^2$, $\overline{\omega} = 0.5$, $a = a_1 = 0.1$, $\mu_o = 1/\sqrt{3}$, $\phi_o = \pi/4$

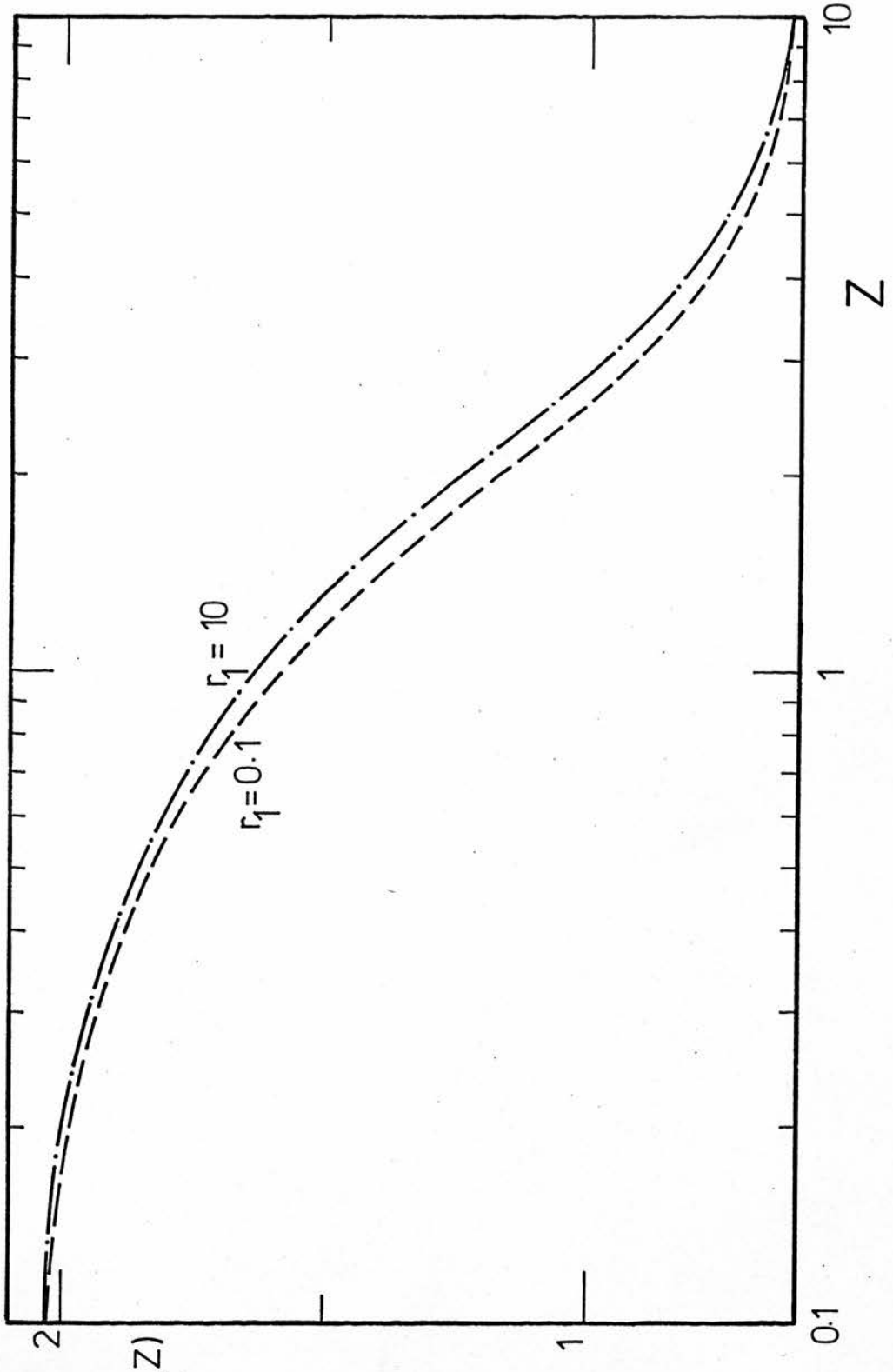

Fig. 6-5b As Fig. 6-5a for r = 2.0.

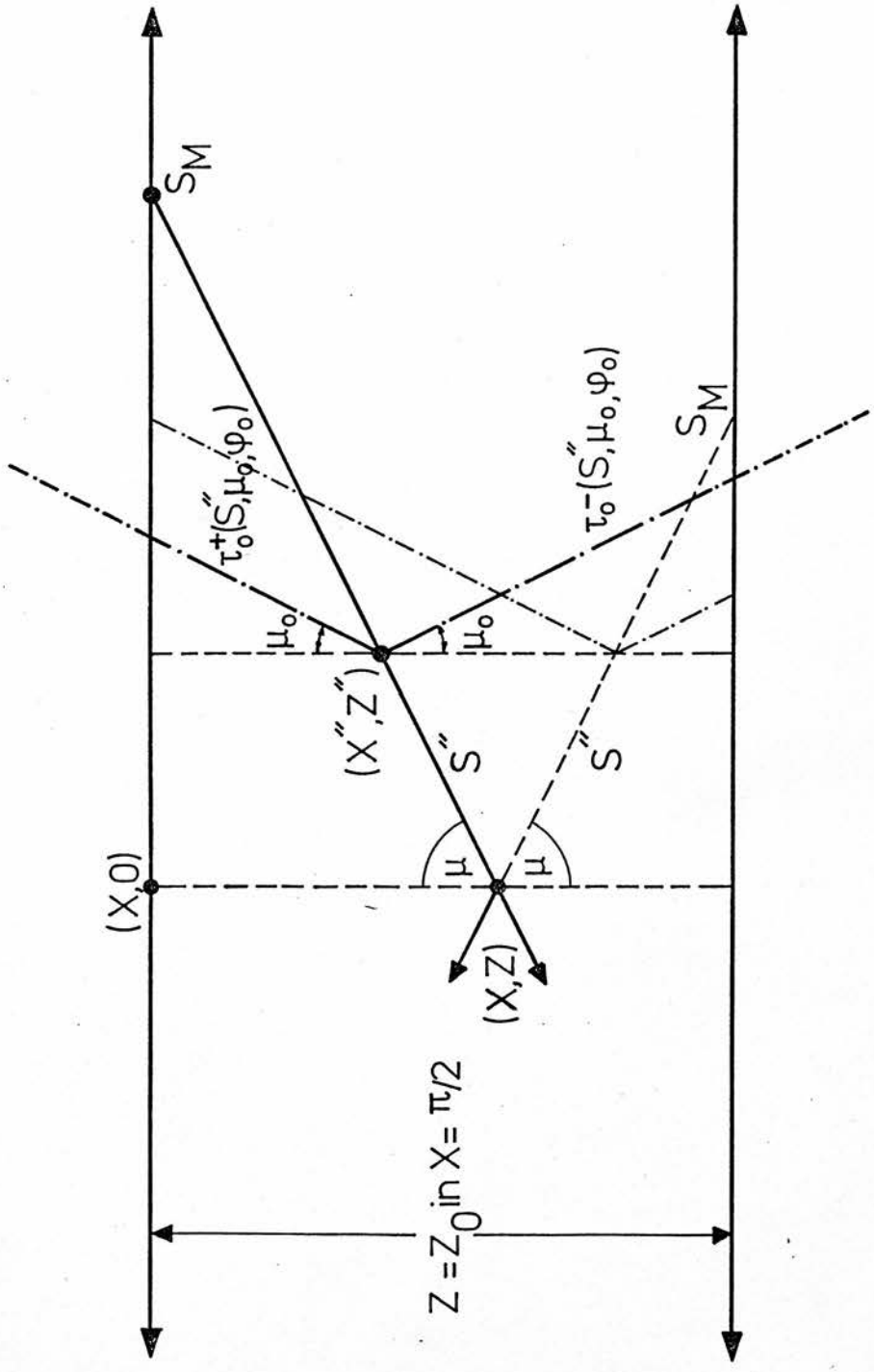

Fig. 6-6 The cross section of an inhomogeneous semi-infinite cloud of mean optical thickness Z_o in the plane of the incident radiation for $\phi = \phi_o$.

the boundary τ_o denoted by $\bar{\tau}_o$ is introduced, i.e.

$$\bar{\tau}_o(S'') = \frac{Z_o - (Z - S''\mu)}{\mu_o} + \frac{a}{r\sin\theta_o\cos\phi_o}\left\{ \sin\left[X + rS''\sin\theta\cos\phi + \frac{Z_o - (Z - S''\mu)}{\mu_o} r\sin\theta_o\cos\phi_o \right] - \sin\left[X + rS''\sin\theta\cos\phi \right] \right\} \quad (6\text{-}36)$$

The results are shown graphically in figures 6-7a,b,c,d for Z_o = 1.0, 5.0, 10.0 and 20.0, and not much more information is obtained about the quantity of interest, i.e. the fluctuation $\left[T(\pi,Z) - T(o,Z)\right] / T(\pi/2,Z)$, than is obtained from the analytical solution for a semi-infinite cloud. But the results reinforce the conclusions of Sections 5 and 6, in the sense that they are not affected in essence because of the finite nature of the cloud.

For Z_o = 1.0, the temperature fluctuations are due mainly to the attenuated field and the sharp decay is shifted towards slightly higher values of r. At the centre, for instance, the strong decay occurs for r ≈ 4.0, i.e. for a fluctuation of thickness $\frac{\lambda_d \kappa}{2} \approx \pi/4$. The insensibility of the fluctuations for values of r < 1.0 is apparent too. Therefore, an inhomogeneous slab of mean thickness Z_o = 1.0 behaves as homogeneous for r < 1.0 in the sense that the temperature at any point corresponds to the temperature of the homogeneous case with the local value of the density.

The much more interesting cases in this study are those in which Z_o = 5.0 and 10.0. If in a first approximation, one considers typical prestellar clouds to be inhomogeneous slabs with thickness of the above

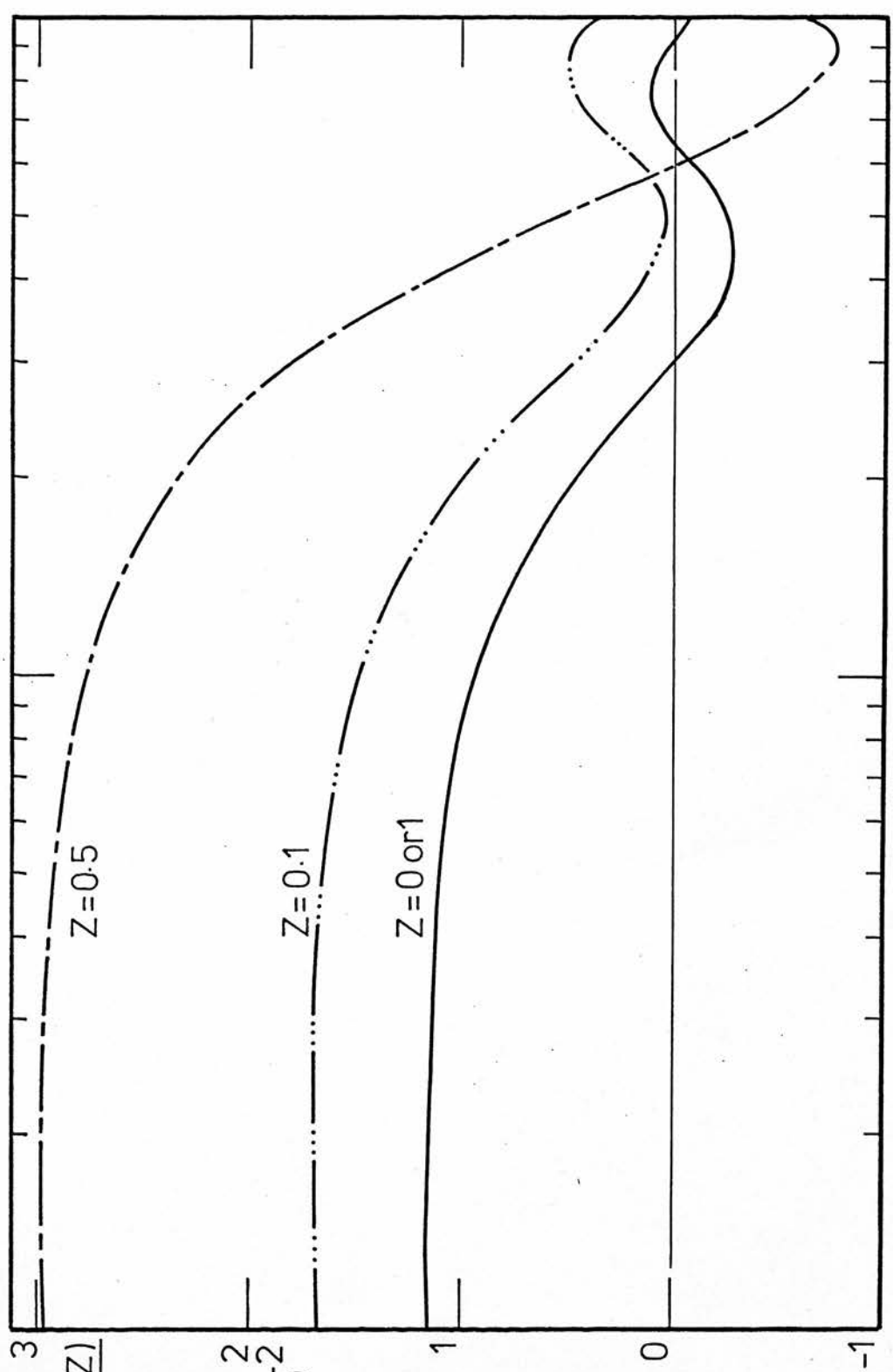

Fig. 6-7a The temperature fluctuation $[T(\pi,z) - T(\pi/2,z)]/T(\pi/2,z)$ as a function of r for different values of Z with mean optical thickness $\mathbf{z}_o = 1.0$. $\eta = 10^2$, $\bar{\omega} = 0.5$, $a = 0.1$, $\mu_o = 1/\sqrt{3}$, $\phi_o = \pi/4$

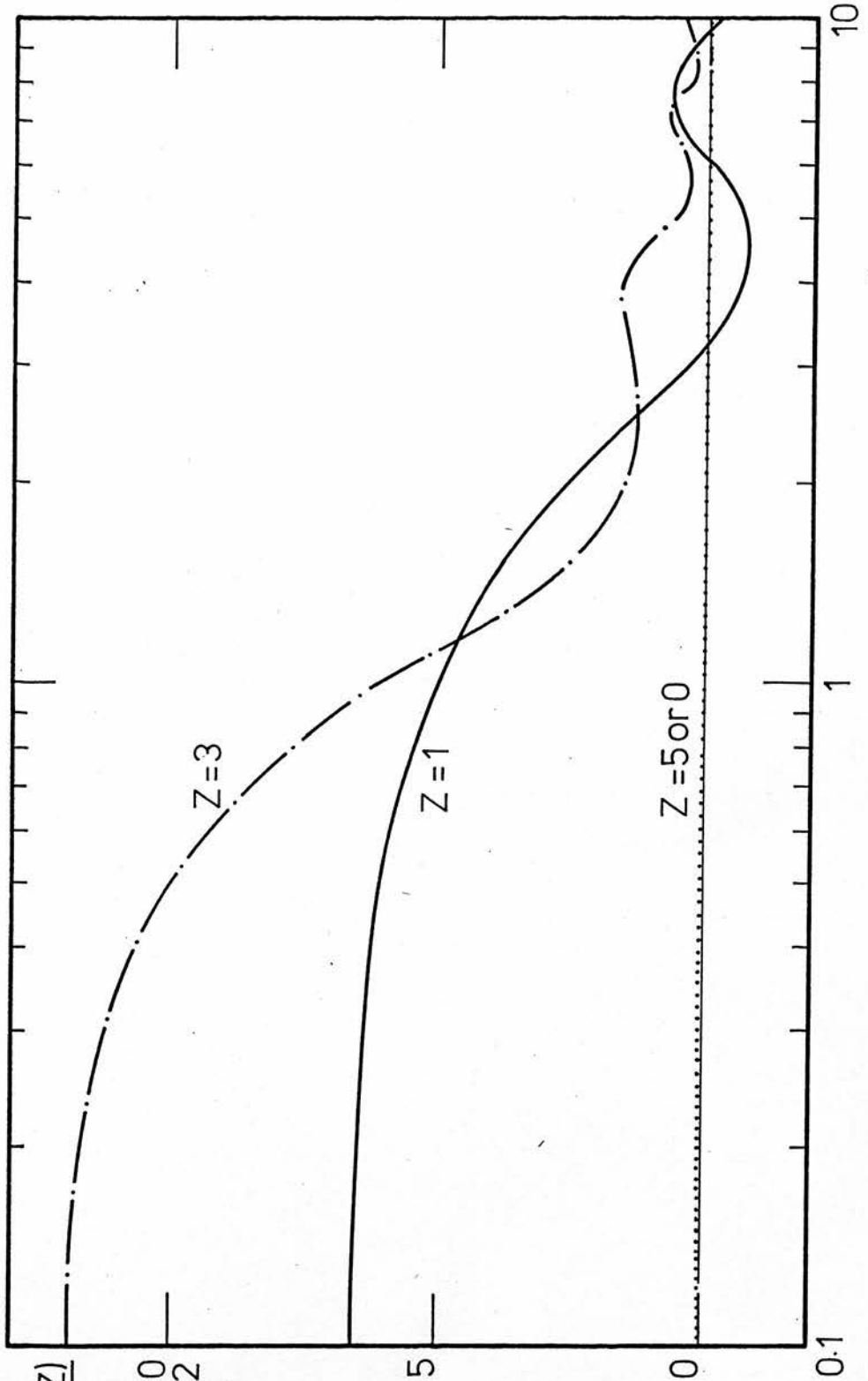

Fig. 6-7b As Fig. 6-7a for Z_o = 5.0.

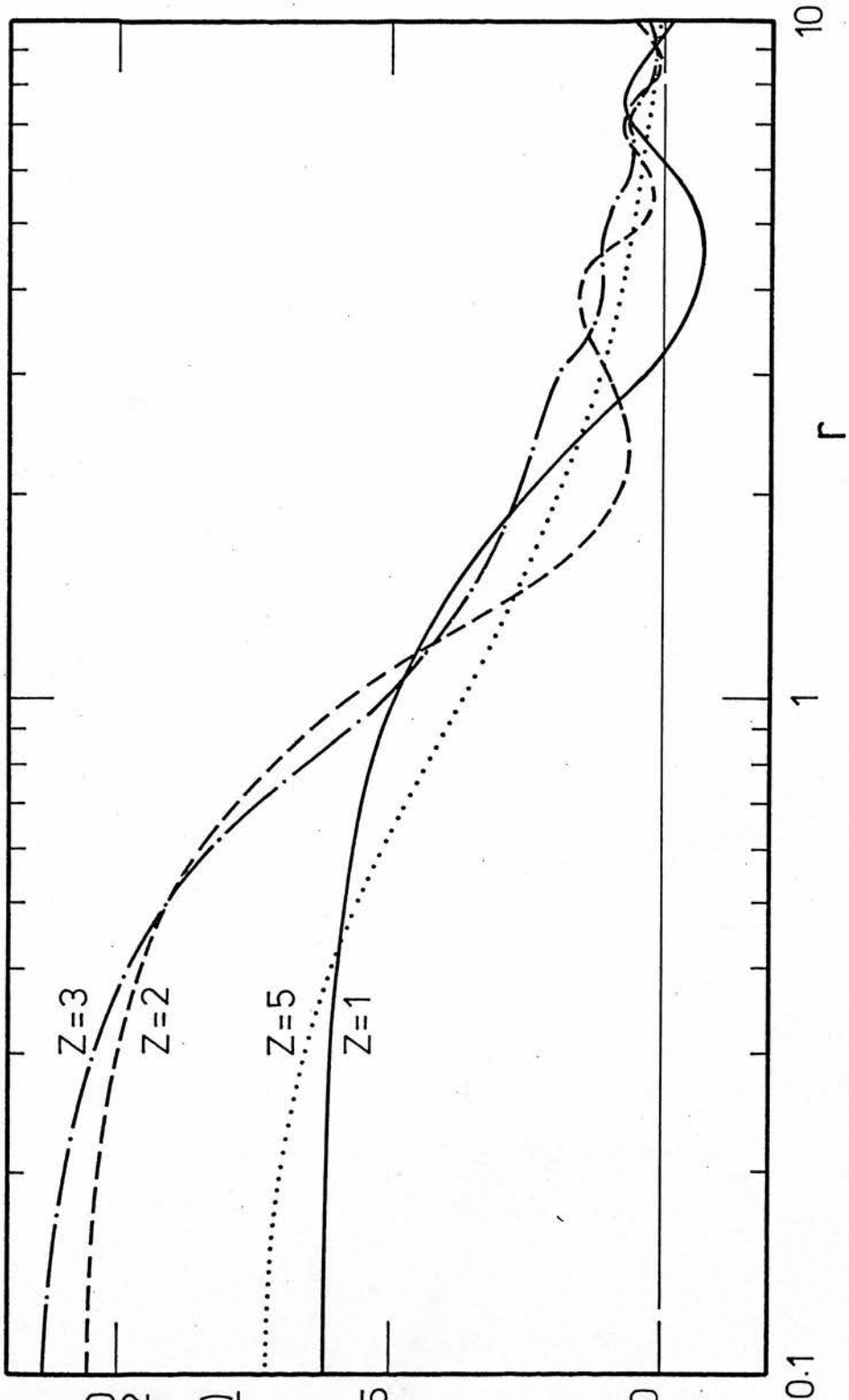

Fig. 6-7c As Fig. 6-7a for Z_o = 10.0.

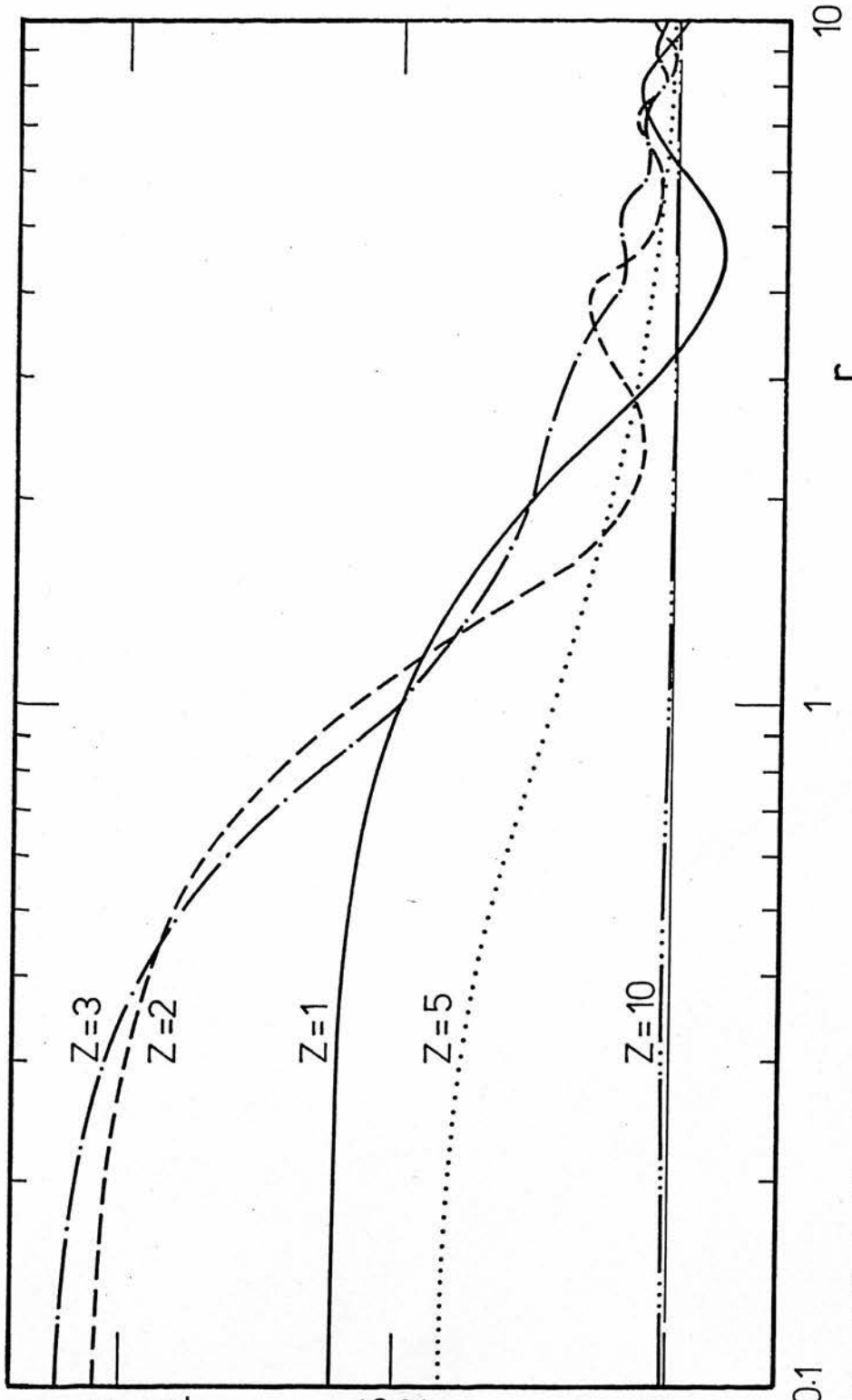

Fig. 6-7d As Fig. 6-7a for Z_o = 20.0.

orders, fluctuations of dust temperature are to be expected at any depth Z. However a strong coupling with Z is evident as can be seen from figure 6-8a,b where the temperature fluctuation has been plotted as a function of Z for the extreme values of r, r = 0.1 and r = 10, and r = 1.0. In particular, it is evident that the strongest effects of inhomogeneities (on the dust temperature) occur towards depths of the order of $Z \simeq 2.5$, a conclusion already drawn from the approximated analytical solution of the semi-infinite model.

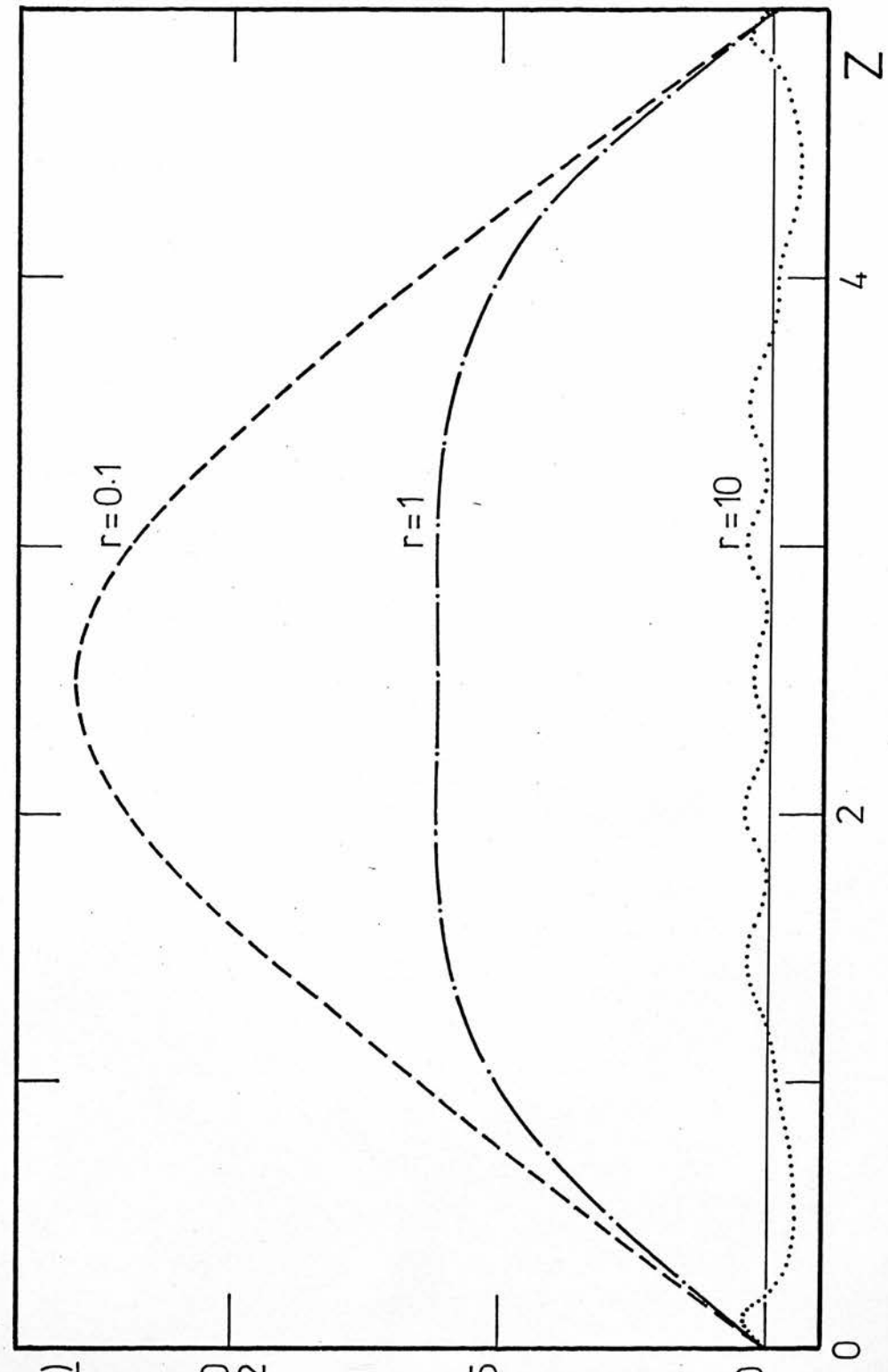

Fig. 6-8a The temperature fluctuation $[T(\pi,Z) - T(0,Z)]/T(\pi/2,Z)$ as a function of Z for several values of r and $Z_o = 5.0$. $\eta = 10^2$, $\bar{\omega} = 0.5$, $a = 0.1$, $\mu_o = 1/3$, $\phi_o = \pi/4$

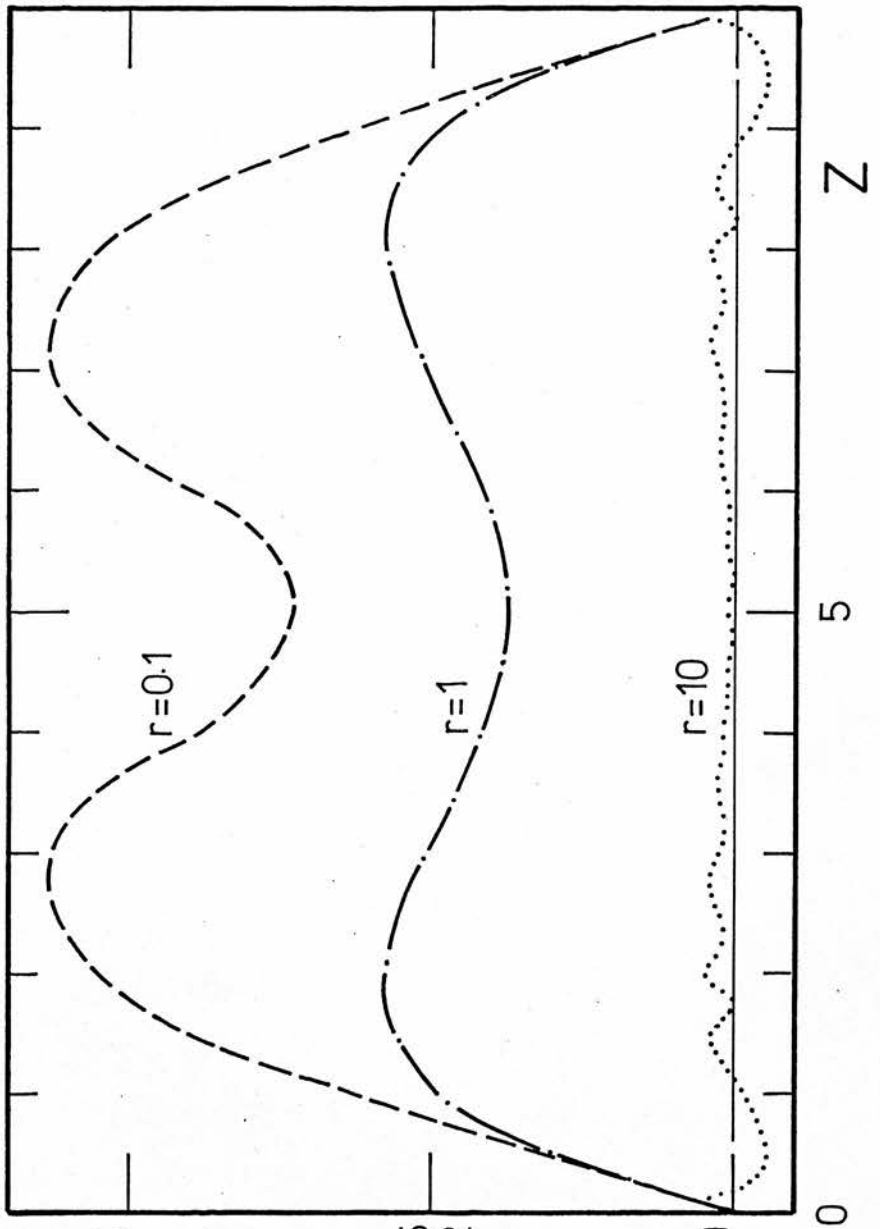

Fig. 6-8b As Fig. 6-8a for Z_o = 10.0.

CHAPTER III

7. LOCAL DENSITY AMPLIFICATIONS DUE TO H_2 FORMATION

The first difficult point that one finds when one tries to follow the evolution of a prestellar cloud is the determination of the cloud conditions at time t = 0, i.e., from which stage of cloud evolution one has to start. One easily sees the necessity of going back in time so that one becomes involved with the problem of galactic evolution and even with the cosmological one, because the way by which prestellar clouds come into being is the main factor that determines initial conditions. No attempt will be made here to go into the whole evolutionary track of prestellar coulds. Instead, as it was pointed out at the beginning of Section 3, a cloud such as that proposed by Roberts (1969) will be considered, and the time t = 0 will be the time at which the atomic cloud has reached the verge of gravitational collapse due to the compression produced by the spiral density wave, i.e. $M \approx M_J$ and gas temperature and density of the order of $T \approx 10^2 K$ and $n \gtrsim 10^2 cm^{-3}$, respectively. Typical masses are of the order of $M \approx 10^4 M_\odot$.

According to Roberts, subsonic turbulence is present in the clouds at the onset of gravitational contraction. Therefore turbulence provides the mechanism generator of fluctuations in the physical parameters characterising the state of the cloud, in particular, spatial fluctuations in density, see appendix B. It is probably unrealistic to work these kind of problems assuming pure statistical fluctuations which are swept out by the turbulent ones, Sasao (1973).

Formally to follow the evolution of the above prestellar clouds,

one would have to establish correlations for pressure, density and temperature of the gas and temperature of the dust, taking into account the gravitational contraction. However, because in the range of values of the temperature and density of the gas and dust temperature, the H_2 formation is controlled by T_d as discussed in Section 3, this complex situation can be schematised, in first approximation, as follows.

The mean density of the cloud, at least at the early stage of the contraction, is determined by the background contraction of the cloud as a whole. The shortest limit for this process is the free-fall which is determined by the equation

$$\frac{1}{\bar{\rho}}\frac{d\bar{\rho}}{dt} = \left[24G\bar{\rho}_o\right]^{\frac{1}{2}}\left\{\frac{\bar{\rho}}{\rho_o}\left[1-\left(\frac{\bar{\rho}_o}{\bar{\rho}}\right)^{1/3}\right]\right\}^{\frac{1}{2}} \qquad (7\text{-}1)$$

see appendix A, where $\bar{\rho}$ is the mean density at any time t and $\bar{\rho}_o$ is the mean density at time $t = 0$, i.e. when the contraction starts.

Turbulence provides density fluctuations superimposed on the mean value $\bar{\rho}$, with a certain spectrum ranging from the size of the cloud to the threshold imposed by viscosity, see appendix B.

According to the relation (6-30), density fluctuations with optical thickness $\lambda_d \bar{\kappa}/2 < \pi/2$* are unable to produce appreciable fluctuation $\Delta T_d/T_{cri}$ and fluctuations with $\lambda_d \frac{\bar{\kappa}}{2} > \pi$ mainly determine the regions where T_d reaches the value T_{cri} first and H_2 formation starts there. Therefore, in a first approximation, one can consider the H_2 formation occurring discontinuously in cells of linear

* Hereafter the subindex s in $\bar{\kappa}_s$ is dropped.

dimensions $\lambda_d/2 \approx \pi/2\overline{\kappa}$ and towards regions where $\overline{T}_d = T_{cri}$ (probably towards the centre of the cloud and towards the peaks of fluctuations at scales $\lambda_d/2 > \pi/\overline{\kappa}$).

With the gas-dynamical problem crudely schematised as above, the crucial point in the Reddish scenario for fragmentation would be, whether or not the H_2 formation can produce an amplification of the density greater than that produced by the contraction of the cloud as a whole and in a time shorter than one free-fall time.

In order to clarify the above aspect we will compare in this section the change $\overline{\rho}(t)$ with the change in ρ and T produced by H_2 formation in cells of dimensions $\lambda_d \frac{\overline{\kappa}}{2} \approx \pi/2$, assuming that at t = 0, the reaction starts simultaneously with the gravitational contraction.

In addition, because of the tendency towards pressure equilibrium, the condition of isobaricity will be introduced in this first approximation. This point is better understood with the help of the following simple ideal laboratory model:

Let us consider an atomic gas of HI and traces of heavy elements confined in a pipe by a piston. At $t < 0$, the gas is maintained at a certain temperature if the heating rate is equal to the cooling rate, $\Lambda = \Gamma$. On the other hand, the temperature T'_d of the walls of the pipe is maintained greater than the critical temperature to H_2 formation. At $t = 0$, $T'_d < T_{cri}$ and the reaction $2HI + (walls) \rightarrow H_2 + (\chi)$ starts. In a first approximation one can set $P_{gas} = P_o$ (external) and because both the number density of particles changes and a <u>new coolant</u> (the H_2) appears, the gas is thermally destabilised regardless

of the nature of Γ and Λ.

It is not necessary to assume that the piston is at rest at $t < 0$, it could be oscillating around some equilibrium position if the nature of the equilibrium $\Gamma = \Lambda$ is stable for such oscillations, in this case one would have $\overline{P}_{gas} = P_o$. Such a motion would give a schematical representation to the initially reversible fluctuations in ρ, T and P due to turbulence.

One must recognise that although the isobaric condition is not very realistic, mainly because the effect of both reduction of the number of particles and the presence of the new coolant is to produce a reduction in pressure with respect to the gravitational force, resulting in an inwards motion, it permits one to gain some insight into the effects of H_2 formation, without entering into the difficult gas-dynamical problem appearing if one removes this condition for a contracting, reacting and turbulent dusty medium*. Additional discussion "a posteriori" of this awkward but simplifying hypothesis of isobaricity will be covered later.

a. Basic Equations and their Solution

In this first attempt, despite the chemical reaction the state equation is

$$P = \frac{R}{2} (1 + x) \rho T \qquad (7\text{-}2)$$

where P, ρ and T are pressure, mass density and temperature of the gas, R the gas constant and $x = n_H/n$ is the chemical parameter indicating the advance of the reaction, n_H and n are the number density of atomic hydrogen and total number of atoms respectively.

* where the reaction rate is controlled by the radiative field through the dust temperature.

In addition to equation (7-2), the chemical and energy equations are introduced, see appendix A, i.e.

$$\frac{dx}{dt} = -\gamma < \tilde{\sigma}_d > \left(\frac{3k}{m_H^3} \right)^{\frac{1}{2}} \left(\frac{n_d}{n} \right) T^{\frac{1}{2}} \rho x \qquad (7\text{-}3)$$

and

$$\rho \frac{du}{dt} = \Gamma - \Lambda + \frac{P}{\rho} \frac{d\rho}{dt} \qquad (7\text{-}4)$$

u being the internal energy per unit mass given by

$$u(x, \rho, T) = \frac{5 + x}{4} RT + \varepsilon x N_o \chi \qquad (7\text{-}5)$$

where ε is the fraction of the binding energy χ(= 4.477 e.v.) going to heat the gas and N_o the Avogadro number.

In order to evaluate <u>only</u> the effects of the H_2 formation in a cell of dimensions $\lambda_d/2 = \pi/2\bar{\kappa}$, the gas will be considered at $t < 0$ with $\Lambda - \Gamma = 0$, which adjust the gas temperature at some value to ($\approx 10^2$ ^oK) and at $t \geq 0$, $\Lambda - \Gamma = \Lambda_{H_2}$. Therefore, from equations (7-4) and (7-5) one obtains the relation

$$\frac{R}{4} \rho (5 + x) \frac{dT}{dt} + \rho \left(\frac{R}{4} T + \varepsilon \chi N_o \right) \frac{dx}{dt} = \Lambda_{H_2} + \frac{P}{\rho} \frac{d\rho}{dt} \qquad (7\text{-}6)$$

Physically, equation (7-6) means that <u>only</u> the compressional heating $\frac{P}{\rho} \frac{d\rho}{dt}$ and the net cooling (or heating) due to H_2 molecules, i.e. $\Lambda_{H_2} - \varepsilon \rho \chi N_o \frac{dx}{dt}$ are under consideration.

Equations (7-2), (7-3) and (7-6) provide the necessary relations to find x, ρ and T as functions of t with initial conditons

$$x(o) = 1.0, \quad \rho(o) = \rho_o \quad \text{and} \quad T(o) = T_o \tag{7-7}$$

Defining the dimensionless density $\tilde{\rho}$, temperature $\tilde{T}$ and time $\tilde{t}$ by the equations

$$\tilde{\rho}(t) = \frac{\rho(t)}{\rho_o} \qquad \text{(a)}$$

$$\tilde{T}(t) = \frac{T(t)}{T_o} \qquad \text{(b)} \tag{7-8}$$

$$\tilde{t} = \frac{t}{t_{ff}} \qquad \text{(c)}$$

where T_{ff} is the free-fall time given by

$$t_{ff} = \left[\frac{3\pi}{32G\rho_o}\right]^{\frac{1}{2}} \tag{7-9}$$

see appendix A, from equations (7-2), (7-3) and (7-6) one obtains the following relations

$$\frac{dx}{d\tilde{t}} = -\theta_o \tilde{T}^{\frac{1}{2}} \tilde{\rho} x \qquad \text{(a)}$$

$$\frac{d\tilde{\rho}}{d\tilde{t}} = \theta_o \{ c_o \frac{1}{1+\xi} \frac{1-x}{7+3x} \frac{\tilde{\rho}}{\tilde{T}} g(\tilde{T}) \exp(-\alpha_o/\tilde{T}) + \left(\frac{4}{1+x} - \frac{\gamma_o}{\tilde{T}}\right) \frac{x\tilde{T}^{\frac{1}{2}}\tilde{\rho}^2}{7+3x} \} \qquad \text{(b)} \tag{7-9}$$

$$\frac{d\tilde{T}}{d\tilde{t}} = \theta_o \{ -c_o \frac{1}{1+\xi} \frac{1-x}{7+3x} g(\tilde{T}) \exp(-\alpha_o/\tilde{T})$$

$$+ (3 + \frac{\gamma_o}{\tilde{T}}) \frac{x\tilde{T}^{3/4}\tilde{\rho}}{7+3x} \} \qquad (c)$$

where

$$\theta_o = \gamma \langle \tilde{\sigma}_d \rangle (\frac{3k}{m_H})^{\frac{1}{2}} (\frac{n_d}{n}) T_o^{\frac{1}{2}} \rho_o t_{ff} \qquad (a)$$

$$c_o = \frac{10.0\, t_{ff}}{R T_o \theta_o} \qquad (b)$$

$$\alpha_o = 512/T_o \qquad (c)$$

$$\gamma_o = \varepsilon \frac{4\chi N_o}{R T_o} \qquad (d) \qquad (7\text{-}10)$$

$$\xi = \frac{\beta_o}{\tilde{T}^{\frac{1}{2}} \tilde{\rho} (1 + 19x)} \qquad (e)$$

$$\beta_o = \frac{840}{n_o T_o^{\frac{1}{2}}} \qquad (f)$$

and $g(\tilde{T})$ is a correction factor in the cooling function of the H_2 molecule greater than 1.0 when $T \gtrsim 150^{o}K$ due to excitation of rotational levels greater than J = 2, Hattori et al (1969).

The system of equations (7-9) with initial conditions (7-7) has been solved numerically like a two boundary value problem using Merson's method and Newton iteration, Haselgrove (1961), Mayers (1962).

b. Discussion of the Results

The solutions of the system of equations (7-9) are plotted in figures (7-1) to (7-16), for different values of: the fraction of the binding energy going as a heat input to the gas ε, the dust-gas number ratio n_d/n, and different values of the initial temperature T_o and number density $n_o cm^{-3}$. In some of these plots, the change in the background mean density $\bar{\rho}(\tilde{t})$ due to the gravitational contraction, corresponding to the same initial density n_o is shown. This function $\bar{\rho}(\tilde{t})$ was calculated using either the numerical solution to equation (7-1) or the analytical one, i.e.

$$\bar{\rho}(t) = \bar{\rho}_o \sec^6 \beta \qquad \text{(a)}$$

$$\beta + \tfrac{1}{2} \sin 2\beta = t \left[\frac{8\pi G \rho_o}{3} \right]^{\frac{1}{2}} \qquad \text{(b)} \qquad (7\text{-}11)$$

see appendix A.

Runs were done for a mean dust cross-section $\langle \sigma_d \rangle = 7.1 \times 10^{-10}$ cm^2, SW (1969), Greenberg (1979), and for different values of the following parameters: fraction of the binding energy going to heat the gas ε and dust to gas ratio n_d/n. The range of variation of these parameters and the initial values of gas temperature T_o and gas

particle density n_o is shown in table 7-1.

Table 7-1

$$0.00 \leq \varepsilon \leq 0.04 \quad *$$

$$10^{-12} \leq \frac{n_d}{n} \leq 10^{-11}$$

$x(o) = 1.0$

$T_o = 120,\ 100,\ 80,\ 60\ ^oK$

$n_o = 10^2,\ 10^3,\ 5 \times 10^3,\ 10^4\ cm^{-3}.$

Generally speaking, from the numerical solutions one sees that the capacity of the H_2 formation as direct amplifier of density inhomogeneities depends sensitively on: the fraction of chemical heating ε, the initial mean density and temperature of the gas at the onset of contraction.

If the H_2 molecule is formed in highly excited rotational levels$^{\neq}$ and the remainder of the binding energy is radiated by the grains $\varepsilon = 0$, i.e. no heat input to the gas occurs, the corresponding solutions of equations (7-9) are those plotted in figures (7-1) to (7-8).

For $n_d/n = 10^{-12} cm^{-3}$ the following results emerge: For $n_o = 10^2 cm^{-3}$, effective density amplification by H_2 formation would

* Upper limit calculated by Hunter and Watson (1978).

$\neq$ The timescale for spontaneous radiative decay from these levels to the ground one is of the order of 10^{10}s, which is three orders of magnitude smaller than the timescales under consideration and therefore the H_2 cooling function adopted in equation (7-9) is correct in first approximation.

require a rather high initial gas temperature, probably $T_o > 80^oK$. For example, for $T_o = 120^oK$, figure 7-1b, the amplification produced by H_2 formation would be a factor ~ 2.0 at the time $t = 0.4\ t_{ff}$.

Here, it is necessary to emphasise that the factors of density amplification obtained in this section would underestimate the true values* because the free-fall time is the shortest limit to the gravitational contraction and clouds do not start to collapse free of pressure. In addition, the density amplification by H_2 formation is coupled with that produced by the contraction of the cloud as a whole. This non-trivial and strongly non-linear coupling will be explored in future research.

The situation looks much more favourable in the case $n_o = 10^3 cm^{-3}$, figures (7-2a) and (7-2b). For $T_o > 60^oK$ the effect of the new coolant becomes important and an effective enhancement in density occurs.

An interesting aspect to note is that the temperature exhibits a maximum at a time depending on the initial values T_o and n_o. This is because at the start of the H_2 reaction there is not enough H_2 to cool effectively. This maximum scarcely appears at $T_o = 120^oK$ (for $n_o = 10^3 cm^{-3}$), figure (7-2b). At this initial temperature the enhancement of density always appears very strong.

At initial density $n_o = 5.0 \times 10^3 cm^{-3}$, figures (7-3a) and 7-3b), the effects due only to the change of number of particles are already

* Assuming that the uncomfortable hypothesis of isobaricity has some real sense at least as first approximation.

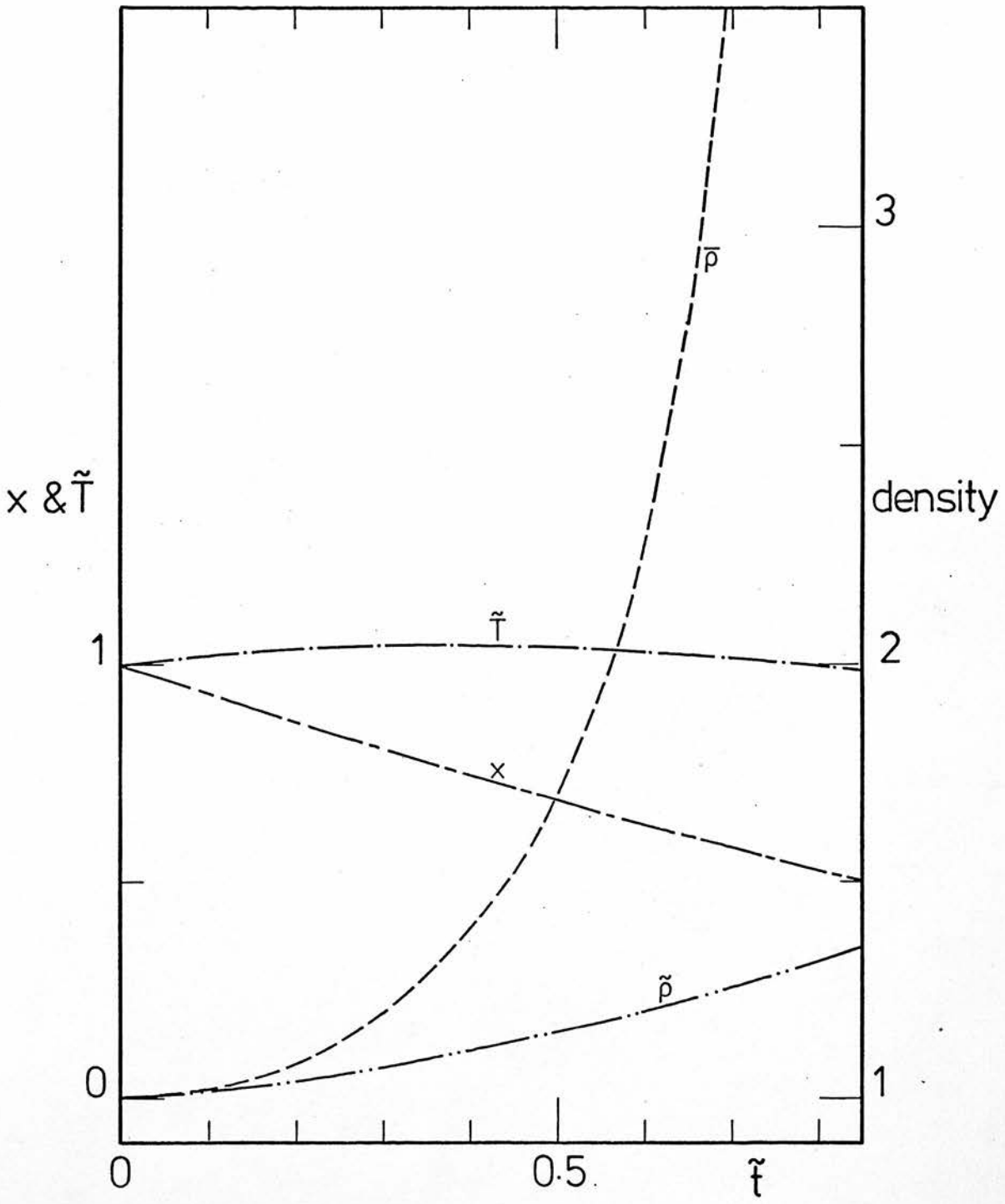

Fig. 7-1a The functions $x(\tilde{t})$, $\tilde{T}(\tilde{t})$, $\tilde{\rho}(\tilde{t})$ and $\bar{\rho}(\tilde{t})$ for $T_o = 60^oK$, $n_o = 10^2 cm^{-3}$, $x_o = 1.0$, $\varepsilon = 0.00$ and $n_d/n = 10^{-12}$.

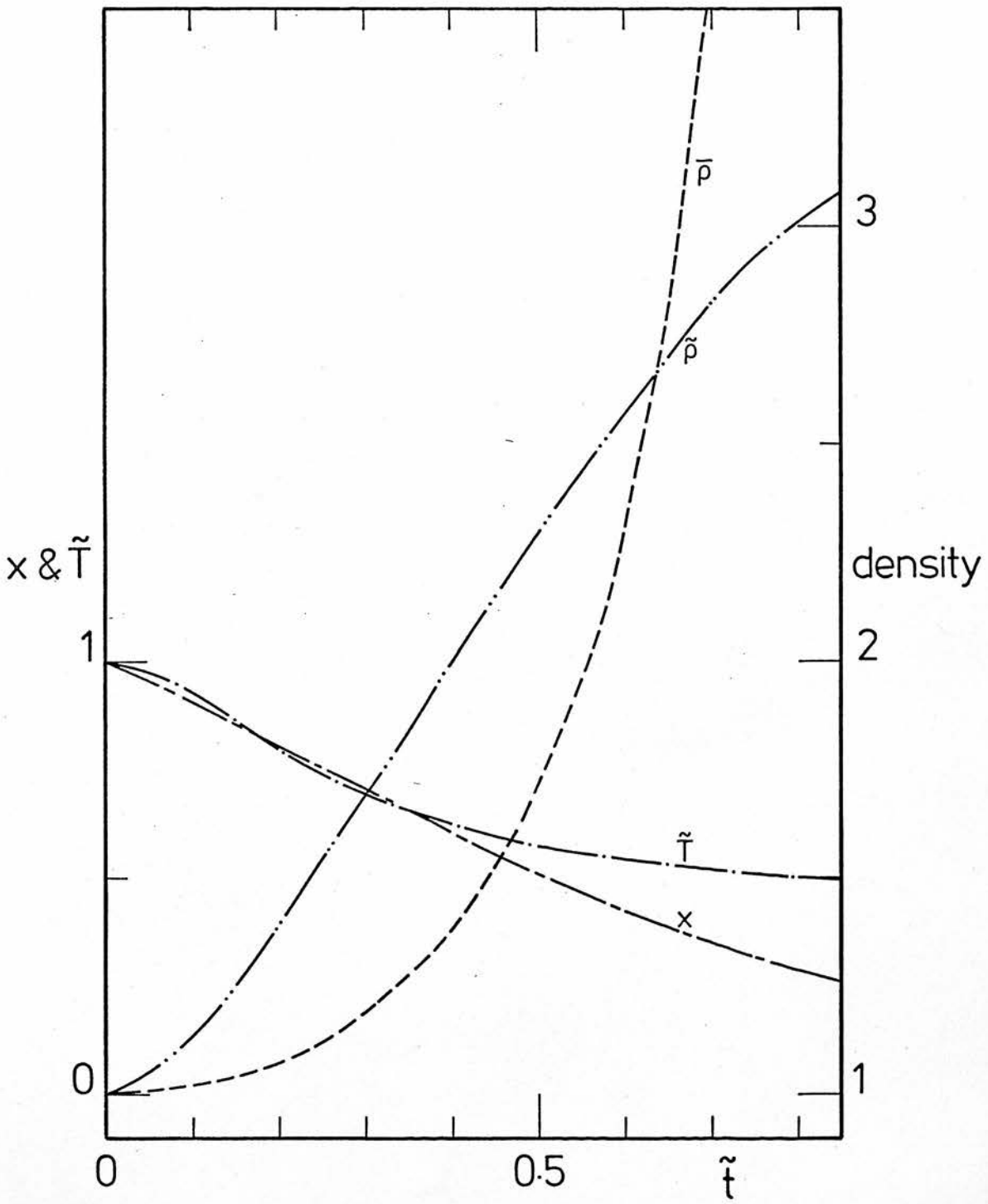

Fig. 7-1b The functions $x(\tilde{t})$, $\tilde{T}(\tilde{t})$ and $\bar{\rho}(\tilde{t})$ for $T_o = 1.2 \times 10^2\ ^oK$, $n_o = 10^2 cm^{-3}$, $x_o = 1.0$, $\varepsilon = 0.00$ and $n_d/n = 10^{-12}$.

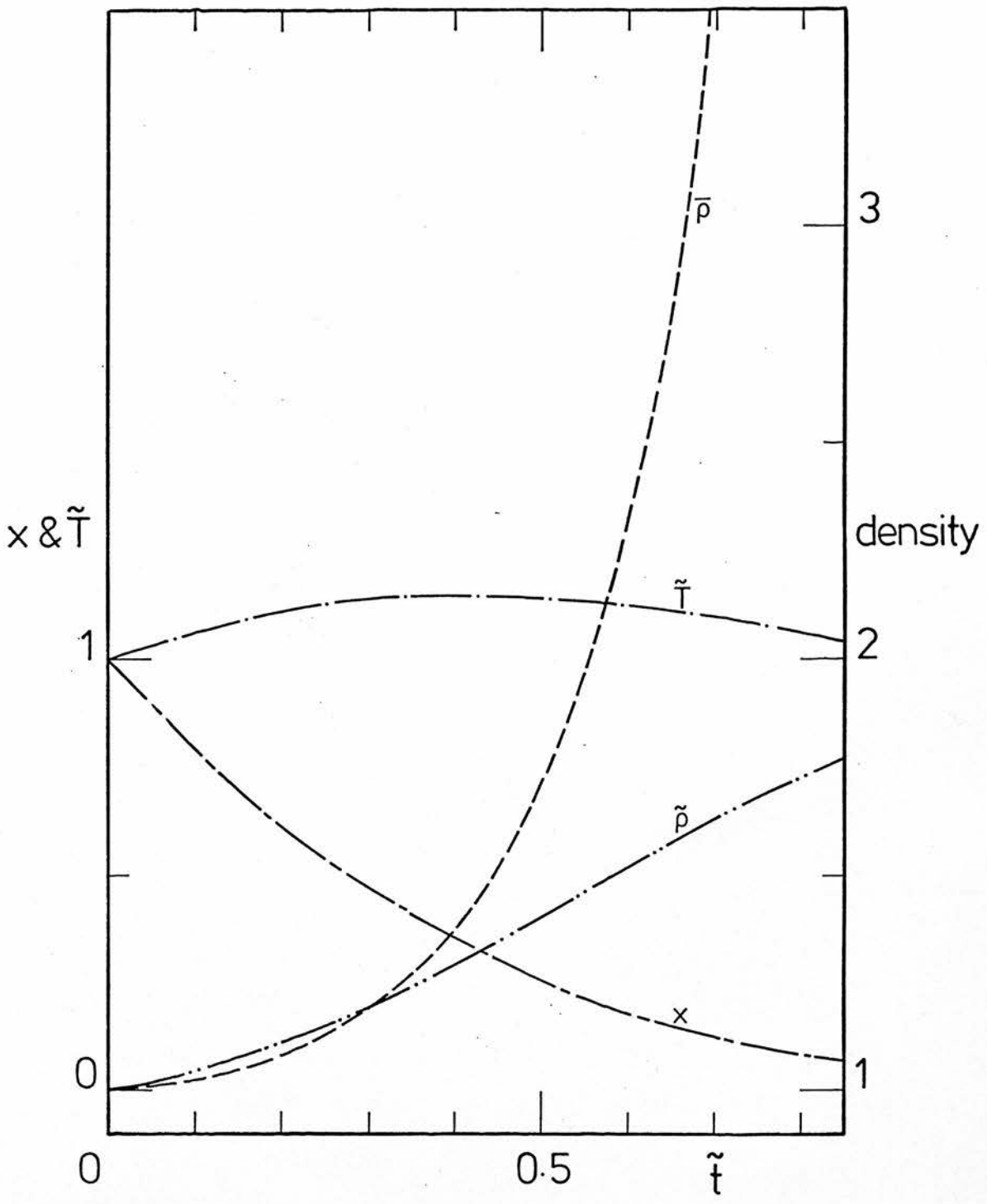

Fig. 7-2a As Fig. 7-1a for $n_o = 10^3 cm^{-3}$.

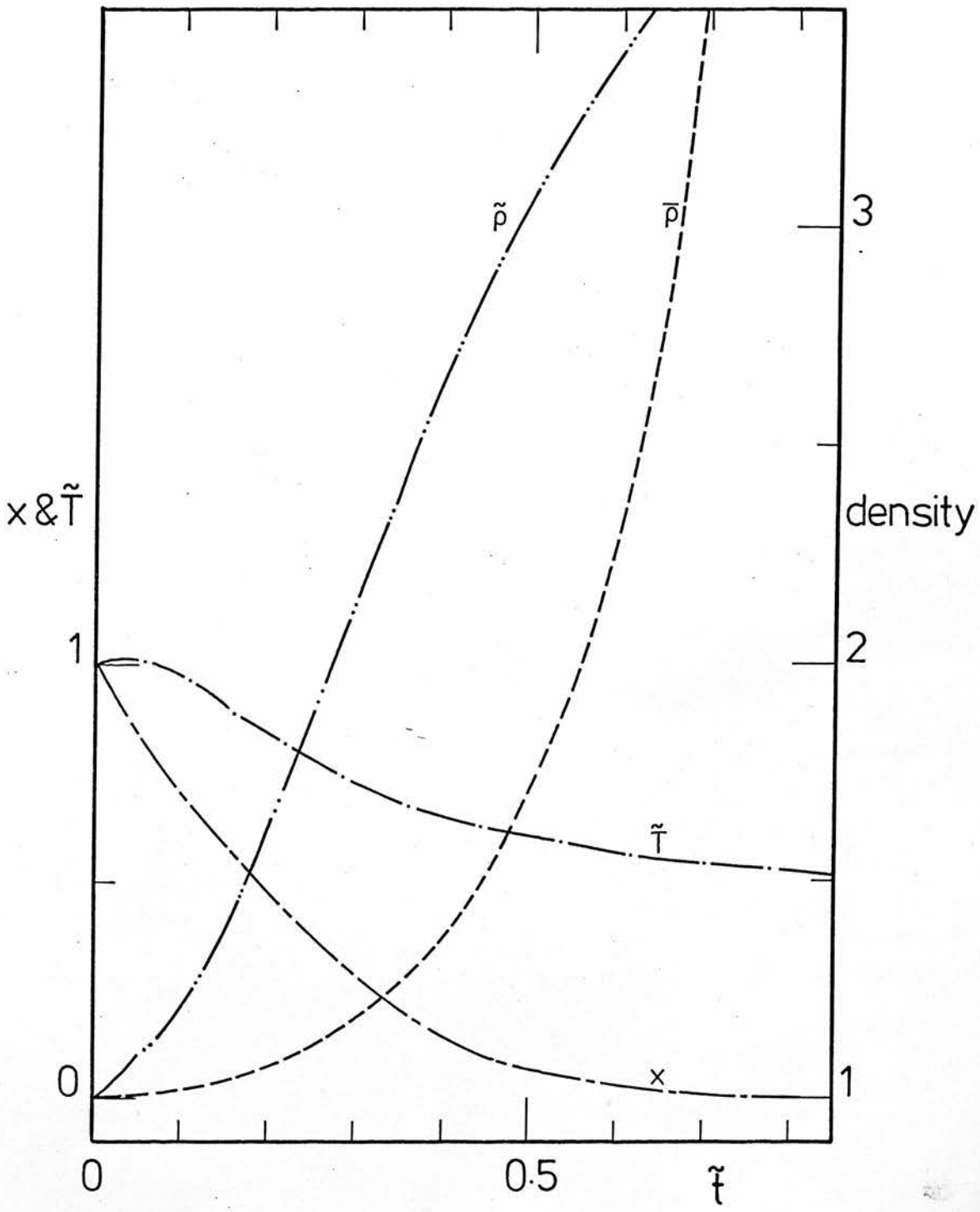

Fig. 7-2b As Fig. 7-1b for $n_o = 10^3 cm^{-3}$.

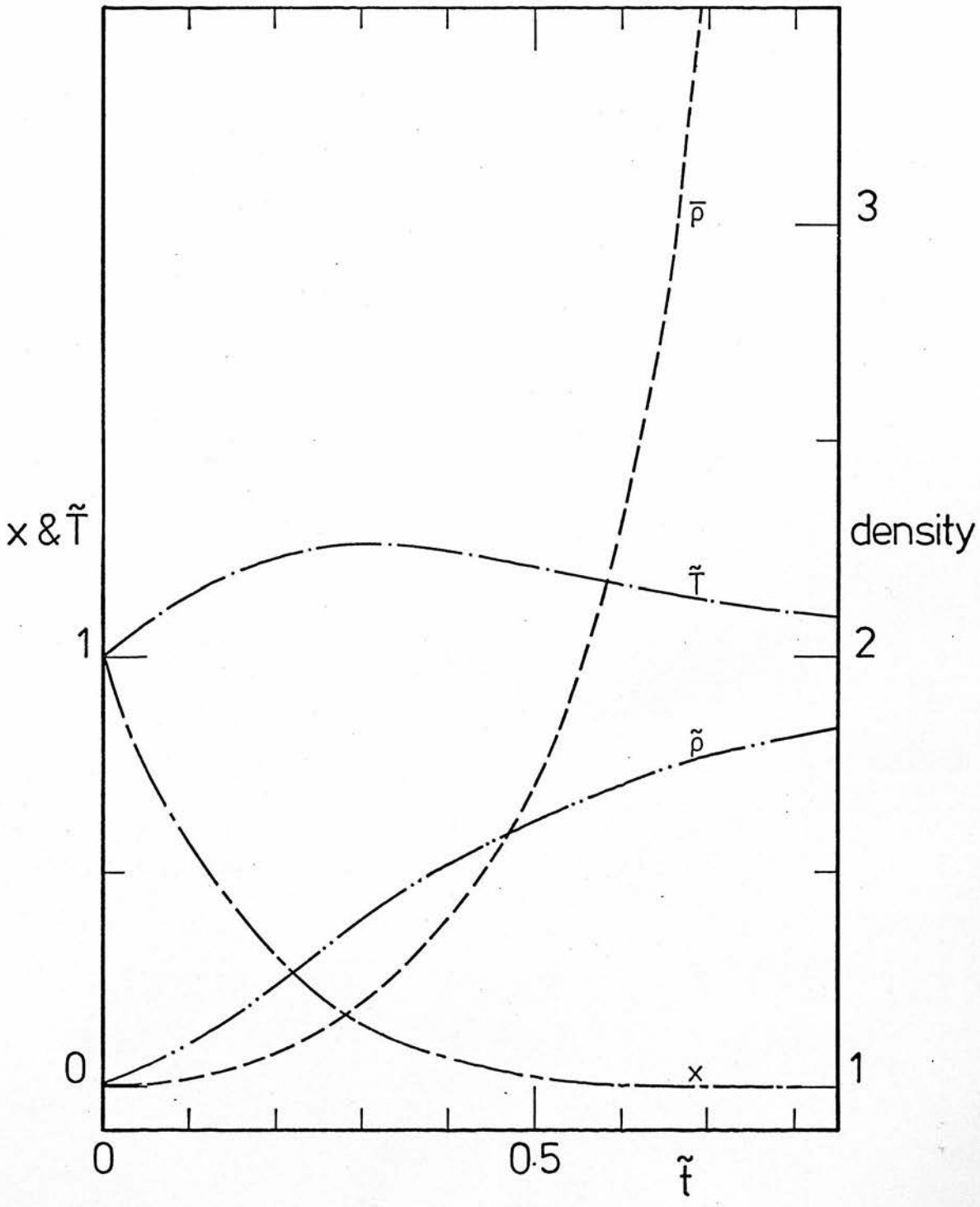

Fig. 7-3a As Fig. 7-1a for $n_o = 5 \times 10^3 cm^{-3}$.

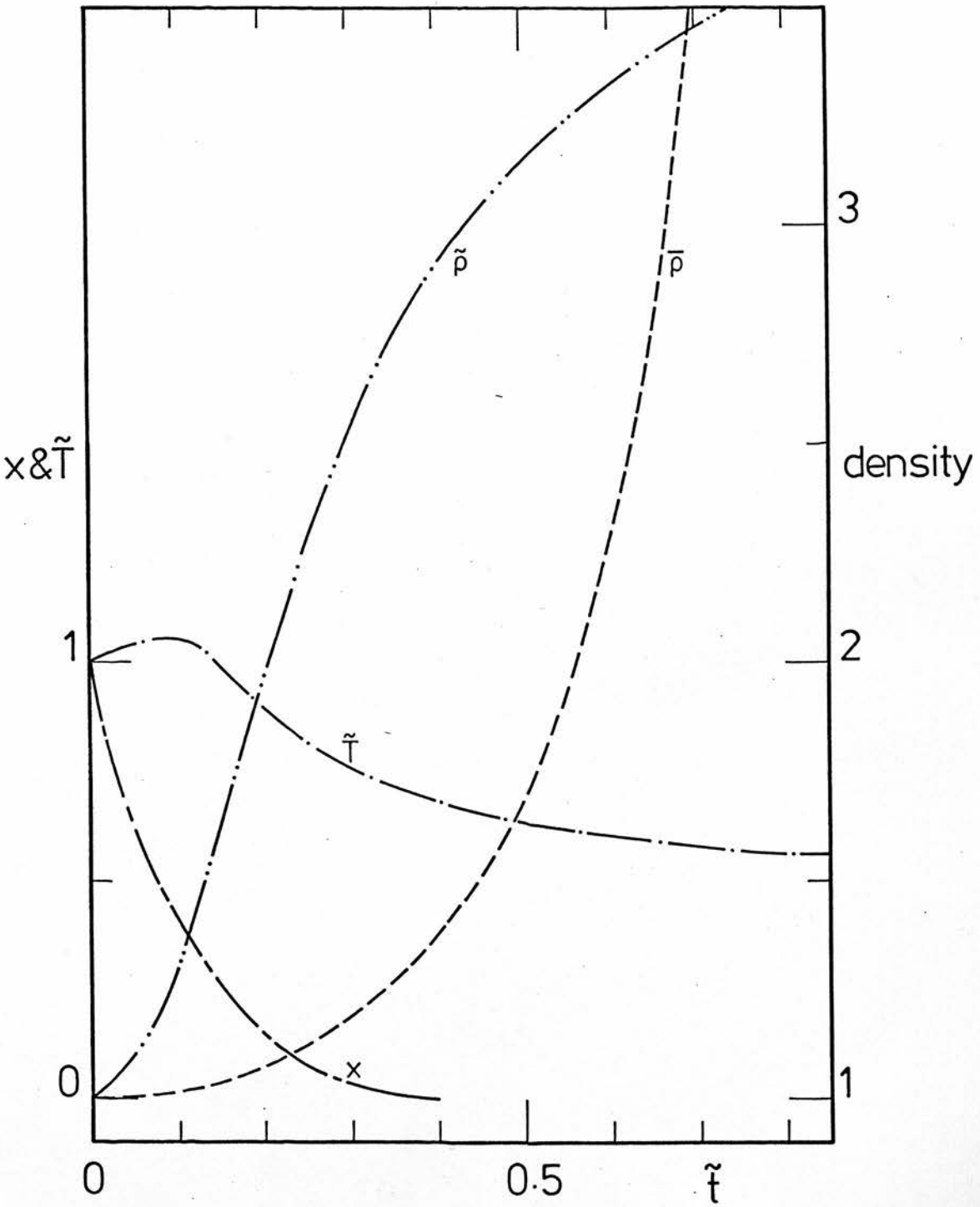

Fig. 7-3b As Fig 7-1b for $n_o = 5 \times 10^3 cm^{-3}$.

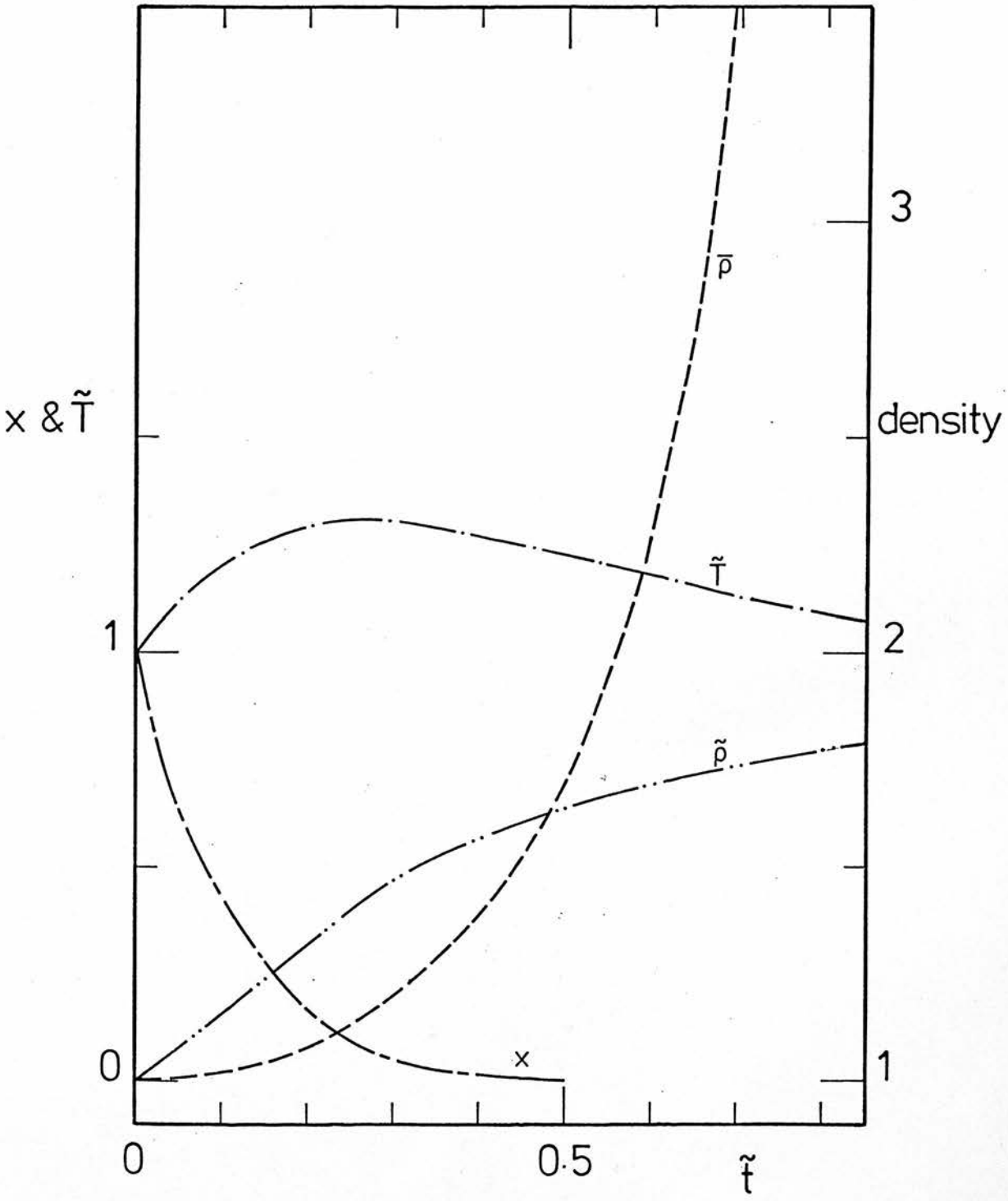

Fig. 7-4a As Fig. 7-1a for $n_o = 10^4 cm^{-3}$.

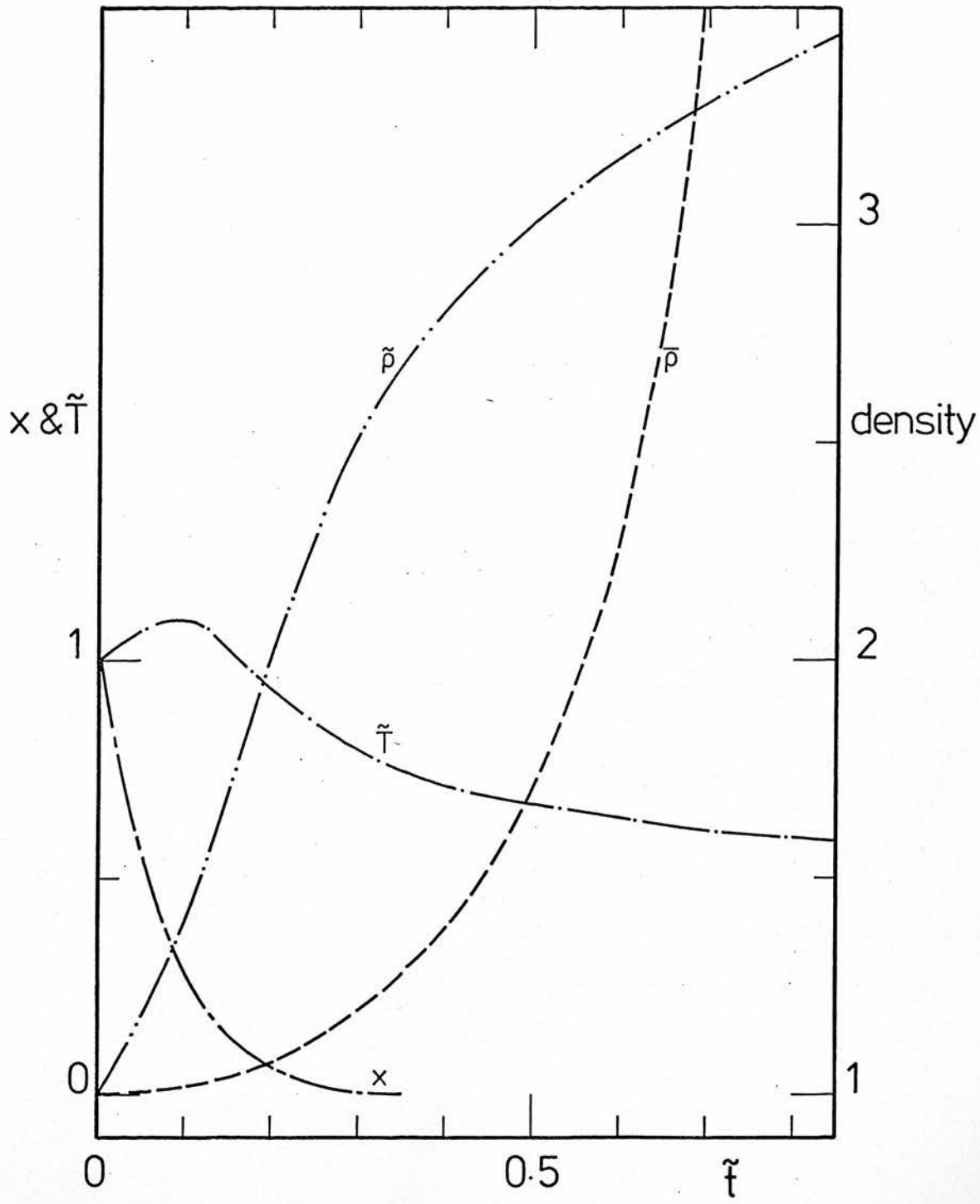

Fig. 7-4b As Fig. 7-1b for $n_o = 10^4 cm^{-3}$.

appreciable, as can be seen from figure (7-3a), where the cooling effects of the H_2 are ineffective because the gas temperature is too low ($60^{o}K$).

It has been found that the H_2 molecule is unable to cool the gas below about $60^{o}K$, the exact temperature depending on n, as is expected from simple physical considerations.

The results for the rather high initial density value of $n_o = 10^4 cm^{-3}$ have been plotted in figures (7-4a) and (7-4b). The behaviour of x, $\tilde{\rho}$ and $\tilde{T}$ are qualitatively the same as the case $n_o = 5.0 \times 10^3 cm^{-3}$, but the effects of H_2 formation are shifted towards earlier epochs of the contraction. In particular the atomic hydrogen is exhausted at

$$t < 0.4\ t_{ff}.$$

The case $\frac{n_d}{n} = 10^{-11}$ has been plotted in figures (7-5) to (7-8) Effective enhancement in density due to H_2 formation appears at times $< 0.1\ t_{ff}$, for the whole range of initial density and temperature of the gas given in table 7-1. This case could be of particular interest if the clouds reach the verge of gravitational contraction with an irregular dust distribution caused by any of the mechanisms capable of decoupling dust and gas in the interstellar medium, see for instance Harrison (1978) and Flannery and Krook (1978).

The solutions of equations (7-10) are not altered in essence if $\chi\varepsilon \lesssim \frac{kT_o}{2}$, i.e. $\gamma_o < 2$ and therefore

$$\frac{d\tilde{\rho}}{d\tilde{t}} > 0 \qquad \text{at } t = 0.$$

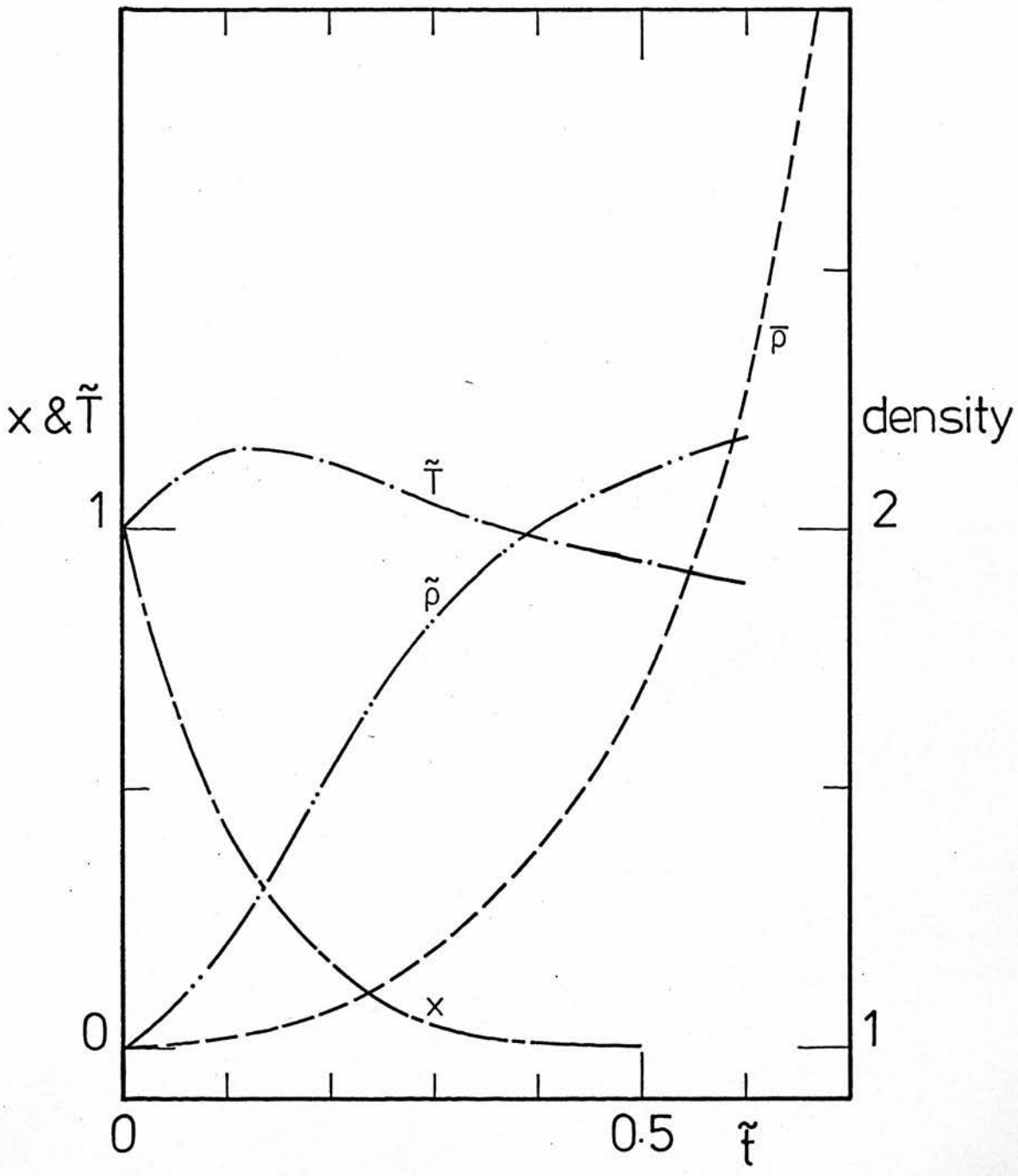

Fig. 7-5a The functions $x(\tilde{t})$, $\tilde{T}(\tilde{t})$, $\tilde{\rho}(\tilde{t})$ and $\bar{\rho}(\tilde{t})$ for $T_o = 60^oK$, $n_o = 10^2 cm^{-3}$, $x_o = 1.0$, $\varepsilon = 0.00$ and $n_d/n = 10^{-11}$.

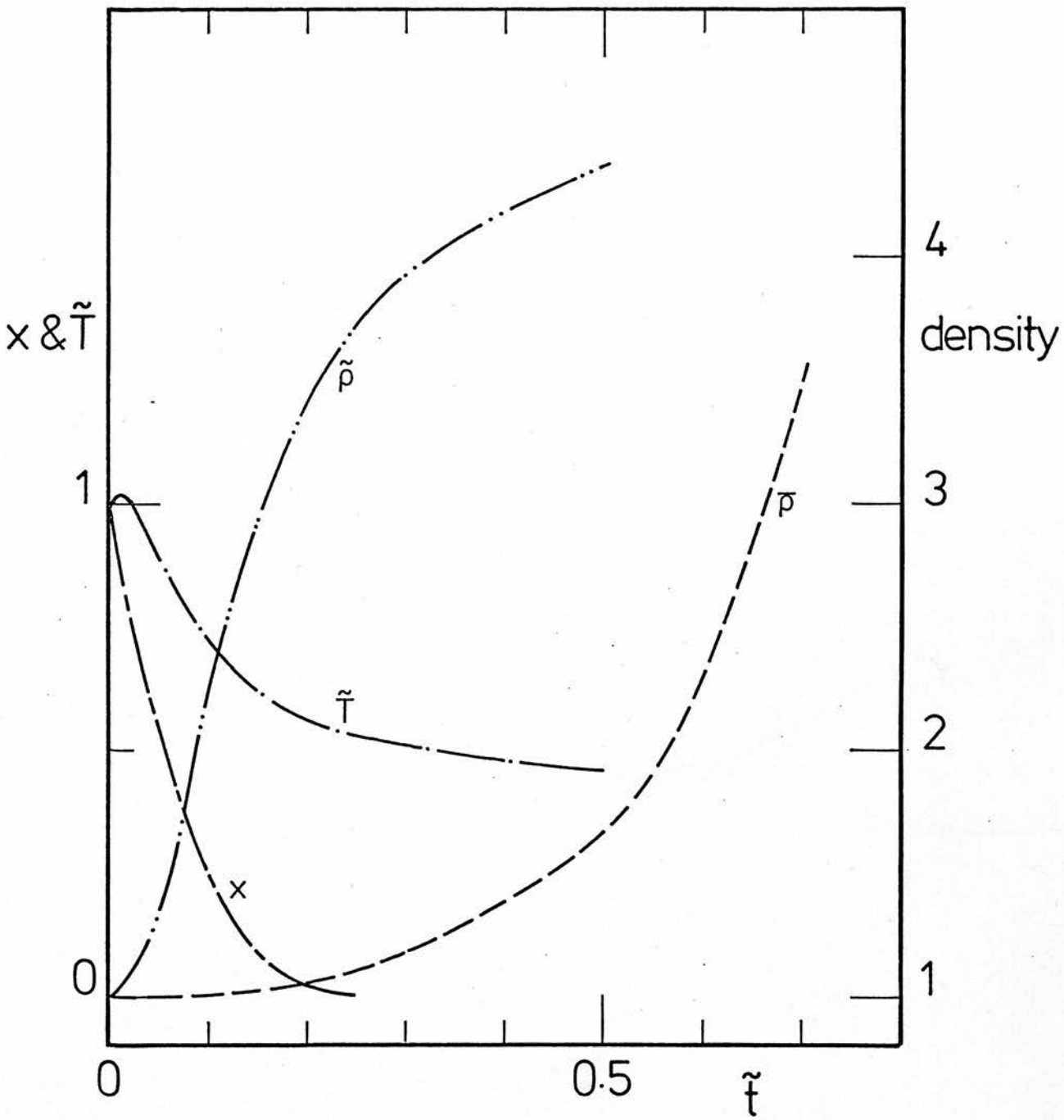

Fig. 7-5b The functions $x(\tilde{t})$, $\tilde{T}(\tilde{t})$, $\tilde{\rho}(\tilde{t})$ and $\bar{\rho}(\tilde{t})$ for $T_o = 1.2 \times 10^2\ ^oK$, $n_o = 10^2 cm^{-3}$, $x_o = 1.0$, $\varepsilon = 0.00$, $n_d/n = 10^{-11}$.

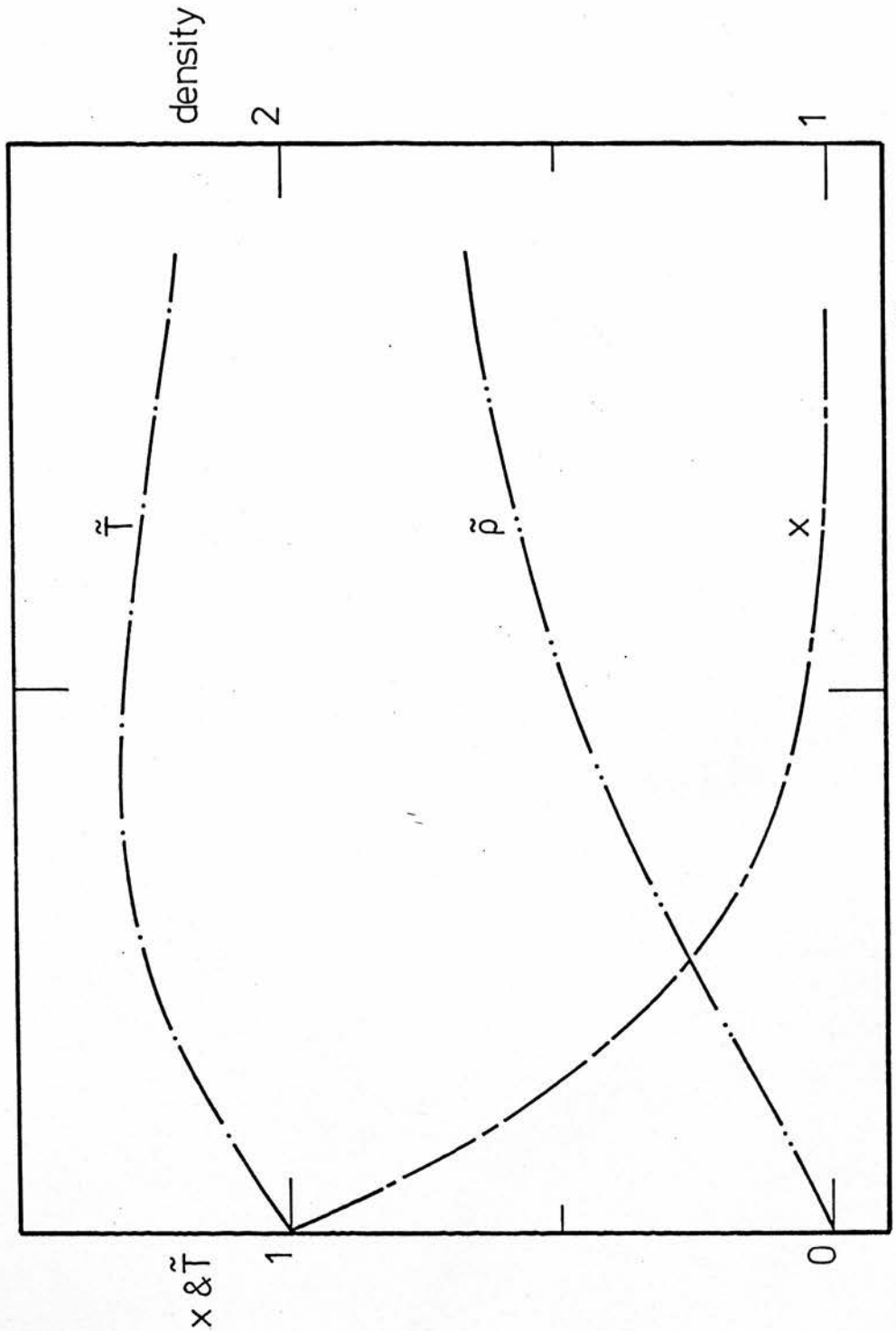

Fig. 7-6a The functions $x(\tilde{t})$, $\tilde{T}(\tilde{t})$ and $\tilde{\rho}(\tilde{t})$ for $T_o = 60^oK$, $n_o = 10^3 cm^{-3}$, $x_o = 1.0$, $\varepsilon = 0.00$ and $n_d/n = 10^{-11}$.

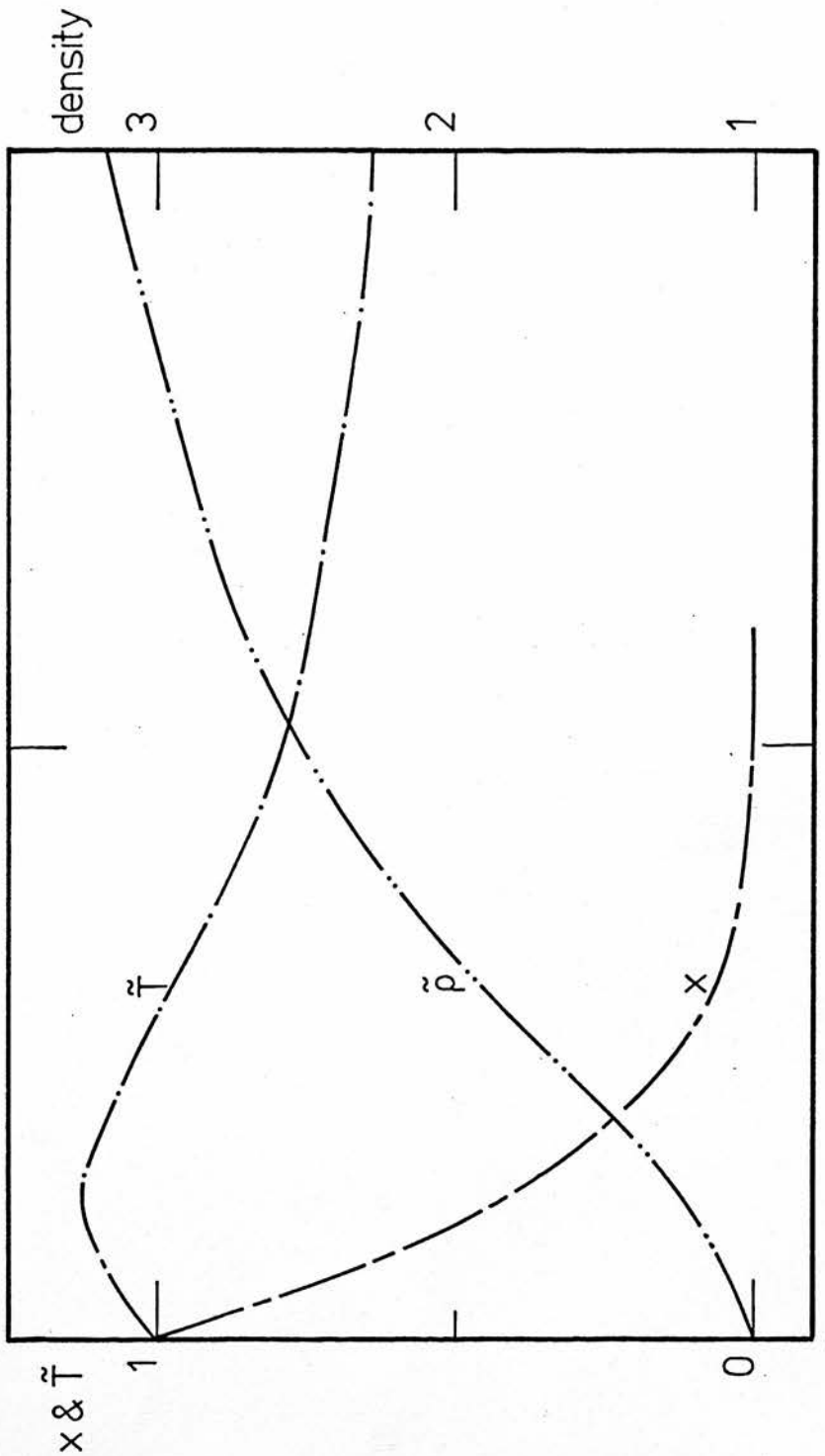

Fig. 7-6b The functions $x(\tilde{t})$, $\tilde{T}(\tilde{t})$ and $\tilde{\rho}(\tilde{t})$ for $T_o = 1.2 \times 10^2$, $n_o = 10^3 cm^{-3}$, $x_o = 1.0$, $\varepsilon = 0.00$ and $n_d/n = 10^{-11}$.

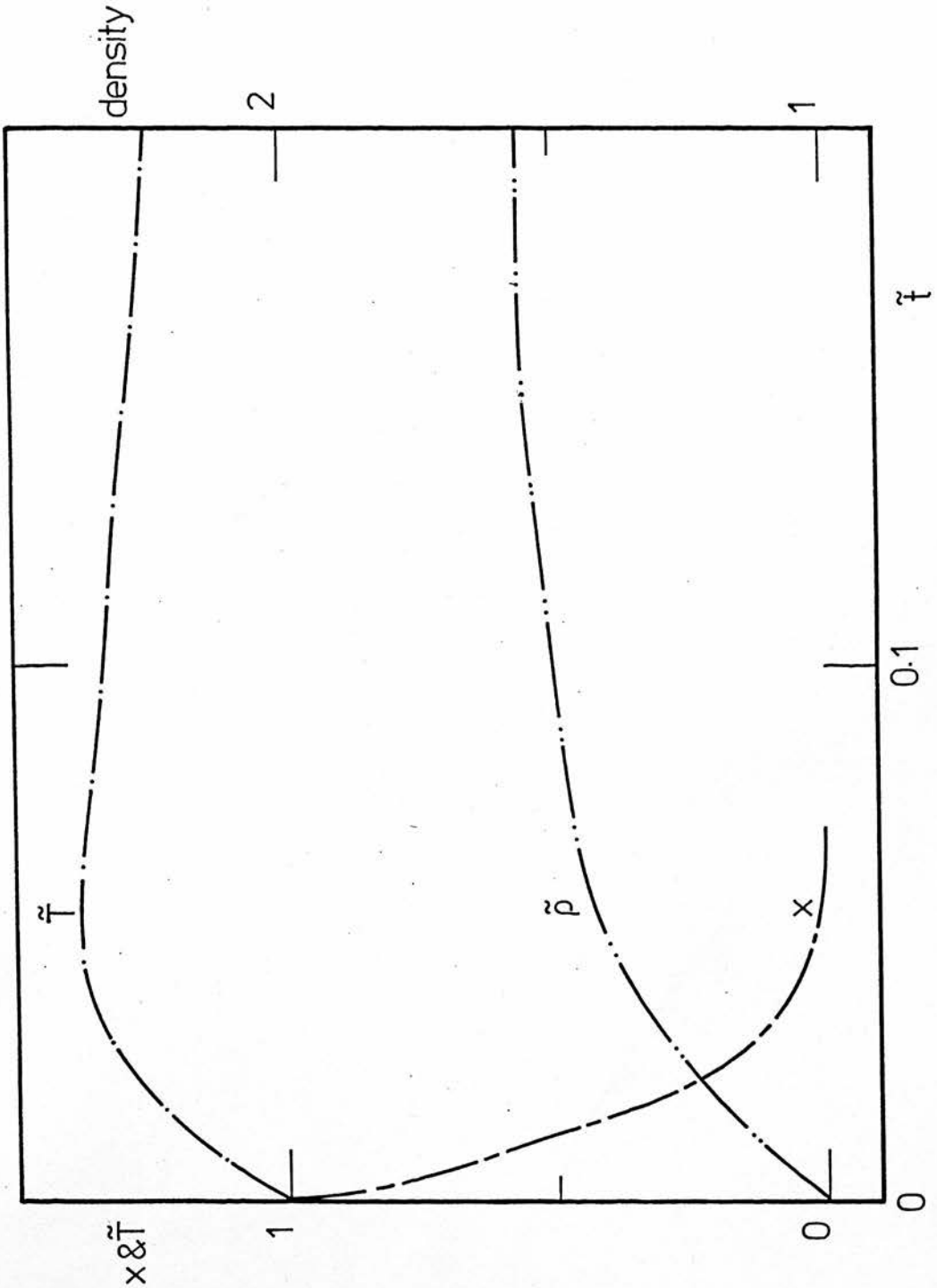

Fig. 7-7a As Fig. 7-6a for $n_o = 5 \times 10^3 cm^{-3}$.

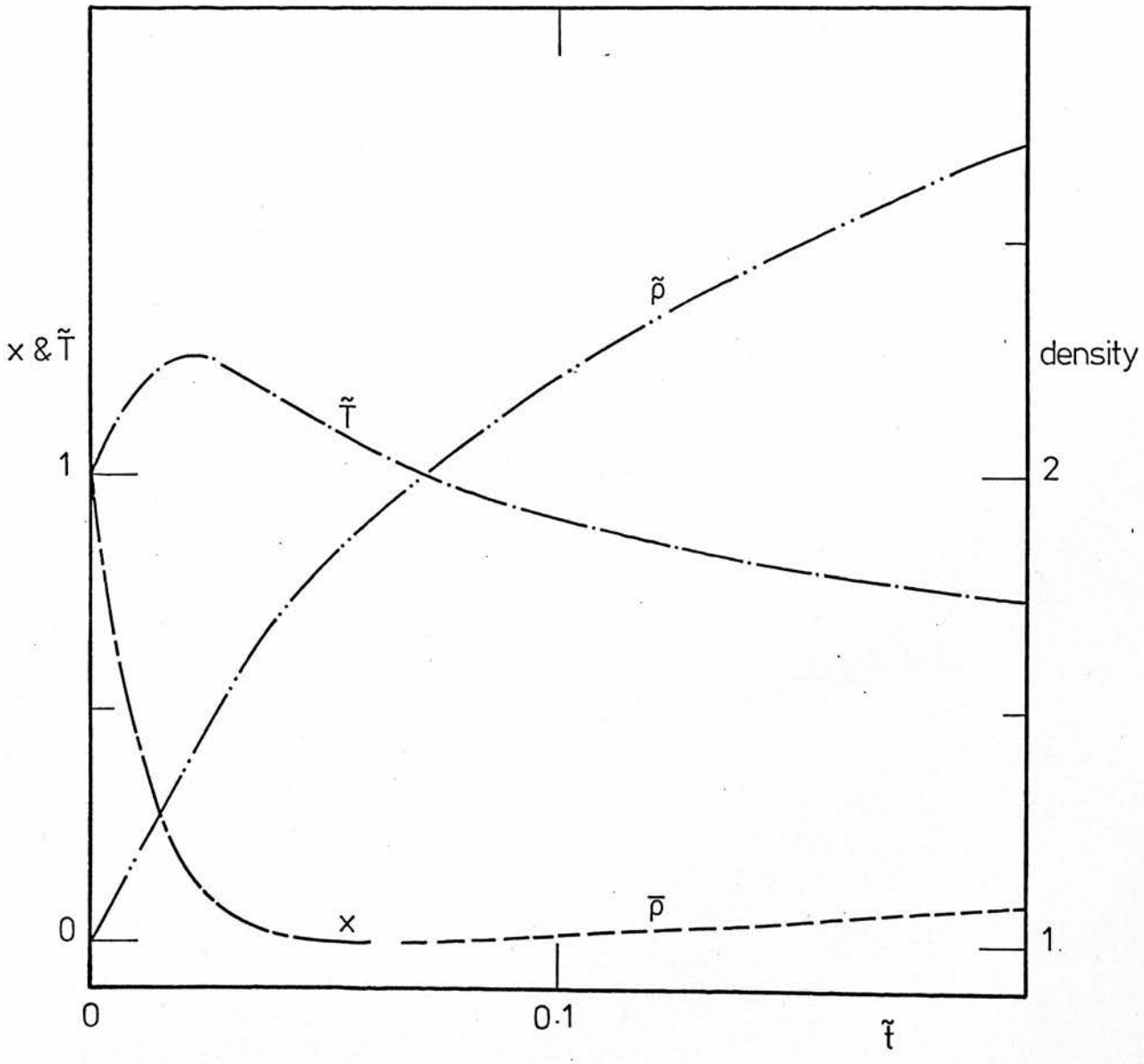

Fig. 7-7b The functions $x(\tilde{t})$, $\tilde{T}(\tilde{t})$, $\tilde{\rho}(\tilde{t})$ and $\bar{\rho}(\tilde{t})$ for $T_o = 1.2 \times 10^2\ ^oK$, $n_o = 10^3 cm^{-3}$, $x_o = 1.0$, $\varepsilon = 0.00$ and $n_d/n = 10^{-11}$.

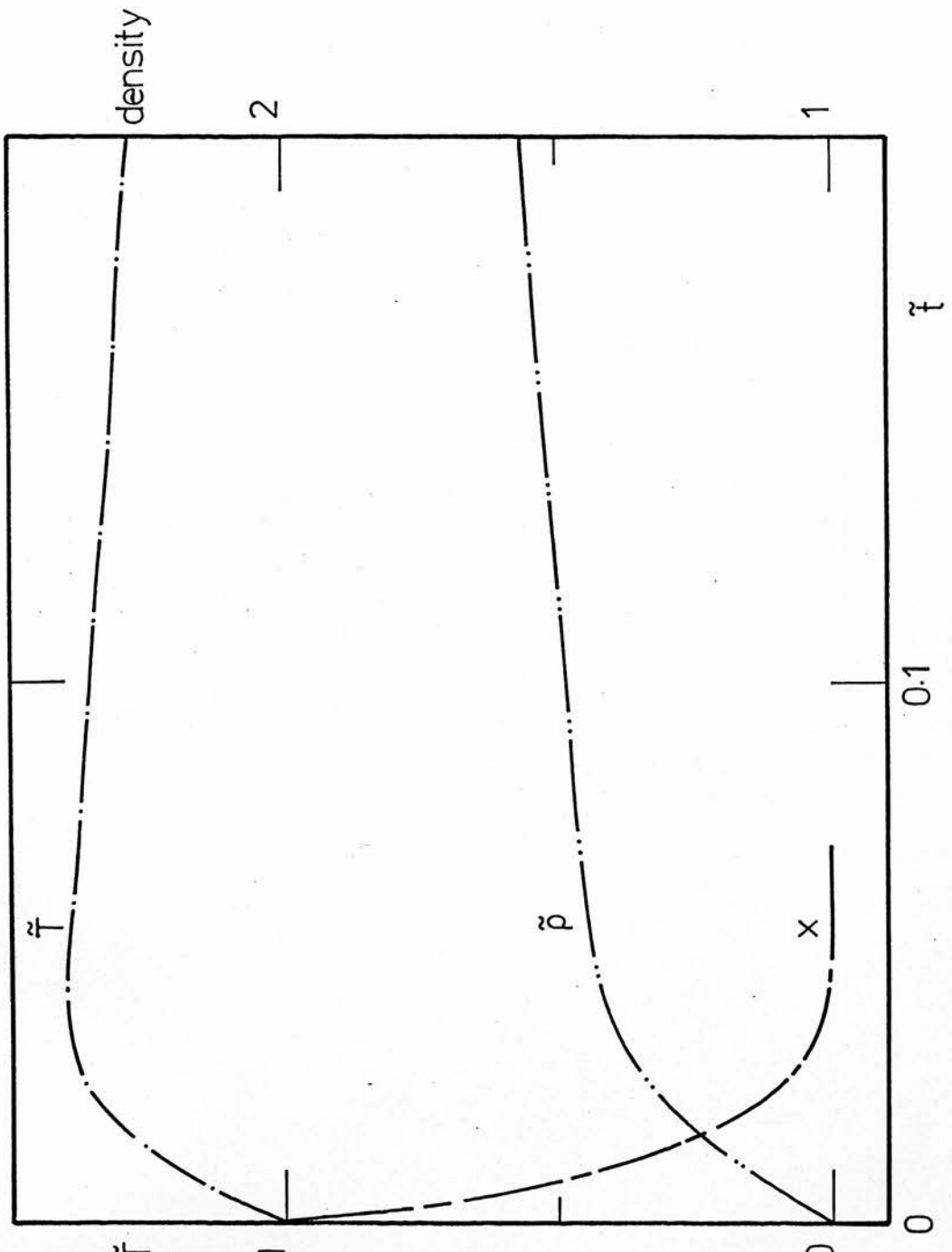

Fig. 7-8a As Fig. 7-6a for $n_o = 10^4 cm^{-3}$.

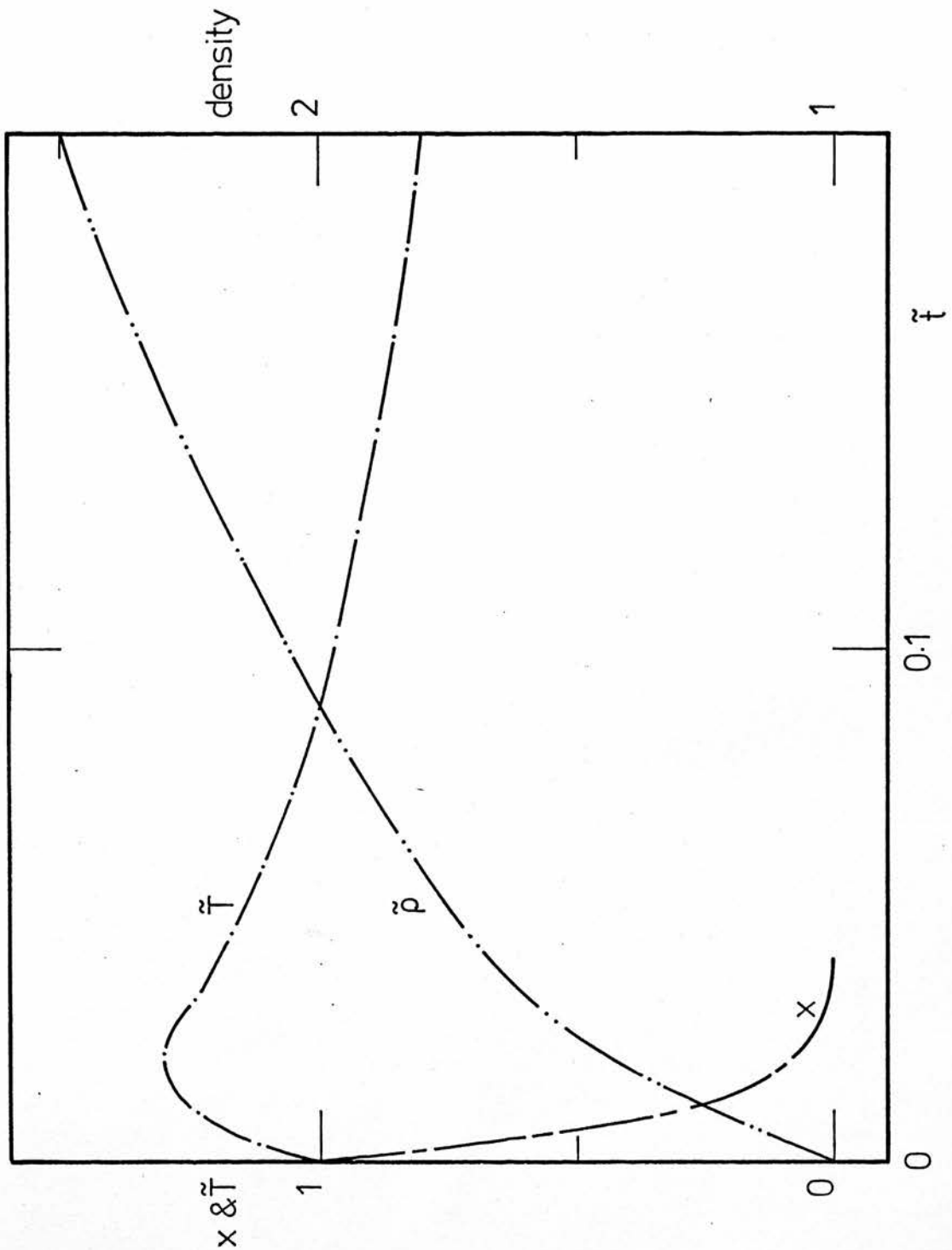

Fig. 7-8b As Fig. 7-6b for $n_o = 10^4 cm^{-3}$.

This condition means physically that the chemical heat input to the gas is less than the thermal energy per particle. For example, for $T_o \approx 10^2\ ^oK$, $\varepsilon \lesssim 1.0 \times 10^{-3}$.

Unfortunately Hunter and Watson (1978) neglected the most probable mechanism by which the remainder of the binding energy is dissipated, SW (1969), in finding the limit for ε. Therefore, this limit has to be taken strictly as an upper limit. However runs were done for $\varepsilon = 0.04$ and they are shown in figures (7-9) to (7-12) for $n_d/n = 10^{-12}$ and figures (7-13) to (7-16) for $n_d/n = 10^{-11}$.

In all the above cases an initial heating and expansion appear followed by a rebound. For $n_d/n = 10^{-12}$ the whole process occurs in times of the order of $0.5\ t_{ff}$ and no effective enhancement in density occurs for initial densities $n_o \lesssim 10^3$. For $n_o \gtrsim 5 \times 10^3$, the heating expansion and rebound occur at shorter times $\approx 0.3\ t_{ff}$ but effective enhancement in density due to H_2 formation would require temperatures higher than 60^oK.

For $\frac{n_d}{n} = 10^{-11}$, effective density amplification occurs for the range of density under consideration providing that $T_o > 60$. For temperatures of the order of $T_o \approx 60$ (the exact value depends on density) the enhancement in density tends to be quenched, this is because at the start of the reaction there are not enough molecules to cool, and the heat input becomes more important than the reduction in the number of particles. The strong peak that the temperature curve presents when $T_o = 60^oK$ is the manifestation of the above effect. The most conspicuous example of this behaviour is apparent from figure (7-16a)

where $\tilde{T}$ reaches its maximum at the time when $\approx 3/5$ of the hydrogen has reacted, which occurs at $t = 0.05\ t_{ff}$.

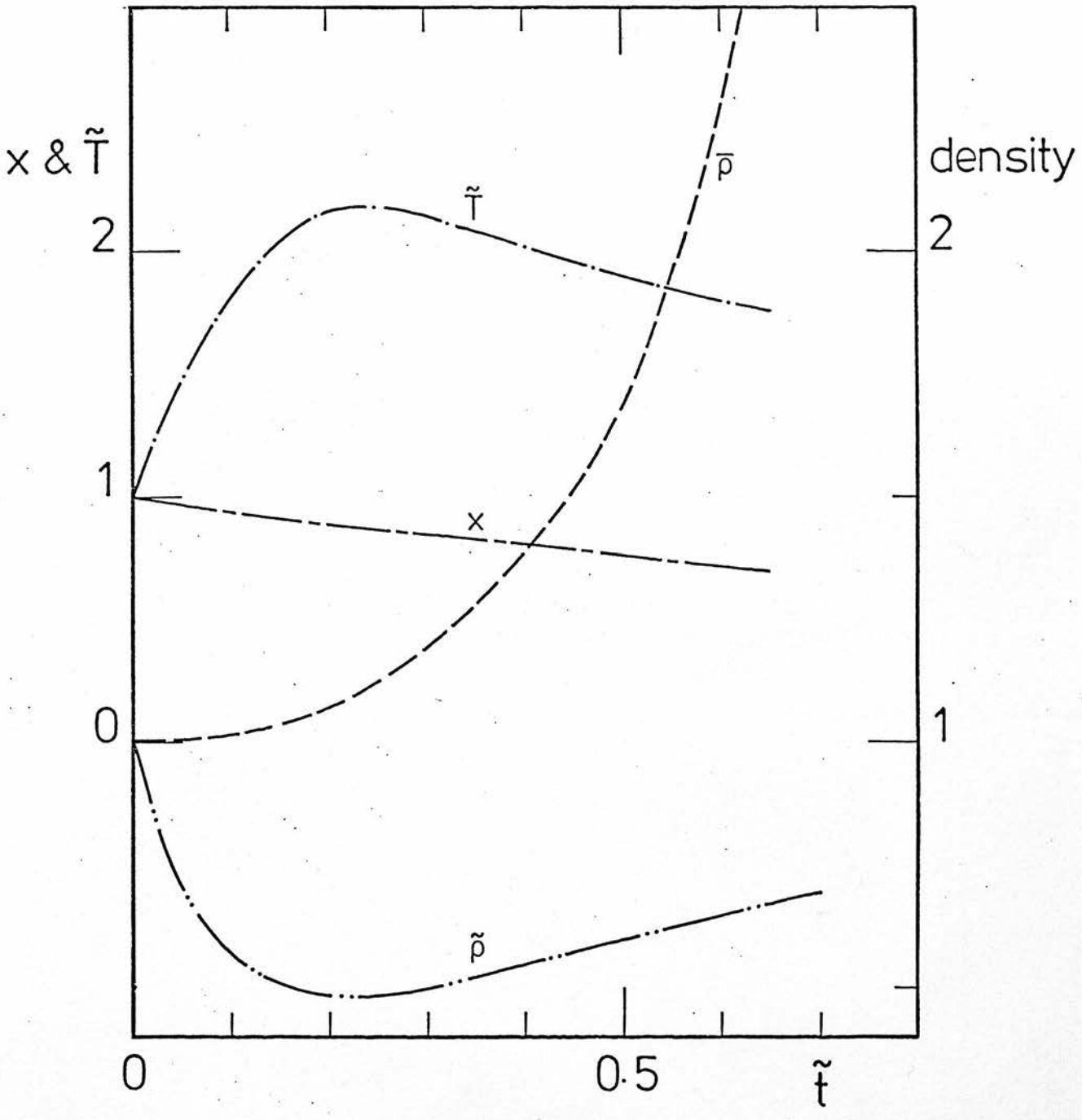

Fig. 7-9a The functions $x(\tilde{t})$, $\tilde{T}(\tilde{t})$, $\tilde{\rho}(\tilde{t})$ and $\bar{\rho}(\tilde{t})$ for $T_o = 60^oK$, $n_o = 10^2 cm^{-3}$, $x_o = 1.0$, $\varepsilon = 0.04$ and $n_d/n = 10^{-12}$.

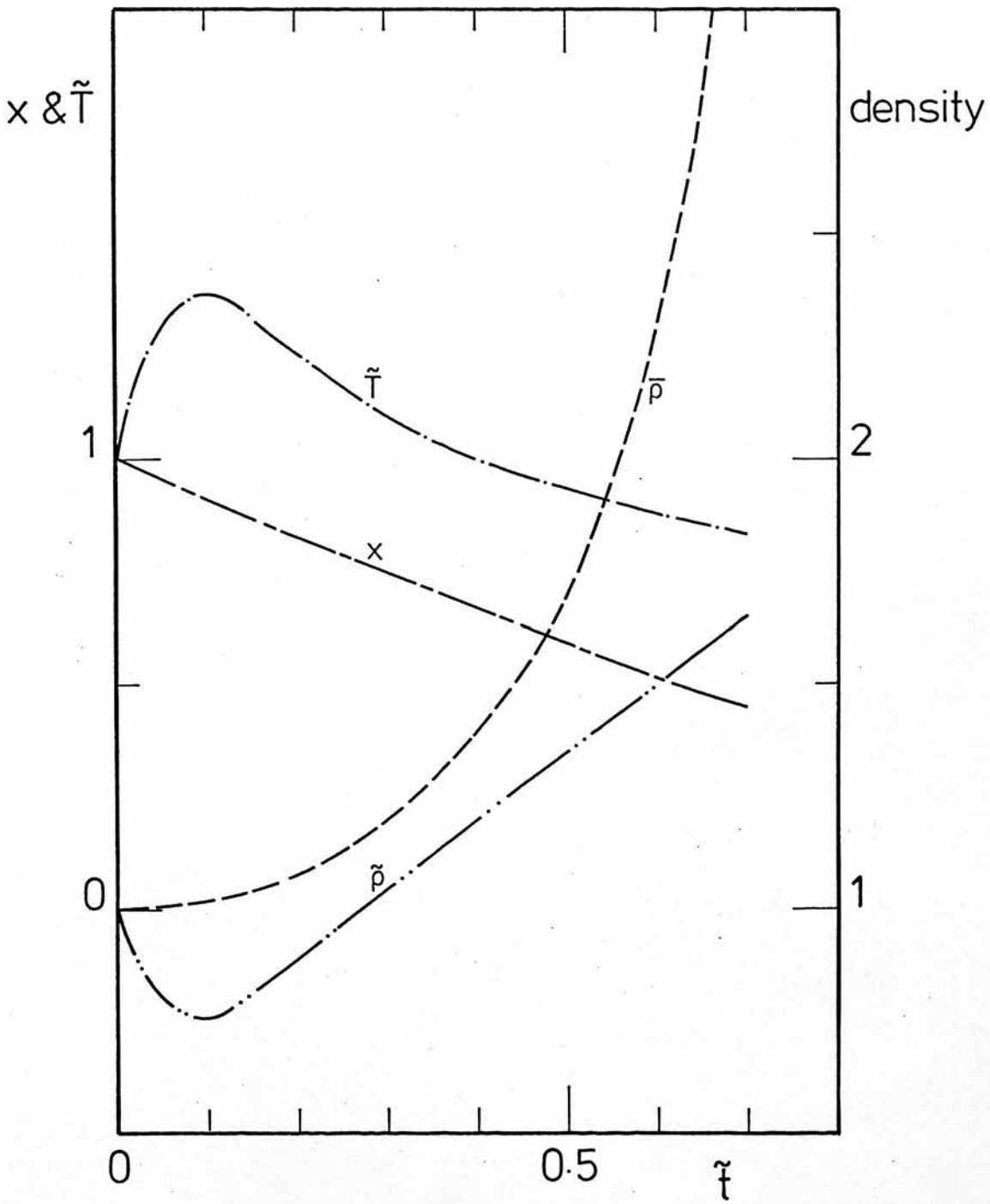

Fig. 7-9b The functions $x(\tilde{t})$, $\tilde{T}(\tilde{t})$, $\tilde{\rho}(\tilde{t})$ and $\bar{\rho}(\tilde{t})$ for $T_o = 1.2 \times 10^2\ ^oK$, $n_o = 10^2 cm^{-3}$, $x_o = 1.0$, $\varepsilon = 0.04$ and $n_d/n = 10^{-12}$.

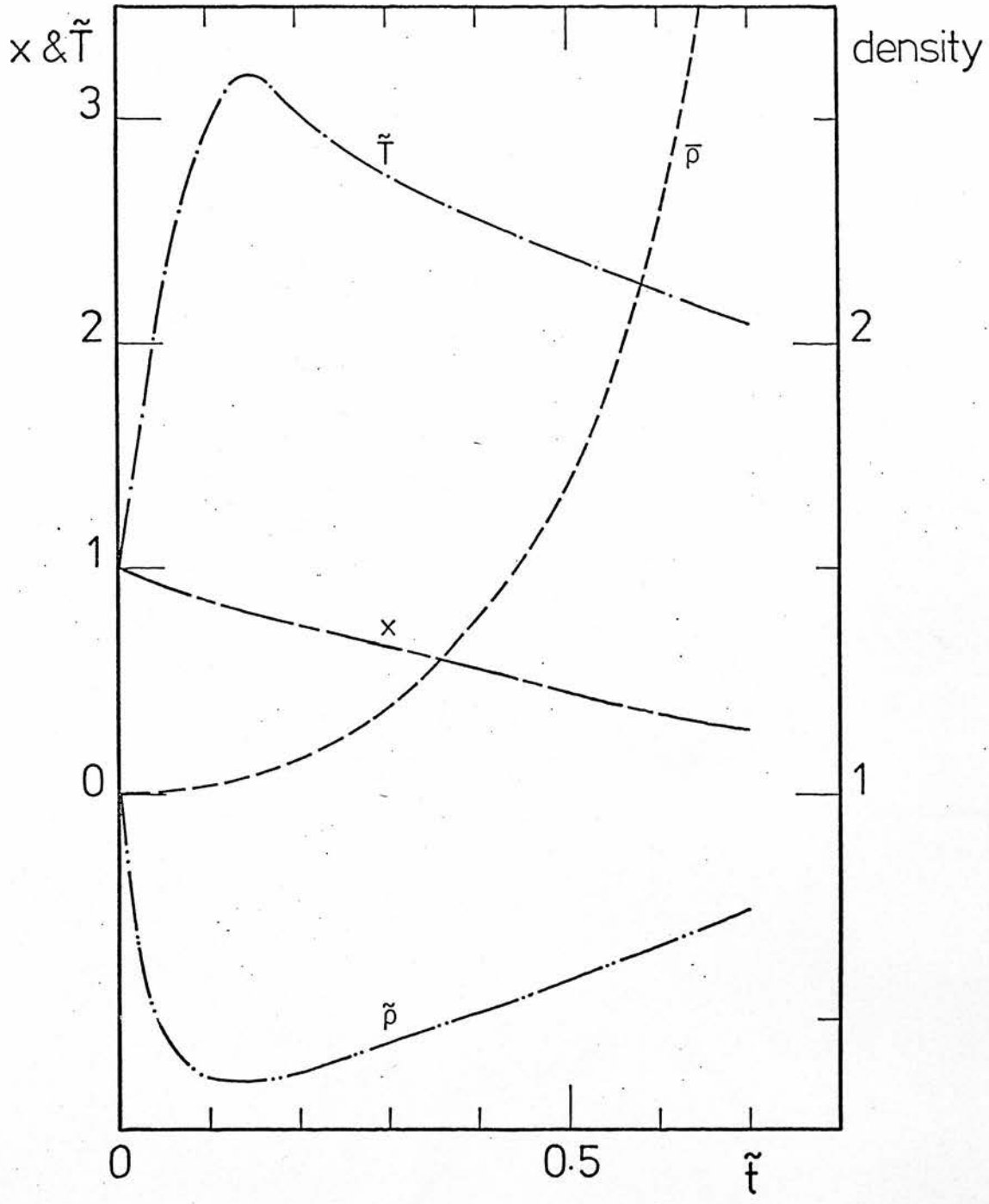

Fig. 7-10a As Fig. 7-9a for $n_o = 10^3 cm^{-3}$.

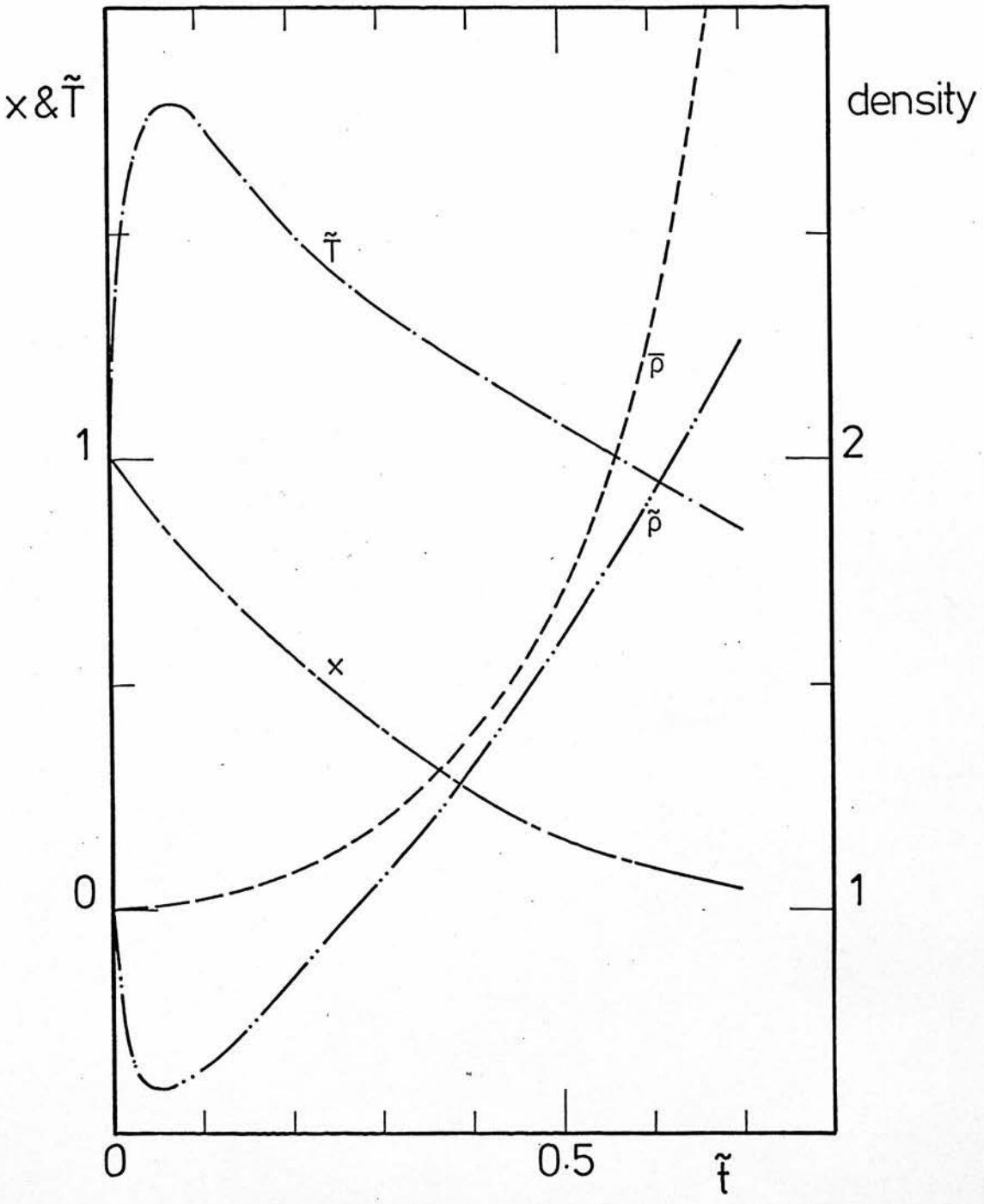

Fig. 7-10b As Fig. 7-9b for $n_o = 10^3 cm^{-3}$.

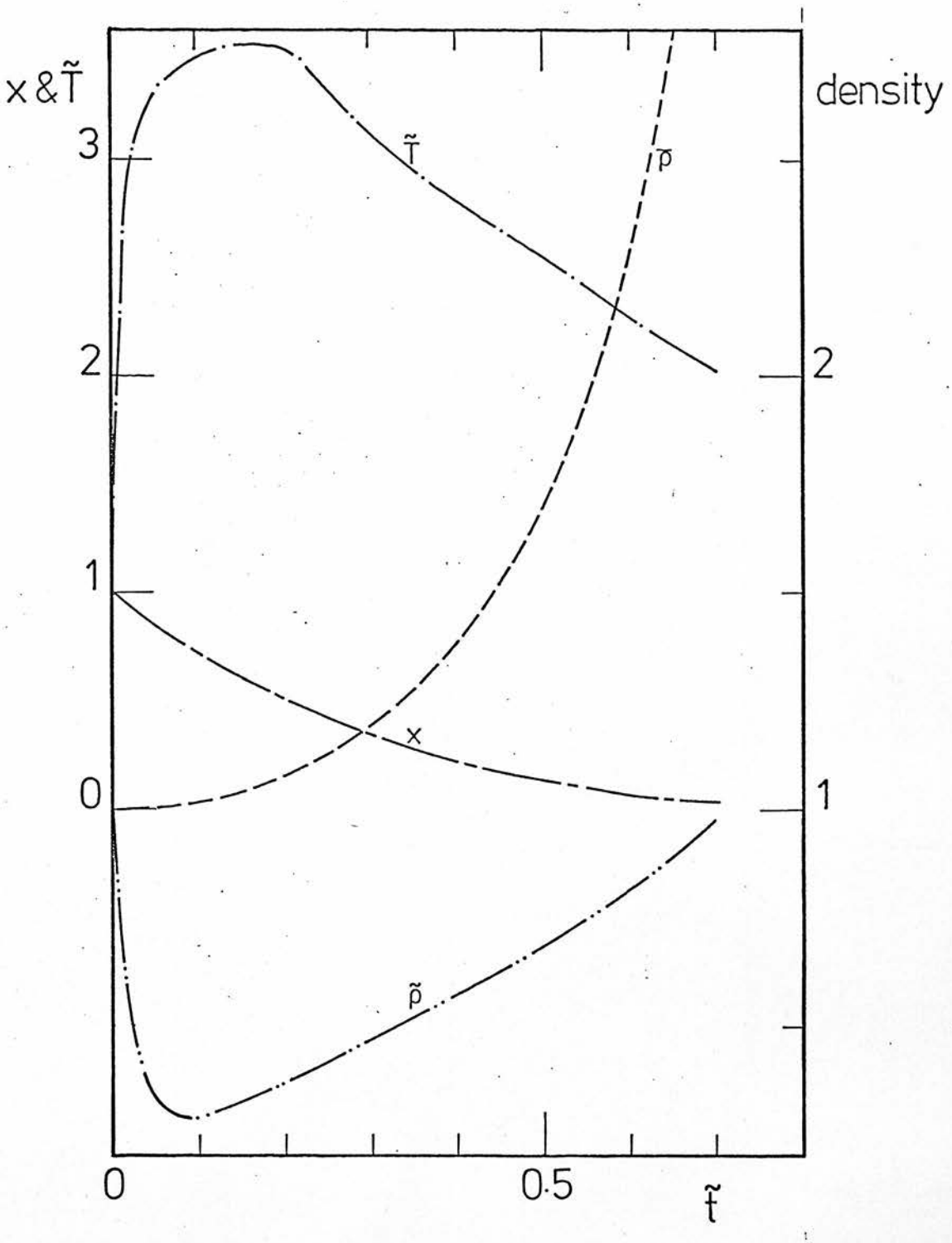

Fig. 7-11a As Fig. 7-9a for $n_o = 5 \times 10^3 cm^{-3}$.

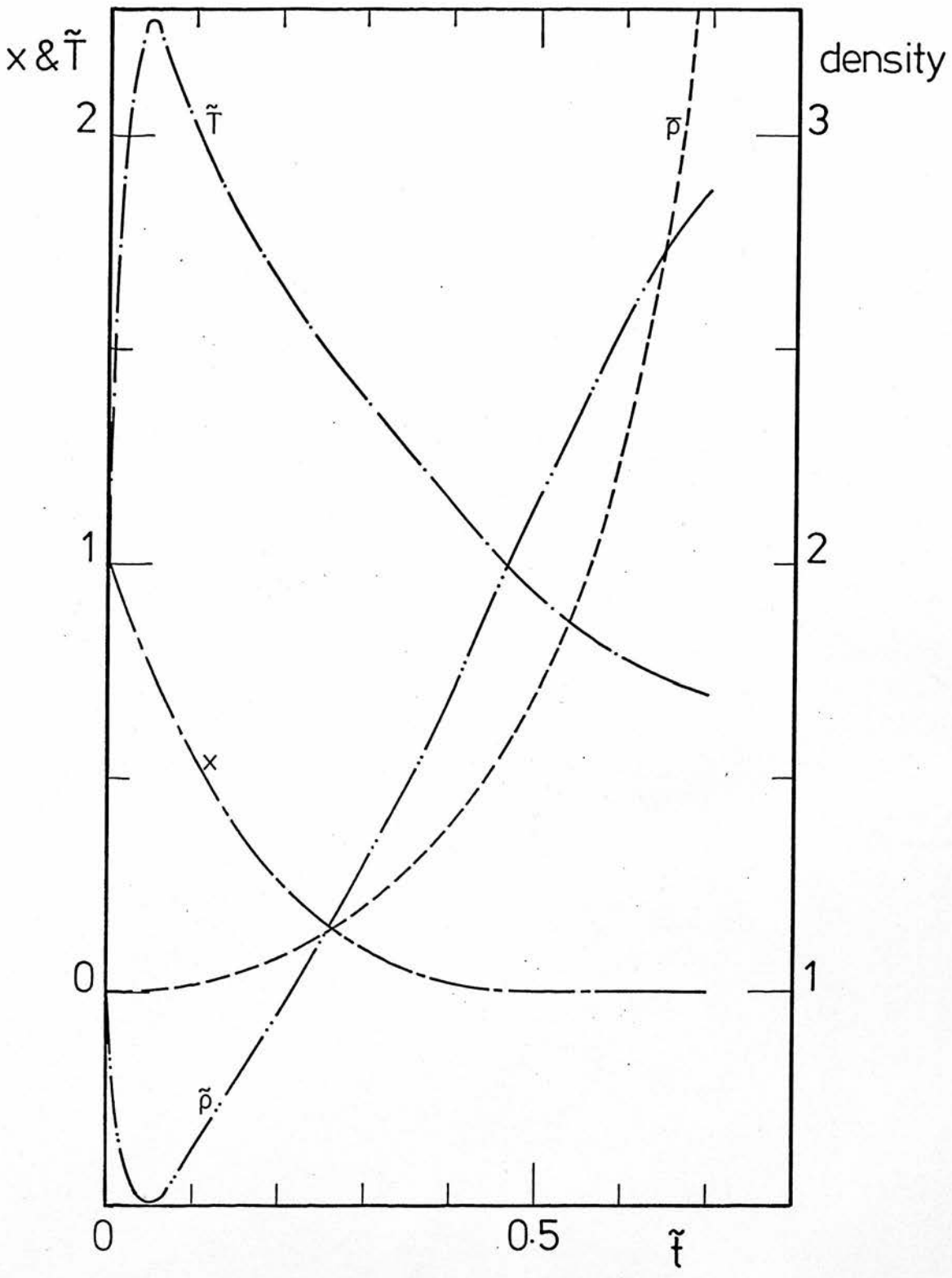

Fig. 7-11b As Fig. 7-9b for $n_o = 5 \times 10^3 cm^{-3}$.

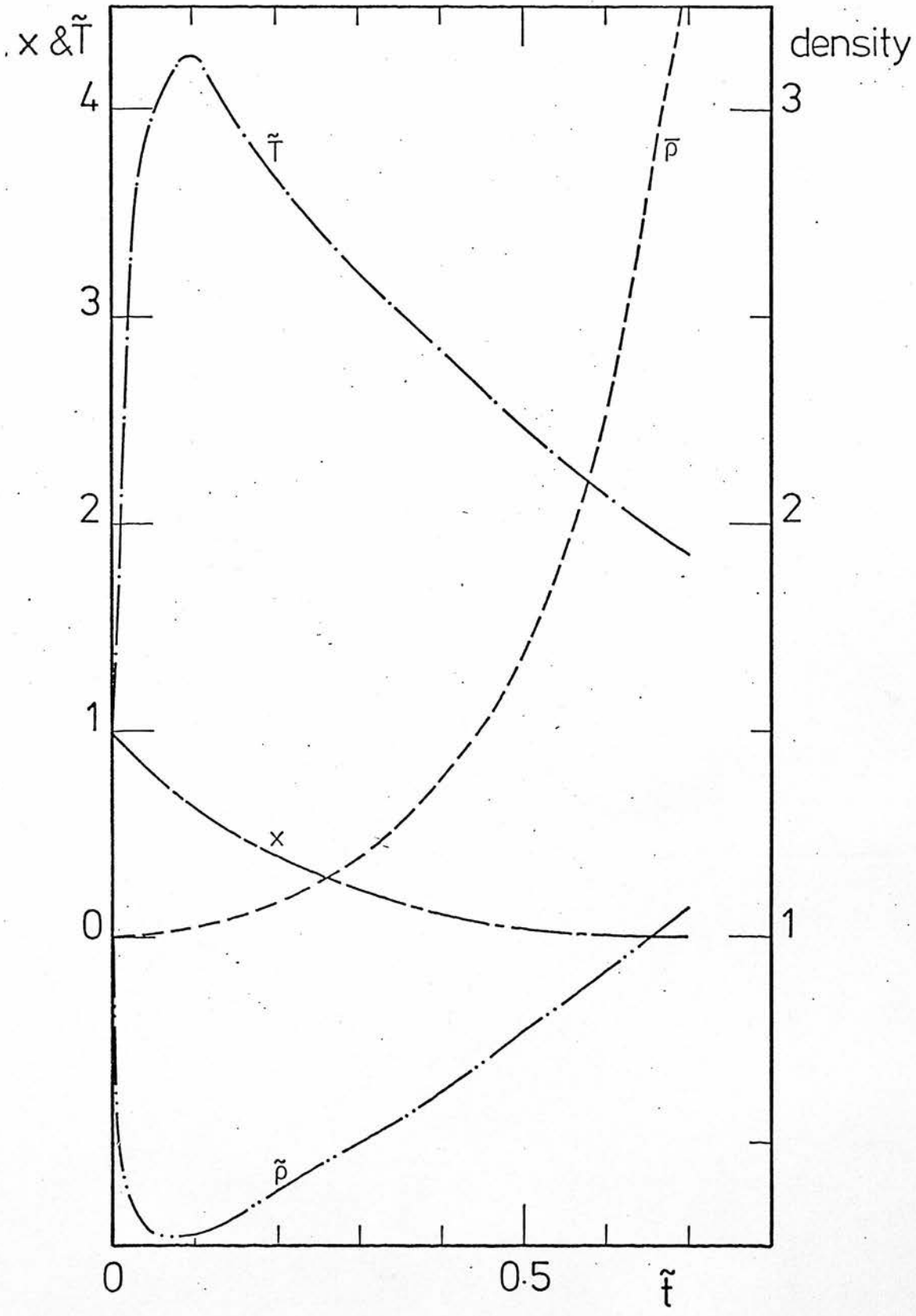

Fig. 7-12a As Fig. 7-9a for $n_o = 10^4 cm^{-3}$.

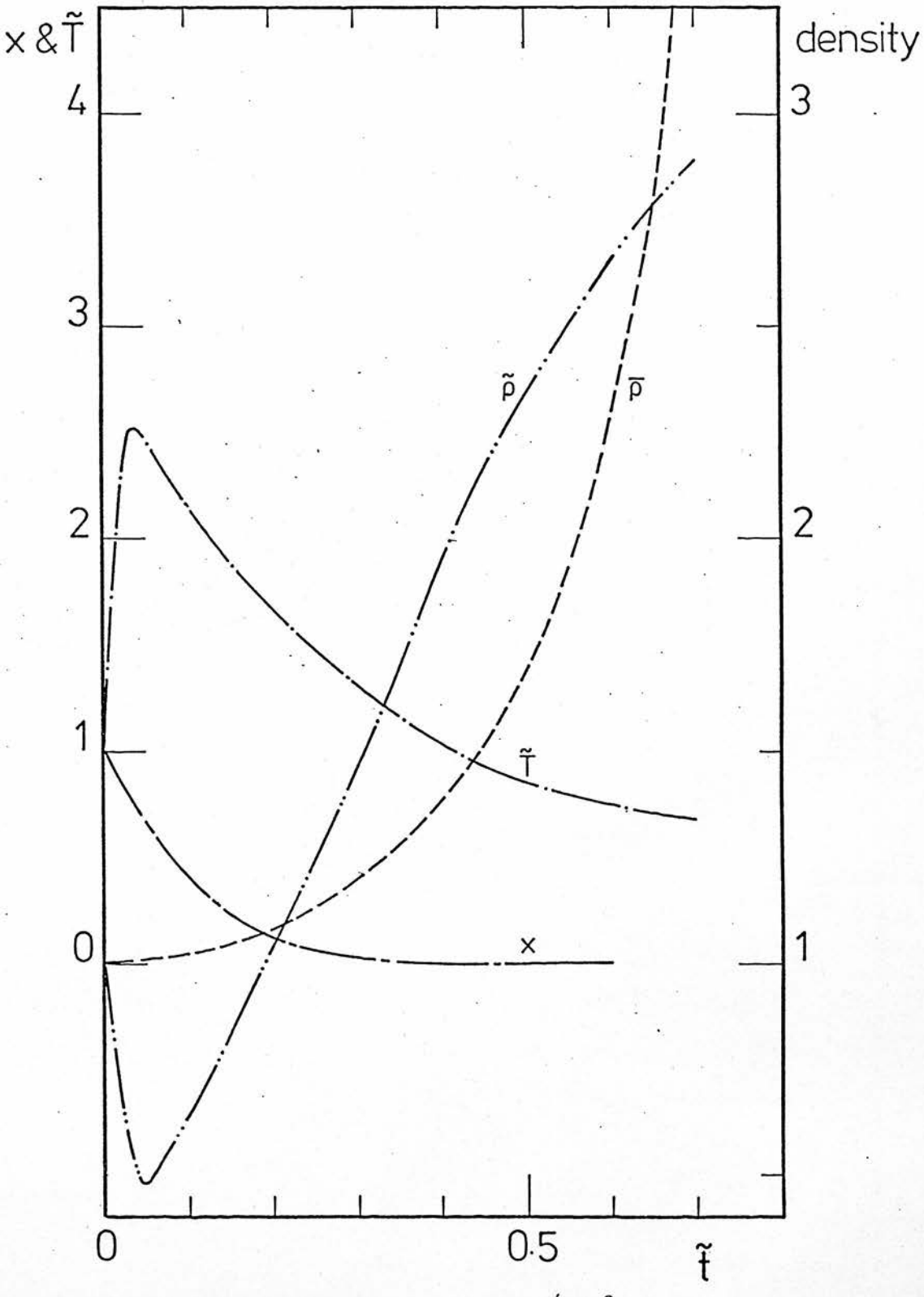

Fig. 7-12b As Fig. 7-9b for $n_o = 10^4 cm^{-3}$.

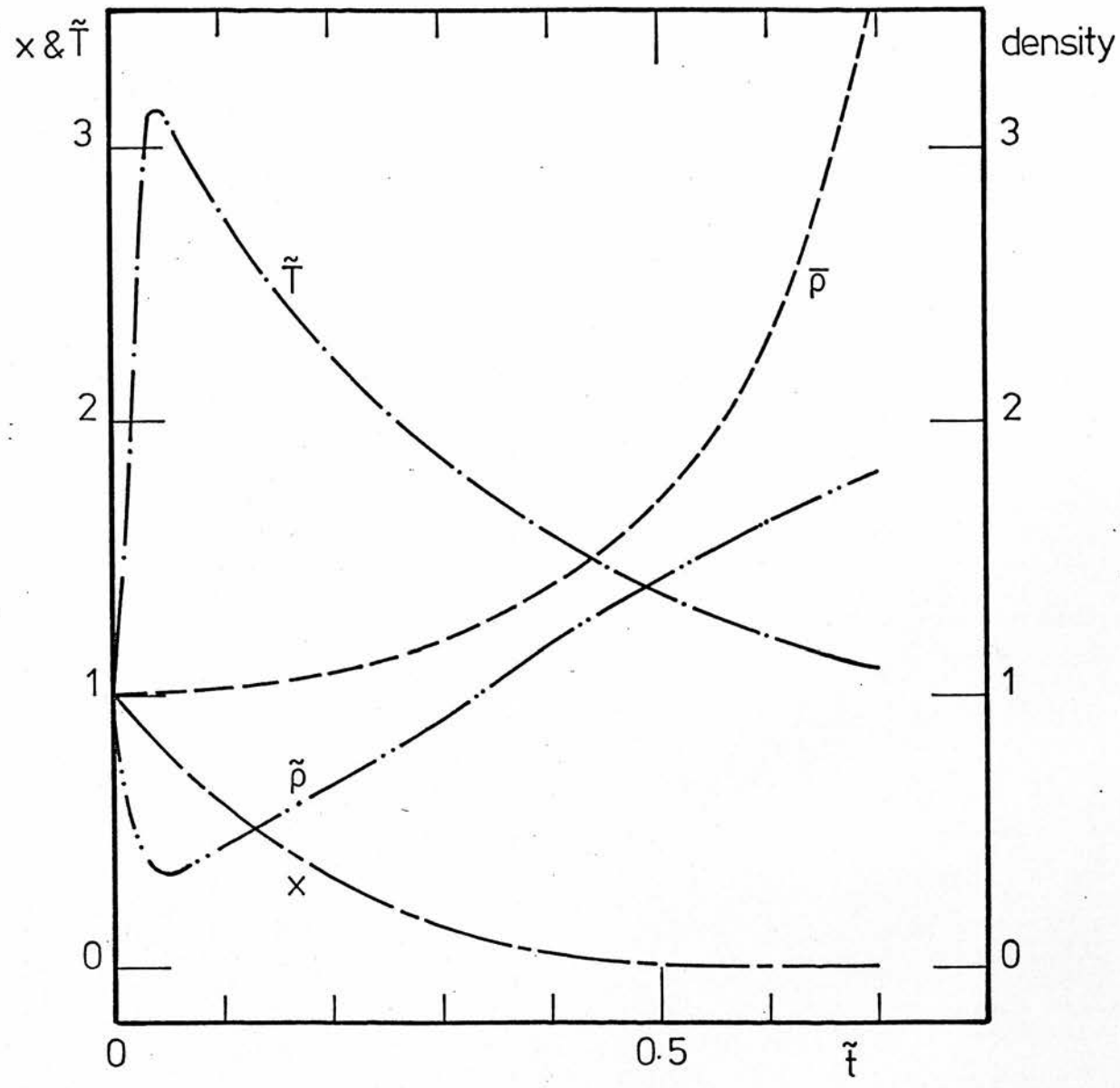

Fig. 7-13a The functions $x(\tilde{t})$, $\tilde{T}(\tilde{t})$, $\tilde{\rho}(\tilde{t})$ and $\bar{\rho}(\tilde{t})$ for $T_o = 60^oK$, $n_o = 10^2 cm^{-3}$, $x_o = 1.0$, $\varepsilon = 0.04$ and $n_d/n = 10^{-11}$.

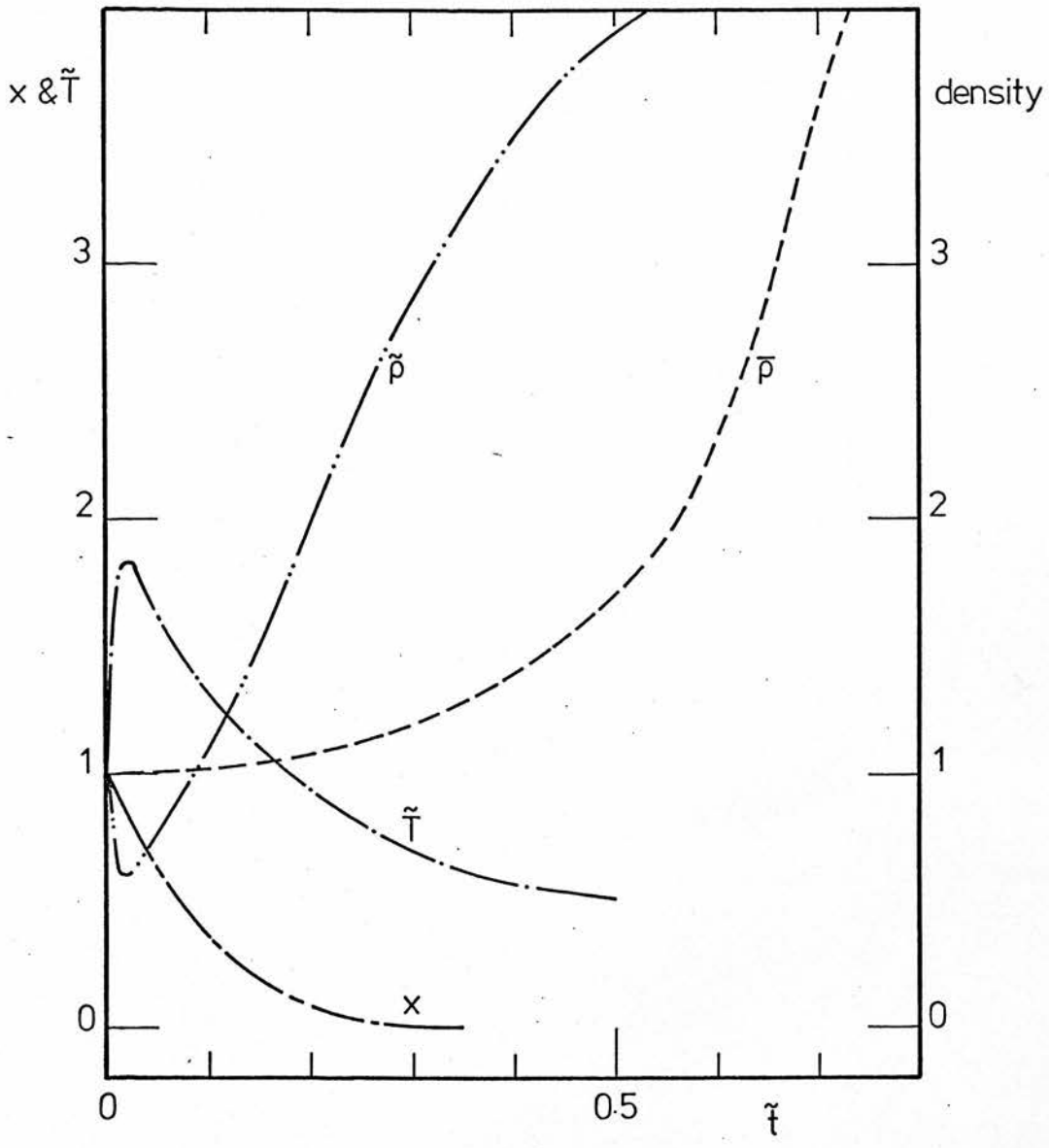

Fig. 7-13b The functions $x(\tilde{t})$, $\tilde{T}(\tilde{t})$, $\tilde{\rho}(\tilde{t})$ and $\bar{\rho}(\tilde{t})$ for $T_o = 1.2 \times 10^2\ ^oK$, $n_o = 10^2 cm^{-3}$, $x_o = 1.0$, $\varepsilon = 0.04$ and $n_d/n = 10^{-11}$.

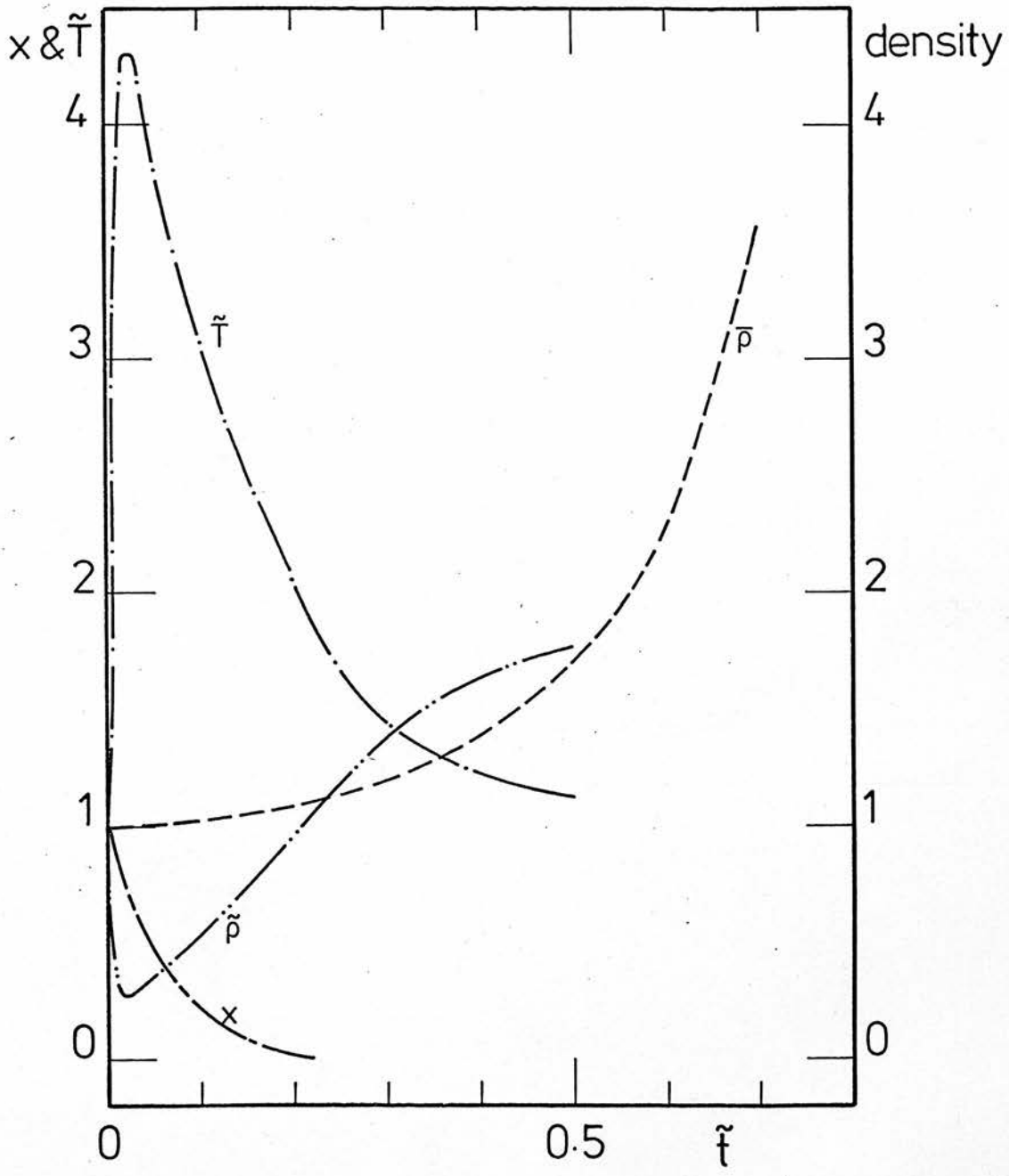

Fig. 7-14a As Fig. 7-13a for $n_o = 10^3 cm^{-3}$.

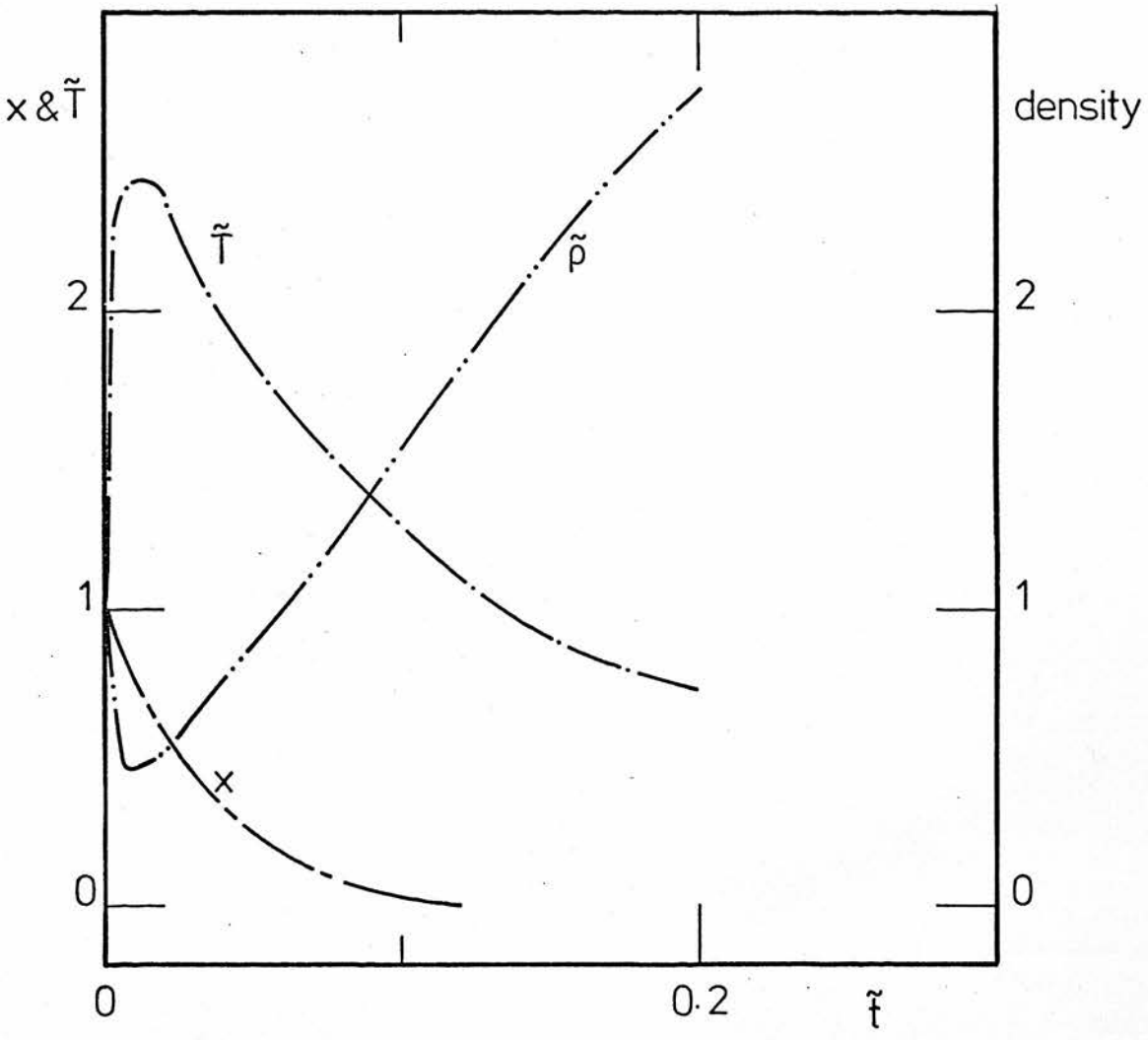

Fig. 7-14b The functions $x(\tilde{t})$, $\tilde{T}(\tilde{t})$ and $\tilde{\rho}(\tilde{t})$ for $T_o = 1.2 \times 10^2\ ^oK$, $n_o = 10^3 cm^{-3}$, $x_o = 1.0$, $\varepsilon = 0.04$ and $n_d/n = 10^{-11}$.

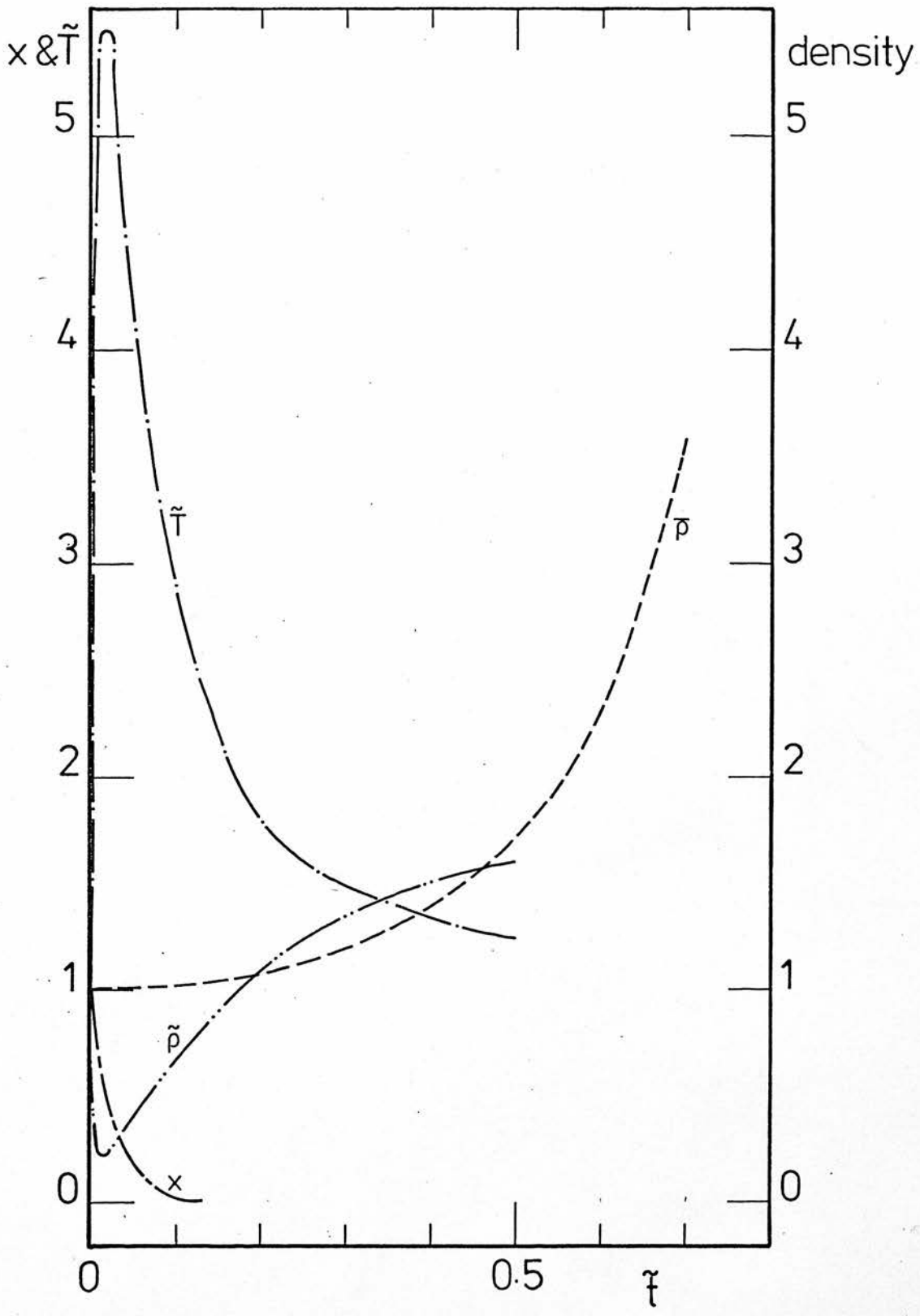

Fig. 7-15a As Fig. 7-13a for $n_o = 5 \times 10^3 cm^{-3}$.

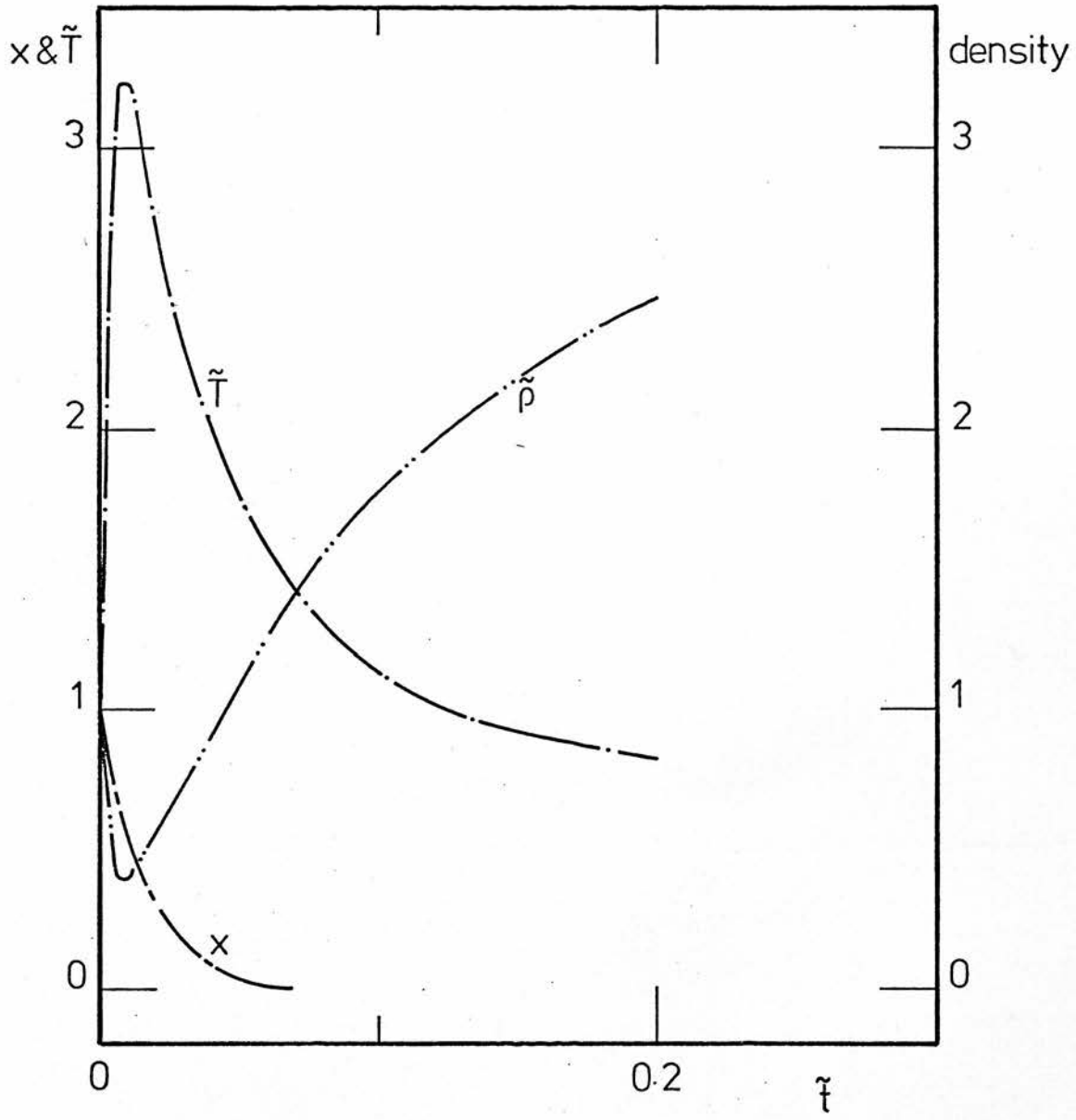

Fig. 7-15b As Fig. 7-14b for $n_o = 5 \times 10^3 cm^{-3}$.

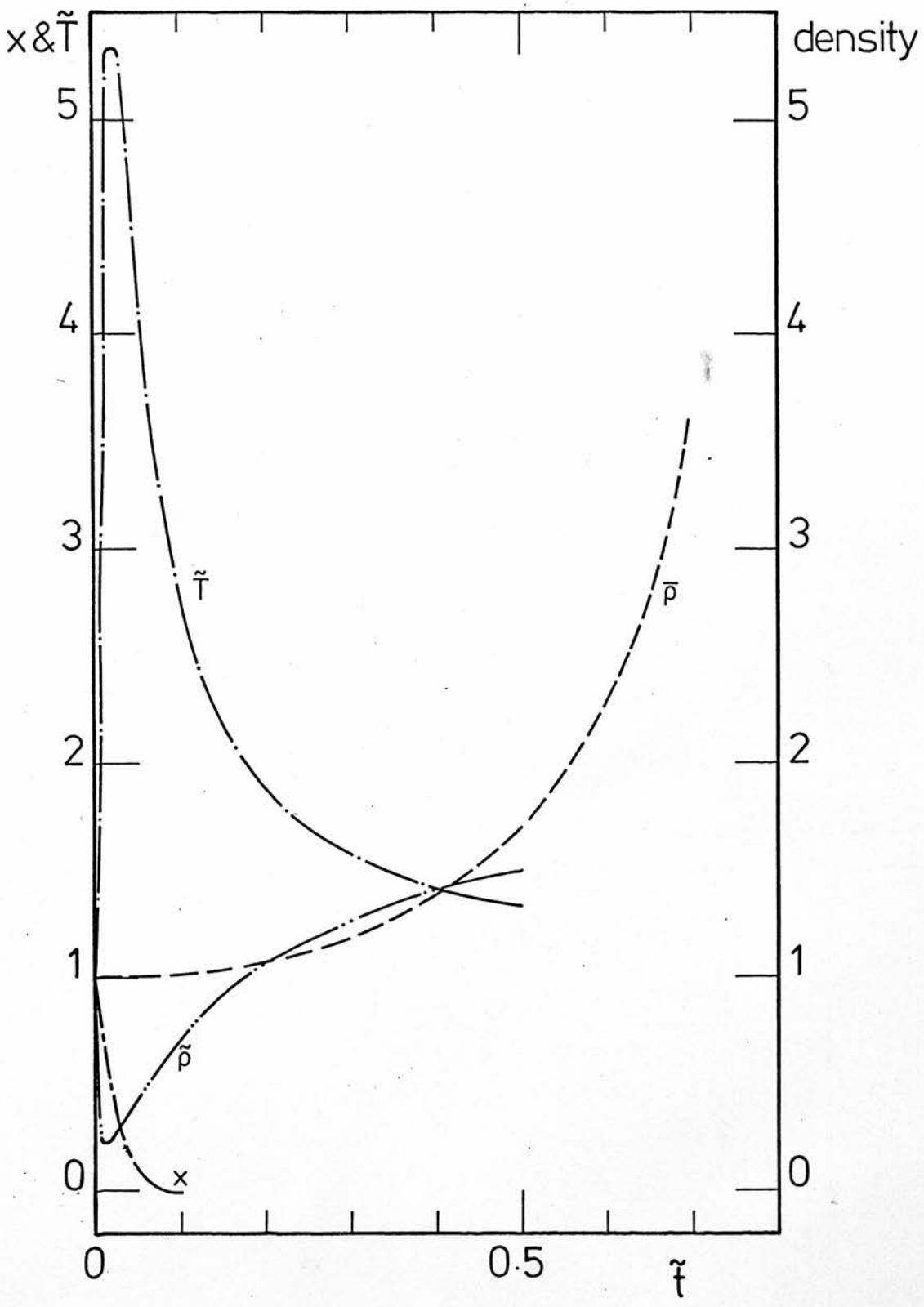

Fig. 7-16a As Fig. 7-13a for $n_o = 10^4 cm^{-3}$.

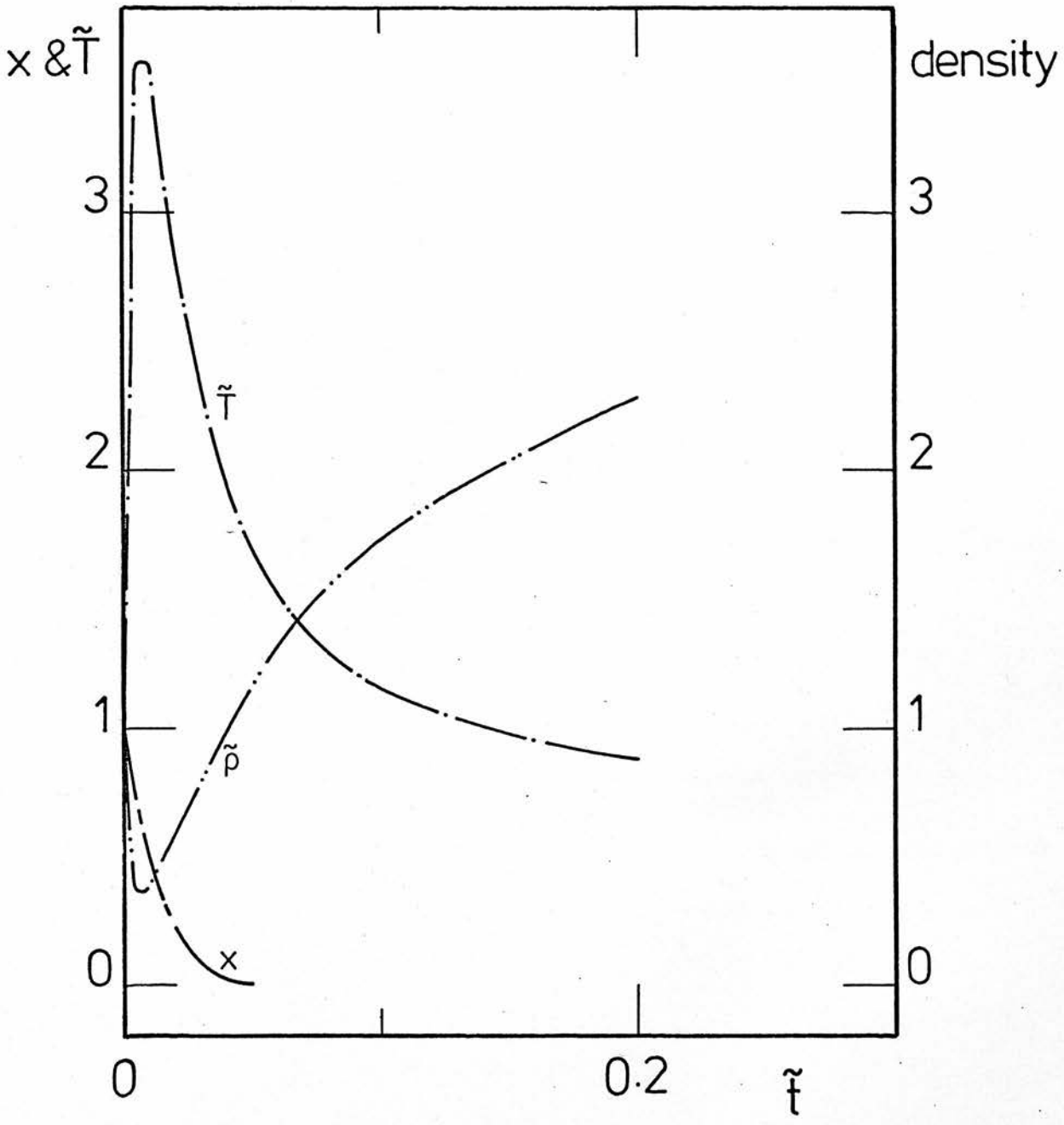

Fig. 7-16b As Fig. 7-14b for $n_o = 10^4 cm^{-3}$.

8. SUMMARY AND DISCUSSION

This attempt to explore the fragmentation process outlined by Reddish (1975, 1978), has been made taking as a working hypothesis a dusty atomic cloud starting gravitational contraction with gas number density $n_o \gtrsim 10^2 cm^{-3}$, gas temperature $T_o \approx 10^{2\,o} K$ and a mean optical thickness for grain extinction $\bar{\tau}_o > 1$. The main point is to see if, under the above conditions, H_2 formation could act as an amplifier of density inhomogeneities which are probably generated by subsonic turbulence.

A fundamental parameter involved in the whole process is the critical temperature of the dust for H_2 formation. Unfortunately, laboratory determinations exist only for a few substrata of interest. Graphite for instance has $T_{cri} = 25^oK$.

It is very interesting to note that determinations of the average grain temperature throughout the galaxy by measurements of the 100μ galactic background give $\bar{T}_d = 24^oK$, Andriesse (1974), and in other galaxies $20 \lesssim \bar{T}_d \lesssim 40$, Hillel (1973)*.

From formal spherical and homogeneous models of IDC, WS (1969) and Leung (1975), the optical depth τ_{cri}, at which $T_d = T_{cri}$, changes over a rather small range, $1 \lesssim \tau_{cri} \lesssim 3$ according to Leung (1975), $3 \lesssim \tau_{cri} \lesssim 7$ according to WS (1969), and τ_{cri} tends to the lower limit when τ_o increases. But τ_{cri} has a very complicated dependence on the total optical depth. These numbers, although calculated for homogeneous models are taken as indicators of the mean values expected in non-homogeneous models.

* These values receive a natural explanation in the context of the Reddish theory because they would be a consequence of the "thermostatic effect", on the whole galactic star formation process, generated by the interaction between radiation field and dust which would control the H_2 formation (and the whole chemistry depending on this molecule) via T_d.

Another curious aspect to note is that for clouds where graphite determines the mean properties of the dust component, the locus of the surface $\tau = \tau_{cri}$ occurs at optical depths $1 \lesssim \tau_{cri} \lesssim 7$ where T_d has a very strong dependence on the visual diffuse field and the effects of inhomogeneities are strong at scales $\lambda_d \frac{\overline{\kappa}}{2} \approx \pi/2$.

To have a rough idea of how H_2 formation progresses through the cloud when it contracts, let us consider for example a spherical and homogeneous cloud of graphite of radius R(t) at time t. Let $r_c(t)$ be the linear radius of the "core" where $T_d \leq T_{cri}$, $\overline{\tau}_c(t)$ its corresponding mean optical depth and $\overline{\tau}_o(t)$ the mean optical depth to the centre. If at t = o,

$$\overline{\tau}_{cri}(o) = \overline{\tau}_o(o) \quad \text{and} \quad R(o) = R_o, \tag{8-1}$$

then at t > o, one has approximately

$$\overline{\tau}_{cri}(t) = \overline{\tau}_o(t) \left[1 - \frac{r_{cri}(t)}{R(t)} \right] \tag{8-2}$$

and

$$\overline{\tau}_o(t) = \overline{\tau}_o(o) \left[\frac{R_o}{R(t)} \right]^2 . \tag{8-3}$$

Therefore

$$\frac{r_{cri}(t)}{R(t)} = 1 - \frac{\overline{\tau}_{cri}(t)}{\overline{\tau}_o(o)} \left[\frac{R(t)}{R_o} \right] \tag{8-4}$$

From Leung (1975) solutions for homogeneous models, it is reasonable to take:

$$\bar{\tau}_o(o) \approx \bar{\tau}_{cri}(o) \approx 3.0 \qquad (8\text{-}5)$$

and when

$$\bar{\tau}_o(t) \approx 10.0, \quad \bar{\tau}_{cri}(t) \approx 1.5$$

Therefore, when the cloud has contracted by a factor ≈ 0.55, i.e. $\frac{R(t)}{R_o} \approx 0.55$, which occurs during a time $t \approx 0.79\ t_{ff}$, $\frac{r_{cri}}{R} \approx 0.73$. This means that the radius of the "core" $T_d = T_{cri}$ has grown from 0.00 to $r_{cri} = 0.73\,R$ and H_2 formation has progressed from the centre towards the edges.

It is expected that the surface $r(t) = r_{cri}(t)$ is rather an irregular and distorted surface due to the inhomogeneities, instead of a spherical and smooth one as it was assumed in the above guess from homogeneous models.

Although the radiative heating problem was solved in very simple inhomogeneous cloud models and in approximate form, two facts were established: (a) only inhomogeneities with optical thickness given by the relation (6-30), i.e., $\lambda_d \bar{\kappa}/2 \approx \pi/2$, are expected to generate strong T_d fluctuations around some mean value, in particular around T_{cri}. (b) Inhomogeneous clouds with mean optical thickness τ_o such that $1 \lesssim \tau_o \lesssim 5$ tend to be much more sensitive to T_d fluctuations towards the centre and those with $\tau_o > 5$ towards optical depths of the order of 2.

The H_2 formation problem was worked out, in a first approximation, as a discontinuity generated by the surface $T_d = T_{cri}$, i.e., H_2 formation can occur inside bubbles where $T_d < T_{cri}$. The effects of H_2 formation in these bubbles were compared with the change in the mean density which would be produced by the fastest form of contraction i.e. free-fall. Strictly speaking gravitational constraction and H_2 formation are coupled with each other. However, the approximation adopted permits the determination to a first approximation of the conditions under which H_2 formation could be important for inducing density amplification.

Although the isobaric condition is not absolutely correct, it has some degree of validity as can be seen from the following simple considerations:

The timescale for a sound wave to travel across a region of dimensions $\lambda_d/4 = \pi/4\overline{\kappa}$ (radius of the cells where $T_d < T_{cri}$) is

$$t_s = \frac{\pi}{4\overline{\kappa}\, c} \tag{8-6}$$

where

$$\overline{\kappa} = < Q_{exd}\ \tilde{\sigma}_d > n_d \tag{8-7}$$

and c the sound speed given by

$$c \approx (\tilde{\gamma}\, R\, T)^{\frac{1}{2}}$$

On the other hand, the timescale for H_2 formation is

$$t_{H_2} = \gamma^{-1} < \tilde{\sigma}_d >^{-1} (3\, R\, T)^{-\frac{1}{2}} \left(\frac{n_d}{n}\right)^{-1} n^{-1} \tag{8-9}$$

see appendix A. Therefore,

$$\frac{t_{H_2}}{t_s} \approx \frac{8 < Q_{ext} >}{\pi} \left(\frac{\tilde{\gamma}}{3} \right)^{\frac{1}{2}} \tag{8-10}$$

where $\left(\frac{\tilde{\gamma}}{3} \right)^{\frac{1}{2}} = \begin{cases} \sqrt{5/9} & \text{for an HI gas} \\ \sqrt{7/15} & \text{for an } H_2 \text{ gas} \end{cases}$ (8-11)

Because the ratio t_{H_2}/t_s only depends on the gas parameters through the specific heat ratio of the gas, it can be taken with confidence.

With the average number $< Q_{ext} > \approx 2$, Wickramasinghe (1973), Greenberg (1979), and with the mean value of $\tilde{\gamma}$ between a gas of pure HI and one of pure H_2, one has

$$\frac{t_{H_2}}{t_s} \approx 3.6 \tag{8-12}$$

That is, the pressure in the bubble with $T_d < T_{cri}$ has time to equalise to the external value while the H_2 reaction proceeds.

The validity of the isobaric condition in the non-steady regime generated by gravitational contraction is difficult to envisage although on physical grounds it is expected that such a condition provides rather a lower limit for the density enhancement due to H_2 formation because of the strong non-linear coupling between both processes and the accelerated increase of the background mean density due to the contraction of the cloud as a whole. This aspect

can only be estimated quantitatively with the help of a self-consistent treatment of the formal multi-dimensional gas dynamic problem enunciated at the beginning of Section 3.

Subsonic turbulence has been invoked as generator of inhomogeneities, particularly density inhomogeneities, but while these fluctuations generated by turbulence are reversible, the production of the H_2 (and of molecules depending on this, mainly CO) introduce irreversibility in turbulent elements at scales $\lambda_d/2 = \pi/2\bar{\kappa}$ and at the early stages of the contraction.

Formal studies of the turbulent generation of density fluctuations in a contracting medium, Sasao (1973) have shown that the amplification of density inhomogeneities resulting only from the turbulence-contraction coupling requires the presence of initially very strong turbulence and effective amplification could only occur at advanced stages of the collapse, $t > 0.9\ t_{ff}$.

It can be argued that, if at length scales $\frac{\lambda_d}{2} \simeq \pi/2\bar{\kappa}$ the time scale characteristic of turbulence t_{t_1} is much shorter than the time necessary to allow appreciable H_2 to form and their effects dominate the very turbulent ones, inhomogeneities could not survive long enough to permit H_2 production to control the situation.

With the assumption of isobaricity ($\bar{P}$ = const.), a quantitative criterion to adopt to determine when H_2 formation effects dominate over the turbulent ones would be that the change in density due to the H_2 formation has to be greater than the density fluctuation produced by

turbulence, i.e.,

$$\left(\frac{\delta\rho}{\bar{\rho}}\right)_{H_2} > \left(\frac{\delta\rho}{\bar{\rho}}\right)_{turb.} \tag{8-13}$$

It seems that this criterion is not very far away from the formal one in a non-isobaric model, because to a first approximation $\left(\frac{\delta\rho}{\bar{\rho}}\right) \sim \left(\frac{\delta P}{\bar{P}}\right)$ for either of the above two different mechanisms and therefore, H_2 formation would dominate over the turbulence if

$$\left(\frac{\delta P}{P}\right)_{H_2} > \left(\frac{\delta P}{P}\right)_{turb.} \tag{8-14}$$

For $\left(\frac{\delta\rho}{\bar{\rho}}\right)_{turb.} \approx 0.1$ for instance, from the numerical solutions of Section 7 one can see that a rather wide and sufficient condition to ensure that (8-13) is valid, is

$$t_{t_1} \approx t_{H_2} \tag{8-15}$$

That this is the case, can be seen from the following simple considerations:

From the Kolmogorov spectral law, appendix B, the timescale characteristic of inhomogeneities at scales $\lambda_d/2 \approx \pi/2\bar{\kappa}$ is

$$t_{t_1} \approx \ell_o^{1/3} \langle v_o \rangle^{-1} \left(\frac{\lambda_d}{2}\right)^{2/3}$$

$$\approx \ell_o^{1/3} \pi^{2/3} \langle 3RT \rangle^{-\frac{1}{2}} \langle Q_{ext} \tilde{\sigma}_d \rangle^{-2/3} \left(\frac{n_d}{n}\right)^{-2/3} n^{-2/3} \tag{8-16}$$

where ℓ_o is the linear dimension of the cloud and $\langle v_o \rangle \approx \langle 3RT \rangle^{\frac{1}{2}}$ in a first approximation. Therefore the ratio t_{H_2}/t_{t_1} is given by

$$t_{H_2}/t_{t_1} \approx 2^{2/3} \pi^{-2/3} \langle Q_{ext} \rangle^{-1/3} \bar{\tau}_o^{-1/3} \tag{8-17}$$

which is rather insensitive to the product $\langle Q_{ext} \rangle \bar{\tau}_o$. For $Q_{ext} \simeq 2$ and $\bar{\tau}_o \simeq 3 - 10$, one obtains

$$t_{H_2}/t_{t_1} \approx 0.3 \tag{8-18}$$

i.e. turbulent elements at scales $\approx \pi/2\bar{\kappa}$ survive long enough to permit H_2 formation in quantities such that molecule formation dominates turbulent effects.

Another point deserving some discussion is the adopted form of the function $\Lambda - \Gamma$. As mentioned in Section 7, interest was focussed only on the direct effects produced by the formation of H_2 molecules on grains, and for that, only a gas of pure HI was considered. In a more realistic model however, traces of heavy elements have to be allowed for, mainly C, O, Fe and Si and probably some ions of them, concentrations of which depend critically on the detailed radiative transport at ionizing wavelengths. In the density range of interest, $n \gtrsim 10^2$ the neutral species probably dominate the atomic cooling. If one goes into this more realistic model, one has to consider all the chemistry depending on H_2 presence, mainly the CO chemistry because of the effectiveness of CO as a coolant. In addition, the agents producing the heating function Γ have to be considered. It is likely that this last aspect is the most puzzling one due to the uncertainty in Γ, Spitzer (1978).

It is likely that given the power of cooling of the CO molecule, the presence of this new molecule enhances the effects produced by H_2. The CO molecule is probably responsible for cooling the gas from about $60^{o}K$ to $5 - 10^{o}K$, temperatures observed in dense molecular clouds. The situation is not as simple as it appears at first glance, and further research, in multi-dimensional and non-homogeneous models, on this particular aspect is required.

Several approximations have been introduced into this study and the problem has been highly schematized in order to go a little further than the very order of magnitude. However, the results show that if HI clouds reach the verge of their gravitational contraction in a subsonic turbulent state, with gas number density $n \gtrsim 10^2$ cm^{-3} and gas temperature $T \approx 10^{2}\ ^{o}K$, their fragmentation would be a consequence of the following chain of processes:

i - subsonic turbulence provides initial density fluctuations with scales of length ranging between the size of the cloud and the threshold imposed by viscosity.

ii - the radiation field imposes a constraint on the spectral range of density fluctuations able to be amplified effectively in times shorter than the contraction time of the cloud as a whole. This constraint is given by the scale length over which fluctuations of the dust temperature occur around the critical value for H_2 formation i.e. $1 \lesssim r \lesssim 2$ where r is the reciprocal of distance measured in units of optical depth.

iii - H_2 formation initiates an irreversible process of density

amplification at the above scales and provides the contracting cloud with an initial pattern of fragmentation. The mass range of fragments is then given by

$$\frac{M}{M_\odot} \approx 4.4 \times 10^{-58} \langle Q_{ext} \tilde{\sigma}_d \rangle \left(\frac{n_d}{n} \right)^{-3} n^{-2} \left(\frac{\pi}{r} \right)^3$$

where $1 \lesssim r \lesssim 2$ and $10^2 \lesssim n \lesssim 10^4$ cm^{-3}.

For standard values of galactic clouds the above mass range would be

$$5.9 \times 10^{-3} \lesssim \frac{M}{M_\odot} \lesssim 4.8 \times 10^2 .$$

9. FURTHER RESEARCH

A. Short Term

a. With simple density distributions and with the help of the Fourier technique, obtain a set of coupled differential equations from the Giovanelli equation and solve them numerically.

b. Consider other geometries: spherical and cylindrical but allowing for inhomogeneities.

c. A self-consistent numerical solution of the Giovanelli equation applying iterative numerical procedure, Varga (1963), Forsythe and Wasow (1960).

d. Look for a simple way to couple the density amplification due to H_2 formation with the gravitational contraction.

e. Re-work Section 7, introducing a more realistic $\Lambda - \Gamma$ function taking into account traces of heavy elements. At the same time introduce the CO chemistry with a simplified treatment of the gas-radiation field interaction.

f. Look for a way to solve in self-consistent form the radiative heating problem taking into account dust and gas simultaneously. In particular, determine whether or not with $T_d > T$, the instability suspected by Silk (1978) appears. The paper of Petrosian and Dana (1975) could serve as a guide.

g. Examine in detail how an atomic cloud compressed by the spiral density wave enters the collapse state. Paper guide: Biermann et al (1972).

h. Look for a quantum mechanical argument to decide which interpretation of the Marenco's experiment (1972) is the correct one.

i. Find the real upper limit of the binding energy of H_2 going as heat input into the gas.

B. Long Term

a. Solution of the radiative heating problem in multi-dimensional and non-uniform clouds using Monte-Carlo techniques. House and Avery (1969), Bernes (1979).

b. The same as problem a but using the Markov chain method, Esposito and House (1978).

c. The same as problem a using the generalised Feautrier's (1964) method, Cannon (1970), Cannon and Rees (1971), Mihalas et al (1978).

d. Solve the problem of radiative smoothing, Spiegel (1957), Le Guet (1972), Delache and Froeschle (1972), Anderson (1973), in a non-homogeneous medium.

e. Calculate the effective cooling rate of the cloud fragmented in places of $\tau_{cool} \approx 1$, Low-Lynden-Bell (1976), integrating numerically the equation of Giovanelli (1957).

f. Does the entropy balance equation give information on the fragmentation process? Groot and Mazur (1962), Nicolis (1979).

g. Repeat the Hollenback et al (1971) calculations for H_2 formation but solving in self-consistent way the radiative

transfer problem following the Petrosian and Dana (1975) paper.

h. Realise the three observational tests suggested by Reddish (1977).

i. Following the paper of Woolfson (1979), repeat the calculation introducing molecular cooling and molecular physics in general instead of atomic cooling and atomic physics.

j. Try to apply the stochastic theory of Chandrasekhar (1943) to the physics of IM. In particular to the grain formation process and to the thermodynamics of the dust clouds.

k. Re-work the Schatzmann's (1958, 1979) problem but in 2-D. In particular, look for the possibility of work in the same general way as the Benard problem, Chandrasekhar (1961).

l. Generalise the 3-D hydrodynamic code of Tohline (1978) to take into account radiative transfer and the chemistry of the H_2 and CO molecule.

m. Re-work the Sasao (1973) paper taking into account the thermodynamics. If this is possible, in a second step, introduce the chemistry and the radiative transport.

REFERENCES

Aiello, S., Mencaraglia, F., Blanco, A., Borghesi, A. & Bussoletti, E., 1977. Mon. Not. R. astr. Soc., 180, 323.

Ambartsumian, V.A., 1955. Observatory, 75, 72.

Ambartsumian, V.A., 1960. Quart. J. Roy. Astron. Soc., 1, 152.

Anderson, D., 1973. Astron. & Astrophys., 29, 23.

Andriesse, C.D., 1974. Astron. & Astrophys., 37, 257.

Andriesse, C.D., 1977. Radiating Cosmic Dust, Vistas in Astronomy, 21, 107. Pergamon Press, Oxford.

Auluck, F.C. & Kothari, D.S., 1954. Nature, 176, 565.

Auluck, F.C. & Kothari, D.S., 1965. Z. Astrophys., 63, 15.

Baade, W., 1944. Astrophys. J., 100, 137.

Bernes, C., 1979. Astron. & Astrophys., 73, 67.

Biermann, P., Kippenhan, R., Tscharnuter, W. & Yorke, H., 1972. Astron. & Astrophys., 19, 113.

Bodenheimer, P., 1968. Astrophys. J., 153, 483.

Bonnor, W.B., 1957. Mon. Not. R. astr. Soc., 117, 104.

Cannon, C.J., 1970. Astrophys. J., 161, 255.

Cannon, C.J. & Rees, D.E., 1971. Astrophys. J., 169, 157.

Chandrasekhar, S., 1943. Rev. Mod. Phys., 15, 1.

Chandrasekhar, S., 1951a. Proc. Roy. Soc., London, A, 210, 18.

Chandrasekhar, S., 1951b. Proc. Roy. Soc., London, A, 210, 26.

Chandrasekhar, S., 1960. Radiative Transfer, Dover Publications, Inc.

Chandrasekhar, S., 1961. Hydrodynamic and Hydromagnetic Stability, Oxford at the Clarendon Press.

Clayton, D.D., 1978. Protostars and Planets, Gehrels, ed. The University of Arizona, Tucson.

Delaché, P. & Froeschle, C., 1972. Astron. & Astrophys., 16, 348.

Disney, M.J., McNally, D. & Wright, A.E., 1969. Mon. Not. R. astr. Soc., 146, 123.

Elmegren, B. & Lada, C., 1977. Astrophys. J., 214, 725.

Esposito, L.W. & House, L.L., 1978. Astrophys. J., 219, 1058.

Feautrier, P., 1964. C.R. Acad. Sc., Paris, 258, 3189.

Federman, S., Glassgold, A.E. & Kwan, J., 1979. Astrophys. J., 227, 466.

Field, G.B., 1965. Astrophys. J., 142, 531.

Flannery, B. & Krook, M., 1978. Astrophys. J., 223, 447.

Forsythe, G.E. & Wasow, N., 1960. Finite-Difference Methods for Partial Differential Equations, John Wiley & Sons, Inc., New York, London.

Frisch, W., Sulem, P. & Nelkin, M., 1978. J. Fluid Mech., 87, 719.

Gamow, G., 1952. Phys. Rev., 86, 251.

Gerola, H. & Glassgold, A.E., 1978. Astrophys. J. Suppl. Series, 37, 1.

Giaretta, D.L., 1977. PhD Thesis, St Catherine's College, Oxford.

Giovanelli, R.G., 1957. Aust. J. Phys., 10, 227.

Giovanelli, R.G., 1959. Aust. J. Phys., 12, 164.

Giovanelli, R.G., 1963. Progr. Optics, 2, 111.

Glassgold, A.E. & Langer, W.D., 1976. Astrophys. J., 204, 403.

Greenberg, J.M., 1971. Astron. & Astrophys., 12, 240.

Greenberg, J.M., 1979. The Moon and the Planets, 20, 15.

Groot, S.R. de & Mazur, P., 1962. Non-Equilibrium Thermodynamics, North Holland Publishing Co., Amsterdam.

Grzedzielski, S., 1966. Mon. Not. R. astr. Soc., 134, 109.

Harrison, E.R., 1978. Astrophys. J., 226, L95.

Haselgrove, C.B., 1961. Computer J., 4, 255.

Hattori, T., Nakano, T. & Hayashi, C., 1969. Progr. Theor. Phys., 42, 781.

Hayashi, C. & Nakano, T., 1965. Progr. Theor. Phys., Japan, 34, 754.

Heisenberg, W., 1947. Zs. f. Phys., 124, 628.

Herbst, E., 1978. Protostars and Planets, Gehrels, Ed. The University of Arizona, Tucson.

Hershberg, R.E., 1964. Izv. Krymsk. Astrofiz. Observ., 31, 100.

Hillel, A.J., 1973. Astrophys. Space Sci., 25, 413.

Hoerner, S. von, 1951. Z. Astrophys., 30, 17.

Hollenbach, D.J. & Salpeter, E.E., 1971. Astrophys. J., 163, 155.

Hollenbach, D.J., Werner, M. & Salpeter, E.E., 1971. Astrophys. J., 163, 165.

House, L.L. & Avery, L.W., 1969. J. Quart. Spectrosc. Radiat. Transfer 9, 1979.

Hoyle, F., 1953. Astrophys. J., 118, 513.

Hulst, H.C., van de, 1946. Recharches Astronomiques de 1'Observatorie d'Utrecht, Vol. XI, pt. 1 & 2, Amsterdam.

Hunter, C., 1962. Astrophys. J., 136, 594.

Hunter, C., 1964. Astrophys. J., 139, 570.

Hunter, D. & Watson, W., 1978. Astrophys. J., 226, 477.

Jeans, J.H., 1928. Astronomy and Cosmogony, Cambridge University Press.

Jong, T. de, 1977. Star Formation, Symp. No. 75, IAU.

Kant, I., 1955, Allgemeine Natur Geschichte und Theorie des Himmels.

Kaplan, S.A. & Pikelner, S.B., 1970. The Interstellar Medium, Harvard University Press.

Kegel, W.H. & Traving, G., 1976. Astron. & Astrophys., 50, 137.

Krishna Swamy, K.S. & Wickramasinghe, N.C., 1968. Mon. Not. R. astr. Soc., 139, 283.

Kruszewski, A., 1961. Acta. Astr., 11, 199.

Landau, L. & Lifschitz, E., 1959. Fluid Mechanics, Pergamon Press, London.

Laplace, P.S. de, 1796, Exposition du Système du Monde.

Larson, R.B., 1969. Mon. Not. R. astr. Soc., 145, 271.

Larson, R.B., 1973. Mon. Not. R. astr. Soc., 161, 133.

Larson, R.B., 1977. Star Formation, IAU Symp. No. 75, de Jong & Maeder (ed.), Reidel Publishing Co., pp.249-281.

Larson, R., 1978. Protostars and Planets, Gehrels, ed., The University of Arizona, Tucson.

Larson, R.B., 1979. Mon. Not. R. astr. Soc., 186, 479.

Layzer, D., 1954. Astrophys. J., 59, 170.

Layzer, D., 1956. Observatory, 76, 73.

Layzer, D., 1963a, Astrophys. J., 137, 351.

Layzer, D., L963b, Astrophys. J., 138, 174.

Layzer, D., 1964. Ann. Rev. Astron. Astrophys., 2, 341.

Lee, T., 1972. Low Temperature Laboratory Astrophysics Experiment, Final Report, Roy. Obs. Edin.

Lee, T., 1975. Astrophys. Space Sci., 34, 123.

Le Guet, F., 1972. Astron. & Astrophys., 16, 356.

Leung, C.M., 1975. Astrophys. J., 199, 340.

Limber, D.N., 1960. Astrophys. J., 131, 168.

Liszt, H.S., 1973. PhD dissertation, Princeton University.

Liszt, H.S., Wilson, R.W., Penzias, A.A., Jefferts, K.B., Wannier, P.G. & Solomon, P.M., 1974. Astrophys. J., 190, 557.

Low, C. & Lynden-Bell, D., 1976. Mon. Not. R. astr. Soc., 176, 367.

Marenco, G., Schutte, A., Scoles, G. & Tommasini, F., 1972. Trans. 5th Int. Vacuum Congress and Int. Conf. on Solid Surfaces, p.824.

Mayers, D.F., 1962. Numerical Solution of Ordinary and Partial Differential Equations, Fox, L. (Ed.), Pergamon Press, pp.16-27.

McCrea, W.H., 1960. Proc. Roy. Soc., A, 256, 245.

McVittie, G.C., 1956. Astron. J., 61, 451.

Mestel, L., 1965. Q. Jl. astr. Soc., 6, 161.

Mihalas, D., Auer, L.H. & Mihalas, B., 1978. Astrophys. J., 220, 1001.

Morgan, D., 1973. PhD Thesis, St Andrews University.

Nariai, H., 1970. Progr. Theor. Phys., Kyoto, 44, 110.

Nariai, H., 1971. Progr. Theor. Phys., Kyoto, 45, 61.

Nicolis, G., 1979. Rep. Prog. Phys., 42, 225.

Oppenheimer, M., 1977. Astrophys. J., 211, 400.

Oppenheimer, M. & Dalgarno, A., 1975. Astrophys. J., 200, 419.

Ozernoi, L.M. & Chernin, A.D., 1968. Sov. Astr., 11, 907.

Ozernoi, L.M. & Chernin, A.D., 1969. Sov. Astr. (A.J.), 12, 901.

Petrosian, V. & Dana, R.A., 1975. Astrophys. J., 196, 733.

Pomraning, G.G., 1973. The Equations of Radiation Hydrodynamics, Pergamon Press, Oxford, pp.47-49.

Reddish, V.C., 1975. Mon. Not. R. astr. Soc., 170, 261.

Reddish, V.C., 1977. Q. Jl. R. astr. Soc., 18, 464.

Reddish, V.C., 1978. Stellar Formation, Pergamon Press.

Rees, M.J., 1976. Mon. Not. R. astr. Soc., 176, 483.

Roberts, W.W., 1969. Astrophys. J., 158, 123.

Sabano, Y. & Kannari, Y., 1978. Publ. Astron. Soc. Japan, 30, 77.

Salpeter, E., 1955. Astrophys. J., 121, 161.

Samuelson, R.E., 1967. Astrophys. J., 147, 782.

Sasao, T., 1971. Publ. Astron. Soc. Japan, 23, 433.

Sasao, T., 1973. Publ. Astron. Soc. Japan, 25, 1.

Schatzman, E., 1958. Rev. Mod. Phys., 30, 1012.

Schatzman, E., 1979. Private Communication.

Silk, J., 1978. Protostars and Planets, Gehrels, ed. The University of Arizona, Tucson.

Smith, R.C., 1977. Mon. Not. R. astr. Soc., 179, 521.

Smith, R.C. & Wright, A.E., 1975. Mon. Not. R. astr. Soc., 172, 221.

Solomon, P.M., 1969. IAU Symp. 26, 320.

Solomon, P.M. & Wickramasinghe, N.C., 1969. Astrophys. J., 158, 449.

Spiegel, E.A., 1957. Astrophys. J., 126, 202.

Spitzer, L., 1976. Q. Jl. R. astr. Soc., 17, 97.

Spitzer, L., 1978. Physical Processes in the Interstellar Medium, John Wiley & Sons.

Stecher, T.P. & Williams, D.A., 1967. Astrophys. J. (Letters), 149, L29.

Stibbs, D.W.N., 1971. Astrophys. J., 168, 155.

Suchkov, A.A. & Shchekinov, Y.A., 1976. Sov. Astr. (A.J.), 19, 403.

Tohline, J.E., 1978. PhD Thesis, University of California.

Tohline, J.E., 1979. Private Communication.

Tomita, K., 1971. Progr. Theor. Phys., Kyoto, 45, 1747.

Tomita, K., 1972. Progr. Theor. Phys., Kyoto, 47, 416.

Unno, W. & Spiegel, E.A., 1966. Publ. Astron. Soc. Japan, 18, 85.

Varga, R.S., 1963. Matrix Iterative Analysis, Prentice-Hall, Inc.

Watson, W.D., 1976. Rev. Mod. Phys., 48, 513.

Weizsacker, C.F. von, 1951. Astrophys. J., 168, 175.

Werner, M. & Salpeter, E., 1969. Mon. Not. R. astr. Soc., 145, 249.

Wickramasinghe, N.C., 1973. Light Scattering Functions for Small Particles, Adam Hilger, London.

Wildt, R., 1966. Icarus, 5, 24.

Wilson, P.A., 1968. Astrophys. J., 151, 1019.

Woodward, P.R., 1978. Ann. Rev. Astron. Astrophys., 16, 555.

Woolfson, M.M., 1979. Phil. Trans. R.S. of London, A 291, 219.

Yoneyama, T., 1973. Publ. Astron. Soc. Japan, 25, 349.

Zimmerman, H., 1964. Astron. Nachr., 288, 95.

Zuckerman, B. & Evans, N.J., II, 1974. Astrophys. J. (Letters), 192, L149.

Zuckerman, B. & Palmer, P., 1974. Ann. Rev. Astr. and Ap., 12, 279.

APPENDIX A

BASIC EQUATIONS GOVERNING A HETEROGENEOUS FLUID

a. Conservation of Mass

A fluid constituted by n components among which r chemical reactions are possible obeys the following relations, De Groot and Mazur (1961)

$$\frac{\delta \rho_k}{\partial t} = - \frac{\partial}{\partial x_\alpha} (\rho_k v_{k\alpha}) + \sum_{j=1}^{r} \nu_{kj} J_j \quad * \qquad (A-1)$$

r = number of reactions

k = 1, ... n

where $\rho_k = m_k n_k$ is the density of the k-component of mass per particle m_k and number density n_k, $v_{k\alpha}$ is the α-th component of the velocity of this k-component, ν_{kj}/m_k ∝ stoichiometric coefficient with which k appears in the chemical reaction j. $\nu_{kj} > 0$ if the component k appears in the second, $\nu_{kj} < 0$ when it appears in the first member of the reaction equation. $\nu_{kj} J_j$ is the mass of k-component generated per unit volume and time in the j^{th} reaction. Equation (A-1) is a balance for each k-component between the local change (left-hand side term) and the flow (first right-hand side term) plus the net production or source term (second right-hand term).

Because there is no creation of mass in the system,

$$\sum_{k=1}^{n} \nu_{kj} J_j = 0 \qquad (A-2)$$

* With Greek letters, Einstein's sum convention will be used.

Therefore,

$$\frac{\partial \rho}{\partial t} = -\frac{\partial}{\partial x_\alpha}\left(\rho v_\alpha\right) \quad \text{- continuity equation -} \tag{A-3}$$

where

$$\rho = \sum_{k=1}^{n} m_k n_k$$

$$v_\alpha = \frac{1}{\rho} \sum_{k=1}^{n} \rho_k v_{k\alpha} \quad \text{- "barycentric velocity" -} \tag{A-4}$$

Defining the "diffusion flow" of substance k by

$$\tilde{J}_{k\alpha} = \rho_k \left(v_{k\alpha} - v_\alpha \right) \tag{A-5}$$

and the mass fraction c_k by

$$c_k = \rho_k/\rho \quad , \qquad \sum_{k=1}^{n} c_k = 1 \tag{A-6}$$

equation (A-1) becomes

$$\rho \frac{dc_k}{dt} = \frac{\partial \tilde{J}_{k\alpha}}{\partial x_\alpha} \tag{A-7}$$

Evidently

$$\sum_{k=1}^{n} \tilde{J}_{k\alpha} = 0 \tag{A-8}$$

b. Motion Equation

$$\rho \frac{dv_\alpha}{dt} = \frac{\partial}{\partial x_\beta} \tilde{P}_{\beta\alpha} + \sum_k \rho_k F_{k\alpha} \qquad \text{(A-9)}$$

where $\tilde{P}_{\beta\alpha}$ are the Cartesian components of the stress tensor of the medium. It is often assumed that $\tilde{P}_{\alpha\beta} = \tilde{P}_{\beta\alpha}$ *. $F_{k\alpha}$ are Cartesian components of the force by unit mass exerted on the k-component. Equation (A-9) is a generalisation of Newton's second law allowing for forces involving short range interaction between particles of the system (first right-hand side term) plus external forces on the system and long-range interaction forces between particles of the system (second right-hand side term).

Defining a momentum flux tensor $\sigma_{\alpha\beta}$ as the part of the momentum flux not due to the direct transfer of momentum with mass of moving fluid, i.e. related with short range interaction, by

$$\sigma_{\alpha\beta} = -P\,\delta_{\alpha\beta} + \sigma'_{\alpha\beta} \qquad \text{(A-10)}$$

where P is the ordinary pressure and $\sigma'_{\alpha\beta}$ is the viscosity stress-tensor, equation (A-9) becomes

$$\frac{\partial}{\partial t}(\rho v_\alpha) = -\frac{\partial}{\partial x_\beta}(\rho v_\alpha v_\beta - \sigma_{\alpha\beta}) + \sum_{k=1}^{n} \rho_k F_{k\alpha} \qquad \text{(A-11)}$$

or in a more familiar form

* This is valid in a first approximation for diluted systems constituted by spherical molecules.

$$\frac{d\underline{v}}{dt} = \nu \Delta \underline{v} + \left(\frac{\xi}{\rho} + \frac{1}{3}\nu \right) \underline{\nabla} \left(\underline{\nabla} . \underline{v} \right) + \sum_{k=1}^{n} \rho_k \underline{F}_k \qquad \text{(A-11')}$$

where η is the coefficient of dynamic viscosity, $\nu = \eta/\rho$ the coefficient of kinematic viscosity and ξ the coefficient of viscosity.

c. Energy Equation

If u is the internal energy per unit mass and

$$\tilde{u} = u + \sum_{k=1}^{n} \tfrac{1}{2} c_k \left(v_{k\alpha} - v_\alpha \right)^2 \qquad \text{(A-12)}$$

the energy equation becomes

$$\rho \frac{d\tilde{u}}{dt} = \Gamma - \Lambda + \frac{P}{\rho} \frac{d\rho}{dt} + \sigma'_{\alpha\beta} \frac{\partial v_\alpha}{\partial x_\beta} + \sum_{k=1}^{n} J_{k\alpha} F_{k\alpha} \qquad \text{(A-13)}$$

where Γ and Λ are the heating and cooling rate per unit volume. This equation can be generalised further to take into account the thermal conduction, Landau and Lifchitz (1959), De Groot and Mazur (1961).

For a fluid with self-gravitation as the unique long-range force and with negligible viscosity and diffusion, the basic equations given in a), b) and c) take the simple form:

Mass conservation

$$\frac{\partial \rho_k}{\partial t} = -\text{div} \left(\rho_k \underline{v}_k \right) + \sum_{j=1}^{r} \nu_{kj} J_j \qquad \text{(A-14)}$$

$$\frac{\partial \rho}{\partial t} = -\text{div} \left(\rho \underline{v} \right) \qquad \text{(A-15)}$$

Motion equation

$$\rho \frac{d\underline{v}}{dt} = -\underline{\nabla} P - \underline{\nabla}\phi \qquad (A\text{-}16)$$

$$\nabla \phi = 4\pi G \rho$$

Energy equation

$$\Gamma - \Lambda = \rho \frac{du}{dt} - \frac{P}{\rho} \frac{d\rho}{dt} \qquad (A\text{-}17)$$

This last equation simply enunciates that for any element of unit volume the net heat input per unit time (left-hand side term in (A-17) is equal to the change of internal energy per unit time (first term on the right-hand side) plus the work done by the element per unit time (second term on the right-hand side). If the element does work (gives energy), $\frac{1}{\rho} \frac{d\rho}{dt} < 0$ and the compressional heating $\frac{P}{\rho} \frac{d\rho}{dt} < 0$. If work is done on the element, $\frac{1}{\rho} \frac{d\rho}{dt} > 0$ and for compressional heating $\frac{P}{\rho} \frac{d\rho}{dt} > 0$.

d. Dynamical and Thermal Timescales. The Jeans Limit.

Equation (A-16) provides two dynamical timescales, the free-fall time t_{ff} and the expansion timescale t_e, and the Jeans limit, in a first approximation.

If in equation (A-16) the pressure term is made smaller than the gravitation one, i.e. $|\nabla P| << \rho |\nabla \phi|$, the equation of motion

becomes

$$\rho \frac{d\underline{v}}{dt} = -\rho \nabla \phi \qquad \text{(A-18)}$$

which in the case of a uniform sphere of initial configuration $\rho(o) = \rho_o$ and $r(o) = R_o$, becomes

$$\frac{d^2 r}{dt^2} = -\frac{4\pi}{3} \frac{G \rho_o R_o^3}{r^2} \qquad \text{(A-19)}$$

The integration of equation (A-19) with the additional condition $\left(\frac{dr}{dt}\right)_{t=0} = 0$ is straightforward and it gives

$$\beta + \tfrac{1}{2} \sin 2\beta = \left[\frac{8\pi G \rho_o}{3}\right]^{\frac{1}{2}} t \qquad \text{(A-20)}$$

where $r/R_o = \cos^2 \beta$, Hunter (1963). Therefore, the time at which any shell reaches the centre, called free-fall time t_{ff} is

$$t_{ff} = \left(\frac{3\pi}{32G}\right)^{\frac{1}{2}} \rho_o^{-\frac{1}{2}} \qquad \text{(A-21)}$$

On the other hand, if in equation (A-16), the pressure force dominates the gravitational one, i.e. $|\nabla P| >> \rho |\nabla \phi|$, this equation reduces to

$$\rho \frac{d\underline{v}}{dt} = -\nabla P \qquad \text{(A-22)}$$

from which the characteristic time t_e for free expansion is defined by

$$t_e = \frac{R_o}{c_S} \tag{A-23}$$

where R_o is the characteristic initial dimension of the cloud and c_S the speed of sound, which for an ideal gas of molecular weight μ is

$$c_S = \left(\tilde{\gamma} \frac{kT}{\mu}\right)^{\frac{1}{2}} \tag{A-24}$$

where $\tilde{\gamma} = c_p/c_v$, the ratio of specific heats. With

$$R_o = \left(\frac{3M}{4\pi\rho}\right)^{1/3} \tag{A-25}$$

where M is the mass of the cloud, the dynamical timescale for free-expansion is

$$t_e = (3M/4\pi\rho) \; / \; \left(\tilde{\gamma} \frac{kT}{\mu}\right)^{\frac{1}{2}} \tag{A-26}$$

Equation (A-16) admits a static solution if

$$\underline{\nabla} P = -\rho \nabla \phi \tag{A-27}$$

which in orders of magnitude gives

$$M_J = \left(\frac{3}{4\pi}\right)^{\frac{1}{2}} \left(\frac{k}{G\mu}\right)^{3/2} T^{3/2} \rho^{-\frac{1}{2}} \tag{A-28}$$

which in a first approximation defines the Jeans limit. For a formal

definition of this limit see Section 2 of the text. Condition (A-28) is equivalent to the statement that in equilibrium $t_e = t_{ff}$ Strictly speaking, $M = M_J$ is not a condition of quasi-hydrostatic equilibrium because in general clouds are open thermodynamical systems, i.e. they are heating or cooling, adiabatic motions can start if $\tilde{\gamma} < 4/3$ or chemical reactions in non equilibrium can appear.

Finally, equation (A-17) provides a timescale for the thermal process. If the cooling (or heating) process is considered as an isochoric one, in a first approximation, equation (A-17) becomes

$$\rho \frac{du}{dt} = \Gamma - \Lambda \qquad \text{(A-29)}$$

and the cooling time would be

$$t_c = (3 k \rho T/2\mu) \; / \; (\Lambda - \Gamma) \qquad \text{(A-30)}$$

if $\Lambda > \Gamma$. This timescale is simply the characteristic time during which the cloud reaches the thermal equilibrium. If $\Gamma > \Lambda$ a change of signs occurs in equation (A-30) and a heating time t_h would be defined.

e. The Chemistry of the H_2

In the particular case of a hydrogen gas reacting on dust particles, equation (A-14) is greatly simplified as follows.

Equation (A-14) can be written involving the particle density rather than the mass density in the form

$$\frac{\partial n_k}{\partial t} + \underline{\nabla} \cdot (n_k \underline{v}_k) = Z_k \qquad \text{(A-31)}$$

where Z_k is the generation rate of particles of type k and k = 1 for atomic hydrogen and 2 for molecular. Defining the parameter x by

$$x = \frac{n_1}{n} \tag{A-32}$$

where $n = n_1 + 2n_2$ is the density number of atoms, the following equation for x can be obtained from equation (A-31)*

$$\frac{dx}{dt} = \frac{1}{n} \text{(dissociation rate)} - \frac{1}{n} \text{(recombination rate)} \tag{A-33}$$

or according to equations (3-1) and (3-7)

$$\frac{dx}{dt} = B \frac{1 - x}{2} - \gamma \langle \tilde{\sigma}_d \rangle \langle v_H \rangle \left(\frac{n_d}{n} \right) n x \tag{A-34}$$

or according to Section 3, simply

$$\frac{dx}{dt} = -\gamma \langle \tilde{\sigma}_d \rangle \langle v_H \rangle \left(\frac{n_d}{n} \right) n x \tag{A-35}$$

From equation (A-35) one can define straightforwardly a timescale for H_2 formation as the e-fold time for x

$$t_{H_2} = \gamma^{-1} \langle \tilde{\sigma}_d \rangle^{-1} \langle v_H \rangle^{-1} \left(\frac{n_d}{n} \right)^{-1} n^{-1} \tag{A-36}$$

i.e., t_{H_2} would be the e-fold time for consuming the atomic hydrogen.

Another quantity of particular interest, involved with the chemistry

* To obtain (A-33) it has been assumed that the velocities for both components are the same and equal to the average one.

of a reacting hydrogen gas, is the internal energy per unit mass u.

If n_1 and n_2 are the particle densities of the two components of a mixture of two gases with molecular masses m_1 and m_2, the internal energy per unit of mass is

$$u = \frac{kT}{n_1 m_1 + n_2 m_2} \; n_1(\varepsilon_1 + \varepsilon_1^o) + n_2(\varepsilon_2 + \varepsilon_2^o) \qquad \text{(A-37)}$$

Herzberg (1950), where ε_i is the internal energy per particle containing the translational plus the energy associated with internal degrees of freedom (rot., vibr., ...)

$$\varepsilon_i = \frac{kT}{\gamma_i - 1} \qquad \text{(A-38)}$$

$\tilde{\gamma}_i = c_{v_i}/c_{\gamma_i}$ is the ratio of the specific heats, and ε_i^o the zero point energy per particle of class i.

Equation (A-37) in terms of the x parameter defined by equation (A-32) becomes

$$u = \left[\frac{x}{\tilde{\gamma}_1 - 1} + \frac{1-x}{2(\tilde{\gamma}_2 - 1)}\right] R\,T + \chi N_o x + \frac{\varepsilon_2^o}{2m_1} \qquad \text{(A-39)}$$

R being the gas constant, N_o the Avogadro number and χ the dissociation energy $2\,\varepsilon_1^o - \varepsilon_2^o$.

From equation (A-39) one finds that the change in internal energy with time in a reacting mixture of hydrogen is

$$\frac{du}{dt} = \frac{5+x}{4}\frac{dT}{dt} + \frac{RT}{4}\frac{dx}{dt} + \chi N_o \frac{dx}{dt} \qquad \text{(A-40)}$$

f. Radiative Transfer Equation

Formally the radiative transport through any medium capable of absorbing, scattering and emitting radiation is governed by the equation

$$\frac{1}{c}\frac{\partial I_\nu}{\partial t}(\underline{r},\underline{\Omega},t) + \underline{\Omega}.\underline{\nabla} I_\nu(\underline{r},\underline{\Omega},t) = \varepsilon_\nu(\underline{r},t)\left[1+\frac{c^2 I_\nu}{2h\nu^3}(\underline{r},\underline{\Omega},t)\right]$$

$$- \alpha_\nu'(\underline{r},t)\, I_\nu(\underline{r},\underline{\Omega},t)$$

$$+ \int_0^\infty d\nu' \int_{4\pi} d\Omega' \frac{\nu}{\nu'}, \sigma_{\nu'\to\nu}(\underline{r},\underline{\Omega}'\underline{\Omega},t)\, I_{\nu'}(\underline{r},\underline{\Omega}';t)\left[1+\frac{c^2}{2h\nu^3} I_\nu(\underline{r},\underline{\Omega},t)\right]$$

$$- \int_0^\infty d_\nu' \int_{4\pi} d\Omega' \sigma_{\nu\to\nu'}(\underline{r},\underline{\Omega}.\underline{\Omega}', t)\, I_\nu(\underline{r},\underline{\Omega},t)\left[1+\frac{c^2}{2h\nu'^3} I_{\nu'}(\underline{r},\underline{\Omega}', t)\right]$$

(A-41)

Pomraning (1973), where the following notation is used:

$I_\nu(\underline{r},\underline{\Omega},t)$ = specific radiation intensity of frequency ν, at the spatial point $\underline{r}$, in the direction defined by the unit vector $\underline{\Omega}$ and at the time t.

$\varepsilon_\nu(\underline{r},t)$ = rate of energy emission due to spontaneous processes

$d\Omega$ = element of solid angle in the direction $\underline{\Omega}$.

$\alpha'_\nu(\underline{r},t)$ = macroscopic absorption coefficient.

$\sigma'_{\nu'\to\nu}(\underline{r},\underline{\Omega}'.\underline{\Omega},t)$ = differential scattering coefficient, i.e. the probability of a photon being scattered from

ν' to ν contained in $d\nu$ and from $\underline{\Omega}'$ to $\underline{\Omega}$ contained in $d\Omega$, in travelling a distance ds is given by

$$\text{probability} = \sigma'_{\nu' \to \nu}(\underline{r}, \underline{\Omega}' . \underline{\Omega}, t)\, d\nu\, d\Omega\, ds. \qquad \text{(A-42)}$$

The boundary condition corresponding to (A-41) becomes

$$I_\nu(\underline{r}_S, \underline{\Omega}, t) = I^o(\underline{r}_S, \nu, \underline{\Omega}, t) \text{ for } \underline{n} . \Omega < 0 \qquad \text{(A-43)}$$

where $I^o(\underline{r}_S, \nu, \underline{\Omega}, t)$ is a known function, $\underline{r}_S$ is the vector of any point on the boundary surface S and $\underline{n}$ is an outward normal unit vector at any point $\underline{r}_S$. This boundary condition enunciates that the specific intensity at all points on the boundary surface S and in the incoming direction is known. Further, the surface S is a non-re-entrant surface, i.e., any photon leaving the volume limited by S re-enters it through S.

The temporal boundary condition provides another well defined function $I_\nu(\underline{r}, \underline{\Omega}, 0)$.

If the assumption of local thermodynamic equilibrium - LTE - is introduced, i.e., the matter at point $\underline{r}$ and time t is considered in thermodynamic equilibrium, regardless of the presence and nature of the radiation field, the RTE takes the simpler form

$$\frac{1}{c} \frac{\partial I_\nu(\underline{r}, \underline{\Omega}, t)}{\partial t} + \underline{\Omega} . \nabla I_\nu(\underline{r}, \underline{\Omega}, t) = \alpha_\nu(\underline{r}, t) \left[B_\nu(\underline{r}, t) - I_\nu(\underline{r}, \underline{\Omega}, t) \right]$$

$$+ \int_0^\infty d\nu' \int_{4\pi} d\Omega' \frac{\nu}{\nu'} \sigma_{\nu' \to \nu}(\underline{r}, \underline{\Omega}' . \underline{\Omega}, t)\, I_{\nu'}(\underline{r}, \underline{\Omega}', t) \left[1 + \frac{c^2}{2h\nu^3} I_\nu(\underline{r}, \underline{\Omega}, t) \right]$$

$$- \int_0^\infty d\nu' \int_{4\pi} d\Omega' \sigma_{\nu \to \nu'}(\underline{r}, \underline{\Omega}.\underline{\Omega}', t)\ I_\nu(\underline{r}, \underline{\Omega}, t) \left[1 + \frac{c^2}{2h\nu'^3} I_{\nu'}(\underline{r}, \underline{\Omega}', t)\right]$$

(A-44)

where $B_\nu(\underline{r},t)$ is the local Planck function and $\alpha_\nu(\underline{r},t)$ is the absorption coefficient taking into account the stimulated emission, i.e.

$$\alpha_\nu(\underline{r},t) = \alpha'_\nu(\underline{r},t) \left[1 - \exp(-h\nu/kT)\right] \qquad \text{(A-45)}$$

If the assumption of LTE is removed, the RTE (A-44) continues to be valid but in such case $B_\nu(\underline{r},t)$ is not the Planck function.

A drastic simplification appears in the RTE (A-44) in the case of coherent scattering. Then the differential scattering coefficient $\sigma_{\nu' \to \nu}(\underline{r}, \underline{\Omega}'.\underline{\Omega}, t)$ contains a $\delta(\nu - \nu')$ function and the non-linear terms in I on the right-hand side of equation (A-44) cancel one another and the RTE (A-44) is reduced to the form

$$\frac{1}{c} \frac{\partial I_\nu(\underline{r},\underline{\Omega},t)}{\partial t} + \underline{\Omega}.\underline{\nabla} I_\nu(\underline{r},\underline{\Omega},t) = \alpha_\nu(\underline{r},t) \left[B_\nu(\underline{r},t) - I_\nu(\underline{r},\underline{\Omega},t)\right]$$

$$-\sigma_\nu(\underline{r},t) \left[I_\nu(\underline{r},\underline{\Omega},t) - \int_{4\pi} d\Omega'\ p(\underline{\Omega}'.\underline{\Omega})\ I_\nu(\underline{r},\underline{\Omega}',t)\right] \qquad \text{(A-46)}$$

where $\sigma_\nu(\underline{r},t)$ is the macroscopic scattering coefficient defined by

$$\sigma_\nu(\underline{r},t) = \frac{1}{4\pi} \int_0^\infty d\nu' \int_{4\pi} d\Omega' \sigma_{\nu \to \nu'}(\underline{r}, \underline{\Omega}.\underline{\Omega}', t) \qquad \text{(A-47)}$$

i.e., $\sigma_\nu(\underline{r},t)ds$ is the probability that a photon is scattered in

travelling a distance ds. $p(\underline{\Omega}'.\underline{\Omega})$ is the angular phase function normalised such that

$$\frac{1}{4\pi} \int_{4\pi} d\Omega' \; p(\underline{\Omega}'.\underline{\Omega}) \quad = \quad 1 \tag{A-48}$$

In the non-time dependent case, equation (A-46) simply becomes

$$\underline{\Omega}.\underline{\nabla} I_\nu (\underline{r},\underline{\Omega}) \quad = \quad \alpha_\nu(\underline{r}) B_\nu (\underline{r}) \; - \left[\alpha_\nu(\underline{r}) + \sigma_\nu(\underline{r})\right] I_\nu(\underline{r},\underline{\Omega})$$

$$+ \; \sigma_\nu(\underline{r}) \int_{4\pi} \frac{d\Omega'}{4\pi} \; p(\underline{\Omega}'.\underline{\Omega}) \; I_\nu(\underline{r},\underline{\Omega}') \tag{A-49}$$

or using the definition of directional derivative along $\underline{\Omega}$

$$\frac{dI_\nu(\underline{r},\Omega)}{ds} \quad = \quad \alpha_\nu(\underline{r}) \; B_\nu(r) \; - \left[\alpha_\nu(r) + \sigma_\nu(\underline{r})\right] I_\nu(\underline{r},\underline{\Omega})$$

$$+ \; \sigma_\nu(\underline{r}) \int_{4\pi} \frac{d\Omega'}{4\pi} \; p(\underline{\Omega}'.\underline{\Omega}) \; I_\nu(\underline{r},\underline{\Omega}') \tag{A-50}$$

Usually an extinction coefficient $\kappa_\nu(\underline{r})$ and a source function S_ν defined by

$$\kappa_\nu(\underline{r}) \quad = \quad \alpha_\nu(\underline{r}) + \sigma_\nu(\underline{r}) \tag{A-51}$$

and

$$S_\nu(\underline{r},\underline{\Omega}) \quad = \quad \frac{\alpha_\nu(\underline{r})}{\kappa_\nu(\underline{r})} \; B_\nu + \frac{\sigma_\nu(\underline{r})}{\kappa_\nu(\underline{r})} \int_{4\pi} \frac{d\Omega'}{4\pi} \; p(\Omega',\Omega) \; I_\nu(\underline{r},\underline{\Omega}') \tag{A-52}$$

are introduced. Therefore, the RTE (A-50) becomes

$$\frac{dI_\nu}{ds} = -\kappa_\nu(I_\nu - S_\nu) = -\kappa_\nu I_\nu + j_\nu \qquad \text{(A-53)}$$

j_ν being the total emission coefficient $\kappa_\nu S_\nu$.

For isotropic scattering $p(\underline{\Omega}'.\underline{\Omega}) = 1$ and

$$S_\nu(\underline{r}) = \frac{\alpha_\nu(\underline{r})}{\kappa_\nu(\underline{r})} B_\nu(\underline{r}) + \frac{\sigma_\nu(\underline{r})}{\kappa_\nu(\underline{r})} J_\nu(\underline{r}) \qquad \text{(A-54)}$$

$J_\nu(\underline{r})$ being the mean intensity defined by

$$J_\nu(\underline{r}) = \frac{1}{4\pi} \int_{4\pi} d\Omega' I_\nu(\underline{r},\underline{\Omega}') \qquad \text{(A-55)}$$

APPENDIX B

TURBULENCE AS A MECHANISM GENERATOR OF DENSITY FLUCTUATION

The problem of generating density fluctuations in a medium where the hydrodynamical equations are valid has been treated by many authors, von Weizsäcker (1951), Chandrasekhar (1951a,b), Gamow (1952), Ozernoi and Chernin (1968, 1969), Nariai (1970, 1971), Tomita (1971, 1972), Sasao (1973). For a recent review see, for instance, Frisch et al (1978). In general, from these works it is clear that density fluctuations must occur as a consequence of turbulent motions. In particular, it is possible, through the hydrodynamical equations, to establish a link between the spectrum of turbulence and that of the density fluctuation.

Simple theoretical considerations suggest that turbulence is present at the early stages of contraction of prestellar clouds.

Simplifying the motion equation (A-11') to the form

$$\frac{\partial \underline{v}}{\partial t} + (\underline{v}.\underline{\nabla})\underline{v} = -\frac{\underline{\nabla} P}{\rho} + \nu \Delta \underline{v} - \underline{\nabla}\phi \qquad \text{(B-1)}$$

It can be shown that the hydrodynamical regimen is turbulent providing that the damping motion (second term in the right-hand side of equation (B-1) is small compared with the transfer of motion (second left-hand term in equation (B-1), Landau and Lifchitz (1959). This fact is usually

indicated by defining the Reynolds number

$$\tilde{R} = \frac{\text{transfer of motion}}{\text{damping of motion}} = \frac{v\ell}{\nu} \qquad \text{(B-2)}$$

where v is the variation of gas velocity at scales of dimension ℓ. Therefore, turbulence appears if $\tilde{R} > \tilde{R}_{cri}$, where $\tilde{R}_{cri}$ is a certain critical value > 10, Kaplan and Pikelner (1970). From the definition of viscosity one has

$$\nu \approx \frac{\eta}{\rho}$$

$$\eta \approx \frac{\langle\lambda\rangle}{\langle v\rangle} n k T \qquad \text{(B-3)}$$

where $\langle\lambda\rangle$ and $\langle v\rangle$ are the mean free-path and mean velocity of the gas particles respectively, and

$$\langle \lambda \rangle = \frac{1}{n \langle\sigma\rangle} \qquad \text{(B-4)}$$

$\langle\sigma\rangle$ being a mean cross-section for collisions between gas particles. Therefore

$$\nu \approx \frac{1}{\langle\sigma\rangle} \left(\frac{k}{3\mu}\right)^{\frac{1}{2}} \frac{T^{\frac{1}{2}}}{n} \qquad \text{(B-5)}$$

and

$$\tilde{R} \approx v\ell \langle\sigma\rangle \left(\frac{3\mu}{k}\right)^{\frac{1}{2}} \frac{n}{T^{\frac{1}{2}}} \qquad \text{(B-6)}$$

Taking $v \approx 7 \times 10^5$ cm and $\ell \approx 5$ pc, Spitzer (1978), the Reynolds numbers for typical HI clouds ($n \approx 10\text{-}10^2 cm^3$, $T \approx 10^2 K$, $\langle\sigma\rangle \approx 8.8 \times 10^{-17}$ cm^2) and molecular clouds ($n \approx 10^4 cm^{-3}$, $T \approx 10 K$, $\langle\sigma\rangle = 6.6 \times 10^{-16} cm^3$) become

$$\tilde{R} \approx 2 \times 10^4 \qquad \text{for HI clouds}$$

$$\tilde{R} \approx 5 \times 10^9 \qquad \text{for molecular clouds.}$$

This indicates that in both the atomic and molecular clouds the hydrodynamic regimen is turbulent.

Three aspects of turbulence are of particular importance in this study: turbulence as a mechanism generator of density inhomogeneities, their spectral distribution and the timescales characteristic of such inhomogeneities. The exploration of these aspects will be done in order of magnitude as follows.

Neglecting gravity, the equation (B-1) becomes

$$\frac{\partial \underline{v}}{\partial t} + (\underline{v}.\underline{\nabla})\underline{v} = -\frac{\underline{\nabla} P}{\rho} + \nu \Delta \underline{v} \qquad \text{(B-7)}$$

On the other hand, from the equation of continuity one has

$$\frac{\partial \rho}{\partial t} = -\nabla(\rho \underline{v}) = \rho \underline{\nabla}.\underline{v} - \underline{v}.\underline{\nabla}\rho \qquad \text{(B-8)}$$

Writing the turbulent velocity v as

$$v = v_p + v_s \qquad \text{(B-9)}$$

where v_s is the velocity of vertical motions and v_p the velocity of potential motions, in orders of magnitude, equations (B-7) and (B-8) become

$$\frac{v}{t_t} + \frac{v^2}{\ell} \approx -c^2 \frac{\delta\rho}{\rho\ell} \qquad \text{(B-10)}$$

$$\frac{\delta\rho}{t_t} \approx -\rho \frac{v_p}{\ell} - \nu \frac{\delta\rho}{\ell} \qquad \text{(B-11)}$$

where c is the sound speed, and t_t is the characteristic timescale associated with turbulent motion at length scales ℓ, defined by

$$t_t \approx \frac{\ell}{v} \qquad \text{(B-12)}$$

From equations (B-11) and (B-12) one obtains

$$\frac{\delta\rho}{\rho} \approx \frac{v_p}{v} \qquad \text{(B-13)}$$

and from equation (B-10) results

$$\frac{v_p}{v} \approx \left(\frac{v}{c}\right)^2 \qquad \text{(B-14)}$$

For subsonic motions $v_p << v_s$ and from equation (B-9) one obtains $v \approx v_s$, which means that

$$\frac{\delta\rho}{\rho} \approx \frac{v_p}{v_s} \qquad \text{(B-15)}$$

and

$$\frac{v_p}{v_s} \approx \frac{v_s^2}{c^2} \qquad \text{(B-16)}$$

Therefore, density fluctuations are generated by the p motions which in turn are generated at the expense of the vortical motions i.e. they are a consequence of the hydrodynamic non-linearity as Ozernoi and Chernin (1968, 1969) pointed out.

Once it has been shown how turbulence generates density fluctuations, and how these two phenomena are linked, it is necessary to look at the spectral distribution.

From either the dimensional analysis or considering the transfer of energy from larger to smaller scales, it is possible to establish the well-known Kolmogorov spectral law, i.e.

$$v \sim \ell^{1/3} \qquad \text{(B-17)}$$

von Weizäcker (1951), Landau and Lifchitz (1959). The relevance of this spectral distribution in interstellar clouds has been emphasised by von Horner (1951), Herschberg (1964), Kaplan and Pikelner (1970), Larson (1979). In addition, the studies of Liszt (1973), Liszt et al (1974), Zuckerman and Palmer (1974) and Zuckerman and Evans (1974), confirm the presence of turbulence in molecular clouds.

Equations (B-15) and (B-16) provide the fundamental relations between turbulence and density fluctuations. In particular, one can consider the range of density inhomogeneities between ℓ_o, the

dimensions of the cloud, and the minimum scale ℓ_m determined by the gas viscosity. According to Heisenberg (1947), the smallest scales correspond to a turbulent viscosity η_ℓ such that

$$\eta_\ell \approx 10\,\eta \tag{B-18}$$

From the definition of turbulent viscosity η_ℓ and assuming the Kolmogorov spectral law one finds

$$\eta_\ell \sim \rho\,\ell\,v \sim \rho\,\ell^{4/3} \tag{B-19}$$

From (B-18) and (B-19) one obtains the order of magnitude of the shortest wavelength scale of spatial density fluctuation ℓ_m which might occur due to turbulent motions, i.e.

$$\ell_m \approx \left[10\ \frac{\langle v\rangle}{n\langle\sigma\rangle}\right]^{\frac{3}{4}} \tag{B-20}$$

This length scale for typical values of HI and molecular clouds becomes

$$\ell_m \approx 2 \times 10^{15}\ \text{cm} \approx 10^{-4}\ \ell_o \text{ for HI clouds}$$

$$\ell_m \approx 3 \times 10^{13}\ \text{cm} \approx 2 \times 10^{-6}\ \ell_o \text{ for molecular clouds}$$

ℓ_o being the length scale for the size of the cloud.

The characteristic timescale for turbulence and therefore for density fluctuations at scales ℓ such that $\ell_m \leq \ell \leq \ell_o$ can be found

from (B-12) and (B-17); it becomes

$$t_t \approx \frac{\ell_o^{1/3}}{v_o} \ell^{2/3} \qquad \text{(B-21)}$$

v_o being the order of magnitude corresponding to the variation of velocity at scales comparable to the cloud size, Landau and Lifchitz (1959).

A timescale of particular interest in this study is the timescale corresponding to fluctuations with optical thickness in grain extinction of the order of $\pi/2$. If in a first approximation, it is supposed that the conventional view holds; i.e. that dust and gas are tied together by either of the two mechanisms: a) gas-dust collisions, or b) coupling of the dust to the weak galactic magnetic field ($\approx 10^{-6}$) frozen in the gas, then the length scale corresponding to the optical thickness $\pi/2$ is

$$\ell_1 = \frac{\pi}{2\bar{\kappa}}$$

$\bar{\kappa}$ being the mean grain extinction, given by

$$\bar{\kappa} = \langle Q_{ext} \tilde{\sigma}_d \rangle \left(\frac{n_d}{n} \right) n \qquad \text{(B-22)}$$

where $\langle \tilde{\sigma}_d \rangle$ is the mean grain cross-section ($\approx 7 \times 10^{-10} cm^2$), and $\frac{n_d}{n}$ the dust gas number ratio. Therefore, the timescale of the turbulence at this scale ℓ_1 becomes

$$t_{t_1} = \frac{\ell_o}{v_o} \frac{\pi}{\langle Q_{ext} \tilde{\sigma}_d \rangle^{2/3} \left(\frac{n_d}{n} \right)^{2/3} n^{2/3}} \qquad \text{(B-23)}$$

APPENDIX C

Derivation of Giovanelli's Equation

The Giovanelli procedure is as follows: one starts writing the radiative transfer equation in the form (4-10), i.e.

$$\frac{dI_\nu}{ds} = - \kappa_\nu I_\nu + \sigma_\nu J_\nu + \kappa_\nu \tilde{S}_\nu \qquad \text{(C-1)}$$

In Cartesian coordinates, the derivative of the left-hand side is simply

$$\frac{dI_\nu}{ds} = \frac{\partial x}{\partial s}\frac{\partial I_\nu}{\partial x} + \frac{\partial y}{\partial s}\frac{\partial I_\nu}{\partial y} + \frac{\partial z}{\partial s}\frac{\partial I_\nu}{\partial z} \qquad \text{(C-2)}$$

but

$$\frac{\partial x}{\partial s} = \sin\theta\cos\phi; \quad \frac{\partial y}{\partial s} = \sin\theta\sin\phi \; ; \quad \frac{\partial z}{\partial s} = \cos\theta \qquad \text{(C-3)}$$

and therefore equation (C-1) becomes

$$\sin\theta\cos\phi\frac{\partial I_\nu}{\partial x} + \sin\theta\sin\phi\frac{\partial I_\nu}{\partial y} + \cos\theta\frac{\partial I_\nu}{\partial z} = -\kappa_\nu I_\nu + \sigma_\nu J_\nu + \kappa_\nu \tilde{S}_\nu \qquad \text{(C-4)}$$

A general representation of I_ν is given by

$$I_\nu = \sum_{n=0}^{\infty} \left[I_n P_n(\mu) + \sum_{m=1}^{n} \left[a_n^m \cos(m\phi) + b_n^m \sin(m\phi) \right] P_n^m(\mu) \right. \qquad \text{(C-5)}$$

Substituting equation (C-5) in (C-4) and integrating with ϕ between 0 to 2π one obtains

$$\sin\theta \int_0^{2\pi} \cos\phi \frac{\partial}{\partial x} \sum_{n=0}^{\infty} I_n P_n(\mu)\, d\phi \; +$$

$$\sin\theta \int_0^{2\pi} \cos\phi \frac{\partial}{\partial x} \sum_{n=0}^{\infty} \sum_{m=1}^{n} \left[a_n^m \cos m\phi + b_n^m \sin m\phi \right] P_m^m(\mu)\, d\phi \; +$$

$$\sin\theta \frac{\partial}{\partial y} \int_0^{2\pi} \sin\phi \frac{\partial}{\partial y} \sum_{n=1}^{\infty} I_n P_n(\mu)\, d\phi \; +$$

$$\sin\theta \int_0^{2\pi} \sin\phi \frac{\partial}{\partial y} \sum_{n=0}^{\infty} \sum_{m=1}^{n} \left[a_n^m \cos m\phi + b_n^m \sin m\phi \right] P_n^m(\mu)\, d\phi \; +$$

$$\cos\theta \int_0^{2\pi} d\phi \frac{\partial}{\partial z} \sum_{n=0}^{\infty} I_n P_n(\mu) \; +$$

$$\cos\theta \int_0^{2\pi} d\phi \frac{\partial}{\partial z} \sum_{n=0}^{\infty} \sum_{m=1}^{n} \left[a_n^m \cos m\phi + b_n^m \sin m\phi \right] P_n^m(\mu) \; =$$

$$-\kappa_\nu \int_0^{2\pi} I_\nu\, d\phi + 2\pi\sigma_\nu J_\nu + 2\pi\kappa_\nu \tilde{S}_\nu \qquad \text{(C-6)}$$

The first left-hand term of equation (C-6) is

$$\sin\theta \int_0^{2\pi} \cos\phi \left[\frac{\partial}{\partial x} \sum_{n=1}^{\infty} I_n P_n(\mu) \right] d\phi = 0 \qquad \text{(C-7a)}$$

because the integrand in brackets does not depend on ϕ.

The second term on the left-hand side of (C-6) is

$$\sin\theta \int_0^{2\pi} \cos\phi \frac{\partial}{\partial x} \sum_{n=0}^{\infty} \sum_{m=1}^{n} \left[a_n^m \cos m\phi + b_n^m \sin m\phi \right] P_n^m(\mu)\, d\phi =$$

$$= \sin\theta \frac{\partial}{\partial x} \left\{ \sum_{n=0}^{\infty} \sum_{m=1}^{n} P_n^m(\mu) \left[a_n^m \int_0^{2\pi} \cos\phi \cos m\phi\, d\phi + b_n^m \int_0^{2\pi} \cos\phi \sin m\phi\, d\phi \right] \right.$$

$$= \pi \sin\theta \frac{\partial}{\partial x} \sum_{n=0}^{\infty} a_n^1 P_n^1(\mu) \qquad \text{(C-7b)}$$

The last equality in equation (C-7b) readily follows from the orthogonality of the trigonometric functions, i.e.

$$\int_0^{2\pi} \cos m\phi \cos\phi\, d\phi = \begin{cases} 0, & m \neq 1 \\ \pi, & m = 1 \end{cases}$$

$$\int_0^{2\pi} \sin m\phi \cos\phi\, d\phi = 0 \text{ for all } m.$$

Similarly to equation (C-7a), the third term on the left-hand side of equation (C-6) becomes zero. The fourth term is

$$\sin\theta \int_0^{2\pi} \sin\phi \frac{\partial}{\partial y} \sum_{n=0}^{\infty} \sum_{m=1}^{n} \left[a_n^m \cos m\phi + b_n^m \sin m\phi \right] P_n^m(\mu)\, d\phi$$

$$= \sin\theta \frac{\partial}{\partial y} \left\{ \sum_{n=0}^{\infty} \sum_{m=1}^{n} P_n^m(\mu) \left[a_n^m \int_0^{2\pi} \sin\phi \cos m\phi\, d\phi + b_n^m \int_0^{2\pi} \sin\phi \sin m\phi\, d\phi \right] \right.$$

$$= \pi \sin\theta \frac{\partial}{\partial y} \sum_{n=0}^{\infty} b_n^1 P_n^1(\mu) \qquad \text{(C-7c)}$$

The last equality follows from the fact that

$$\int_0^{2\pi} \sin m\phi \sin\phi \, d\phi = \begin{cases} 0 & m \neq 1 \\ \pi & m = 1 \end{cases} \quad \text{and}$$

$$\int_0^{2\pi} \sin\phi \cos m\phi \, d\phi = 0 \quad \text{for all } m.$$

The fifth term on the left-hand side of equation (C-6) is

$$\cos\theta \int_0^{2\pi} d\phi \frac{\partial}{\partial z} \sum_{n=0}^{\infty} I_n P_n(\mu) = 2\pi \cos\theta \frac{\partial}{\partial z} \sum_{n=0}^{\infty} I_n P_n(\mu) \qquad \text{(C-7d)}$$

and the sixth one is evidently 0.

Substituting equations (C-7) in equation (C-6) one obtains

$$\mu \sum_{n=0}^{\infty} \left(\frac{\partial I_n}{\partial z} \right) P_n(\mu) + \tfrac{1}{2} \sin\theta \sum_{n=0}^{\infty} \left(\frac{\partial a_n^1}{\partial x} + \frac{\partial b_n^1}{\partial y} \right) P_n^1(\mu)$$

$$= -\kappa_\nu \sum_{n=0}^{\infty} I_n P_n(\mu) + \sigma_\nu J_\nu + \kappa_\nu \tilde{S}_\nu \qquad \text{(C-8)}$$

Multiplying equation (C-8) by $P_m(\mu)$ and integrating from -1 to +1 one obtains

$$\sum_{n=0}^{\infty} \left(\frac{\partial I_n}{\partial z} \right) \int_{-1}^{1} \mu P_n(\mu) P_m(\mu) \, d\mu + \sum_{n=1}^{\infty} \left(\frac{\partial a_n^1}{\partial x} + \frac{b_n^1}{\partial y} \right) \int_{-1}^{1} \tfrac{1}{2}(1-\mu^2)^{\frac{1}{2}} P_n^1(\mu) P_m(\mu) d\mu$$

$$-\kappa_\nu \sum_{n=0}^{\infty} \int_{-1}^{1} I_n P_n(\mu) P_m(\mu) d + \sigma_\nu J_\nu \int_{-1}^{1} P_m(\mu) d\mu + \kappa_\nu \tilde{S}_\nu \int_{-1}^{1} P_m(\mu) d\mu \qquad \text{(C-9)}$$

For m = 0, equation (C-9) becomes

$$\sum_{n=0}^{\infty} \frac{\partial I_n}{\partial z} \int_{-1}^{1} \mu P_n(\mu) P_o(\mu) d\mu + \sum_{n=1}^{\infty} \left(\frac{\partial a_n^1}{\partial x} + \frac{\partial b_n^1}{\partial y} \right) \int_{-1}^{1} \tfrac{1}{2}(1-\mu^2)^{\frac{1}{2}} P_n^1(\mu) P_o(\mu) d\mu$$

$$= -\kappa_\nu \sum_{n=0}^{\infty} \int_{-1}^{1} I_n P_n(\mu) P_0(\mu) + 2\sigma_\nu J_\nu + 2\kappa_\nu \tilde{S}_\nu \qquad \text{(C 10)}$$

From the orthogonality of the Legendre polynomials and associated Legendre functions, i.e.

$$\int_{-1}^{1} P_k(\mu) P_\ell(\mu) d\mu = \frac{2}{2\ell+1} \delta_{k\ell}$$

$$\int_{-1}^{1} P_k^m(\mu) P_\ell^m = \frac{2}{2+1} \frac{(\ell+m)!}{(\ell-m)!} \delta_{k\ell}$$

and using the well known recurrence relations, it follows that

$$\sum_{n=0}^{\infty} \left(\frac{\partial I_n}{\partial z} \right) \int_{-1}^{1} \mu P_n(\mu) d\mu = \frac{2}{3} \frac{\partial I_1}{\partial z} \qquad \text{(C-11a)}$$

$$\sum_{n=1}^{\infty} \left(\frac{\partial a_n^1}{\partial x} + \frac{\partial b_n^1}{\partial y} \right) \int_{-1}^{1} \tfrac{1}{2}(1-\mu^2) P_n^1(\mu) d\mu = \frac{2}{3} \left(\frac{\partial a_1^1}{\partial x} + \frac{\partial b_1^1}{\partial y} \right) \qquad \text{(C-11b)}$$

$$\kappa_\nu \sum_{n=0}^{\infty} \int_{-1}^{1} I_n P_n(\mu) d\mu = 2\kappa_\nu J_\nu \qquad \text{(C-11c)}$$

because

$$J = \frac{1}{4\pi} \int_0^{2\pi} d\phi \int_{-1}^{1} d\mu \, I_\nu = I_o \qquad \text{(C-11d)}$$

Therefore, equation (C-9) becomes

$$\frac{1}{3}\frac{\partial I_1}{\partial z} + \frac{1}{3}\left(\frac{\partial a_1^1}{\partial x} + \frac{\partial b_1^1}{\partial y}\right) = -\alpha_\nu J_\nu + \kappa_\nu \tilde{S}_\nu \qquad \text{(C-12)}$$

Similarly for m = 1, the terms of equation (C-9) become

$$\sum_{n=0}^{\infty} \frac{\partial I_n}{\partial z} \int_{-1}^{1} \mu P_n(\mu)\, P_1(\mu) d\mu = \frac{2}{3}\frac{\partial I_o}{\partial z} + \frac{4}{15}\frac{\partial I_2}{\partial z} \qquad \text{(C-13a)}$$

$$\sum_{n=1}^{\infty} \left(\frac{\partial a_n^1}{\partial x} + \frac{\partial b_n^1}{\partial y}\right) \int_{-1}^{1} \tfrac{1}{2}(1-\mu^2)^{\frac{1}{2}} P_n^1(\mu) P_1(\mu)\, d\mu = \frac{2}{5}\left(\frac{\partial a_2^1}{\partial x} + \frac{\partial b_2^1}{\partial y}\right) \qquad \text{(C-14b)}$$

$$\kappa_\nu \sum^{\infty} \int_{-1}^{1} I_n P_n(\mu)\, P_1(\mu)\, d\mu = \frac{2}{3}\kappa_\nu I_1$$

and one obtains

$$\frac{\partial J_\nu}{\partial z} + \frac{2}{5}\frac{\partial I_2}{\partial z} + \frac{3}{5}\left(\frac{\partial a_2^1}{\partial x} + \frac{\partial b_2^1}{\partial y}\right) = -\kappa_\nu I_1 \qquad \text{(C-15)}$$

and with the approximation

$$\frac{\partial I_2}{\partial z} = \frac{\partial a_2^1}{\partial x} = \frac{\partial a_2^1}{\partial z} = 0$$

equation (C-15) becomes

$$\frac{\partial J_\nu}{\partial z} = -\kappa_\nu I_1 \qquad \text{(C-16)}$$

By symmetry

$$\frac{\partial J_\nu}{\partial x} = -\kappa_\nu a_1^1 \quad ; \qquad \frac{\partial J_\nu}{\partial y} = -\kappa_\nu b_1^1 \tag{C-17}$$

Therefore, if the vector $\underline{I}_1$ is defined by

$$\underline{I}_1 = (a_1^1 , b_1^1 , I_1)$$

then from equations (C-12) and (C-17) it follows that

$$\frac{1}{3} \underline{\nabla} . \underline{I}_1 = -\alpha_\nu J_\nu + \kappa_\nu \tilde{S}_\nu \tag{C-18}$$

and

$$\underline{I}_1 = -\frac{1}{\kappa_\nu} \underline{\nabla} J_\nu \tag{C-19}$$

from where the Giovanelli equation is obtained, i.e.

$$\underline{\nabla} . \left[\frac{1}{\kappa_\nu(\underline{r})} \underline{\nabla} J_\nu(\underline{r}) \right] = 3 \left[\alpha_\nu(\underline{r}) J_\nu(\underline{r}) - \kappa_\nu(\underline{r}) \tilde{S}_\nu(\underline{r}) \right] \tag{C-20}$$